

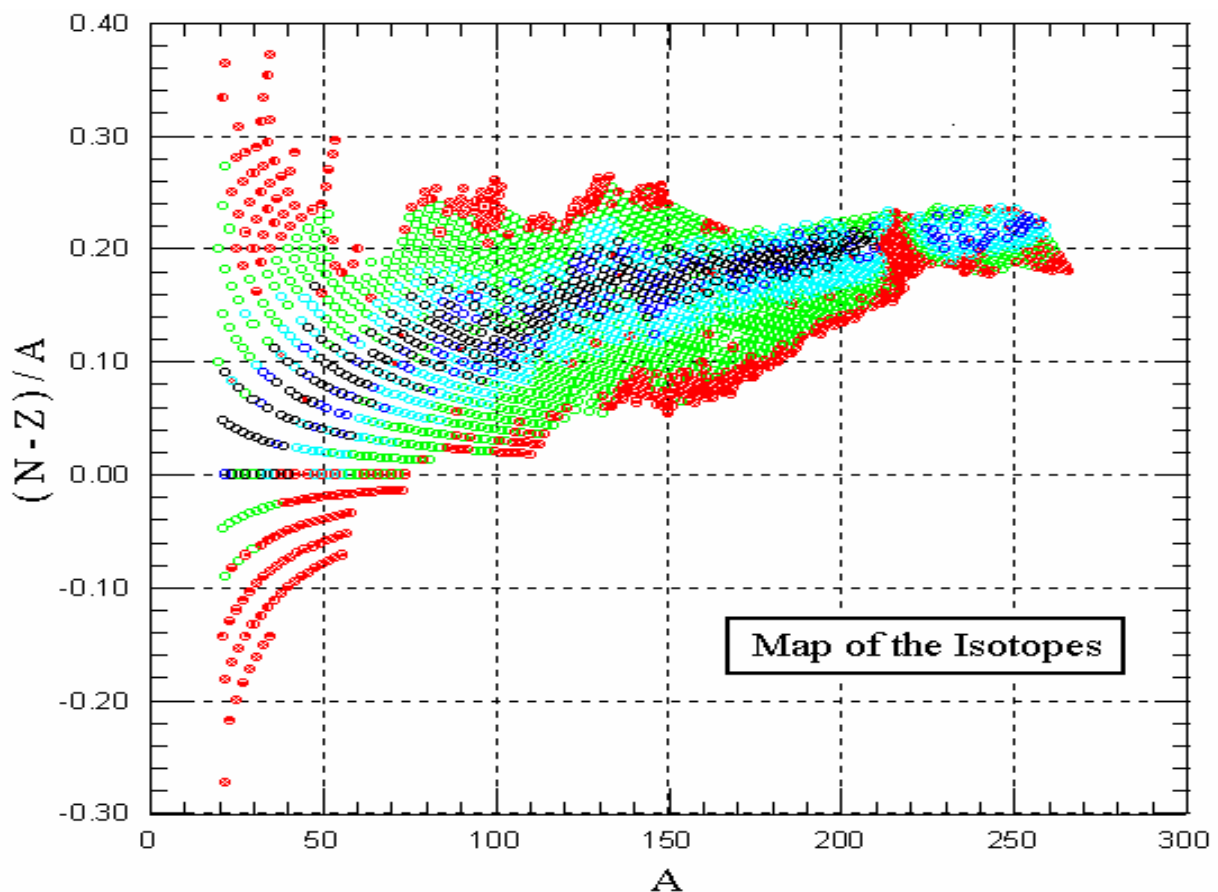
NUCLEAR DATA AND MEASUREMENT SERIES

ANL/NDM-158

**A Survey of Experimental and Evaluated Fast Neutron Helium
Production Cross Section Data for Fusion Energy Applications**

Donald L. Smith

May 2004



ARGONNE NATIONAL LABORATORY

9700 SOUTH CASS AVENUE

ARGONNE, ILLINOIS 60439, U.S.A.

Operated by THE UNIVERSITY OF CHICAGO for the U.S.
DEPARTMENT OF ENERGY under Contract W-31-109-Eng-38

Argonne National Laboratory, with facilities in the states of Illinois and Idaho, is owned by the United States Government, and operated by The University of Chicago under the provisions of Contract W-31-109-Eng-38 with the U.S. Department of Energy.

-----**DISCLAIMER**-----

This report was prepared as an account of work sponsored by an agency of the United States Government. Neither the United States Government nor any agency thereof, nor The University of Chicago, nor any of their employees or officers, makes any warranty, express or implied, or assumes any legal liability or responsibility for the accuracy, completeness, or usefulness of any information, apparatus, product, or process disclosed, or represents that its use would not infringe privately owned rights. Reference herein to any specific commercial product, process, or service by trade name, trademark, manufacturer, or otherwise, does not necessarily constitute or imply its endorsement, recommendation, or favoring by the United States Government or any agency thereof. The views and opinions of document authors expressed herein do not necessarily state or reflect those of the United States Government or any agency thereof, Argonne National Laboratory, or The University of Chicago.

***** NOTICE *****

This report is only available as a PDF document that can be downloaded with no cost or restriction from the following Internet site: <http://www.td.anl.gov/reports/index.html>.

ANL/NDM-158

**A Survey of Experimental and Evaluated Fast Neutron Helium
Production Cross Section Data for Fusion Energy Applications^a**

Donald L. Smith^b

Nuclear Engineering Division
Argonne National Laboratory
9700 South Cass Avenue
Argonne, Illinois 60439
U.S.A.

May 2004

Keywords

SURVEY. Nuclear data, neutron cross sections, helium production, fusion technology.

^a This work was supported through a grant provided by TSI Research, Solana Beach, California, with funding obtained from the U.S. Department of Energy, Office of Science, Office of Fusion Energy Sciences.

^b *Author contact:* 1710 Avenida del Mundo #1506, Coronado, California 92118, U.S.A.;
Tel - +1(619)435-6724; E-mail - Donald.L.Smith@anl.gov.

Nuclear Data and Measurement Series

The Nuclear Data and Measurement Series documents results of studies in the field of microscopic nuclear data. The primary objective is the dissemination of information in the comprehensive form required for nuclear technology applications. This Series is devoted to: a) measured microscopic nuclear parameters, b) experimental techniques and facilities employed in measurements, c) the analysis, correlation and interpretation of nuclear data, and d) the compilation and evaluation of nuclear data. Contributions to this Series are reviewed to assure technical competence and, unless otherwise stated, the contents can be formally referenced. This Series does not supplant formal journal publication, but it does provide the more extensive information required for technological applications (*e.g.*, tabulated numerical data) in a timely manner.

Table of Contents

- Information About Other Issues of the ANL/NDM Series
 - Abstract
 - Acknowledgements
1. Introduction
 2. Helium Producing Nuclear Reactions
 3. CINDA Helium Producing Neutron Reaction Citations
 4. CSISRS Helium Producing Neutron Reaction Experimental Data
 5. Evaluated Helium Producing Neutron Reaction Cross Sections
 6. Comments on a Neutron Materials Radiation Test Facility for Fusion
 7. Summary and Recommendations

Information About Other Issues of the ANL/NDM Series

Information about all other reports in this Series is available from Argonne National Laboratory via the Internet at the following Internet site:

<http://www.td.anl.gov/reports/index.html>

There one can also find a list of titles and authors, abstracts, and specific reports available for viewing or downloading as PDF files with no cost or restriction.

If any questions arise concerning the above-mentioned Internet site or the present report or any other report in this Series, please direct them to:

Dr. Filip G. Kondev
Nuclear Data Program
Nuclear Engineering Division
Building 362
Argonne National Laboratory
9700 South Cass Avenue
Argonne, Illinois 60439
U.S.A.

Tel: +1(630)252-4484
Fax: +1(630)252-5287
E-mail: kondev@anl.gov

A Survey of Experimental and Evaluated Fast Neutron Helium Production Cross Section Data for Fusion Energy Applications^a

by

Donald L. Smith^b

Nuclear Engineering Division, Argonne National Laboratory
Argonne, Illinois 60439, U.S.A.

Abstract

It is well established that the high fluences of fast neutrons likely to be encountered in the environments of fusion reactors or fusion materials test facilities will generate substantial quantities of helium (both ^4He and ^3He isotopes), and that the presence of this gas in bulk material can produce serious damage in engineering structures due to swelling. The present study was undertaken to survey the current status (as of early 2004) of the available fast neutron cross section information for helium production in several major structural elements of interest for the development of fusion energy systems. The scope of this study encompasses both compiled experimental cross section data and evaluated cross sections available from major nuclear data libraries used in the analysis of fusion systems. The main conclusion from this work is that the contemporary knowledge of those individual neutron reaction cross sections important for helium production is, in general, very inadequate for the purpose of producing reliable designs for fusion reactors (e.g., ITER) and materials irradiation test facilities (e.g., IFMIF). Since the number of distinct neutron reactions that must be considered is large, and the capabilities (both experimental and theoretical) of the nuclear physics community to adequately determine the cross sections for specific reactions is limited for various reasons, it is recommended, as a consequence of the present investigation, that an engineering approach be undertaken to provide the data needed for system design purposes. The suggested technical approach would involve irradiating small specimens of candidate materials in high fluence neutron fields whose spectra resemble as closely as possible those to be encountered in real fusion facilities, and that direct integrated yield measurements then be made of helium production in these samples, inclusive of all the contributing neutron reaction channels.

^a This work was supported through a grant provided by TSI Research, Solana Beach, California, with funding obtained from the U.S. Department of Energy, Office of Science, Office of Fusion Energy Sciences.

^b *Author contact:* 1710 Avenida del Mundo #1506, Coronado, California 92118, U.S.A.; Tel - +1(619)435-6724; E-mail - Donald.L.Smith@anl.gov.

Acknowledgements

The author is indebted to Dr. Edward T. Cheng, President, TSI Research, Solana Beach, California, for suggesting this research project. A grant to support the work was provided by TSI Research with funding obtained from the U.S. Department of Energy, Office of Science, Office of Fusion Energy Sciences. The author is also grateful to Dr. Filip Kondev, Argonne Nuclear Data Program, for posting the present document on the Argonne National Laboratory Internet site reserved for reports of the ANL/NDM Series.

1. Introduction

The recognition that fast neutrons originating from D-T fusion reactions in a thermonuclear fusion device will produce significant quantities of helium gas via reactions in structural materials has led to the need for reliable neutron induced helium production cross section data. Some pertinent information is available in compilations and libraries maintained at data centers around the world. However, the demand for numerical data is extensive due to the wide range of materials that needs to be considered and the long list of reactions involved, not only for neutron energies in the range 13 - 15 MeV but also for higher and lower energies as a consequence of secondary processes. Furthermore, it has been proposed to develop a fusion materials test facility based on the thick target charged particle neutron producing reaction processes $d + Li$. Such a facility will generate neutrons with energies up to several tens of MeV. The number of open reaction channels, including ones that generate 3He or 4He as byproducts, is known to increase roughly exponentially with increasing incident neutron energy. Therefore, a legitimate question has arisen as to whether the contemporary databases (both experimental and theoretical) of information on the pertinent helium producing reactions are adequate for purpose of producing reliable designs for both fusion energy and fusion materials testing devices. The present investigation was undertaken to explore this issue. The goal of this study was to produce a survey of existing data that would serve to answer the question: "Is the nuclear data base for helium reactions adequate for fusion applications?" The present report documents the results from this investigation for the following specific elements that are considered important for fusion materials damage assessment: carbon, silicon, titanium, vanadium, chromium, iron, nickel, and tungsten.

Section 2 examines basic nuclear physics issues associated with fast neutron helium production. The isotopes of the above-mentioned elements that are considered worthy of consideration (natural abundance in excess of 1%) are identified. The general characteristics of nuclear reactions are discussed, with particular emphasis given to helium producing reactions. Based on these considerations, an algorithm has been proposed for reducing the list of reactions likely to be important for neutron energies up to 60 MeV. These selected reactions are listed with Q-values, threshold energies, and helium particle yields per reaction. Those reactions that need to be considered for energies up to 14 MeV are highlighted since this is the energy region likely to be of greatest importance for a true thermonuclear reactor. Section 3 summarizes the information compiled in the computer bibliography CINDA which is produced by the Nuclear Data Section of the International Atomic Energy Agency (IAEA-NDS), in collaboration with other data centers around the world. In particular, the mix of experimental, theoretical, evaluation, compilation, and review citations is indicated in tabular and graphical form for the isotopes surveyed in the present investigation. Section 4 examines the existing database of experimental information that is compiled in EXFOR format. The results of this survey are exhibited in the form of plots of data that were generated and downloaded using an online routine available at the National Nuclear Data Center (NNDC), Brookhaven National Laboratory, U.S.A. The objective of this presentation is to provide a sense of the scope (and limitation) of the existing database

without burdening the reader with obscure tables of numerical results. Section 5 examines the general purpose evaluated neutron data files for the selected elements and isotopes, as available from the major evaluation projects, ENDF (U.S.), JENDL (Japan), JEF (Europe), Brond (Russia), and CENDL (China). Again, the collected information is provided in the form of plots generated and downloaded online from the NNDC. Where possible, comparison is made between the evaluated predictions from the various data evaluation projects in order to provide the reader with an understanding of the uncertainty that persists in the data for various helium producing reactions. In addition, pre-formed plots were downloaded from the IAEA-NDS that show individual evaluations from the Fusion Evaluated Nuclear Data Library (FENDL) along with experimental data where available. FENDL is the neutron reaction data library prepared specifically for use by the fusion community. Section 6 examines briefly the nature of the spectrum that would likely be produced at a materials irradiation test facility based on the $d + Li$ neutron source reaction. In particular, the objective is to provide the reader with an understanding of the relative numbers of neutrons below and above 15 MeV for this source, since many of these neutrons exhibit energies external to the 13 – 15 MeV primary energy range for D-T fusion neutrons. Finally, Section 7 provides a summary of the present study and offers recommendations for future investigation in this technical area.

2. Helium Producing Neutron Reactions

2.1 Physics Considerations

Before reviewing the information available on helium production by fast neutrons it is necessary to examine which nuclear reactions involving carbon, silicon, titanium, vanadium, chromium, iron, nickel, and tungsten are responsible for generating helium. Each isotope of these various elements has its own individual characteristics, but there are some basic physics principles governing helium production that are discussed in this sub-section.

The nuclear processes responsible for generating helium are governed by quantum mechanics. Furthermore, those reactions that do emit one or more helium nuclei must compete with other reaction channels that do not generate helium. As is seen below, at neutron energies up to 60 MeV there are numerous competing reaction channels. Available computer codes implement nuclear models which, in principle, can be used to calculate cross sections and particle emission spectra and angular distributions for these various reactions. Such calculations can be very helpful in providing qualitative information for estimating the relative importance of various processes. However, the present state of the art does not allow for sufficiently accurate results to be obtained this way in most cases, especially for complex reaction channels involving several emitted particles. One reason is that the models themselves are simplified by comparison to what actually happens in nuclear collisions. Were they not, the calculations would be intractable. Furthermore, even these simplified models require the input of extensive information about nuclear potentials, nuclear level energies, spins, parities, and widths (lifetimes) that is either not available or is known rather sketchily. This suggests that experimentation might be a better approach to determining the relevant cross sections. Alas, the situation is even more difficult for experimentalists than for theorists. Mono-energetic neutrons needed to measure energy differential cross sections directly can be obtained only in very limited neutron-energy regions such as at 14 MeV and in the keV and low-MeV domains. Sample materials are difficult to obtain in many cases, especially for minor isotopes. Also, there are severe limitations in defining unique measurable signatures for individual reactions.

Those physical considerations that define which helium-producing reactions are likely to be significant for present purposes, and which are probably of lesser consequence, are discussed in conceptual terms in this sub-section. This step is necessary to reduce to practical proportions the lists of reactions that need to be considered. Without pruning, such lists can amount to several hundred open channels at 60 MeV for a single isotope! One of the ways used here to limit the number of reactions considered is to treat major and minor isotopes somewhat differently. The total helium production for an element is generally dominated by reactions involving the major isotope(s) of that element, if there is more than a single stable isotope. Table 2.1 lists the elements included and indicates the abundances in percent of the various isotopes. Referring to Table 2.1, for present purposes an isotope is considered to be major (green highlight) if it comprises

10% or more of the total, minor (yellow highlight) if 1 - 10%, and negligible if < 1% (pink highlight). These choices are arbitrary, of course, but appear to be reasonable.

Table 2.1: Isotopic abundances for the considered elements ^a

<u>Element</u>	<u>Symbol</u>	<u>Z</u>	<u>A</u>	<u>Abundance*</u>
Carbon	C	6	12	98.890%
			13	1.110%
Silicon	Si	14	28	92.230%
			29	4.683%
			30	3.087%
Titanium	Ti	22	46	8.250%
			47	7.440%
			48	73.720%
			49	5.410%
			50	5.180%
Vanadium	V	23	50	0.250%
Chromium	Cr	24	50	99.750%
			51	4.345%
Iron	Fe	26	52	83.789%
			53	9.501%
			54	2.365%
			54	5.845%
			56	91.754%
Nickel	Ni	28	56	2.119%
			57	0.282%
			58	68.077%
			60	26.223%
			61	1.140%
Tungsten	W	74	62	3.634%
			64	0.926%
			180	0.120%
			182	26.500%
			183	14.310%
			184	30.640%
			186	28.430%

^a J.K. Tuli, *Nuclear Wallet Cards*, National Nuclear Data Center, BNL, 2000.

The incident neutron is a single nucleon, a relatively simple nuclear particle. However, even for carbon isotopes, the target nuclei are complex collections of bound neutrons and protons. To initiate reactions, including radiative capture, scattering, and transmutation processes, requires that the incident neutron interact with the target causing disruption. In some cases net positive energy is released (exoergic reactions), but in most cases energy is consumed (endoergic reactions). The parameters used to assess the

energetics of a reaction process are the Q-value (equal to the total mass of the reacting particles in the entrance channel minus the total mass of the product particles in the exit channel) or, comparably, the minimum energy required – in principle – to initiate the reaction (i.e., the threshold energy). The Q-value and corresponding threshold energy can be calculated from knowledge of the masses of the particles involved using well-known formulas (e.g., R.D. Evans, *The Atomic Nucleus*, McGraw Hill Publishers, NY, 1955). These calculations can be quite tedious if performed by hand using mass tables, especially when there are many reaction channels to consider as in the present situation. Fortunately, computational utilities can be found on the Internet to help with this task (e.g., Q-Tool Utility, T-16 Division, LANL: <http://t2.lanl.gov>). Q-Tool was employed to determine reaction Q-values and threshold energies for incident neutrons up to 60 MeV. The results of these calculations were downloaded into EXCEL spreadsheets for further analysis. One potential shortcoming of the Q-Tool utility is that it is limited to 7 particles in the exit channel. However, for energies up to 60 MeV it is unlikely that this limitation causes any important reaction channels to be overlooked. Furthermore, the present study ignores all reaction channels involving more than 5 particles in the exit channel, as discussed below.

A positive difference between the actual incident neutron energy and the threshold energy is important because it corresponds to the amount of energy available for sharing by the interacting particles in the exit channel, after accounting for the additional center-of-mass energy required to conserve momentum as the reaction proceeds. It is seen below why the availability of net positive energy in the exit channel has such an important influence on determining the reaction cross section.

At energies up to 60 MeV, neutron induced reactions are dominated by a combination of compound and pre-compound reaction mechanisms. Briefly, a compound process is one where the neutron merges with the target nucleus and particles are subsequently emitted only after the composite nuclear system reaches equilibrium. A pre-compound process does not involve equilibration of the composite nucleus. Instead, particles are emitted before the composite nucleus comes into equilibrium. In reality, these concepts offer an oversimplified image of what actually goes on in the collisions to aid scientists in visualizing reaction processes. Compound and pre-compound mechanisms are admixed to varying degrees in the energy domain of present interest. Recall that all these reactions are governed by quantum mechanics, and a true understanding of them lies imbedded in solutions to complicated Schroedinger equations. Nevertheless, for argument sake, consider a reaction in which the incident neutron merges with the target and two light particles plus a product nucleus emerge in the exit channel. Then, imagine one light particle being emitted first and a second light particle subsequently, thereby leading to the final collection of reaction products. This picture of the reaction process differs considerably from spallation in which it is imagined that the incident neutron literally explodes nucleus. Spallation is really observed only at energies of several hundred MeV to several GeV, well beyond the region of current interest. Another point is that detailed nuclear structure issues remain important at energies up to 60 MeV, whereas in spallation they tend to have much less influence.

As each light particle is formed and emitted while the reaction proceeds, it must surmount barriers. All particles must overcome the so-called centrifugal barrier if non-zero angular momentum is involved (non *s*-state transitions). Furthermore, charged particles must surmount a Coulomb barrier; the higher their atomic number, the more difficult it is for these particles to penetrate this Coulomb barrier. Obviously, neutrons are not affected by the Coulomb problem and thus are emitted more easily for a given amount of available energy. Another consideration is the energy involved in forming a complex particle within the nucleus, e.g., a deuteron, a triton, or an alpha particle. Of course, this is not an issue in the emission of protons and neutrons. Here, the production of helium is of interest so the formation and emission of alpha particles (^4He) and helions (^3He) is relevant. For these light particles, there is a great deal of variation in the effective binding energies, as is indicated in Table 2.2. The significance of the information in Table 2.2 can be summarized by stating that alpha particles are very tightly bound and are relatively easy to form inside the nucleus whereas the other light composite particles are weakly bound and less readily produced; it takes more energy per nucleon to assemble them and they also tend to be larger in size. Actually, energy is gained in the formation of alpha particles and generally is consumed in forming the other particles. If several light particles – either charged or uncharged – are present in the outgoing channel, then they must share the surplus energy (when the incident neutron energy exceeds the threshold energy). Thus, the more particles present in the exit channel, the smaller (on average) the energy available to any single particle in the collection. This is an important factor that tends to inhibit reactions involving a large number of particles in the exit channel, especially charged particles that must overcome the Coulomb barrier.

Table 2.2: Light-particle binding energies per nucleon ^a

Particle	Binding Energy per Nucleon (MeV)
^2H (deuteron)	1.11
^3H (triton)	2.83
^3He (helion)	2.57
^4He (alpha particle)	7.07

^a R.D. Evans, *The Atomic Nucleus*, McGraw Hill Publishing Company, NY, 1955.

Based on the qualitative physics considerations discussed above, it was decided to prune the lists of all possible neutron-induced reactions for the isotopes listed in Table 2.1 by imposing the following acceptance conditions:

- To be considered, a reaction must emit at least one helium particle (^3He or ^4He).
- Carbon: For the major isotope ^{12}C , consideration is limited to reactions involving no more than 5 particles in the exit channel (including the product nucleus). If there are 5 particles, at least 2 must be neutrons. If there are 4 particles, at least 1 one must a neutron. If there are 3 particles there is no restriction. For the minor isotope ^{13}C , consideration is limited to reactions with no more than 4 particles in

the exit channel (including the product nucleus). If there are 4 particles, then 2 must be neutrons. If there are 3 particles then 1 must be a neutron; otherwise, there is no restriction.

- Silicon, Titanium, Vanadium, Chromium, Iron, and Nickel: For the major isotopes, consideration is limited to reactions involving no more than 4 particles in the exit channel (including the product nucleus). If there are 4 particles, then at least 1 must be a neutron; otherwise, there is no restriction. For the minor isotopes consideration is limited to reactions involving no more than 3 particles. If there are 3 particles, then 1 must be a neutron; otherwise, there is no restriction.
- Tungsten: All the isotopes are major. Consideration is limited to reactions involving no more than 3 particles in the exit channel (including the product nucleus). If there are 3 particles, then 1 must be a neutron; otherwise, there is no restriction.

Upon reflection, it becomes evident that these somewhat arbitrarily imposed restrictions are reasonable from a practical point of view and, as will be seen, they do lead to significant pruning of otherwise very large lists of reactions suggested by consideration of energetics alone. In spite of this pruning, the lists of reactions, especially for the major isotope of carbon and for silicon through nickel, still remain rather large. This suggests that an experimental integral approach to assessing helium production in fusion materials might be superior to considering individual reactions separately and then adding their inevitably rather uncertain contributions. This point is examined further in this report.

For carbon, there exist several open reaction channels that generate moderately light reaction-product nuclei that are unstable to particle decay. Some of these yield additional helium. This would not be evident from a casual inspection of the contents of the reaction channels listed by the Q-Tool utility. These “exotic” light product nuclei are listed in Table 2.3 with their decay modes, half-lives, etc. The reaction products listed in Table 2.3 are rarely observed for silicon and the heavier target element in Table 2.1.

Table 2.3: Moderately light and particle-unstable nuclear reaction products^{a,b}

<u>Element</u>	<u>Z</u>	<u>A</u>	<u>Symbol</u>	<u>Decay Half Life</u>	<u>Decay Mode</u>	<u>⁴He per Decay</u>
Helium	2	5	⁵ He	7 x 10 ⁻²² sec	n + ⁴ He (100%)	1
Lithium	3	5	⁵ Li	3 x 10 ⁻²² sec	p + ⁴ He (100%)	1
		8	⁸ Li	0.838 sec	beta + 2 ⁴ He (100%)	2
Beryllium	4	6	⁶ Be	5 x 10 ⁻²¹ sec	2 p + ⁴ He (100%)	1
		8	⁸ Be	7 x 10 ⁻¹⁷ sec	2 ⁴ He (100%)	2
Boron	5	7	⁷ B	3 x 10 ⁻²² sec	3 p + ⁴ He (100%)	1
		8	⁸ B	0.770 sec	EC + 2 ⁴ He (100%)	2
Carbon	6	8	⁸ C	2 x 10 ⁻²¹ sec	4 p + ⁴ He (100%)	1
		9	⁹ C	0.127 sec	p + 2 ⁴ He (100%)	2

^a J.K. Tuli, *Nuclear Wallet Cards*, National Nuclear Data Center, BNL, 2000.

^b R.B. Firestone et al., *Table of Isotopes (8th Edition)*, Wiley Interscience Publishing Company, NY, 1996.

2.2 Specific Elements

The details for specific elements are examined next to guide the generation of reaction lists for further investigation. The total numbers of reaction channels open for neutron energies up to 60 MeV are established. All channels that actually produce helium are ascertained only for the major isotopes while pruned lists of helium producing reactions that emerge from consideration of the chosen pruning criteria indicated above are provided for both the major and minor isotopes of C, Si, Ti, V, Cr, Fe, Ni, and W.

Carbon

^{12}C

This is the major isotope of carbon. The number of open reaction channels for incident neutron energy to 60 MeV is 141. Of these, the present analysis has determined that 97 involve emission of helium in the exit channel. A rapid increase in the number of energetically allowed helium generating reaction channels with increasing neutron energy is evident from Fig. 2.1. In fact, most of these reaction channels are open only at energies above 15 MeV. Also, it is seen that the number of energetically accessible channels approximately doubles between 50 and 60 MeV. Finally, it is apparent from Fig. 2.1 that the number of open reaction channels increases nearly exponentially (linear on a logarithmic scale) above 30 MeV! This behavior is observed for the major isotopes of other elements considered in this study. Thus, it may be difficult to estimate the material damage due to helium production in the environment of a fusion reactor (dominated by 14 MeV neutrons) by examining the damage produced in a materials testing environment if the latter involves a spectrum having a considerable fraction of higher energy neutrons.

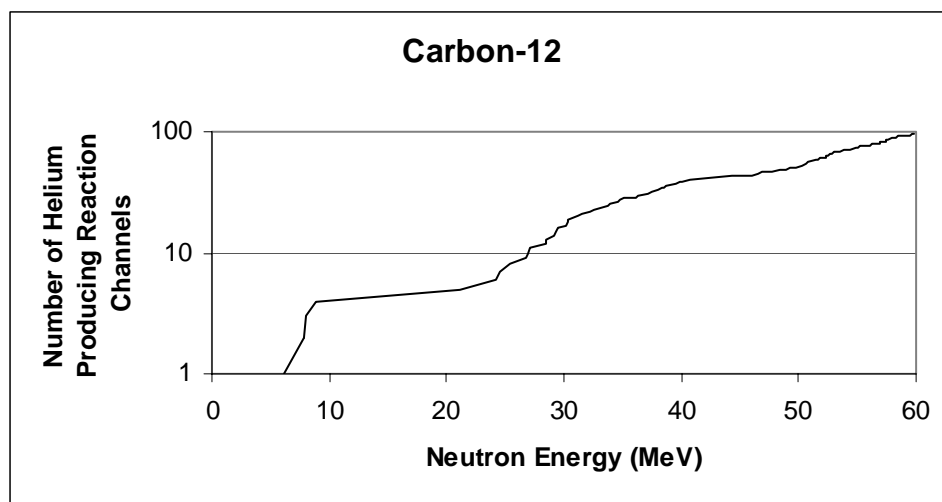


Figure 2.1: Number of helium-producing reaction channels for ^{12}C vs. neutron energy

Application of the pruning criteria indicated above reduces the number of helium-producing reactions that are potentially significant for ^{12}C to 43, a factor of about 2 less than the total but still a rather large number. These reactions are listed in Table 2.4. Helium reactions with thresholds up to 14 MeV are highlighted. This supports the point that is made above concerning the potential impact on damage of the difference between helium production by neutrons below and above 15 MeV.

Table 2.4: Potentially significant helium producing reactions for ^{12}C up to 60 MeV

Reaction Products	Q-value (MeV)	Threshold (MeV)	n	CP	Total Particles	He per Reaction
$^9\text{Be} + ^4\text{He}$	-5.70122	6.18044	0	2	2	1
$^{10}\text{Be} + ^3\text{He}$	-19.46662	21.10289	0	2	2	1
$^8\text{Be} + n + ^4\text{He}$	-7.36663	7.98584	1	2	3	3
$^5\text{He} + 2\ ^4\text{He}$	-8.1648	8.85109	0	3	3	3
$^7\text{Li} + d + ^4\text{He}$	-22.39716	24.27977	0	3	3	1
$^8\text{Li} + p + ^4\text{He}$	-22.58894	24.48766	0	3	3	3
$^6\text{Li} + t + ^4\text{He}$	-23.38988	25.35593	0	3	3	1
$^8\text{Be} + d + t$	-24.95605	27.05375	0	3	3	2
$^9\text{Be} + n + ^3\text{He}$	-26.279	28.48789	1	2	3	1
$^6\text{He} + ^3\text{He} + ^4\text{He}$	-26.87914	29.13847	0	3	3	1
$^7\text{Li} + t + ^3\text{He}$	-36.71765	39.80396	0	3	3	1
$^9\text{Li} + p + ^3\text{He}$	-39.10307	42.38989	0	3	3	1
$^8\text{Li} + d + ^3\text{He}$	-40.94213	44.38353	0	3	3	3
$^7\text{He} + 2\ ^3\text{He}$	-47.90174	51.92814	0	3	3	2
$n + 3\ ^4\text{He}$	-7.27479	7.88628	1	3	4	3
$^7\text{Li} + n + p + ^4\text{He}$	-24.62175	26.69135	1	3	4	1
$^7\text{Be} + 2n + ^4\text{He}$	-26.26594	28.47373	2	2	4	1
$^8\text{Be} + n + p + t$	-27.18064	29.46532	1	3	4	2
$^8\text{Be} + 2n + ^3\text{He}$	-27.94441	30.29329	2	2	4	3
$^5\text{He} + n + ^3\text{He} + ^4\text{He}$	-28.74258	31.15855	1	3	4	3
$^5\text{Li} + n + t + ^4\text{He}$	-29.05382	31.49595	1	3	4	2
$^6\text{Li} + n + d + ^4\text{He}$	-29.64718	32.13919	1	3	4	1
$^8\text{Be} + n + 2d$	-31.21336	33.83701	1	3	4	2
$^7\text{Li} + n + d + ^3\text{He}$	-42.97495	46.58722	1	3	4	1
$^8\text{Li} + n + p + ^3\text{He}$	-43.16672	46.79511	1	3	4	3
$^6\text{Li} + n + t + ^3\text{He}$	-43.96767	47.66339	1	3	4	1
$^8\text{B} + 2n + t$	-45.94249	49.8042	2	2	4	2
$^6\text{He} + n + 2\ ^3\text{He}$	-47.45692	51.44593	1	3	4	2

${}^6\text{Be} + n + 2t$	-48.27444	52.33217	1	3	4	1
$2n + {}^3\text{He} + 2{}^4\text{He}$	-27.85257	30.19373	2	3	5	2
${}^6\text{Li} + 2n + p + {}^4\text{He}$	-31.87177	34.55077	2	3	5	1
${}^8\text{Be} + 2n + p + d$	-33.43794	36.24858	2	3	5	2
${}^5\text{Li} + 2n + d + {}^4\text{He}$	-35.31112	38.27921	2	3	5	2
${}^6\text{Be} + 3n + {}^4\text{He}$	-36.94232	40.04752	3	2	5	2
${}^7\text{Li} + 2n + p + {}^3\text{He}$	-45.19954	48.9988	2	3	5	1
${}^7\text{Be} + 3n + {}^3\text{He}$	-46.84372	50.78119	3	2	5	1
$3n + 2{}^3\text{He} + {}^4\text{He}$	-48.43036	52.50119	2	3	5	3
${}^5\text{He} + 2n + 2{}^3\text{He}$	-49.32036	53.46601	2	3	5	3
${}^5\text{Li} + 2n + t + {}^3\text{He}$	-49.6316	53.80341	2	3	5	2
${}^6\text{Li} + 2n + d + {}^3\text{He}$	-50.22496	54.44664	2	3	5	1
${}^4\text{Li} + 2n + t + {}^4\text{He}$	-50.76661	55.03382	2	3	5	1
${}^8\text{B} + 3n + d$	-52.19979	56.58747	3	2	5	2
${}^9\text{C} + 4n$	-53.12805	57.59375	4	1	5	2

${}^{13}\text{C}$

This is the minor isotope of carbon. The number of open reaction channels existing for incident neutron energy to 60 MeV is 159. The total number of these reactions that produce helium was not determined explicitly, but it is readily evident from inspection of the Q-Tool output that the ratio is qualitatively similar to ${}^{12}\text{C}$. Application of the above-mentioned pruning criteria suggests that among all these helium producing reactions only 6 are likely to be significant. These are listed in Table 2.5. Helium reactions with thresholds up to 14 MeV are highlighted.

Table 2.5: Potentially significant helium producing reactions for ${}^{13}\text{C}$ up to 60 MeV

Reaction Products	Q-value (MeV)	Threshold (MeV)	n	CP	Total Particles	He per Reaction
${}^{11}\text{Be} + {}^3\text{He}$	-23.90904	25.76365	0	2	2	1
${}^{10}\text{Be} + {}^4\text{He}$	-3.83519	4.13268	1	2	3	1
${}^9\text{Be} + n + {}^4\text{He}$	-10.64757	11.4735	1	2	3	1
${}^{10}\text{Be} + n + {}^3\text{He}$	-24.41297	26.30667	1	2	3	1
${}^8\text{Be} + 2n + {}^4\text{He}$	-12.31298	13.2681	2	2	4	3
${}^9\text{Be} + 2n + {}^3\text{He}$	-31.22535	33.64749	2	2	4	1

Silicon

²⁸Si

This is the major isotope of silicon. The number of open reaction channels for incident neutron energy to 60 MeV is 258. Of these, the present analysis has determined that 185 involve emission of helium in the exit channel. It is apparent from Fig. 2.2 that the number of open helium producing reaction channels increases nearly exponentially with advancing neutron energy, approximately doubling between 50 and 60 MeV. Application of the pruning criteria indicated above reduces the number of helium producing reactions that are potentially significant for ²⁸Si to 24. These reactions are listed in Table 2.6. Helium reactions with thresholds up to 14 MeV are highlighted.

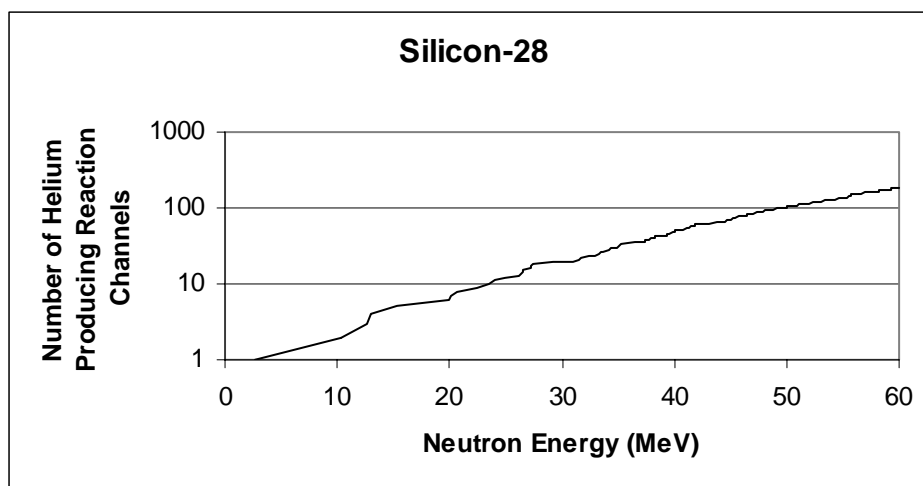


Figure 2.2: Number of helium-producing reaction channels for ²⁸Si vs. neutron energy

Table 2.6: Potentially significant helium producing reactions for ²⁸Si up to 60 MeV

Reaction Products	Q-value (MeV)	Threshold (MeV)	n	CP	Total Particles	He per Reaction
²⁵ Mg + ⁴ He	-2.65368	2.74935	0	2	2	1
²⁶ Mg + ³ He	-12.1383	12.57592	0	2	2	1
²⁴ Mg + n + ⁴ He	-9.9844	10.34437	1	2	3	1
²¹ Ne + 2 ⁴ He	-12.53967	12.99177	0	3	3	2
²⁴ Na + p + ⁴ He	-14.71787	15.2485	0	3	3	1
²³ Na + d + ⁴ He	-19.45277	20.15411	0	3	3	1
²² Ne + ³ He + ⁴ He	-22.75343	23.57376	0	3	3	2
²⁵ Mg + n + ³ He	-23.23146	24.06903	1	2	3	1
²² Na + t + ⁴ He	-25.61428	26.53776	0	3	3	1
²⁵ Na + p + ³ He	-26.28439	27.23204	0	3	3	1

$^{24}\text{Na} + d + ^3\text{He}$	-33.07106	34.26339	0	3	3	1
$^{23}\text{Na} + t + ^3\text{He}$	-33.77325	34.9909	0	3	3	1
$^{23}\text{Ne} + 2\ ^3\text{He}$	-38.13055	39.50528	0	3	3	2
$^{20}\text{Ne} + n + 2\ ^4\text{He}$	-19.30084	19.9967	1	3	4	2
$^{23}\text{Na} + n + p + ^4\text{He}$	-21.67736	22.4589	1	3	4	1
$^{23}\text{Mg} + 2\ n + ^4\text{He}$	-26.51657	27.47259	2	2	4	1
$^{24}\text{Mg} + 2\ n + ^3\text{He}$	-30.56218	31.66405	2	2	4	1
$^{22}\text{Na} + n + d + ^4\text{He}$	-31.87158	33.02066	1	3	4	1
$^{21}\text{Ne} + n + ^3\text{He} + ^4\text{He}$	-33.11745	34.31145	1	3	4	2
$^{24}\text{Na} + n + p + ^3\text{He}$	-35.29565	36.56818	1	3	4	1
$^{21}\text{Na} + n + t + ^4\text{He}$	-36.68353	38.0061	1	3	4	1
$^{23}\text{Na} + n + d + ^3\text{He}$	-40.03055	41.47379	1	3	4	1
$^{22}\text{Ne} + n + 2\ ^3\text{He}$	-43.3312	44.89344	1	3	4	2
$^{22}\text{Na} + n + t + ^3\text{He}$	-46.19206	47.85744	1	3	4	1

^{29}Si

This is a minor isotope of silicon. The number of open reaction channels existing for incident neutron energy to 60 MeV is 256. The total number of these reactions that produce helium was not determined explicitly, but it is readily evident from inspection of the Q-Tool output that the ratio is qualitatively similar to ^{28}Si . Application of the above-mentioned pruning criteria suggests that among all these helium producing reactions only 4 are likely to be significant. These are listed in Table 2.7. Helium reactions with thresholds up to 14 MeV are highlighted.

Table 2.7: Potentially significant helium producing reactions for ^{29}Si up to 60 MeV

Reaction Products	Q-value (MeV)	Threshold (MeV)	Total Particles
$^{26}\text{Mg} + ^4\text{He}$	-0.03414	0.03533	2
$^{27}\text{Mg} + ^3\text{He}$	-14.16852	14.66172	2
$^{25}\text{Mg} + n + ^4\text{He}$	-11.1273	11.51464	3
$^{26}\text{Mg} + n + ^3\text{He}$	-20.61192	21.32942	3

^{30}Si

This is a minor isotope of silicon. The number of open reaction channels existing for incident neutron energy to 60 MeV is 229. The total number of these reactions that produce helium was not determined explicitly, but it is readily evident from inspection of the Q-Tool output that the ratio is qualitatively similar to ^{28}Si . Application of the above-

mentioned pruning criteria suggests that among all these helium producing reactions only 4 are likely to be significant. These are listed in Table 2.8. Helium reactions with thresholds up to 14 MeV are highlighted.

Table 2.8: Potentially significant helium producing reactions for ^{30}Si up to 60 MeV

<u>Reaction Products</u>	<u>Q-value (MeV)</u>	<u>Threshold (MeV)</u>	<u>Total Particles</u>
$^{27}\text{Mg} + ^4\text{He}$	-4.2	4.34134	2
$^{28}\text{Mg} + ^3\text{He}$	-16.27414	16.82179	2
$^{26}\text{Mg} + n + ^4\text{He}$	-10.6434	11.00157	3
$^{27}\text{Mg} + n + ^3\text{He}$	-24.77778	25.61159	3

Titanium

^{46}Ti

This is a minor isotope of titanium. The number of open reaction channels existing for incident neutron energy to 60 MeV is 384. The total number of these reactions that produce helium was not determined explicitly, but it is readily evident from inspection of the Q-Tool output that the ratio is qualitatively similar to ^{48}Ti . Application of the above-mentioned pruning criteria suggests that among all these helium producing reactions only 4 are likely to be significant. These are listed in Table 2.9. Helium reactions with thresholds up to 14 MeV are highlighted.

Table 2.9: Potentially significant helium producing reactions for ^{46}Ti up to 60 MeV

<u>Reaction Products</u>	<u>Q-value (MeV)</u>	<u>Threshold (MeV)</u>	<u>Total Particles</u>
$^{43}\text{Ca} + ^4\text{He}$	-0.07049	0.07204	2
$^{44}\text{Ca} + ^3\text{He}$	-9.51621	9.72509	2
$^{42}\text{Ca} + n + ^4\text{He}$	-8.00355	8.17923	3
$^{43}\text{Ca} + n + ^3\text{He}$	-20.64827	21.1015	3

^{47}Ti

This is a minor isotope of titanium. The number of open reaction channels existing for incident neutron energy to 60 MeV is 372. The total number of these reactions that produce helium was not determined explicitly, but it is readily evident from inspection of the Q-Tool output that the ratio is qualitatively similar to ^{48}Ti . Application of the above-mentioned pruning criteria suggests that among all these helium producing

reactions only 4 are likely to be significant. These are listed in Table 2.10. Helium reactions with thresholds up to 14 MeV are highlighted.

Table 2.10: Potentially significant helium producing reactions for ^{47}Ti up to 60 MeV

Reaction Products	Q-value (MeV)	Threshold (MeV)	Total Particles
$^{44}\text{Ca} + ^4\text{He}$	2.18378	0	2
$^{45}\text{Ca} + ^3\text{He}$	-10.97917	11.21503	2
$^{43}\text{Ca} + n + ^4\text{He}$	-8.94827	9.14051	3
$^{44}\text{Ca} + n + ^3\text{He}$	-18.394	18.78916	3

^{48}Ti

This is the major isotope of titanium. The number of open reaction channels for incident neutron energy to 60 MeV is 309. Of these, the present analysis has determined that 216 involve emission of helium in the exit channel. It is apparent from Fig. 2.3 that the number of open helium producing reaction channels increases nearly exponentially with advancing neutron energy, approximately doubling between 50 and 60 MeV.

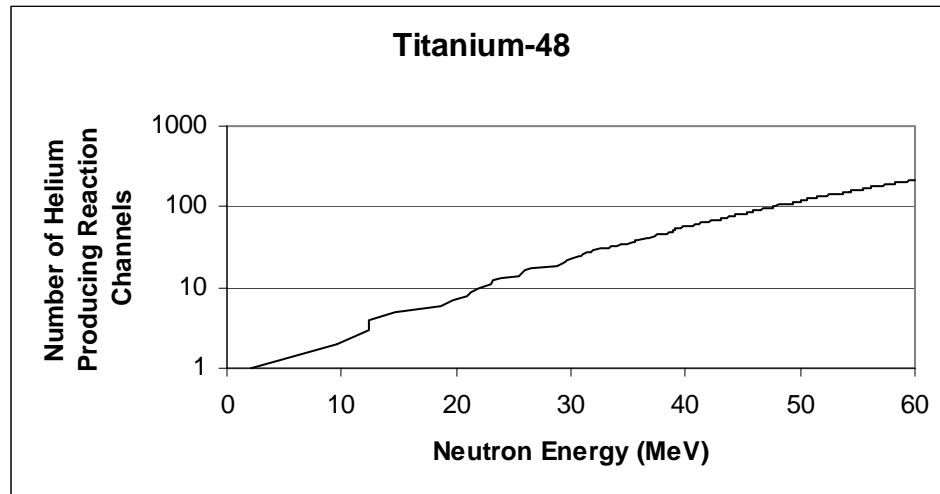


Figure 2.3: Number of helium producing reaction channels for ^{48}Ti vs. neutron energy

Application of the pruning criteria indicated above reduces the number of helium producing reactions that are potentially significant for ^{48}Ti to 24. These reactions are listed in Table 2.11. Helium reactions with thresholds up to 14 MeV are highlighted.

Table 2.11: Potentially significant helium producing reactions for ^{48}Ti up to 60 MeV

Reaction Products	Q-value (MeV)	Threshold (MeV)	n	CP	Total Particles	He per Reaction
$^{45}\text{Ca} + ^4\text{He}$	-2.02807	2.07074	0	2	2	1
$^{46}\text{Ca} + ^3\text{He}$	-12.21207	12.46897	0	2	2	1
$^{44}\text{Ca} + n + ^4\text{He}$	-9.4429	9.64155	1	2	3	1
$^{41}\text{Ar} + 2\ ^4\text{He}$	-12.19834	12.45495	0	3	3	2
$^{44}\text{K} + p + ^4\text{He}$	-14.31946	14.62069	0	3	3	1
$^{43}\text{K} + d + ^4\text{He}$	-19.38342	19.79118	0	3	3	1
$^{45}\text{Ca} + n + ^3\text{He}$	-22.60585	23.08141	1	2	3	1
$^{42}\text{K} + t + ^4\text{He}$	-22.76925	23.24824	0	3	3	1
$^{42}\text{Ar} + ^3\text{He} + ^4\text{He}$	-23.34992	23.84112	0	3	3	2
$^{45}\text{K} + p + ^3\text{He}$	-26.02803	26.57557	0	3	3	1
$^{44}\text{K} + d + ^3\text{He}$	-32.67265	33.35997	0	3	3	1
$^{43}\text{K} + t + ^3\text{He}$	-33.7039	34.41292	0	3	3	1
$^{43}\text{Ar} + 2\ ^3\text{He}$	-38.30087	39.10659	0	3	3	2
$^{40}\text{Ar} + n + 2\ ^4\text{He}$	-18.29708	18.68199	1	3	4	2
$^{43}\text{Ca} + 2n + ^4\text{He}$	-20.57496	21.00779	2	2	4	1
$^{43}\text{K} + n + p + ^4\text{He}$	-21.60801	22.06257	1	3	4	1
$^{42}\text{K} + n + d + ^4\text{He}$	-29.02655	29.63717	1	3	4	1
$^{44}\text{Ca} + 2n + ^3\text{He}$	-30.02068	30.65222	2	2	4	1
$^{41}\text{K} + n + t + ^4\text{He}$	-30.30308	30.94056	1	3	4	1
$^{41}\text{Ar} + n + ^3\text{He} + ^4\text{He}$	-32.77612	33.46562	1	3	4	2
$^{44}\text{K} + n + p + ^3\text{He}$	-34.89724	35.63136	1	3	4	1
$^{43}\text{K} + n + d + ^3\text{He}$	-39.9612	40.80185	1	3	4	1
$^{42}\text{K} + n + t + ^3\text{He}$	-43.34703	44.25891	1	3	4	1
$^{42}\text{Ar} + n + 2\ ^3\text{He}$	-43.9277	44.85179	1	3	4	2

^{49}Ti

This is a minor isotope of titanium. The number of open reaction channels existing for incident neutron energy to 60 MeV is 297. The total number of these reactions that produce helium was not determined explicitly, but it is readily evident from inspection of the Q-Tool output that the ratio is qualitatively similar to ^{48}Ti . Application of the above-mentioned pruning criteria suggests that among all these helium producing

reactions only 4 are likely to be significant. These are listed in Table 2.12. Helium reactions with thresholds up to 14 MeV are highlighted.

Table 2.12: Potentially significant helium producing reactions for ^{49}Ti up to 60 MeV

Reaction Products	Q-value (MeV)	Threshold (MeV)	Total Particles
$^{46}\text{Ca} + ^4\text{He}$	0.22329	0	2
$^{47}\text{Ca} + ^3\text{He}$	-13.07833	13.34784	2
$^{45}\text{Ca} + n + ^4\text{He}$	-10.1705	10.38008	3
$^{46}\text{Ca} + n + ^3\text{He}$	-20.3545	20.77394	3

^{50}Ti

This is a minor isotope of titanium. The number of open reaction channels existing for incident neutron energy to 60 MeV is 237. The total number of these reactions that produce helium was not determined explicitly, but it is readily evident from inspection of the Q-Tool output that the ratio is qualitatively similar to ^{48}Ti . Application of the above-mentioned pruning criteria suggests that among all these helium producing reactions only 4 are likely to be significant. These are listed in Table 2.13. Helium reactions with thresholds up to 14 MeV are highlighted.

Table 2.13: Potentially significant helium producing reactions for ^{50}Ti up to 60 MeV

Reaction Products	Q-value (MeV)	Threshold (MeV)	Total Particles
$^{47}\text{Ca} + ^4\text{He}$	-3.43977	3.50923	2
$^{48}\text{Ca} + ^3\text{He}$	-14.0711	14.35527	2
$^{46}\text{Ca} + n + ^4\text{He}$	-10.71593	10.93235	3
$^{47}\text{Ca} + n + ^3\text{He}$	-24.01755	24.5026	3

Vanadium

^{51}V

This is the major isotope of vanadium. The only other isotope of vanadium is ^{50}V and the abundance is negligible. The number of open reaction channels for incident neutron energy to 60 MeV is 298. The present analysis has determined that 202 involve emission of helium in the exit channel. It is apparent from Fig. 2.4 that the number of

open helium producing reaction channels increases nearly exponentially with advancing neutron energy, approximately doubling between 50 and 60 MeV.

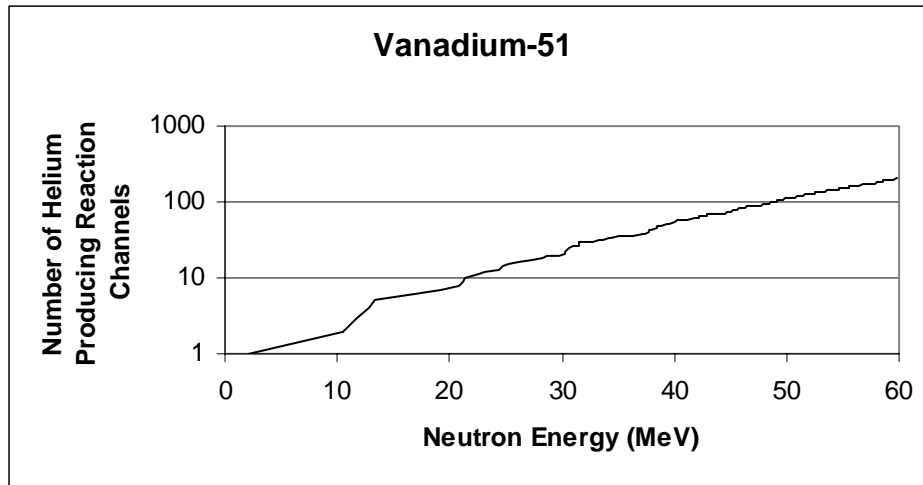


Figure 2.4: Number of helium producing reaction channels for ^{51}V vs. neutron energy

Application of the pruning criteria indicated above reduces the number of helium-producing reactions that are potentially significant for ^{51}V to 24. These reactions are listed in Table 2.14. Helium reactions with thresholds up to 14 MeV are highlighted.

Table 2.14: Potentially significant helium producing reactions for ^{51}V up to 60 MeV

Reaction Products	Q-value (MeV)	Threshold (MeV)	n	CP	Total Particles	He per Reaction
$^{48}\text{Sc} + ^4\text{He}$	-2.05828	2.09903	0	2	2	1
$^{49}\text{Sc} + ^3\text{He}$	-12.5052	12.75279	0	2	2	1
$^{47}\text{Ca} + \text{p} + ^4\text{He}$	-11.50045	11.72815	0	3	3	1
$^{44}\text{K} + 2\ ^4\text{He}$	-13.16588	13.42656	0	3	3	2
$^{46}\text{Ca} + \text{d} + ^4\text{He}$	-16.55202	16.87974	0	3	3	1
$^{45}\text{Ca} + \text{t} + ^4\text{He}$	-20.68851	21.09813	0	3	3	1
$^{48}\text{Ca} + \text{p} + ^3\text{He}$	-22.13178	22.56998	0	3	3	1
$^{48}\text{Sc} + \text{n} + ^3\text{He}$	-22.63606	23.08425	1	2	3	1
$^{45}\text{K} + ^3\text{He} + ^4\text{He}$	-24.87446	25.36696	0	3	3	2
$^{47}\text{Ca} + \text{d} + ^3\text{He}$	-29.85364	30.44473	0	3	3	1
$^{46}\text{Ca} + \text{t} + ^3\text{He}$	-30.87251	31.48376	0	3	3	1
$^{46}\text{K} + 2\ ^3\text{He}$	-38.56995	39.33362	0	3	3	2
$^{47}\text{Sc} + \text{n} + ^4\text{He}$	-10.29085	10.49461	1	3	4	1

$^{46}\text{Ca} + n + p + ^4\text{He}$	-18.77661	19.14838	1	3	4	1
$^{43}\text{K} + n + 2\ ^4\text{He}$	-20.45443	20.85942	1	3	4	2
$^{46}\text{Sc} + 2\ n + ^4\text{He}$	-20.93526	21.34976	2	2	4	1
$^{45}\text{Ca} + n + d + ^4\text{He}$	-26.94581	27.47932	1	3	4	1
$^{44}\text{Ca} + n + t + ^4\text{He}$	-28.10334	28.65977	1	3	4	1
$^{47}\text{Sc} + 2\ n + ^3\text{He}$	-30.86863	31.47982	2	2	4	1
$^{47}\text{Ca} + n + p + ^3\text{He}$	-32.07823	32.71336	1	3	4	1
$^{44}\text{K} + n + ^3\text{He} + ^4\text{He}$	-33.74367	34.41177	1	3	4	2
$^{46}\text{Ca} + n + d + ^3\text{He}$	-37.1298	37.86496	1	3	4	1
$^{45}\text{Ca} + n + t + ^3\text{He}$	-41.26629	42.08334	1	3	4	1
$^{45}\text{K} + n + 2\ ^3\text{He}$	-45.45224	46.35217	1	3	4	2

Chromium

^{50}Cr

This is a minor isotope of chromium. The number of open reaction channels existing for incident neutron energy to 60 MeV is 375. The total number of these reactions that produce helium was not determined explicitly, but it is readily evident from inspection of the Q-Tool output that the ratio is qualitatively similar to ^{52}Cr . Application of the above-mentioned pruning criteria suggests that among all these helium producing reactions only 4 are likely to be significant. These are listed in Table 2.15. Helium reactions with thresholds up to 14 MeV are highlighted.

Table 2.15: Potentially significant helium producing reactions for ^{50}Cr up to 60 MeV

<u>Reaction Products</u>	<u>Q-value (MeV)</u>	<u>Threshold (MeV)</u>	<u>Total Particles</u>
$^{47}\text{Ti} + ^4\text{He}$	0.32368	0	2
$^{48}\text{Ti} + ^3\text{He}$	-8.62741	8.80164	2
$^{46}\text{Ti} + n + ^4\text{He}$	-8.5541	8.72685	3
$^{47}\text{Ti} + n + ^3\text{He}$	-20.2541	20.66313	3

^{52}Cr

This is the major isotope of chromium. The number of open reaction channels for incident neutron energy to 60 MeV is 307. The present analysis has determined that 215 involve emission of helium in the exit channel. It is apparent from Fig. 2.5 that the number of open helium producing reaction channels increases nearly exponentially with advancing neutron energy, approximately doubling between 50 and 60 MeV. Application

of the pruning criteria indicated above reduces the number of helium-producing reactions that are potentially significant for ^{52}Cr to 26. These reactions are listed in Table 2.16 Helium reactions with thresholds up to 14 MeV are highlighted.

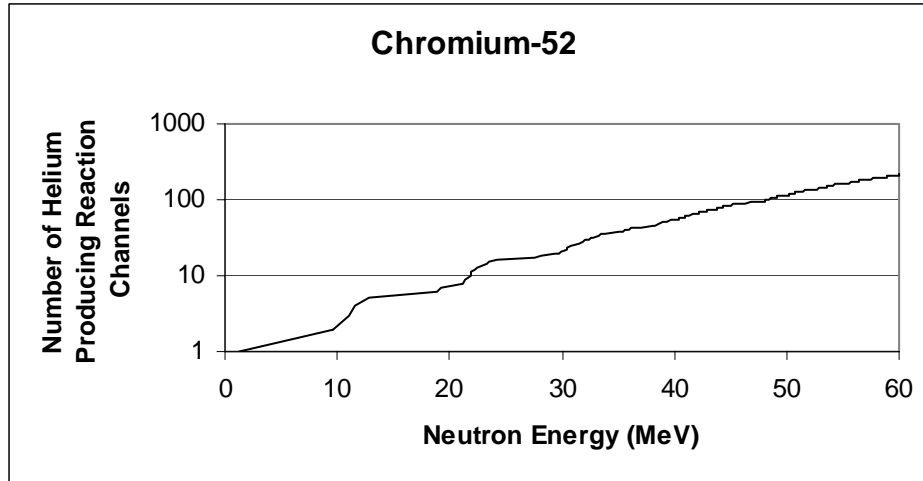


Figure 2.5: Number of helium producing reaction channels for ^{52}Cr vs. neutron energy

Table 2.16: Potentially significant helium producing reactions for ^{52}Cr up to 60 MeV

Reaction Products	Q-value (MeV)	Threshold (MeV)	n	CP	Total Particles	He per Reaction
$^{49}\text{Ti} + ^4\text{He}$	-1.20835	1.23182	0	2	2	1
$^{50}\text{Ti} + ^3\text{He}$	-10.84692	11.05756	0	2	2	1
$^{48}\text{Ti} + n + ^4\text{He}$	-9.35078	9.53237	1	2	3	1
$^{45}\text{Ca} + 2\ ^4\text{He}$	-11.37886	11.59983	0	3	3	2
$^{48}\text{Sc} + p + ^4\text{He}$	-12.56264	12.8066	0	3	3	1
$^{47}\text{Sc} + d + ^4\text{He}$	-18.57062	18.93126	0	3	3	1
$^{46}\text{Ca} + ^3\text{He} + ^4\text{He}$	-21.56285	21.9816	0	3	3	2
$^{49}\text{Ti} + n + ^3\text{He}$	-21.78614	22.20922	1	2	3	1
$^{46}\text{Sc} + t + ^4\text{He}$	-22.95773	23.40356	0	3	3	1
$^{49}\text{Sc} + p + ^3\text{He}$	-23.00956	23.45639	0	3	3	1
$^{48}\text{Sc} + d + ^3\text{He}$	-30.91583	31.51621	0	3	3	1
$^{47}\text{Sc} + t + ^3\text{He}$	-32.89111	33.52984	0	3	3	1
$^{47}\text{Ca} + 2\ ^3\text{He}$	-34.86447	35.54153	0	3	3	2
$^{44}\text{Ca} + n + 2\ ^4\text{He}$	-18.79369	19.15865	1	3	4	2
$^{47}\text{Sc} + n + p + ^4\text{He}$	-20.79521	21.19905	1	3	4	1

$^{47}\text{Ti} + 2\text{n} + ^4\text{He}$	-20.97747	21.38485	2	2	4	1
$^{47}\text{Ca} + 2\text{p} + ^4\text{He}$	-22.00481	22.43213	0	4	4	1
$^{46}\text{Ca} + \text{p} + \text{d} + ^4\text{He}$	-27.05638	27.58181	0	4	4	1
$^{46}\text{Sc} + \text{n} + \text{d} + ^4\text{He}$	-29.21503	29.78237	1	3	4	1
$^{48}\text{Ti} + 2\text{n} + ^3\text{He}$	-29.92857	30.50977	2	2	4	1
$^{45}\text{Sc} + \text{n} + \text{t} + ^4\text{He}$	-31.71842	32.33438	1	3	4	1
$^{45}\text{Ca} + \text{n} + ^3\text{He} + ^4\text{He}$	-31.95664	32.57722	1	3	4	2
$^{48}\text{Sc} + \text{n} + \text{p} + ^3\text{He}$	-33.14042	33.784	1	3	4	1
$^{47}\text{Sc} + \text{n} + \text{d} + ^3\text{He}$	-39.1484	39.90865	1	3	4	1
$^{46}\text{Ca} + \text{n} + 2\ ^3\text{He}$	-42.14063	42.95899	1	3	4	2
$^{46}\text{Sc} + \text{n} + \text{t} + ^3\text{He}$	-43.53551	44.38095	1	3	4	1

^{53}Cr

This is a minor isotope of chromium. The number of open reaction channels existing for incident neutron energy to 60 MeV is 310. The total number of these reactions that produce helium was not determined explicitly, but it is readily evident from inspection of the Q-Tool output that the ratio is qualitatively similar to ^{52}Cr . Application of the above-mentioned pruning criteria suggests that among all these helium producing reactions only 4 are likely to be significant. These are listed in Table 2.17. Helium reactions with thresholds up to 14 MeV are highlighted.

Table 2.17: Potentially significant helium producing reactions for ^{53}Cr up to 60 MeV

Reaction Products	Q-value (MeV)	Threshold (MeV)	Total Particles
$^{50}\text{Ti} + ^4\text{He}$	1.79164	0	2
$^{51}\text{Ti} + ^3\text{He}$	-12.41376	12.65028	2
$^{49}\text{Ti} + \text{n} + ^4\text{He}$	-9.14758	9.32187	3
$^{50}\text{Ti} + \text{n} + ^3\text{He}$	-18.78614	19.14407	3

^{54}Cr

This is a minor isotope of chromium. The number of open reaction channels existing for incident neutron energy to 60 MeV is 279. The total number of these reactions that produce helium was not determined explicitly, but it is readily evident from inspection of the Q-Tool output that the ratio is qualitatively similar to ^{52}Cr . Application of the above-mentioned pruning criteria suggests that among all these helium producing

reactions only 4 are likely to be significant. These are listed in Table 2.18. Helium reactions with thresholds up to 14 MeV are highlighted.

Table 2.18: Potentially significant helium producing reactions for ^{54}Cr up to 60 MeV

Reaction Products	Q-value (MeV)	Threshold (MeV)	Total Particles
$^{51}\text{Ti} + ^4\text{He}$	-1.55507	1.58415	2
$^{52}\text{Ti} + ^3\text{He}$	-14.3243	14.59216	2
$^{50}\text{Ti} + \text{n} + ^4\text{He}$	-7.92745	8.0757	3
$^{51}\text{Ti} + \text{n} + ^3\text{He}$	-22.13285	22.54674	3

Iron

^{54}Fe

This is a minor isotope of iron. The number of open reaction channels existing for incident neutron energy to 60 MeV is 377. The total number of these reactions that produce helium was not determined explicitly, but it is readily evident from inspection of the Q-Tool output that the ratio is qualitatively similar to ^{56}Fe . Application of the above-mentioned pruning criteria suggests that among all these helium producing reactions only 4 are likely to be significant. These are listed in 2.19. Helium reactions with thresholds up to 14 MeV are highlighted.

Table 2.19: Potentially significant helium producing reactions for ^{54}Fe up to 60 MeV

Reaction Products	Q-value (MeV)	Threshold (MeV)	Total Particles
$^{51}\text{Cr} + ^4\text{He}$	0.84277	0	2
$^{52}\text{Cr} + ^3\text{He}$	-7.69555	7.83946	2
$^{50}\text{Cr} + \text{n} + ^4\text{He}$	-8.41893	8.57636	3
$^{51}\text{Cr} + \text{n} + ^3\text{He}$	-19.73501	20.10405	3

^{56}Fe

This is the major isotope of iron. The number of open reaction channels for incident neutron energy to 60 MeV is 343. The present analysis has determined that 242 involve emission of helium in the exit channel. It is apparent from Fig. 2.6 that the number of open helium producing reaction channels increases nearly exponentially with advancing neutron energy, approximately doubling between 50 and 60 MeV. Application

of the pruning criteria indicated above reduces the number of helium-producing reactions that are potentially significant for ^{56}Fe to 24. These reactions are listed in Table 2.20. Helium reactions with thresholds up to 14 MeV are highlighted.

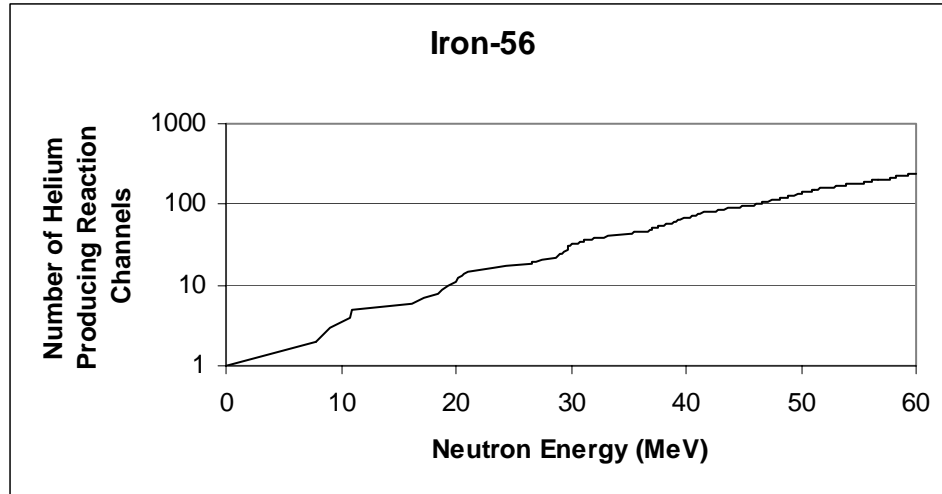


Figure 2.6: Number of helium producing reaction channels for ^{56}Fe vs. neutron energy

Table 2.20: Potentially significant helium producing reactions for ^{56}Fe up to 60 MeV

Reaction Products	Q-value (MeV)	Threshold (MeV)	n	CP	Total Particles	He per Reaction
$^{53}\text{Cr} + ^4\text{He}$	0.32604	0	0	2	2	1
$^{54}\text{Cr} + ^3\text{He}$	-10.53265	10.72258	0	2	2	1
$^{52}\text{Cr} + n + ^4\text{He}$	-7.61318	7.75047	1	2	3	1
$^{49}\text{Ti} + 2\ ^4\text{He}$	-8.82154	8.98061	0	3	3	2
$^{52}\text{V} + p + ^4\text{He}$	-10.80624	11.00111	0	3	3	1
$^{51}\text{V} + d + ^4\text{He}$	-15.89295	16.17955	0	3	3	1
$^{50}\text{Ti} + ^3\text{He} + ^4\text{He}$	-18.4601	18.79299	0	3	3	2
$^{53}\text{Cr} + n + ^3\text{He}$	-20.25174	20.61694	1	2	3	1
$^{50}\text{V} + t + ^4\text{He}$	-20.68702	21.06006	0	3	3	1
$^{53}\text{V} + p + ^3\text{He}$	-22.90544	23.31849	0	3	3	1
$^{52}\text{Cr} + 2n + ^3\text{He}$	-28.19096	28.69933	2	1	3	1
$^{52}\text{V} + d + ^3\text{He}$	-29.15944	29.68526	0	3	3	1
$^{51}\text{V} + t + ^3\text{He}$	-30.21344	30.75827	0	3	3	1
$^{51}\text{Ti} + 2\ ^3\text{He}$	-32.6655	33.25455	0	3	3	2
$^{48}\text{Ti} + n + 2\ ^4\text{He}$	-16.96397	17.26987	1	3	4	2

$^{51}\text{V} + n + p + ^4\text{He}$	-18.11754	18.44425	1	3	4	1
$^{51}\text{Cr} + 2n + ^4\text{He}$	-19.65264	20.00703	2	2	4	1
$^{50}\text{V} + n + d + ^4\text{He}$	-26.94432	27.4302	1	3	4	1
$^{49}\text{Ti} + n + ^3\text{He} + ^4\text{He}$	-29.39932	29.92947	1	3	4	2
$^{49}\text{V} + n + t + ^4\text{He}$	-30.01977	30.56112	1	3	4	1
$^{52}\text{V} + n + p + ^3\text{He}$	-31.38403	31.94997	1	3	4	1
$^{51}\text{V} + n + d + ^3\text{He}$	-36.47073	37.1284	1	3	4	1
$^{50}\text{Ti} + n + 2\ ^3\text{He}$	-39.03788	39.74185	1	3	4	2
$^{50}\text{V} + n + t + ^3\text{He}$	-41.2648	42.00892	1	3	4	1

^{57}Fe

This is a minor isotope of iron. The number of open reaction channels existing for incident neutron energy to 60 MeV is 365. The total number of these reactions that produce helium was not determined explicitly, but it is readily evident from inspection of the Q-Tool output that the ratio is qualitatively similar to ^{56}Fe . Application of the above-mentioned pruning criteria suggests that among all these helium producing reactions only 4 are likely to be significant. These are listed in 2.21. Helium reactions with thresholds up to 14 MeV are highlighted.

Table 2.21: Potentially significant helium producing reactions for ^{57}Fe up to 60 MeV

Reaction Products	Q-value (MeV)	Threshold (MeV)	Total Particles
$^{54}\text{Cr} + ^4\text{He}$	2.39904	0	2
$^{55}\text{Cr} + ^3\text{He}$	-11.93239	12.14378	2
$^{53}\text{Cr} + n + ^4\text{He}$	-7.32005	7.44973	3
$^{54}\text{Cr} + n + ^3\text{He}$	-18.17874	18.50079	3

Nickel

^{58}Ni

This is one of two major isotopes of nickel. The number of open reaction channels for incident neutron energy to 60 MeV is 420. The present analysis has determined that 308 involve emission of helium in the exit channel. It is apparent from Fig. 2.7 that the number of open helium-producing reaction channels increases nearly exponentially with advancing neutron energy, approximately doubling between 50 and 60 MeV. Application of the pruning criteria indicated above reduces the number of helium producing reactions

that are potentially significant for ^{58}Ni to 24. These reactions are listed in Table 2.22. Helium reactions with thresholds up to 14 MeV are highlighted.

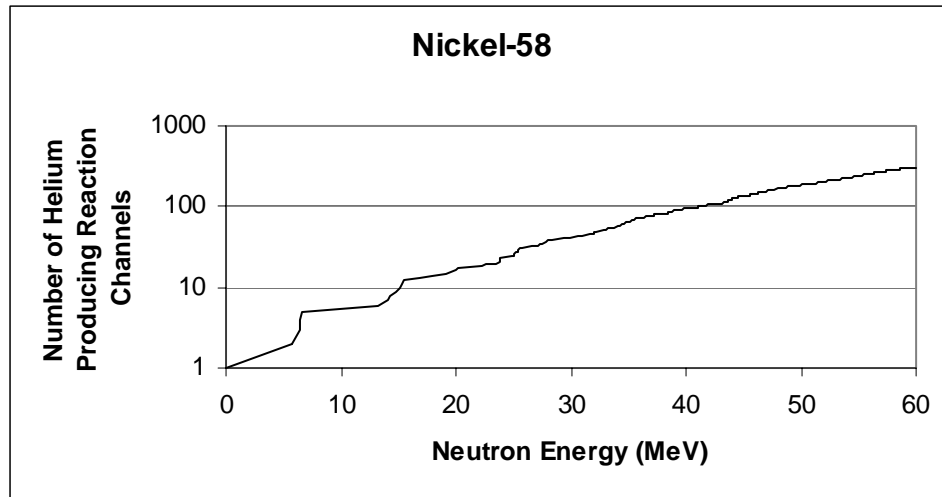


Figure 2.7: Number of helium producing reaction channels for ^{58}Ni vs. neutron energy

Table 2.22: Potentially significant helium producing reactions for ^{58}Ni up to 60 MeV

Reaction Products	Q-value (MeV)	Threshold (MeV)	n	CP	Total Particles	He per Reaction
$^{55}\text{Fe} + ^4\text{He}$	2.89843	0	0	2	2	1
$^{56}\text{Fe} + ^3\text{He}$	-6.48194	6.59479	0	2	2	1
$^{51}\text{Cr} + 2\ ^4\text{He}$	-5.5568	5.65354	0	3	3	2
$^{54}\text{Mn} + \text{p} + ^4\text{He}$	-6.31435	6.42429	0	3	3	1
$^{54}\text{Fe} + \text{n} + ^4\text{He}$	-6.39957	6.51099	1	2	3	1
$^{53}\text{Mn} + \text{d} + ^4\text{He}$	-13.0288	13.25564	0	3	3	1
$^{52}\text{Cr} + ^3\text{He} + ^4\text{He}$	-14.09512	14.34052	0	3	3	2
$^{55}\text{Mn} + \text{p} + ^3\text{He}$	-16.66562	16.95577	0	3	3	1
$^{55}\text{Fe} + \text{n} + ^3\text{He}$	-17.67936	17.98716	1	2	3	3
$^{52}\text{Mn} + \text{t} + ^4\text{He}$	-18.82541	19.15316	0	3	3	1
$^{54}\text{Mn} + \text{d} + ^3\text{He}$	-24.66755	25.09701	0	3	3	1
$^{53}\text{Cr} + 2\ ^3\text{He}$	-26.73368	27.19912	0	3	3	2
$^{53}\text{Mn} + \text{t} + ^3\text{He}$	-27.34929	27.82545	0	3	3	1
$^{50}\text{Cr} + \text{n} + 2\ ^4\text{He}$	-14.8185	15.07649	1	3	4	2
$^{53}\text{Mn} + \text{n} + \text{p} + ^4\text{He}$	-15.2534	15.51896	1	3	4	1
$^{53}\text{Fe} + 2\ \text{n} + ^4\text{He}$	-19.77814	20.12248	2	2	4	1
$^{52}\text{Mn} + \text{n} + \text{d} + ^4\text{He}$	-25.08271	25.51941	1	3	4	1
$^{51}\text{Cr} + \text{n} + ^3\text{He} + ^4\text{He}$	-26.13458	26.58959	1	3	4	2

$^{54}\text{Mn} + n + p + {}^3\text{He}$	-26.89214	27.36033	1	3	4	1
$^{54}\text{Fe} + 2n + {}^3\text{He}$	-26.97735	27.44703	2	2	4	1
$^{51}\text{Mn} + n + t + {}^4\text{He}$	-29.361	29.87218	1	3	4	1
$^{53}\text{Mn} + n + d + {}^3\text{He}$	-33.60659	34.19168	1	3	4	1
$^{52}\text{Cr} + n + 2 {}^3\text{He}$	-34.6729	35.27657	1	3	4	2
$^{52}\text{Mn} + n + t + {}^3\text{He}$	-39.40319	40.08921	1	3	4	1

^{60}Ni

This is one of two major isotopes of nickel. The number of open reaction channels for incident neutron energy to 60 MeV is 397. The present analysis has determined that 287 involve emission of helium in the exit channel. It is apparent from Fig. 2.8 that the number of open helium-producing reaction channels increases nearly exponentially with advancing neutron energy, approximately doubling between 50 and 60 MeV. Application of the pruning criteria indicated above reduces the number of helium producing reactions that are potentially significant for ^{60}Ni to 24. These reactions are listed in Table 2.23. Helium reactions with thresholds up to 14 MeV are highlighted.

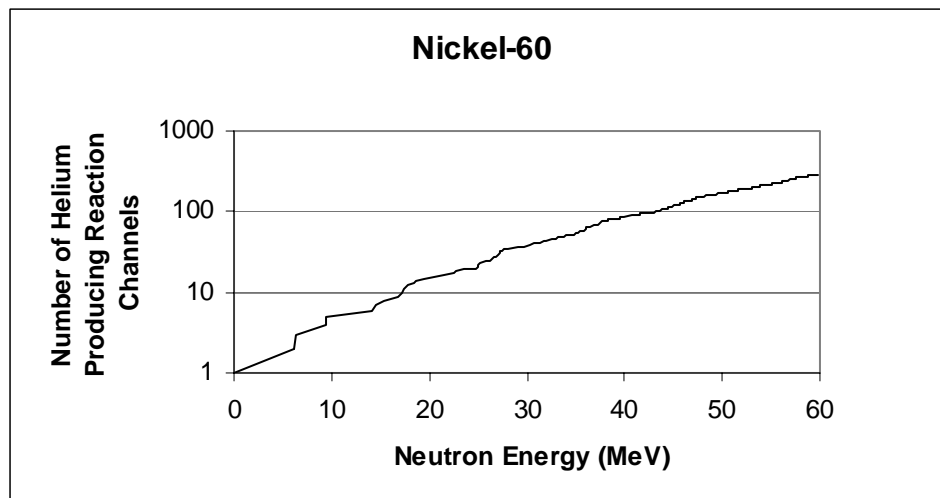


Figure 2.8: Number of helium producing reaction channels for ^{60}Ni vs. neutron energy

Table 2.23: Potentially significant helium producing reactions for ^{60}Ni up to 60 MeV

Reaction Products	Q-value (MeV)	Threshold (MeV)	n	CP	Total Particles	He per Reaction
$^{57}\text{Fe} + {}^4\text{He}$	1.35403	0	0	2	2	1
$^{58}\text{Fe} + {}^3\text{He}$	-9.17922	9.33371	0	2	2	1
$^{53}\text{Cr} + 2 {}^4\text{He}$	-5.96602	6.06643	0	3	3	2
$^{56}\text{Fe} + n + {}^4\text{He}$	-6.29206	6.39796	1	2	3	1

$^{56}\text{Mn} + \text{p} + ^4\text{He}$	-9.20518	9.36011	0	3	3	1
$^{55}\text{Mn} + \text{d} + ^4\text{He}$	-14.25114	14.491	0	3	3	1
$^{54}\text{Cr} + ^3\text{He} + ^4\text{He}$	-16.82471	17.10788	0	3	3	1
$^{54}\text{Mn} + \text{t} + ^4\text{He}$	-18.22037	18.52703	0	3	3	1
$^{57}\text{Fe} + \text{n} + ^3\text{He}$	-19.22375	19.5473	1	2	3	1
$^{57}\text{Mn} + \text{p} + ^3\text{He}$	-21.13227	21.48794	0	3	3	1
$^{56}\text{Mn} + \text{d} + ^3\text{He}$	-27.55838	28.0222	0	3	3	1
$^{55}\text{Mn} + \text{t} + ^3\text{He}$	-28.57163	29.0525	0	3	3	1
$^{55}\text{Cr} + 2\ ^3\text{He}$	-31.15615	31.68052	0	3	3	2
$^{52}\text{Cr} + \text{n} + 2\ ^4\text{He}$	-13.90524	14.13927	1	3	4	2
$^{55}\text{Mn} + \text{n} + \text{p} + ^4\text{He}$	-16.47573	16.75303	1	3	4	1
$^{55}\text{Fe} + 2\ \text{n} + ^4\text{He}$	-17.48948	17.78383	2	2	4	1
$^{54}\text{Mn} + \text{n} + \text{d} + ^4\text{He}$	-24.47766	24.88964	1	3	4	1
$^{53}\text{Cr} + \text{n} + ^3\text{He} + ^4\text{He}$	-26.5438	26.99055	1	3	4	2
$^{56}\text{Fe} + 2\ \text{n} + ^3\text{He}$	-26.86984	27.32207	2	2	4	1
$^{53}\text{Mn} + \text{n} + \text{t} + ^4\text{He}$	-27.15941	27.61651	1	3	4	1
$^{56}\text{Mn} + \text{n} + \text{p} + ^3\text{He}$	-29.78297	30.28423	1	3	4	1
$^{55}\text{Mn} + \text{n} + \text{d} + ^3\text{He}$	-34.82893	35.41512	1	3	4	1
$^{54}\text{Cr} + \text{n} + 2\ ^3\text{He}$	-37.40249	38.03199	1	3	4	2
$^{54}\text{Mn} + \text{n} + \text{t} + ^3\text{He}$	-38.79815	39.45114	1	3	4	1

^{61}Ni

This is a minor isotope of nickel. The number of open reaction channels existing for incident neutron energy to 60 MeV is 414. The total number of these reactions that produce helium was not determined explicitly, but it is readily evident from inspection of the Q-Tool output that the ratio is qualitatively similar to ^{58}Ni . Application of the above-mentioned pruning condition suggests that among all these helium producing reactions only 4 are likely to be significant. These are listed in Table 2.24. Those helium-producing reaction channels with threshold energies up to 14 MeV are highlighted.

Table 2.24: Potentially significant helium producing reactions for ^{61}Ni up to 60 MeV

Reaction Products	Q-value (MeV)	Threshold (MeV)	Total Particles
$^{58}\text{Fe} + ^4\text{He}$	3.57851	0	2
$^{59}\text{Fe} + ^3\text{He}$	-10.41832	10.59078	2
$^{57}\text{Fe} + \text{n} + ^4\text{He}$	-6.46603	6.57307	3
$^{58}\text{Fe} + \text{n} + ^3\text{He}$	-16.99927	17.28068	3

⁶²Ni

This is a minor isotope of nickel. The number of open reaction channels existing for incident neutron energy to 60 MeV is 374. The total number of these reactions that produce helium was not determined explicitly, but it is readily evident from inspection of the Q-Tool output that the ratio is qualitatively similar to ⁵⁸Ni. Application of the above-mentioned pruning condition suggests that among all these helium-producing reactions only 4 are likely to be significant. These are listed in Table 2.25. Those helium producing reaction channels with threshold energies up to 14 MeV are highlighted.

Table 2.25: Potentially significant helium producing reactions for ⁶²Ni up to 60 MeV

<u>Reaction Products</u>	<u>Q-value (MeV)</u>	<u>Threshold (MeV)</u>	<u>Total Particles</u>
⁵⁹ Fe + ⁴ He	-0.43786	0.44499	2
⁶⁰ Fe + ³ He	-12.19575	12.39439	2
⁵⁸ Fe + n + ⁴ He	-7.01882	7.13314	3
⁵⁹ Fe + n + ³ He	-21.01564	21.35794	3

Tungsten

There are four major isotopes of tungsten (^{182,183,184,186}W) and one that has negligible abundance for present purposes (¹⁸⁰W). The open reaction channels available up to incident neutron energy of 60 MeV for the major isotopes are: ¹⁸²W (852), ¹⁸³W (852), ¹⁸⁴W (841), and ¹⁸⁶W (817). The total number of these reactions that produce helium was not determined explicitly for each of these isotopes, but it is readily evident from inspection of the Q-Tool output that the ratio to the total open reaction channels is substantial. In fact, it is concluded from an examination of the various elements considered in this study that the fraction of open reaction channels that emit helium, in particular alpha particles, increases with mass number. In any event, the number of helium producing reaction channels is limited to 4 for each considered tungsten isotope by the selected criteria for limitation, as discussed above. Thus, the reactions included in the pruned lists are given in Tables 2.6 – 2.9.

¹⁸²W

Table 2.26: Potentially significant helium producing reactions for ¹⁸²W up to 60 MeV

<u>Reaction Products</u>	<u>Q-value (MeV)</u>	<u>Threshold (MeV)</u>	<u>Total Particles</u>
¹⁷⁹ Hf + ⁴ He	7.87316	0	2
¹⁸⁰ Hf + ³ He	-5.31666	5.34614	2
¹⁷⁸ Hf + n + ⁴ He	1.77407	0	3
¹⁷⁹ Hf + n + ³ He	-12.70462	12.77505	3

^{183}W Table 2.27: Potentially significant helium producing reactions for ^{183}W up to 60 MeV

Reaction Products	Q-value (MeV)	Threshold (MeV)	Total Particles
$^{180}\text{Hf} + ^4\text{He}$	9.07038	0	2
$^{181}\text{Hf} + ^3\text{He}$	-5.81168	5.84373	2
$^{179}\text{Hf} + \text{n} + ^4\text{He}$	1.68242	0	3
$^{180}\text{Hf} + \text{n} + ^3\text{He}$	-11.5074	11.57084	3

 ^{184}W Table 2.28: Potentially significant helium producing reactions for ^{184}W up to 60 MeV

Reaction Products	Q-value (MeV)	Threshold (MeV)	Total Particles
$^{181}\text{Hf} + ^4\text{He}$	7.3543	0	2
$^{182}\text{Hf} + ^3\text{He}$	-6.50628	6.54196	2
$^{180}\text{Hf} + \text{n} + ^4\text{He}$	1.65858	0	3
$^{181}\text{Hf} + \text{n} + ^3\text{He}$	-13.22348	13.29599	3

 ^{186}W Table 2.29: Potentially significant helium producing reactions for ^{186}W up to 60 MeV

Reaction Products	Q-value (MeV)	Threshold (MeV)	Total Particles
$^{183}\text{Hf} + ^4\text{He}$	6.42071	0	2
$^{184}\text{Hf} + ^3\text{He}$	-7.87125	7.91395	2
$^{182}\text{Hf} + \text{n} + ^4\text{He}$	1.12344	0	3
$^{183}\text{Hf} + \text{n} + ^3\text{He}$	-14.15707	14.23386	3

3. CINDA Helium Producing Neutron Reaction Citations

3.1 The CINDA Index

CINDA, the Computer Index of Neutron Data, contains bibliographic references to measurements, calculations, reviews, and evaluations of neutron cross sections and other microscopic neutron data; it also includes index references to computer libraries of numerical neutron data available from four regional neutron data centers. The compilation of CINDA is the result of worldwide cooperation involving the following four data centers:

The USA National Nuclear Data Center at Brookhaven National Laboratory, USA.
The Russian Nuclear Data Center at the Fiziko-Energeticheskij Institut, Obninsk, Russia.
The NEA Data Bank at Paris, France.
The IAEA Nuclear Data Section, Vienna, Austria.

Although CINDA is probably the most complete index available for information on neutron induced reactions, it is far from complete. In particular, concerning helium producing reactions CINDA is limited to the following reaction processes (with indicated CINDA lookup codes):

(n, α) Reaction	(NA)
(n,n α) Reaction	(NNA)
(n, ³ He) Reaction	(NHE)
(n,He-emission) Reactions	(AEM)

The code AEM refers to total helium atom emission. It is used to denote measurements in which helium nuclei are detected without regard to their origin from a particular reaction channel. This list obviously fails to include many of the open and considered reaction channels mentioned in Section 2. Nevertheless, this selection is based on the fact that few if any data or related information (e.g., theoretical results from models) are published and documented. This list probably encompasses the most important sources of helium production up to 15 MeV and possibly to 20 MeV. Consequently, the discussion in this section is limited to these four processes, as available from CINDA.

CINDA can be accessed at the Internet sites for the four major data centers around the world. In the U.S., this is the National Nuclear Data Center (NNDC) at Brookhaven National Laboratory. The Internet address is <http://www.nndc.bnl.gov/nndc/cinda/>. This is an interactive site that allows the user to select the target isotope and reaction desired. It also allows for selection of the desired energy range, limitations on dates of the entries, laboratory, author(s), type of publication, and so on, in order to reduce the list of citations to the one especially desired by the user. In the present investigation, no such limitations were placed; all references pertaining to a particular isotope and reaction were retrieved. A typical retrieved ASCII file is shown in Table 3.1.

Table 3.1: CINDA retrieval for the $^{53}\text{Cr}(n,\alpha)$ reaction

National Nuclear Data Center

** CINDA Retrieval **
21-JAN-2004

Element	:	CR
Mass	:	53
Quantity	:	NA
Laboratory	:	
Publication Date	:	
Energy Range(eV)	:	
Publication Type	:	ALL
Work Type	:	ALL

CR-53:Quantity	Energy range	Lab	Reference/Comments
(n,alfa)	Fiss	CRC Eval	Rept CRC-1003 6012 Roy+,ESTIMATED AVG SIG=3.0MB
(n,alfa)	1.4+7	IIT Theo	Jour NP 60 49 6411 Gardner+PREDICTED BY EMPIRICAL FORM
(n,alfa)	Fiss	AE Theo	Prog EANDC(OR)-73 6801 Eriksson. STAT MOD CALC
(n,alfa)	5.9+6	NEU Expt	Jour HPA 45 439 7208 Foroughi+ UPPER LIMIT TO SIG GIVEN
	6.0+6	NEU Expt	Prog EANDC(OR)-90 6906 Foroughi+,COUNTER TELESCOP
	5.9+6	NEU Expt	Data EXFOR20832.014 7901 1PNT.D/DA
(n,alfa)	Tr 1.8+7	FEI Theo	Rept FEI-699 7600 Bychkov+ STATMOD ANAL,LVL DENS EFFCT
(n,alfa)	1.0+7 2.0+7	TRM Theo	Conf 76AHMEDA 2 13 7612 Garg. VERY BRIEF.CALC SIG AT 4ES GVN
(n,alfa)	5.0+5 2.0+7	TRM Eval	Prog INDC(SEC)-61 7710 Garg. P89,ABST. STATMOD EVAL,NDG.
(n,alfa)	4.0+6 1.5+7	KFK Eval	Rept KFK-2386 2 88 7703 Meyer.KEDAK3 RECOMMENDED CURVE
	4.0+6 1.5+7	KFK Eval	Rept KFK-2233 1 7512 Goel. GRAPH OF KEDAK DATA
	4.0+6 1.5+7	KFK Eval	Data KEDAK-3 7510 27 DATA SETS
(n,alfa)	2.3+6 2.0+7	GEL Comp	Conf 77GEEL 261 7712 Paulsen. GRPH.TBL. EXPTS CFD KEDAK
(n,alfa)	Fiss	FEI Eval	Rept YK- 3(30) 11 7800 Abagyan+ EVAL SIG(U235-SPEC) GIVEN
	4.0+6 7.0+7	FEI Eval	Rept YK- 3(30) 11 7800 Abagyan+ EVAL SIGS(E-GROUPS),TABLE
(n,alfa)	1.5+7	FEI Eval	Rept YK- 2(33) 51 7900 Bychkov+ COMPIL+RECOM SIG-DATA.TABLE
	1.4+7 1.5+7	FEI Eval	Rept INDC(CCP)-146 8007 .PG 104.ENGLISH OF YK-33(2) 51
(n,alfa)	Fiss	MUN Comp	Jour JRC 52 219 7901 Gryntakis., 4 VALUES GIVEN.
(n,alfa)	1.2+3 1.4+6	DUB Theo	Conf 80KIEV 3 306 8009 Gledenov+ CALC SIG AT 10 ES,TBL
(n,alfa)	Tr 2.0+7	TRM Eval	Prog BARC-1183 27 8200 Garg+ H-F+PRE-EQUIL EXCITON MDL.NDG
(n,alfa)	3.8+6 2.0+7	ORL Theo	Rept ORNL-TM-10381 8705 Shibata+ GRPH.STAT.MDL,DIR.INT.CALC.
(n,alfa)	1.7+6 2.0+7	FEI Eval	Jour YK 1990 3 53 9010 Zelenetskij+ 'BROND'LIBR.A-SPEC,NDG
(n,alfa)	2.0+6 2.0+7	IAE Revw	Conf 92TRIEST 775 9203 Konshin.LECTURE:MDLS CFD.GRPH SIG(E)

Notice that CINDA utilizes a number of codes to indicate the nature of the retrieved information, e.g., the laboratory, type of information, energy range, etc. Concerning the type of information, CINDA utilizes six categories: experimental data

(Expt), theoretical results from nuclear models (Theo), combination of experimental and theoretical results (ExTh), evaluations (Eval), compilations (Comp), and reviews (Revw).

3.2 CINDA citations for C, Si, Ti, V, Cr, Fe, Ni, and W

The information retrieved from CINDA for the present investigation is outlined in Tables 3.2 - 3.9 for isotopes of the elements C, Si, Ti, V, Cr, Fe, Ni, and W. What is shown in these tables are the number of entries in CINDA for each indicated isotope, reaction type, and information type, as well as an indication of the energy ranges that pertain to information provided in the files. For convenience, the energy ranges are color coded to enable the reader to discern from a quick glance the degree of coverage in energy of the reported works. There are many limitations to these tables that must be kept in mind in assessing the true amount and quality of available information. CINDA is non-discriminatory. Journal articles, conference proceedings, progress reports, etc., are listed together. Also, there is repetition. For example, the appearance of 98 entries labeled “Expt” does not necessarily suggest that 98 independent experiments have been performed. Often an individual work will be listed several times, e.g., when a report is prepared, a journal article is published, data are submitted to one of the centers, etc. One experiment may also report information for more than one type of reaction and thus be listed under several headings. This is particularly true for nuclear modeling studies. The appearance of a shaded block in the “Energy Range” field merely indicates that at least one report was documented pertinent to that energy range. In fact, the vast majority of reported data are in the 13 - 15 MeV range, greatly outweighing contributions corresponding to other energy ranges. Very little information exists above 20 MeV. Also, the relative coverage of the indicated energy ranges by experiment vs. theory cannot be deduced from these tables; only a detailed study of the retrieved files and subsequent referral to the mentioned works will reveal this detailed information.

Table 3.2: Information available in CINDA for carbon isotopes

C-12

<u>Reaction</u>	<u>Expt</u>	<u>ExTh</u>	<u>Theo</u>	<u>Eval</u>	<u>Comp</u>	<u>Revw</u>	<u>Total</u>	<u>Energy Range (MeV)</u>			
								<u><13</u>	<u>13-15</u>	<u>15-20</u>	<u>>20</u>
NA	98	1	13	18	7	9	146				
NHE	12	0	1	0	0	0	13				
NNA	78	2	4	14	2	2	102				
AEM	41	0	0	0	0	0	41				

C-13

<u>Reaction</u>	<u>Expt</u>	<u>ExTh</u>	<u>Theo</u>	<u>Eval</u>	<u>Comp</u>	<u>Revw</u>	<u>Total</u>	<u>Energy Range (MeV)</u>			
								<u><13</u>	<u>13-15</u>	<u>15-20</u>	<u>>20</u>
NA	2	0	1	2	2	0	7				
NHE	0	0	0	0	0	0	0				
NNA	0	0	0	0	0	0	0				
AEM	0	0	0	0	0	0	0				

It is evident from Table 3.2 that considerable information is available for ^{12}C , the dominant isotope of natural carbon. Most of this material consists of citations to experimental work, but nuclear modeling and evaluation studies have also been reported. Although the (n,α) reaction has been studied extensively at lower energies, no citations are given for work above 20 MeV. However, some results for helium emission are cited above 20 MeV. This could provide useful information for present purposes. Fewer results are cited for the minor isotope ^{13}C , but its abundance is quite low in natural carbon.

Table 3.3: Information available in CINDA for silicon isotopes

Si-28

Reaction	Expt	ExTh	Theo	Eval	Comp	Revw	Total	Energy Range (MeV)			
								<13	13-15	15-20	>20
NA	98	3	16	11	4	1	133				
NHE	4	0	3	1	0	0	8				
NNA	0	0	0	1	0	0	1				
AEM	7	0	1	0	0	0	8				

Si-29

Reaction	Expt	ExTh	Theo	Eval	Comp	Revw	Total	Energy Range (MeV)			
								<13	13-15	15-20	>20
NA	4	0	1	4	3	1	13				
NHE	0	0	0	0	0	0	0				
NNA	0	0	0	0	0	0	0				
AEM	0	0	0	0	0	0	0				

Si-30

Reaction	Expt	ExTh	Theo	Eval	Comp	Revw	Total	Energy Range (MeV)			
								<13	13-15	15-20	>20
NA	62	0	2	6	3	2	75				
NHE	0	0	0	0	0	0	0				
NNA	0	0	0	0	0	0	0				
AEM	0	0	0	0	0	0	0				

The helium-producing reactions for the dominant isotope ^{28}Si of natural silicon appear to have been studied extensively, although it is interesting to note once again the apparent absence of (n,α) results above 20 MeV. Much less is known about the minor isotopes ^{29}Si and ^{30}Si . The only reported results are for the (n,α) reaction. This may not be a limitation for present purposes since these two isotopes together account for < 8% of the total atoms found in natural silicon. Under these circumstances, estimates of the reaction cross sections from nuclear model calculations might well suffice to determine whether the contribution to helium production from these two isotopes is significant.

Table 3.4: Information available in CINDA for titanium isotopes

Ti-46

Reaction	Expt	ExTh	Theo	Eval	Comp	Revw	Total	Energy Range (MeV)			
								<13	13-15	15-20	>20
NA	0	0	12	1	1	1	15	█	█	█	
NHE	0	0	2	0	0	0	2		█		
NNA	0	0	0	0	0	0	0				
AEM	19	0	2	0	0	1	22		█		

Ti-47

Reaction	Expt	ExTh	Theo	Eval	Comp	Revw	Total	Energy Range (MeV)			
								<13	13-15	15-20	>20
NA	4	0	2	2	1	0	9	█	█		
NHE	0	0	0	0	0	0	0				
NNA	0	0	0	0	0	0	0				
AEM	4	0	0	0	0	0	4		█		

Ti-48

Reaction	Expt	ExTh	Theo	Eval	Comp	Revw	Total	Energy Range (MeV)			
								<13	13-15	15-20	>20
NA	19	1	21	4	2	5	52		█	█	█
NHE	0	0	0	0	0	0	0				
NNA	0	0	1	0	0	0	1			█	
AEM	19	0	2	0	0	1	22		█		

Ti-49

Reaction	Expt	ExTh	Theo	Eval	Comp	Revw	Total	Energy Range (MeV)			
								<13	13-15	15-20	>20
NA	0		1	1	1	0	3		█		
NHE	0	0	0	0	0	0	0				
NNA	0	0	0	0	0	0	0				
AEM	4	0	0	0	0	0	4		█		

Ti-50

Reaction	Expt	ExTh	Theo	Eval	Comp	Revw	Total	Energy Range (MeV)			
								<13	13-15	15-20	>20
NA	53	1	8	4	4	2	72	█	█	█	█
NHE	0	0	0	0	0	0	0				
NNA	0	0	0	0	0	0	0				
AEM							0		█		

Although some information is cited in CINDA for all the stable isotopes of titanium, it is rather surprising that the amount of information that has been produced is

relatively modest, even for the dominant isotope ^{48}Ti . In particular, the data available for energies above 20 MeV is quite limited. This would clearly hamper arriving at any conclusions about the relative helium production by neutrons corresponding to thick target sources such as $^7\text{Li}(d,n)$ which have been proposed for materials radiation testing purposes.

Table 3.5: Information available in CINDA for vanadium isotopes

V-51

<u>Reaction</u>	<u>Expt</u>	<u>ExTh</u>	<u>Theo</u>	<u>Eval</u>	<u>Comp</u>	<u>Revw</u>	<u>Total</u>	Energy Range (MeV)			
								<13	13-15	15-20	>20
NA	170	0	26	24	7	10	237				
NHE	11	0	2	2	0	0	15				
NNA	31	0	3	7	0	0	41				
AEM	21	4	3	1	1	1	31				
	<u>Expt</u>	<u>ExTh</u>	<u>Theo</u>	<u>Eval</u>	<u>Comp</u>	<u>Revw</u>	<u>Total</u>				
Sums	233	4	34	34	8	11	324				

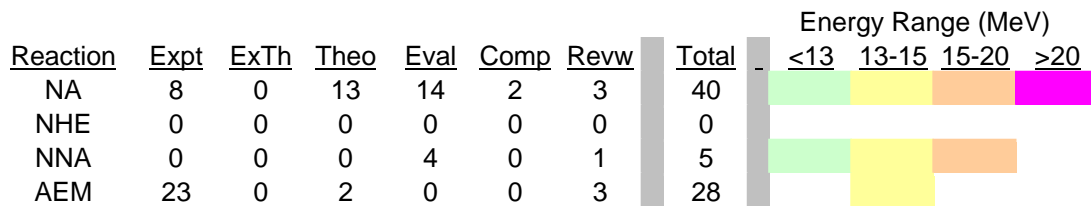
Considerable information is reported in CINDA for vanadium, an element that consists almost entirely of ^{51}V . Only a detailed examination of the reported results can determine whether this information is adequate for the purpose of estimating helium production in fusion energy applications. This issue will be examined in more detail in later sections of this report, not only for vanadium but for the other considered elements as well.

At this point it is worthwhile discussing the general issues of quality and reliability for the information retrieved from CINDA. The wide range of quality, reliability, and utility of the results reported in the literature is a well known issue in the nuclear data field. Discrepancies are commonplace, not only for experimental results but also for the information generated by nuclear modeling. Cross sections are never measured directly. They are derived from raw experimental data following the application of many corrections. Extensive auxiliary information related to properties of the neutron source, nature of the sample material, radiation detector characteristics, etc., have to be considered in generating reported cross sections. While older experiments are not necessarily of poorer quality than more recent ones, there is a tendency for more recent investigations to carry out more thorough determinations than the older works of auxiliary parameters (sample properties, neutron scattering, etc.) that must be incorporated in deriving cross sections. This point is particularly evident in the extensive body of 14-MeV data compiled from the literature. Discrepancies on the order of a factor of two are not uncommon, as is evident from plots of experimental results presented in later sections of this report. Furthermore, while experimental work offers many problems and challenges, so does theoretical work. The competition between the calculated cross sections for various energetically allowed reaction channels at a given incident neutron energy is very sensitively dependent upon the assumed model parameters, many of which

are poorly known. Furthermore, the models themselves are just approximations of the true, complex many-body interactions of which a nuclear reaction is comprised. Weak reaction channels with small cross sections can be severely influenced by assumptions concerning the strong channels, e.g., neutron elastic and inelastic scattering, and multiple neutron emission such as (n,2n), (n,3n), etc. It has been demonstrated in blind nuclear modeling inter-comparison studies that discrepancies of a factor of ten are not unusual for various independent predictions of cross sections for the weak reaction channels.

Table 3.6: Information available in CINDA for chromium isotopes

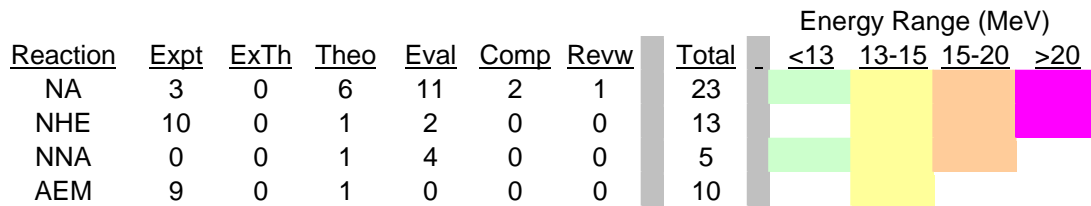
Cr-50



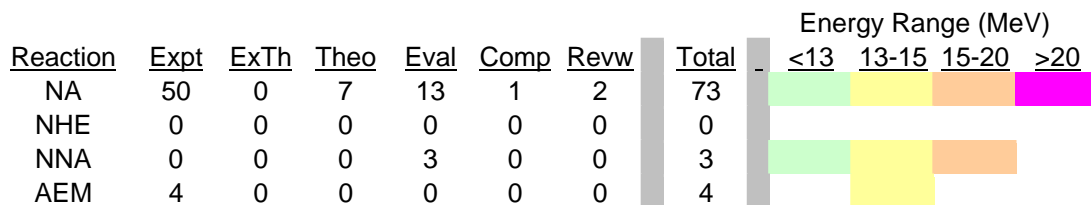
Cr-52



Cr-53



Cr-54



Substantial information is available on helium producing reactions for the various chromium isotopes. Nevertheless, it is surprising that no results have been reported for

the dominant isotope ^{52}Cr at energies above 20 MeV. This would clearly hamper arriving at any conclusions about the relative helium production by neutrons corresponding to thick target sources such as $^7\text{Li}(d,n)$ which have been proposed for materials radiation testing purposes.

Table 3.7: Information available in CINDA for iron isotopes

Fe-54

Reaction	Expt	ExTh	Theo	Eval	Comp	Revw	Total	Energy Range (MeV)			
								<13	13-15	15-20	>20
NA	128	3	34	28	6	13	212				
NHE	1	0	2	0	0	0	3				
NNA	3	1	2	3	0	0	9				
AEM	25	0	3	0	0	2	30				

Fe-56

Reaction	Expt	ExTh	Theo	Eval	Comp	Revw	Total	Energy Range (MeV)			
								<13	13-15	15-20	>20
NA	14	1	32	21	5	6	79				
NHE	1	0	0	0	0	0	1				
NNA	5	0	6	4	0	1	16				
AEM	35	0	14	2	0	4	55				

Fe-57

Reaction	Expt	ExTh	Theo	Eval	Comp	Revw	Total	Energy Range (MeV)			
								<13	13-15	15-20	>20
NA	6	0	6	9	1	1	23				
NHE	0	0	0	0	0	0	0				
NNA	0	0	1	2	0	0	3				
AEM	8	0	0	0	0	0	8				

As might be expected, studies of helium production in iron have been quite extensive. Iron is a dominant element in structural materials proposed for fusion energy systems. The dominant isotope is ^{56}Fe . The remaining isotopes account for < 10% of the atoms of natural iron. Because of the special importance of iron, careful inspection of the details of the available database is essential. Plots of the experimental data, nuclear model results, and evaluated information are provided in later sections of this report.

It should be evident to the reader that the approach of examining all individual helium producing reactions for each elements of interest for fusion is probably not the best method for estimating total helium production in materials, given contemporary limitations of experimental and theoretical physics. From an engineering point of view, a more realistic approach is probably to undertake experiments that will measure the total

helium production from the various materials of interest for those particular neutron spectra that are characteristic of fusion or materials testing environments.

Table 3.8: Information available in CINDA for nickel isotopes

Ni-58

Reaction	Expt	ExTh	Theo	Eval	Comp	Revw	Total	Energy Range (MeV)			
								<13	13-15	15-20	>20
NA	69	0	36	27	5	9	146				
NHE	1	0	0	0	0	0	1				
NNA	6	1	6	5	1	1	20				
AEM	46	0	5	2	0	4	57				

Ni-60

Reaction	Expt	ExTh	Theo	Eval	Comp	Revw	Total	Energy Range (MeV)			
								<13	13-15	15-20	>20
NA	11	1	18	19	3	3	55				
NHE	1	0	0	0	0	0	1				
NNA	1	0	1	3	0	1	6				
AEM	42	0	5	4	0	3	54				

Ni-61

Reaction	Expt	ExTh	Theo	Eval	Comp	Revw	Total	Energy Range (MeV)			
								<13	13-15	15-20	>20
NA	11	0	2	10	2	1	26				
NHE	0	0	0	0	0	0	0				
NNA	0	0	0	2	0	0	2				
AEM	9	0	0	0	0	0	9				

Ni-62

Reaction	Expt	ExTh	Theo	Eval	Comp	Revw	Total	Energy Range (MeV)			
								<13	13-15	15-20	>20
NA	55	1	9	18	3	8	94				
NHE	0	0	0	0	0	0	0				
NNA	0	0	1	1	0	0	2				
AEM	8	0	1	0	0	0	9				

The body of information on helium producing reactions for nickel exceeds that for iron. Both ^{58}Ni and ^{60}Ni , the two major isotopes of natural nickel, are well represented and reasonably extensive information is available even for the minor isotopes ^{61}Ni and ^{62}Ni . Nickel is not regarded as a particularly favorable structural material for fusion applications because of its tendency to activate under neutron bombardment. The $^{58}\text{Ni}(n,p)$ reaction yields 70.88-day ^{58}Co and the $^{58}\text{Ni}(n,\gamma)$ reaction produces 76,000-year ^{59}Ni . The former reaction can be problematic for fusion reactor maintenance

considerations whereas the latter reaction is potentially a problem for waste disposal at the end of the fusion reactor life cycle. While neither of these reactions involves the production of helium, at least not directly, both must nevertheless be considered when assessing the relative merits of various materials to be used in fusion environments.

Table 3.9: Information available in CINDA for tungsten isotopes

W-182

<u>Reaction</u>	<u>Expt</u>	<u>ExTh</u>	<u>Theo</u>	<u>Eval</u>	<u>Comp</u>	<u>Revw</u>	<u>Total</u>	<u>Energy Range (MeV)</u>			
								<u><13</u>	<u>13-15</u>	<u>15-20</u>	<u>>20</u>
NA	2	0	0	2	2	1	7	█	█	█	
NHE	0	0	0	0	0	0	0				
NNA	14	0	1	3	2	1	21		█	█	
AEM	5	0	0	0	0	0	5		█		

W-183

<u>Reaction</u>	<u>Expt</u>	<u>ExTh</u>	<u>Theo</u>	<u>Eval</u>	<u>Comp</u>	<u>Revw</u>	<u>Total</u>	<u>Energy Range (MeV)</u>			
								<u><13</u>	<u>13-15</u>	<u>15-20</u>	<u>>20</u>
NA	2	0	0	2	1	1	6		█		
NHE	0	0	0	0	0	0	0				
NNA	0	0	0	0	0	0	0				
AEM	5	0	0	0	0	0	5		█		

W-184

<u>Reaction</u>	<u>Expt</u>	<u>ExTh</u>	<u>Theo</u>	<u>Eval</u>	<u>Comp</u>	<u>Revw</u>	<u>Total</u>	<u>Energy Range (MeV)</u>			
								<u><13</u>	<u>13-15</u>	<u>15-20</u>	<u>>20</u>
NA	11	0	0	5	1	1	18	█	█	█	
NHE	0	0	0	0	0	0	0				
NNA	0	0	0	0	0	0	0				
AEM	1	0	0	0	0	0	1		█		

W-186

<u>Reaction</u>	<u>Expt</u>	<u>ExTh</u>	<u>Theo</u>	<u>Eval</u>	<u>Comp</u>	<u>Revw</u>	<u>Total</u>	<u>Energy Range (MeV)</u>			
								<u><13</u>	<u>13-15</u>	<u>15-20</u>	<u>>20</u>
NA	20	0	1	6	2	1	30	█	█	█	
NHE	2	0	0	0	0	0	2	█	█	█	█
NNA	0	0	0	0	0	0	0				
AEM	5	0	0	0	0	0	5		█		

The helium producing reactions on tungsten are expected to have relatively small cross sections due to the previously mentioned Coulomb barrier effect. Nevertheless, some information is available and it has been indexed in CINDA, as indicated above.

An overview of the database indexed by CINDA is given in Table 3.10 and visually in Fig. 3.1. The table and figure summarize the total citations for each element, without regard to particular isotopes, but they do give a breakout by information type. It is seen that for the four processes considered, (n, α), (n, ^3He), (n,n α), and (n,He-emission), there are nearly 2400 citations for the eight elements included in the present study.

Table 3.10:

Element	Expt	ExTh	Theo	Eval	Comp	Revw	Total
C	231	3	19	34	11	11	309
Si	175	3	23	23	10	4	238
Ti	122	2	51	12	9	10	206
V	233	4	34	34	8	11	324
Cr	127	1	63	72	7	17	287
Fe	226	5	100	69	12	27	439
Ni	260	3	84	91	14	30	482
W	67	0	2	18	8	5	100
Sums	1441	21	376	353	79	115	2385

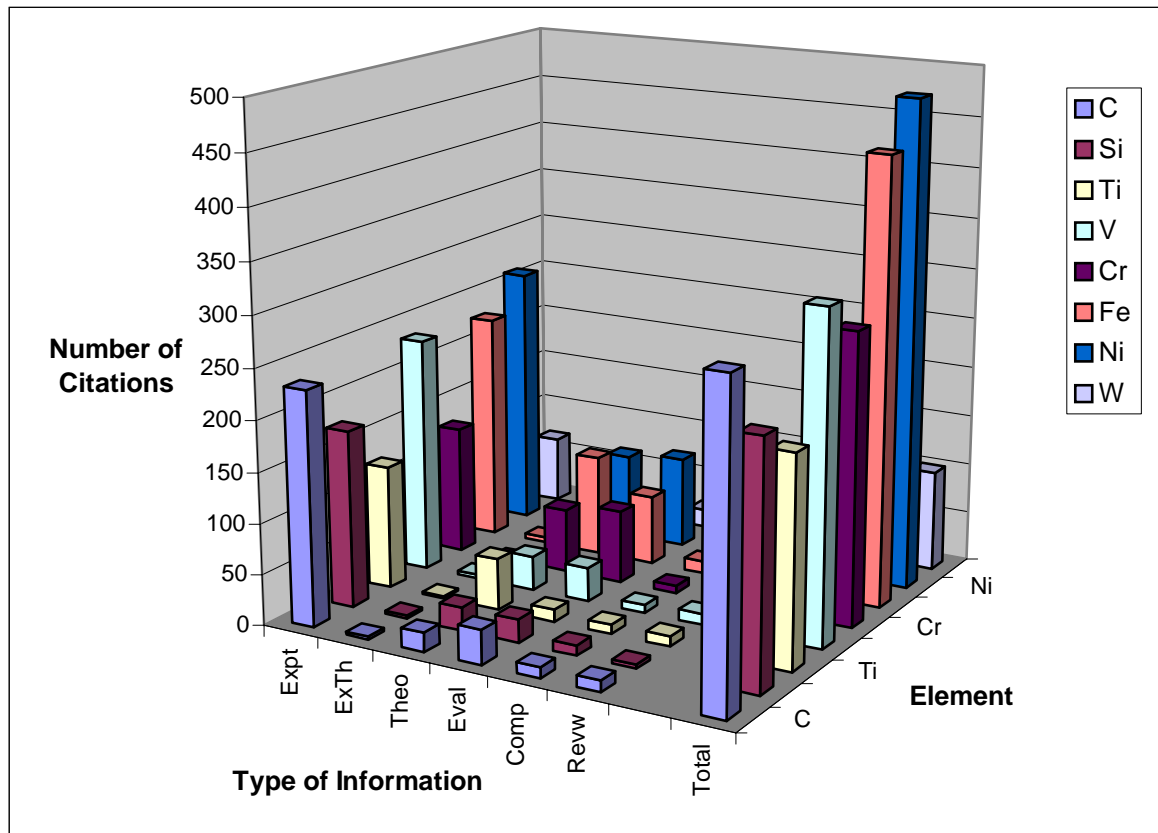


Figure 3.1: Summary of CINDA citations for helium production

One observes at a glance that most of the citations in CINDA refer to experimental work. Most of the remaining citations involve nuclear modeling studies or data evaluations with just a few compilations and reviews. This is a reasonable mix of information considering that modeling that is not guided by experimental data is rather unreliable, and a few compilations and reviews are all that the applied nuclear community requires since all such studies must inevitably refer to a common contemporary database of numerical results. However, a very troubling aspect of all this is that a plethora of measurements and modeling results often generates more confusion than enlightenment due to the presence of unresolved discrepancies.

4. CSISRS Helium Producing Neutron Reaction Experimental Data

4.1 CSISRS Retrieval of EXFOR Data Files

A large body of experimental nuclear reaction data has been archived by the worldwide Nuclear Reaction Data Center network coordinated by the IAEA Nuclear Data Section (<http://www-nds.iaea.org/>). These data are compiled and exchanged between the regional data centers so that each center can provide access to the same database within its service area. The 80-column ASCII format used in archiving these nuclear data is called EXFOR (Exchange Format). A sample retrieved data file appears in Table 4.1.

Table 4.1: Sample EXFOR data file

```

REQUEST      3377001   20040214           5           0  0  0
ENTRY        20739           840201           20739000  1
SUBENT       20739001      840201           20739001  1
BIB          15           26           20739001  2
INSTITUTE    (2GERKFK)           20739001  3
REFERENCE    (J,RCA,10,15,68)       20739001  4
AUTHOR       (H.BRAUN,L.NAGY)       20739001  5
TITLE        -FISSION SPECTRUM AVERAGE CROSS SECTIONS FOR THE
              (N,P)-,(N,A)- AND (N,2N)-REACTIONS OF CO-59, NI-58,
              FE-54 AND Y-89.- (IN GERMAN). 20739001  6
INC-SOURCE   (REAC ) FR-2 REACTOR IN KARLSRUHE. 20739001  9
INC-SPECT    .FAST REACTOR NEUTRON FLUX. 20739001 10
SAMPLE       .Y(2)O(3) , NI-58 (99.89 PER CENT ENRICHED),FE-54
              (71.8 PER CENT ENRICHED). 20739001 12
METHOD       (ACTIV) ACTIVATION AND CHEMICAL SEPARATION. 20739001 13
DETECTOR     (NAICR) NAI(TL)-DETECTOR. 20739001 14
              (PROPC) 4PI-BETA PROPORTIONAL COUNTER FOR THE SR-89
              20739001 15
ACTIVITY     . 20739001 16
ANALYSIS     .IRRADIATION WITH CADMIUM FILTER. 20739001 17
              .CHEMICAL SEPARATIONS BY CATION EXCHANGE. 20739001 18
MONITOR      .NI-FOILS AS FAST NEUTRON FLUX MONITOR. 20739001 19
CORRECTION   .THE FAST NEUTRON SPECTRUM HAS IN GOOD PRECISION
              A SIMILAR CONTRIBUTION AS THE FISSON SPECTRUM. 20739001 21
ERR-ANALYS  .FOR THE NEUTRON FLUX 10 PER CENT ERRORS. 20739001 22
              .FOR THE ACTIVITY MEASUREMENTS. 20739001 23
              .0.5 PER CENT ERROR FOR THE UNCERTAINTY IN THE WIGHT. 20739001 24
              .THE GIVEN ERROR IS THE ABSOLUTE ERROR. 20739001 25
STATUS       .TAKEN FROM RADIOCHIMICA ACTA 10(1968)15. 20739001 26
HISTORY      (770419C) 20739001 27
              (780307E) 20739001 28
ENDBIB      26           20739001 29
COMMON      1           3           20739001 30
EN-DUMMY    20739001      840201           20739001 31
MEV         1.5000E+00           20739001 32
              20739001 33
ENDCOMMON   1           3           20739001 34
ENDSUBENT   1           2073900199999
SUBENT      20739008      840201           20739008  1
BIB         1           1           20739008  2
REACTION    (28-NI-58(N,A)26-FE-55,,SIG,,FIS) 20739008  3
ENDBIB      1           20739008  4
NOCOMMON    0           0           20739008  5
DATA        2           1           20739008  6
DATA        DATA-ERR 20739008  7
MB          PER-CENT 20739008  8
              2.9500E+00 3.2000E+01 20739008  9
ENDDATA     3           20739008 10
ENDSUBENT   2           2073900899999
ENDENTRY    2           2073999999999
ENDREQUEST  1           Z999999999999

```

A useful description of the U.S. EXFOR data retrieval procedure is provided in an EXFOR Help file that can be found by clicking on the CSISRS link at the Home page of

the Brookhaven National Laboratory National Nuclear Data Center (NNDC) Website (<http://www.nndc.bnl.gov>). The following material is reproduced verbatim from that file:

“The EXFOR retrieval page gives you access to the EXFOR experimental nuclear reaction data library (in USA usually called CSISRS). This data base contains data compiled as the result of the cooperative efforts of the world-wide Nuclear Reaction Data Center network which is coordinated by the IAEA Nuclear Data Section.

The neutron data part of EXFOR is relatively complete due to the long history of neutron data compilation activities of the four neutron data centers. In particular, the data for incident neutrons below 20 MeV energy are assumed to be complete. The charged particle and photonuclear data contained in this library are not so comprehensive because of the much smaller and more intermittent support given to the compilation of such data.

All data are compiled by the publication in which the data appears and each publication gets a unique entry or accession number. Desired data may be selected by this accession number. The compiled neutron data are indexed in the neutron data bibliography, CINDA, where these accession numbers are associated with the publications describing the data. For non-neutron data no such index presently exists.

Alternatively, the user may specify a reaction (or a desired residual nucleus and projectile) and the program will generate a list of data sets which satisfy the retrieval criteria. The user may then select to see and/or save all or some of those data sets, either in original EXFOR format or in a computational format which is more suitable if the data are to be processed by the user's own programs.”

The present focus is entirely on integrated, mono-energetic, microscopic cross section data, denoted by the code CS in the EXFOR System. A number of other codes required to utilize the retrieval procedures are also conveniently defined in the above-mentioned EXFOR Help file. Furthermore, there is an EXFOR manual that is available on-line.

4.2 Experimental Neutron Data for Helium Production in C, Si, Ti, V, Cr, Fe, Ni, and W

The CSISRS data retrieval utility at the NNDC Website has been used in the present investigation to survey the status of neutron-induced helium production experimental cross-section data. Results from this survey are summarized in Table 4.2.

Table 4.2: Summary of experimental information retrieved from the EXFOR System

Carbon-12

<u>Reaction</u>	<u># Listed Data Files</u>	<u>BNL-325 Plot</u>	<u>Figure</u>
(N,N+2A)	12 (7)	Yes	Fig. 1
(N,A)	6 (3)	Yes	Fig. 2
(N,A+N)	1	None	

Carbon-13

<u>Reaction</u>	<u># Listed Data Files</u>	<u>BNL-325 Plot</u>	<u>Figure</u>
(N,P+A)	1 (0)	None	
(N,A)	5 (4)	Yes	Fig. 3

No He-4 or He-3 emission cross-section data are available

Silicon-28

<u>Reaction</u>	<u># Listed Data Files</u>	<u>BNL-325 Plot</u>	<u>Figure</u>
(N,P+A)	1 (0)	None	
(N,A)	5 (4)	Yes	Fig. 3

Silicon-29

<u>Reaction</u>	<u># Listed Data Files</u>	<u>BNL-325 Plot</u>	<u>Figure</u>
(N,A)	3 (2)	Yes	Fig. 4

Silicon-30

<u>Reaction</u>	<u># Listed Data Files</u>	<u>BNL-325 Plot</u>	<u>Figure</u>
(N,A)	23 (19)	Yes	Fig. 5

Titanium-46

<u>Reaction</u>	<u># Listed Data Files</u>	<u>BNL-325 Plot</u>	<u>Figure</u>
(N,P+A)	1 (0)	None	
(N,A)	5 (4)	Yes	Fig. 3

No He-4 or He-3 emission cross-section data are available

Titanium-47

<u>Reaction</u>	<u># Listed Data Files</u>	<u>BNL-325 Plot</u>	<u>Figure</u>
(N,P+A)	1 (0)	None	
(N,A)	5 (4)	Yes	Fig. 3

No He-4 or He-3 emission cross-section data are available

Titanium-48

<u>Reaction</u>	<u># Listed Data Files</u>	<u>BNL-325 Plot</u>	<u>Figure</u>
(N,A)	5 (5)	Yes	Fig. 6

Titanium-49

<u>Reaction</u>	<u># Listed Data Files</u>	<u>BNL-325 Plot</u>	<u>Figure</u>
(N,P+A)	1 (0)	None	
(N,A)	5 (4)	Yes	Fig. 3

No He-4 or He-3 emission cross-section data are available

Titanium-50

<u>Reaction</u>	<u># Listed Data Files</u>	<u>BNL-325 Plot</u>	<u>Figure</u>
(N,A)	17 (16)	Yes	Fig. 7

Vanadium-51

<u>Reaction</u>	<u># Listed Data Files</u>	<u>BNL-325 Plot</u>	<u>Figure</u>
(N,N+A)	13 (11)	Yes	Fig.8
(N,He-3)	3	None	

(N,A)	56 (40)	Yes	Fig. 9
-------	---------	-----	--------

Chromium-50

<u>Reaction</u>	<u># Listed Data Files</u>	<u>BNL-325 Plot</u>	<u>Figure</u>
(N,A)	1	None	

Chromium-52

<u>Reaction</u>	<u># Listed Data Files</u>	<u>BNL-325 Plot</u>	<u>Figure</u>
(N,N+A)	1	None	

Chromium-53

<u>Reaction</u>	<u># Listed Data Files</u>	<u>BNL-325 Plot</u>	<u>Figure</u>
(N,He-3)	3	None	

Chromium-54

<u>Reaction</u>	<u># Listed Data Files</u>	<u>BNL-325 Plot</u>	<u>Figure</u>
(N,A)	16 (15)	Yes	Fig. 10

Iron-54

<u>Reaction</u>	<u># Listed Data Files</u>	<u>BNL-325 Plot</u>	<u>Figure</u>
(N,A)	39 (25)	Yes	Fig. 11

Iron-56

<u>Reaction</u>	<u># Listed Data Files</u>	<u>BNL-325 Plot</u>	<u>Figure</u>
(N,N+A)	1	None	
(N,A)	1	None	

Iron-57

<u>Reaction</u>	<u># Listed Data Files</u>	<u>BNL-325 Plot</u>	<u>Figure</u>
-----------------	----------------------------	---------------------	---------------

No He-4 or He-3 emission cross-section data are available

Nickel-58

<u>Reaction</u>	<u># Listed Data Files</u>	<u>BNL-325 Plot</u>	<u>Figure</u>
(N,N+A)	3	None	
(N,P+A)	1 (1)	Yes	Fig. 12
(N,A)	19 (12)	Yes	Fig. 13
(N,A+N)	2	None	

Nickel-60

<u>Reaction</u>	<u># Listed Data Files</u>	<u>BNL-325 Plot</u>	<u>Figure</u>
-----------------	----------------------------	---------------------	---------------

No He-4 or He-3 emission cross-section data are available

Nickel-61

<u>Reaction</u>	<u># Listed Data Files</u>	<u>BNL-325 Plot</u>	<u>Figure</u>
(N,A)	4	None	

Nickel-62

<u>Reaction</u>	<u># Listed Data Files</u>	<u>BNL-325 Plot</u>	<u>Figure</u>
(N,A)	19 (14)	Yes	Fig. 14

Tungsten-182

<u>Reaction</u>	<u># Listed Data Files</u>	<u>BNL-325 Plot</u>	<u>Figure</u>
(N,N+A)	4 (4)	Yes	Fig. 15
(N,A)	1	None	

Tungsten-183

<u>Reaction</u>	<u># Listed Data Files</u>	<u>BNL-325 Plot</u>	<u>Figure</u>
(N,A)	1	None	

Tungsten-184

<u>Reaction</u>	<u># Listed Data Files</u>	<u>BNL-325 Plot</u>	<u>Figure</u>
(N,A)	5 (4)	Yes	Fig. 16

Tungsten-186

<u>Reaction</u>	<u># Listed Data Files</u>	<u>BNL-325 Plot</u>	<u>Figure</u>
(N,A)	7 (7)	Yes	Fig. 17

This table requires some explanation. First, only those isotopes whose natural abundance is significant, as defined in Section 2, are included in this table. In the column “Reaction” for each portion of the table there appear various reaction codes, such as (N,A), (N,N+A), etc. Here, “A” means an alpha particle (^4He nucleus) and “N” means neutron. The number of these codes listed varies for each isotope, and in some cases there are no entries at all. These listed codes define the totality of archived neutron cross-section data (as described above) available for retrieval from the EXFOR System for the indicated target isotope. The column “# Listed Date Files” indicates the number of “hits” generated by the data retrieval software. Not all of these “hits” correspond to files that actually contain cross-section data of the indicated type. Furthermore, a search on “(N,A)” may also retrieve data in which contributions from both (N,A) and (N,N+A) appear. Consequently, a second number (usually smaller) frequently appears in parentheses in Table 4.2. This number indicates the actual number of “hits” that correspond uniquely to the reaction type specified. In cases where data are available for plotting, the actual number of plotted data sets may be smaller still since not all of the “hits” scored by the retrieval software correspond to files that contain numerical data.

The NNDC retrieval procedures include a data plotting routine. One can generate plots interactively in what is referred to as the “BNL-325” format. However, some of the

available data cannot be plotted using the NNDC software. An example would be if only a single cross section at a single energy exists in a particular file. Graphical output is available in either PostScript or GIF (Graphics Interchange Format), and for the latter a choice of three plot sizes (small, medium, or large) is provided. The resolution (clarity) of these BNL-325 plots is rather limited, but they have the advantage that the files do not require much computer storage space and the GIF format can be imported readily into EXCEL or Microsoft Word documents (as has been done in the preparation of the present report). These plots offer the reader a qualitative overview of the quantity and quality of the available data for neutron induced helium producing reactions. In some cases, one or more evaluations can also be imported into the plot to provide “eye guide(s)” to the data. For the present report, only ENDF/B-VI was selected for plotting whenever it was found to be available. Otherwise, either no evaluation was available or another available sole evaluation was used for the eye guide. The existence of a plot is indicated in Table 4.2 by “Yes”. Furthermore, the cell is shaded in light green to indicate visually that a plot is available. The corresponding figure number is also indicated in Table 4.2.

Altogether, 17 plots were generated and downloaded from the NNDC Website for inclusion in the present report. These appear as Figs. 4.1 - 4.17. Since the target isotope, reaction type, and evaluation (if present) are rather difficult to decipher in these small survey plots, this information is included in the figure captions to aid the reader in interpreting the information provided by the plot.

It is rather remarkable that the quantity of available information to plot should be as small as it is considering the large number of reactions that can generate helium, as discussed in Section 2, and the considerable number of citations to experimental work given in CINDA (Section 3)! Furthermore, a review of these plots shows that only in a few cases are the data sufficient to adequately define the shape and magnitude of the cross section excitation function over a reasonable energy range. Serious discrepancies are evident in the vicinity of 14 MeV. Finally, there is a paucity of information available above 20 MeV. It should be stressed here that many of the citations to experimental work mentioned in CINDA do not actually refer to compiled data files. Progress reports, abstracts, and other mentions of preliminary work are included and these generally do not present numerical values.

Why should the available experimental data be so limited after decades of laboratory work at accelerator facilities around the world? The answer to this important question lies in understanding the nature and limitations of experimental work in this field. To review the details in their entirety would occupy a large volume. However, to impress upon the reader that experimentalists are not lazy, incompetent individuals, an attempt will be made here to review the key issues and problem areas involved in measuring cross sections for helium producing reactions.

- Samples: There are many limitations associated with making samples that can be used to measure accurate cross sections. These have to do with chemistry, physical properties, isotopic abundance, impurities, cost, etc. Sample related

limitations are among the most important factors to consider in determining whether accurate cross sections can be measured.

- Neutron sources: Mono-energetic or nearly mono-energetic neutron fields can be provided in only a very limited number of situations. These are mostly at lower energies, and they are produced by bombardment of specific materials such as lithium, deuterium, and tritium with charged particles. It is virtually impossible to obtain mono-energetic sources of higher energy neutrons (above 20 MeV).
- Isotopic interference: The $(n, n\alpha)$ reaction on ^{61}Ni yields the same reaction product as the (n, α) reaction on ^{60}Ni , for example. So, distinguishing between these two reactions is very difficult unless isotopically pure samples of nickel are available (virtually impossible in many instances) or, at the very least, several samples with varying but well-known isotopic compositions are available to help sort out the effects of these two reactions. This phenomenon is observed in reaction studies for many other elements as well.
- Unique signature of a reaction: In order to insure that the experimenter is observing a specific reaction, free from interference due to other background reactions, there needs to be a unique signature that identifies the reaction. Such signatures do exist in some cases, but not in as many situations as might be desired. Neutron induced helium producing reactions that produce a radioactive residual nucleus are generally the easiest to measure accurately. The decays of the byproduct nuclei generally involve unique radioactive decay signatures, e.g., emission of well defined gamma rays following de-excitation of excited levels of a daughter nucleus formed by radioactive decay of the product nucleus. This is a complicated business that demands a great deal of ingenuity on the part of experimenters, some cooperation from Nature, and accurate quantitative knowledge of the decay properties of many radioactive nuclei. Unfortunately, Nature is not as helpful as one might hope in the case of helium producing reactions. For example, consider the (n, α) reactions for the isotopes listed in Section 2. These reactions generally figure as the most prominent ones in helium production for these materials, at least for energies below 20 MeV. As one can see from Table 4.3, many of the reaction byproducts are stable or, in a few cases, so long-lived that they might as well be stable. In such cases, the only signature of the reaction is the emitted α particles. They are difficult to measure because they are so easily absorbed in materials, thus necessitating the use of very thin samples and specially designed detectors. Even so, many of the lowest energy particles never escape the sample or yield signals that lie below the noise and background levels of the particle detectors used in such measurements. Finally, these particles are generally anisotropically emitted with respect to the incident neutron beam. Angle-integrated cross sections are then quite hard to measure.
- Detector limitations: Following many decades of nuclear radiation detector development, experimentalists are still faced with serious limitations. For example, very low energy radiations are difficult to measure accurately due to the

effects of detector noise and various background radiations. Limitations in detector efficiency make it difficult to measure very small cross sections. Accurate detector calibration remains as much an art as a science.

- Various additional experimental perturbations: There are so many experimental perturbations that influence the relationship between what is sought and what is actually measured that it would be impossible to be comprehensive here. Among the most critical are background neutron effects, sample absorption effects, contaminants, electronic instabilities, and so on. Skilled experimentalists develop procedures for dealing with many of these effects within the context their particular laboratories. Nevertheless, serious systematic differences between the results measured at various laboratories are evident in most compiled data files. These factors limit the accuracy that can be anticipated from experimental work.

This brief discussion is intended to encourage the reader to be more appreciative of the problems faced by experimentalists, and thus to understand why there are shortcomings in the experimental database. For the foreseeable future, one should not expect experimental work to resolve all the uncertainties and data deficiencies associated with individual reactions leading to the production of helium by fast neutrons. In a later section of this report, it is explained why there exists considerable hope that an experimental engineering approach could lead to the acquisition of information that would satisfy the needs of the fusion research community for helium production data.

Table 4.3: Properties of (n, α) reactions for major C, Si, Ti, V, Cr, Fe, Ni, and W isotopes

Element	Symbol	Z	A	Abundance*	(N,A) Reaction Product	Half Life*	Decay Mode
Carbon	C	6	12	98.890%	Be-9	Stable	beta-
			13	1.110%	Be-10	1.51E6 y	
Silicon	Si	14	28	92.230%	Mg-25	Stable	beta-/gamma
			29	4.683%	Mg-26	Stable	
			30	3.087%	Mg-27	9.458 m	
Titanium	Ti	22	46	8.250%	Ca-43	Stable	beta-/No gamma** 2*beta- beta-/gamma
			47	7.440%	Ca-44	Stable	
			48	73.720%	Ca-45	162.61 d	
			49	5.410%	Ca-46	>0.28E16 y	
			50	5.180%	Ca-47	4.536 d	
Vanadium	V	23	50	0.250%			
Chromium	Cr	24	51	99.750%	Sc-48	43.67 h	beta-/gamma
			52	83.789%	Ti-49	Stable	
Iron	Fe	26	53	9.501%	Ti-50	Stable	beta-/gamma EC/gamma
			54	2.365%	Ti-51	5.76 m	
			54	5.845%	Cr-51	27.7025 d	
			56	91.754%	Cr-53	Stable	
			57	2.119%	Cr-54	Stable	
			58	0.282%			

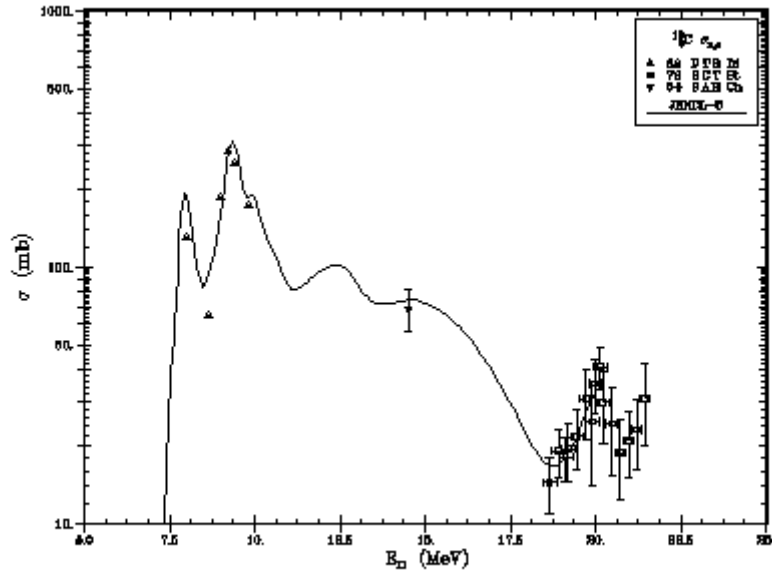


Fig 4.2: $^{12}\text{C}(n,\alpha)$ cross section data with JENDL-3 evaluation shown

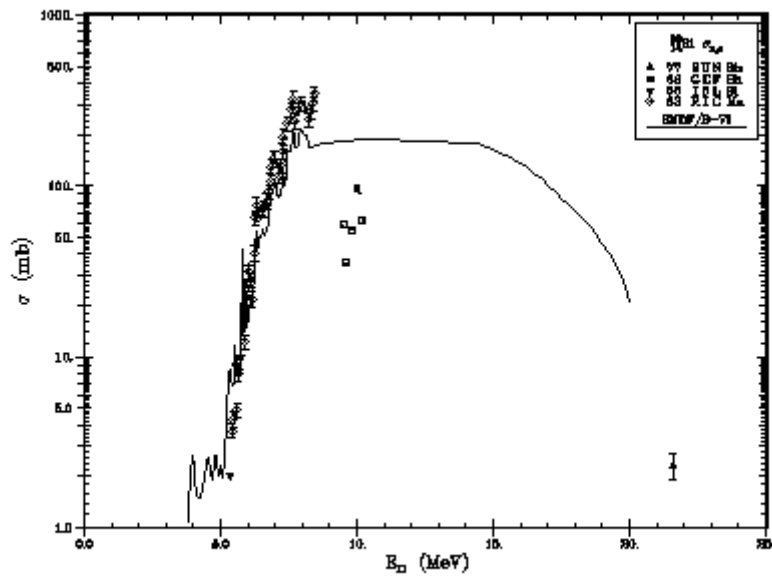


Fig 4.3: $^{28}\text{Si}(n,\alpha)$ cross section data with ENDF/B-VI evaluation shown

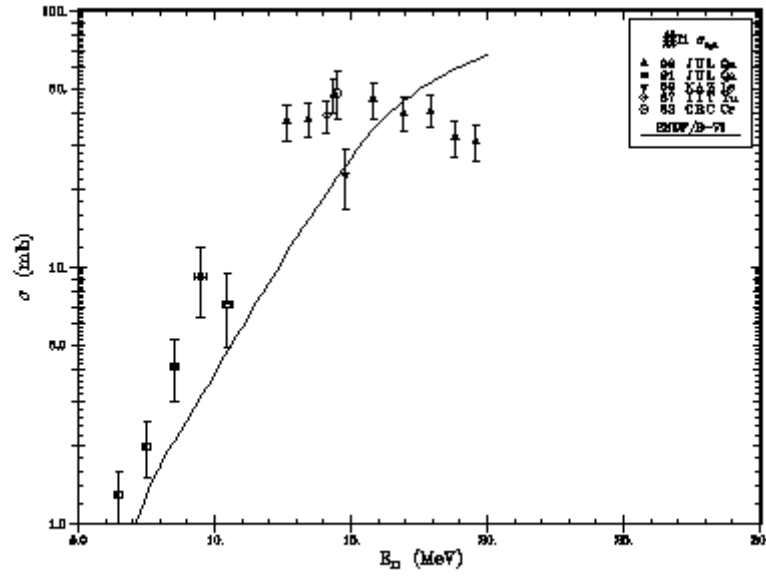


Fig. 4.6: $^{48}\text{Ti}(n,\alpha)$ cross section data with ENDF/B-VI evaluation shown

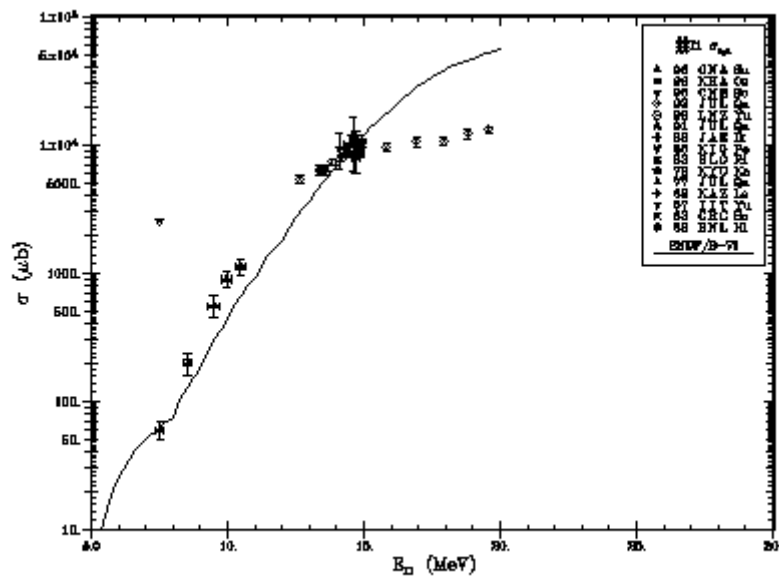


Fig. 4.7: $^{50}\text{Ti}(n,\alpha)$ cross section data with ENDF/B-VI evaluation shown

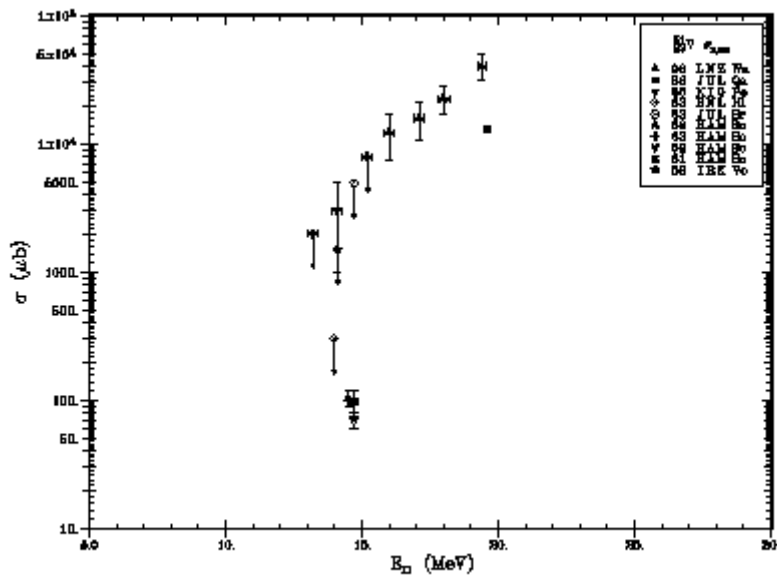


Fig. 4.8: $^{51}\text{V}(n,\alpha)$ cross section data with no evaluation shown

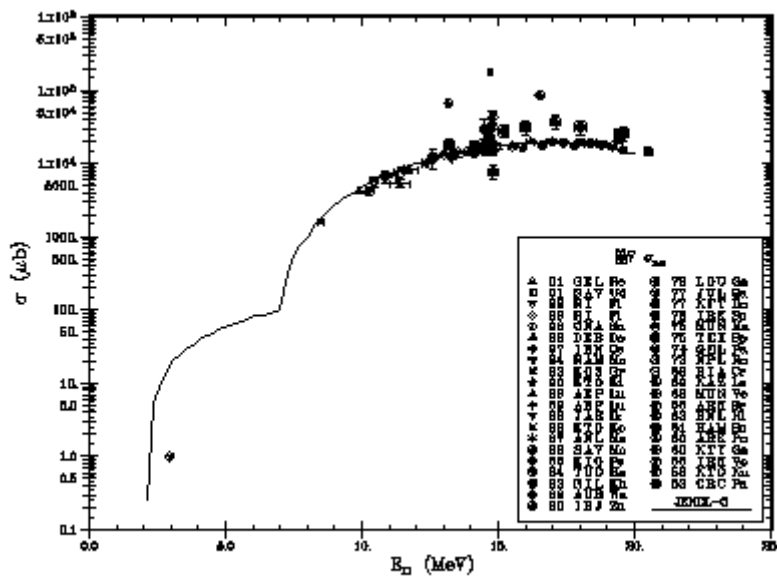


Fig. 4.9: $^{51}\text{V}(n,\alpha)$ cross section data with ENDF/B-VI evaluation shown

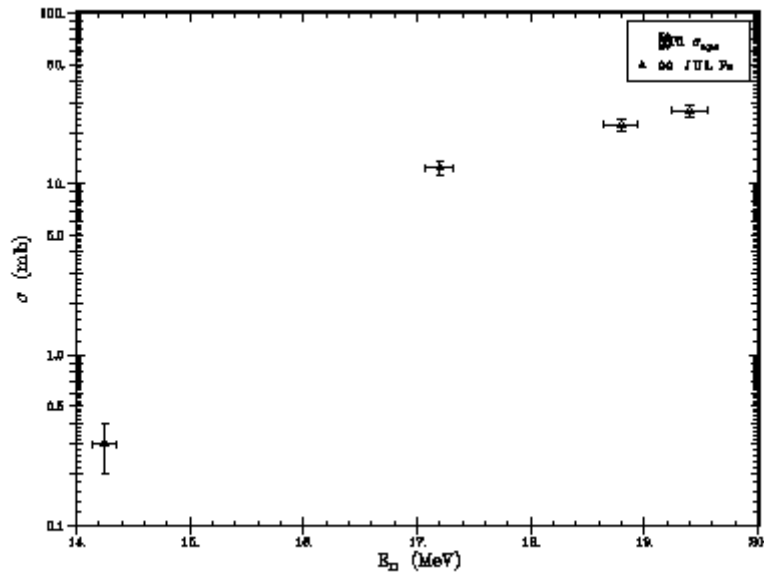


Fig. 4.12: $^{58}\text{Ni}(n,\alpha)$ cross section data with no evaluation shown

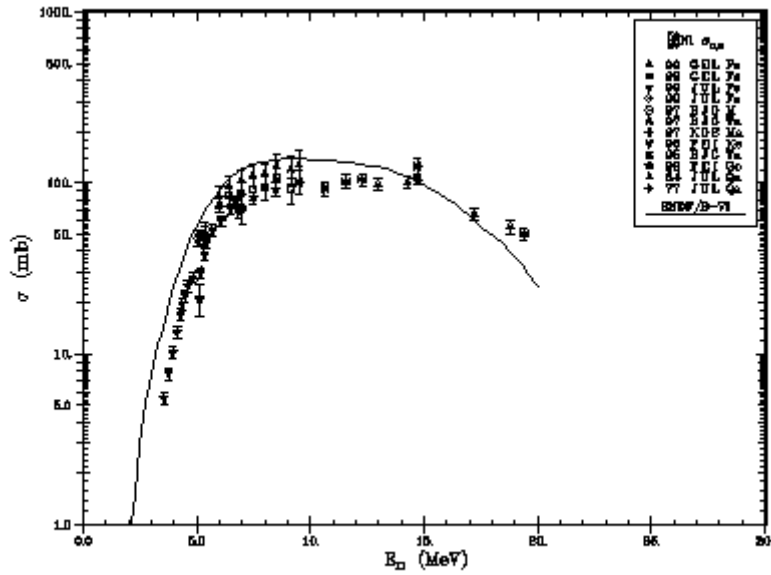


Fig. 4.13: $^{58}\text{Ni}(n,\alpha)$ cross section data with ENDF/B-VI evaluation shown

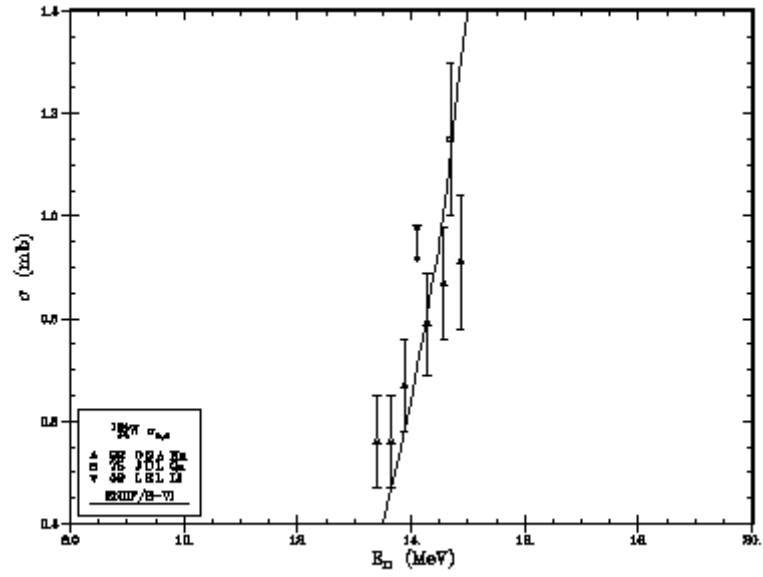


Fig. 4.16: $^{184}\text{W}(n,\alpha)$ cross section data with ENDF/B-VI evaluation shown

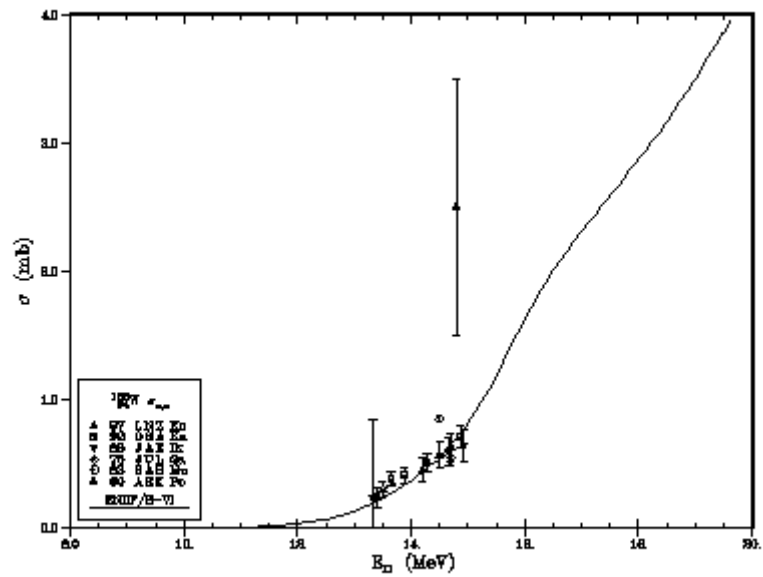


Fig. 4.17: $^{186}\text{W}(n,\alpha)$ cross section data with ENDF/B-VI evaluation shown

4.3 Comments on specific helium producing reactions

The following comments are based solely on the information shown in Figs. 4.1 – 4.17, as retrieved from the EXFOR System.

$^{12}\text{C}(n,n\alpha)$:

Experimental data are available from about 12 - 21 MeV, but the discrepancies are evidently of the order of 50% in the vicinity of 14 MeV for this reaction. Furthermore, there are no data near threshold or at higher energies. The peak cross section appears to be around 0.45 barn near 17 MeV.

$^{12}\text{C}(n,\alpha)$:

The JENDL-3 evaluation for this reaction appears to be based on nuclear model calculations that are guided by the sparse cross section data available in the vicinity of 18 - 20 MeV and at a few scattered lower energies. Only a single experimental point is available near 14 MeV. It is estimated that the uncertainty in this cross section is around 30% near 14 MeV and even larger at other energies above and below this point, based on the data retrieved from the EXFOR System. The peak cross section appears to be about 300 millibarn at around 9 MeV.

$^{28}\text{Si}(n,\alpha)$:

The cross section is reasonably well defined by experimental data from threshold up to around 8 MeV. There are a few scattered points between 9 and 10 MeV and a single point around 21 MeV. The ENDF/B-VI evaluation appears to be based on nuclear modeling guided by experimental data near threshold. There are no data available near 14 MeV so the cross-section uncertainty near this energy could amount to nearly a factor of two. The peak cross section appears to be about 300 - 400 millibarn around 9 MeV.

$^{29}\text{Si}(n,\alpha)$:

The shape of the cross section near threshold, including broad resonance structure, appears to be reasonably well defined by experimental data up to about 4 MeV. There are some data available up to about 6.5 MeV, but none are archived in the EXFOR System at higher energies. ENDF/B-VI fails to reproduce the observed structure, and the lack of compiled data near 14 MeV and above is a serious deficiency for present purposes. The uncertainty could be in excess of a factor of two near 14 MeV and even larger at higher energies. The peak cross section appears to be about 100 millibarn around 6.5 MeV based on experimental data, although the ENDF/B-VI evaluation suggests that it might be even larger at higher energies. It is not clear that the evaluated curve is realistic in this energy region since there is likely to be competition from other reaction channels that could easily lead to the decline of this cross section with increasing energy rather than the steady increase shown in the plot.

$^{30}\text{Si}(n, \alpha)$:

This cross section is reasonably well defined by experimental data from near threshold to nearly 18 MeV. Discrepancies on the order of a factor of two are observed near 14 MeV. This is not unusual; nevertheless, the cross section is probably known to about 30% accuracy in this region based on a comparison with nuclear modeling results and various experimental data at energies both above and below 14 MeV. The maximum cross section appears to be about 100 millibarn around 15 MeV.

$^{48}\text{Ti}(n, \alpha)$:

The plotted data give a reasonable impression of the shape of the cross section from threshold to about 20 MeV, but the uncertainties are large near threshold and around 20% in the vicinity of 14 MeV (excluding one apparently low point). The agreement between the ENDF/B-VI evaluation and these data is quite poor, with significant differences evident in both shape and normalization. The maximum cross section appears to be about 50 millibarn around 15 MeV.

$^{50}\text{Ti}(n, \alpha)$:

The shape and normalization of the cross section from threshold to around 20 MeV is reasonably well defined by experimental data. There are extensive data in the vicinity of 14 MeV and, with the exception of some outliers, the cross section in this region is probably known to about 10%. While the ENDF/B-VI evaluation agrees with the data near 14 MeV, it differs significantly from experiment at most other energies. The maximum cross section appears to be about 10 millibarn around 20 MeV.

$^{51}\text{V}(n, n\alpha)$:

Although considerable data are available, there are serious discrepancies near the threshold that, unfortunately, occurs around 15 MeV, a significant energy for fusion applications. The cross section is about 50 millibarn at 20 MeV.

$^{51}\text{V}(n, \alpha)$:

The experimental data available for this reaction is quite extensive from threshold to around 20 MeV. Although there are discrepancies, most of the data are reasonably consistent suggesting that this cross section is rather well defined by experimental work. The ENDF/B-VI evaluation agrees rather well with the majority of the available data. The maximum cross section is about 20 millibarn in the vicinity of 15 MeV.

$^{54}\text{Cr}(n, \alpha)$:

Although there are a number of experimental data sets available, the discrepancies are very large, especially in the vicinity of 15 MeV where the uncertainty is probably 50% or larger. The maximum cross section is about 15 millibarn around 15 MeV.

$^{54}\text{Fe}(n, \alpha)$:

This cross section is rather well defined by data and an evaluation up to around 20 MeV. Although there are discrepancies evident in the 14-MeV data, most of the data sets are consistent, thus suggesting that the uncertainty is probably < 10% around 14 - 15 MeV.

$^{58}\text{Ni}(n, p\alpha)$:

There is just a single data set for this reaction and very few points. Nevertheless, the quality of these results is high and they probably define the cross section to about 10 - 20%, depending on the energy. The maximum cross section is about 30 millibarn around 20 MeV.

$^{58}\text{Ni}(n, \alpha)$:

There are extensive data available for this reaction and the consistency of results is quite good. However, the ENDF/B-VI reaction is systematically higher than the data over most of the energy range below 15 MeV. The reason for this discrepancy is not immediately evident. The maximum cross section is in the range 80 - 120 millibarn around 10 MeV, depending on whether one believes the data or the evaluation.

$^{62}\text{Ni}(n, \alpha)$:

The cross section excitation function is reasonably well defined by experimental data from threshold to 20 MeV. The uncertainty around 15 MeV appears to be around 15 - 20%. The ENDF/B-VI evaluation is in qualitative agreement with the data, but differences on the order of the data uncertainties are evident. The maximum cross section is about 30 millibarn around 14 MeV.

$^{182}\text{W}(n, n\alpha)$:

The experimental data are so discrepant that they are virtually useless. They do suggest, however, that the cross section may be somewhere in the range 10 - 25 microbarn in the vicinity of 14 - 15 MeV.

$^{184}\text{W}(n, \alpha)$:

The available data provide only a qualitative sense of the magnitude and shape of the cross section near threshold. The uncertainties are large, on the order of 30 - 50%, and the energy range is limited to 13 - 15 MeV. Compounding the difficulty is the fact that the cross section changes rapidly with energy in this range. The cross section around 14 MeV appears to be about 0.5 millibarn. The ENDF/B-VI evaluation is in qualitative agreement with the experimental data. However, it is not evident from the shape whether

this evaluation is based on a nuclear model calculation is simply an eye guide to the experimental data.

$^{186}\text{W}(n, \alpha)$:

The cross section in the energy range 13 - 15 MeV is quite well defined by good quality data with an uncertainty of perhaps 10 - 20%. At other energies the uncertainty is much greater and practically no data exist. The cross section appears to be about 0.5 millibarn in the vicinity of 14 MeV, and the ENDF/B-VI evaluation appears to be strongly influenced by the 14-MeV data.

The reader is again reminded that the comments given above for specific reactions are based entirely on the plots included in the present report. As mentioned above, there are data sets archived in the EXFOR System for which no plots are given, e.g., data sets involving single cross section values at a single energy. Also, there are undoubtedly some additional new data sets that have not yet been archived in the EXFOR System. One that comes to mind would be from the work of Haight and coworkers at Los Alamos National Laboratory, in which direct measurements of α -particle emission have been made up to around 40 - 50 MeV at the LANL LANSCE white-source neutron facility. This group has obtained results for helium production from nickel, and work on other structural materials has been mentioned in progress reports. It is unlikely that a more thorough search of the literature than provided by the current CSISRS retrieval of EXFOR data will provide a great deal of additional information that would substantially alter the present observation that the database for neutron induced helium producing reactions is quite inadequate for fusion applications at neutron energies up to 60 MeV, especially if it is required to know the specific contributions from individual reactions involving various fusion material isotopes.

5. Evaluated Helium Producing Neutron Reaction Cross Sections

5.1 Sources of Cross Section Information

There exist various sources for evaluated cross section information. Since the objective of the present investigation is to provide a survey of the status of nuclear data that offers the reader some indication as to how well the cross sections are actually known, it was decided to limit the present work to consideration of the evaluated general purpose libraries from the U.S. (ENDF/B-VI), Europe (JEF), Japan (JENDL), Russia (Brond), and China (CENDL), as well as the IAEA FENDL Library (<http://www-nds.iaea.org/>). Listings of tabulated numerical information alone are of little use. Consequently, it was decided to present the information entirely in the form of GIF survey plots. These plots are generated interactively, on-line, using software available at the IAEA Nuclear Data Section (NDS) and U.S. National Nuclear Data Center (<http://www.nndc.bnl.gov>) Internet sites. Similar software and databases can be found at the NEA Nuclear Data Bank (<http://www.nea.fr>), but it was decided to limit this exercise to the two preceding sources of information. There is much redundancy in the library contents of these (and other) national and regional data centers. The main differences between them lie in the software they provide for visualization and downloading of data.

5.2 Evaluated Data from General Purpose Files

The U.S. National Nuclear Data Center (NNDC) was selected as the site for downloading plots that compare evaluated cross sections from the above-mentioned general purpose nuclear data libraries. None of the general purpose libraries include all the helium producing reaction cross sections of interest for the present investigation. In fact the limited extent of reaction coverage provided by these data libraries is somewhat disconcerting. The situation is summarized in Table 5.1.

Table 5.1: Helium producing neutron cross sections from general purpose libraries ^a

<u>Element</u>	<u>Isotope</u>	<u>Reaction</u>	<u>ENDF</u>	<u>JENDL</u>	<u>JEF</u>	<u>BROND</u>	<u>CENDL</u>	
<i>Carbon</i>	C-12	(N,A)		JENDL-3				
	C-13	None						
	C-nat	(N,A)	ENDF/B-VI	JENDL-3	JEF-2	Brond-2		
<i>Silicon</i>	Si-28	(N,NA)	ENDF/B-VI	JENDL-3				
		(N,A)	ENDF/B-VI	JENDL-3				
	Si-29	(N,NA)	ENDF/B-VI	JENDL-3				
		(N,A)	ENDF/B-VI	JENDL-3				
	Si-30	(N,NA)	ENDF/B-VI	JENDL-3				
		(N,A)	ENDF/B-VI	JENDL-3				
	Si-nat	(N,NA)			JENDL-3	JEF-2	Brond-2	CENDL-2
		(N,A)			JENDL-3	JEF-2	Brond-2	CENDL-2

<i>Titanium</i>	Ti-46	(N,NA)		JENDL-3			
		(N,3He)		JENDL-3			
		(N,A)		JENDL-3			
	Ti-47	(N,NA)		JENDL-3			
		(N,3He)		JENDL-3			
		(N,A)		JENDL-3			
	Ti-48	(N,NA)		JENDL-3			
		(N,3He)		JENDL-3			
		(N,A)	ENDF/B-VI	JENDL-3			
	Ti-49	(N,NA)		JENDL-3			
		(N,3He)		JENDL-3			
		(N,A)		JENDL-3			
	Ti-50	(N,NA)		JENDL-3			
		(N,3He)		JENDL-3			
		(N,A)	ENDF/B-VI	JENDL-3			
Ti-nat	(N,NA)	ENDF/B-VI	JENDL-3	JEF-2		CENDL-2	
	(N,PA)	ENDF/B-VI					
	(N,3He)	ENDF/B-VI		JEF-2		CENDL-2	
	(N,A)	ENDF/B-VI	JENDL-3	JEF-2		CENDL-2	
<i>Vanadium</i>	V-51	(N,NA)		JENDL-3			
		(N,A)		JENDL-3			
	V-nat	(N,NA)	ENDF/B-VI	JENDL-3	JEF-2		CENDL-2
		(N,PA)	ENDF/B-VI				
		(N,3He)	ENDF/B-VI				
	(N,A)	ENDF/B-VI	JENDL-3	JEF-2		CENDL-2	
<i>Chromium</i>	Cr-50	(N,NA)	ENDF/B-VI	JENDL-3	JEF-2		
		(N,3He)		JENDL-3			
		(N,A)	ENDF/B-VI	JENDL-3	JEF-2	Brond-2	
	Cr-52	(N,NA)	ENDF/B-VI	JENDL-3	JEF-2		
		(N,3He)		JENDL-3			
		(N,A)	ENDF/B-VI	JENDL-3	JEF-2	Brond-2	
	Cr-53	(N,NA)		JENDL-3			
		(N,3He)		JENDL-3			
		(N,A)	ENDF/B-VI	JENDL-3	JEF-2	Brond-2	
	Cr-54	(N,NA)		JENDL-3	JEF-2		
		(N,3He)		JENDL-3			
		(N,A)	ENDF/B-VI	JENDL-3	JEF-2	Brond-2	
	Cr-nat	(N,NA)		JENDL-3		Brond-2	CENDL-2
		(N,A)		JENDL-3		Brond-2	CENDL-2
	<i>Iron</i>	Fe-54	(N,NA)	ENDF/B-VI	JENDL-3	JEF-2	

		(N,A)	ENDF/B-VI	JENDL-3	JEF-2	Brond-2	
	Fe-56	(N,NA)	ENDF/B-VI	JENDL-3	JEF-2	Brond-2	
		(N,A)	ENDF/B-VI	JENDL-3	JEF-2	Brond-2	
	Fe-57	(N,NA)	ENDF/B-VI	JENDL-3	JEF-2		
		(N,A)	ENDF/B-VI	JENDL-3	JEF-2	Brond-2	
	Fe-nat	(N,NA)		JENDL-3		Brond-2	CENDL-2
		(N,A)		JENDL-3		Brond-2	CENDL-2
<i>Nickel</i>	Ni-58	(N,NA)	ENDF/B-VI	JENDL-3	JEF-2	Brond-2	
		(N,3He)		JENDL-3			
		(N,A)	ENDF/B-VI	JENDL-3	JEF-2	Brond-2	
	Ni-60	(N,NA)	ENDF/B-VI	JENDL-3	JEF-2		
		(N,3He)		JENDL-3			
		(N,A)	ENDF/B-VI	JENDL-3	JEF-2	Brond-2	
	Ni-61	(N,NA)		JENDL-3			
		(N,3He)		JENDL-3			
		(N,A)	ENDF/B-VI	JENDL-3	JEF-2	Brond-2	
	Ni-62	(N,NA)	ENDF/B-VI	JENDL-3	JEF-2		
		(N,3He)		JENDL-3			
		(N,A)	ENDF/B-VI	JENDL-3	JEF-2	Brond-2	
Ni-nat	(N,NA)		JENDL-3			CENDL-2	
	(N,3He)		JENDL-3				
	(N,A)		JENDL-3		Brond-2	CENDL-2	
<i>Tungsten</i>	W-182	(N,NA)		JENDL-3			
		(N,A)	ENDF/B-VI	JENDL-3	JEF-2	Brond-2	
	W-183	(N,NA)		JENDL-3			
		(N,A)	ENDF/B-VI	JENDL-3	JEF-2	Brond-2	
	W-184	(N,NA)		JENDL-3			
		(N,A)	ENDF/B-VI	JENDL-3	JEF-2	Brond-2	
	W-186	(N,NA)		JENDL-3			
		(N,A)	ENDF/B-VI	JENDL-3	JEF-2	Brond-2	
	W-nat	(N,NA)		JENDL-3			
		(N,A)	ENDF/B-VI	JENDL-3			

^a Green shading indicates that library has a file for the listed reaction. Library versions are also designated.

It is evident that the most extensive general purpose library for evaluated helium producing neutron reaction cross sections is JENDL-3. The other four libraries are considerably sparser in the extent their coverage of these reactions. Nevertheless, a number of the survey plots given below do exhibit more than one evaluated file for a particular reaction. Thus, these plots serve to provide a good indication of the uncertainty in contemporary knowledge of many of the cross sections of interest for helium production. Nevertheless, it should be noted that, with few exceptions, these plots are limited to the (n, α), (n, $n\alpha$), and (n, ^3He) reactions, a small subset of the universe of all reactions of potential interest for helium production, as discussed in Sections 2 - 4.

Furthermore, these evaluations are generally confined to neutron energies no higher than 20 MeV. The plots generated during the course of this investigation are presented below.

What is very evident from these plots is the considerable disagreement between many of the comparable curves of evaluated cross sections, except in some cases where one evaluation is a copy of another. Disagreements in both shape and normalization are particularly acute for independent evaluations in those situations where there are few if any data to guide these evaluations. Many (most in fact) of the contemporary evaluations are based on nuclear model calculations, even when extensive data are available. The reasons for this are well known. Among them is the fact that general purpose files must provide cross section values for all the significant reaction channels up to at least 20-MeV neutron energy, and the partial cross sections must add up exactly to the total cross section at all energies. It is very easy to meet this requirement when nuclear modeling is used to generate the evaluated results. Another consideration is the fact that there are few isotopes (or elements) where the experimental data are sufficiently comprehensive to guide evaluations without the help of nuclear models.

It is very interesting to examine the region of 14-MeV in these various plots. Since the experimental data in this region are more extensive than for other energies (see Section 4), one would expect that the cross sections should be the best known there and, consequently, that the various evaluations should exhibit better agreement there than elsewhere. Surprisingly, this is frequently NOT the case. Another point that the reader should be aware of is that differences in the cross section curves near threshold can be considerably greater than indicated by appearances. A small shift in the energy scale can lead to significant differences in the corresponding numerical values.

The contemporary trend is to provide evaluated files for individual isotopes of elements rather than elemental files. It is argued that elemental values can be constructed from isotopic values. Furthermore, nuclear models generally compute cross section values for individual isotopes, not for elements. Since nuclear models are imperfect, and experimental values have errors, there are many opportunities for inconsistencies to arise in the production of evaluated cross sections. As a result of these inconsistencies, the evaluation generated for a particular reaction channel may very well not be the best possible one based on all the existing information. For example, if there are extensive and reasonably accurate data for a particular reaction channel, the final evaluated curve may not actually pass within the range of the data uncertainties at all energies when the evaluation is based on a nuclear model. The evaluator/modeler charged with producing a vertical (all channels included) evaluation for a particular isotope of a general purpose file must be cognizant of the state of affairs for all the reaction channels. Thus, he will tend to adjust the parameters of the model to produce the best overall agreement with experimental data for the most significant reaction channels while, at the same time adhering as much as possible to known systematic considerations. For this reason, evaluations for specific reaction channels of importance in certain applications, e.g., neutron dosimetry cross sections or standard cross sections, may very well be carried out in a manner to optimize agreement between the evaluation and experimental data without concern for other reaction channels. Thus, inconsistencies between the predicted evaluations in general purpose files and those produced for specific applications may be unavoidable. The reader (and user of these files) needs to be aware of the fact that such inconsistencies do exist and must deal with these files carefully and not apply them beyond the scope for which they were intended by the original evaluators.

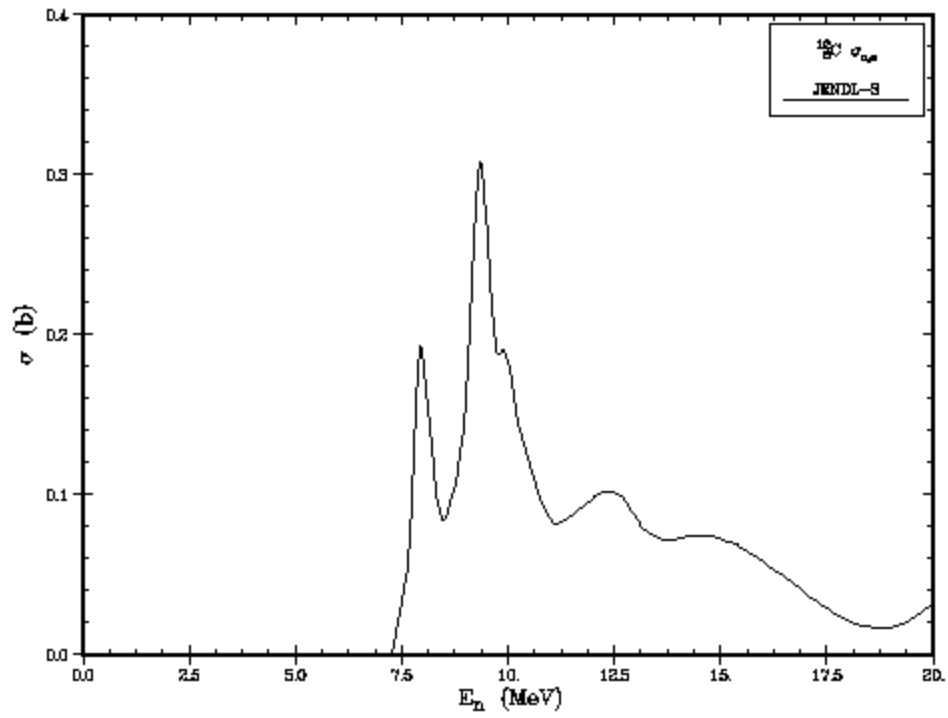


Figure 5.1: $^{12}\text{C}(n,\alpha)$ reaction cross section

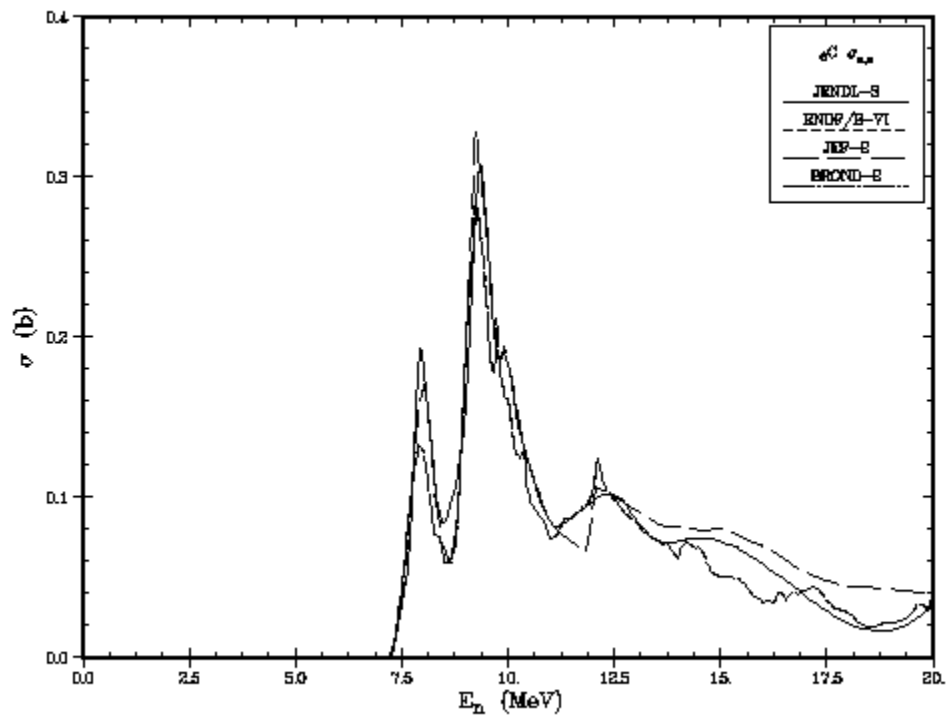


Figure 5.2: $^{\text{nat}}\text{C}(n,\alpha)$ reaction cross section

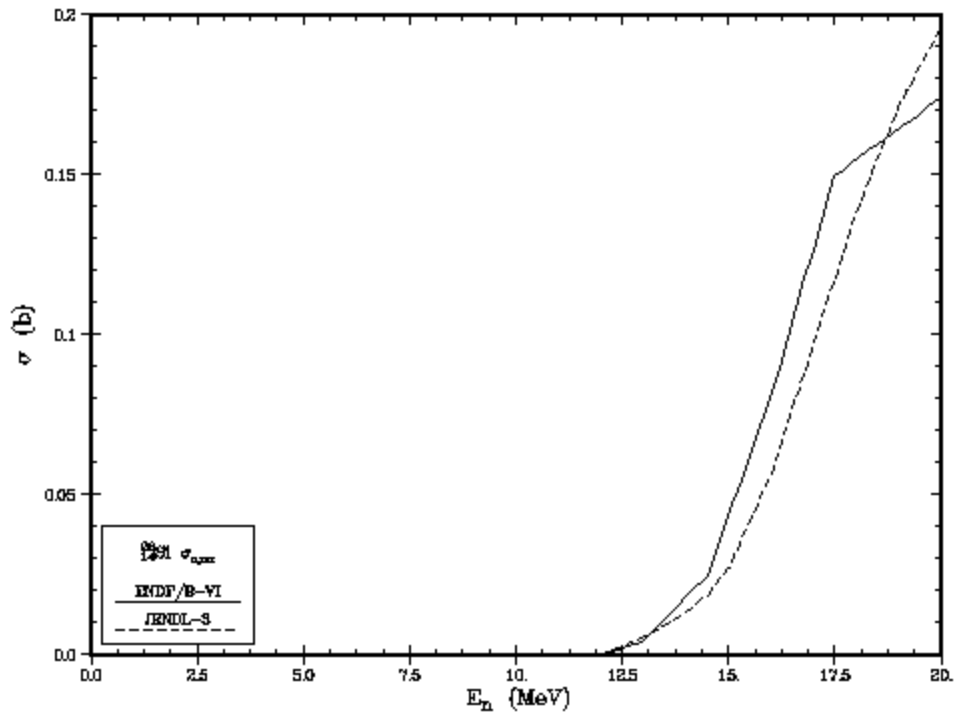


Figure 5.3: $^{28}\text{Si}(n,\alpha)$ reaction cross section

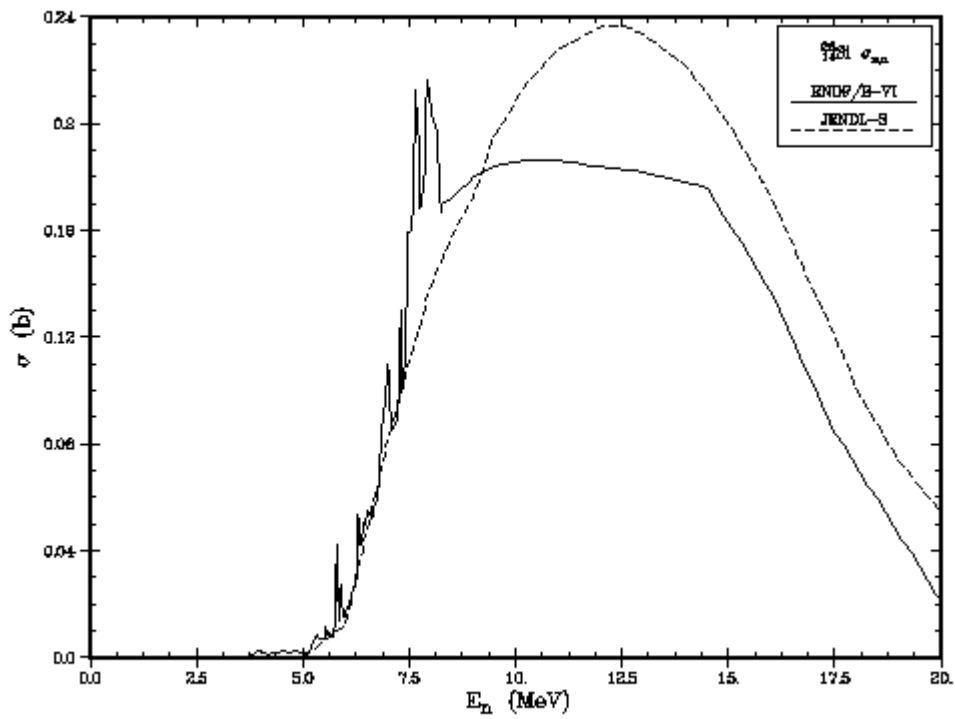


Figure 5.4: $^{28}\text{Si}(n,\alpha)$ reaction cross section

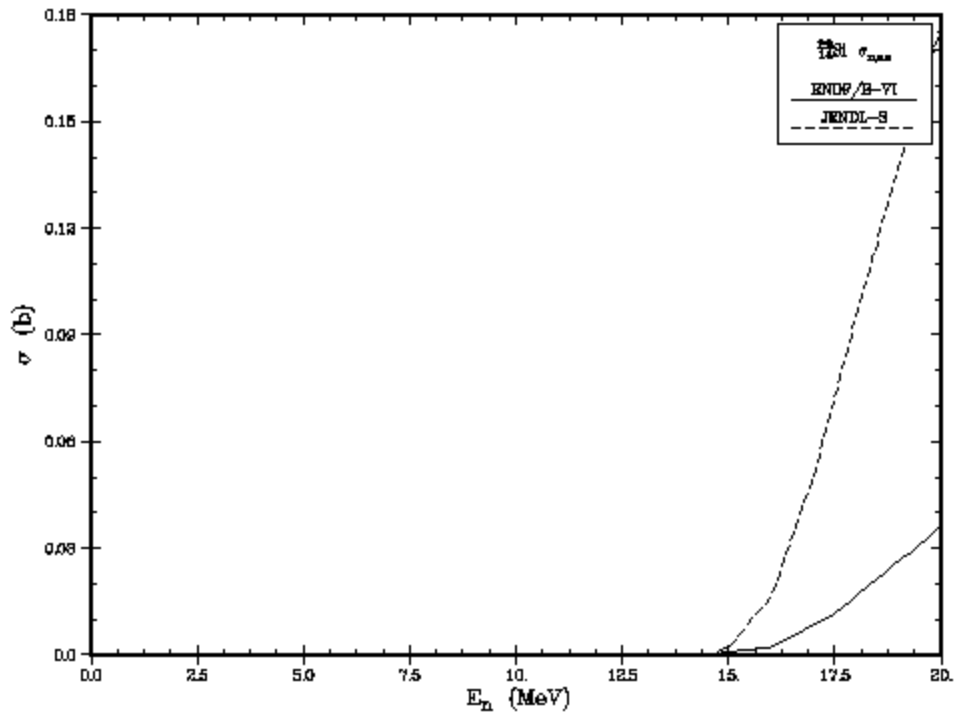


Figure 5.5: $^{29}\text{Si}(n,\alpha)$ reaction cross section

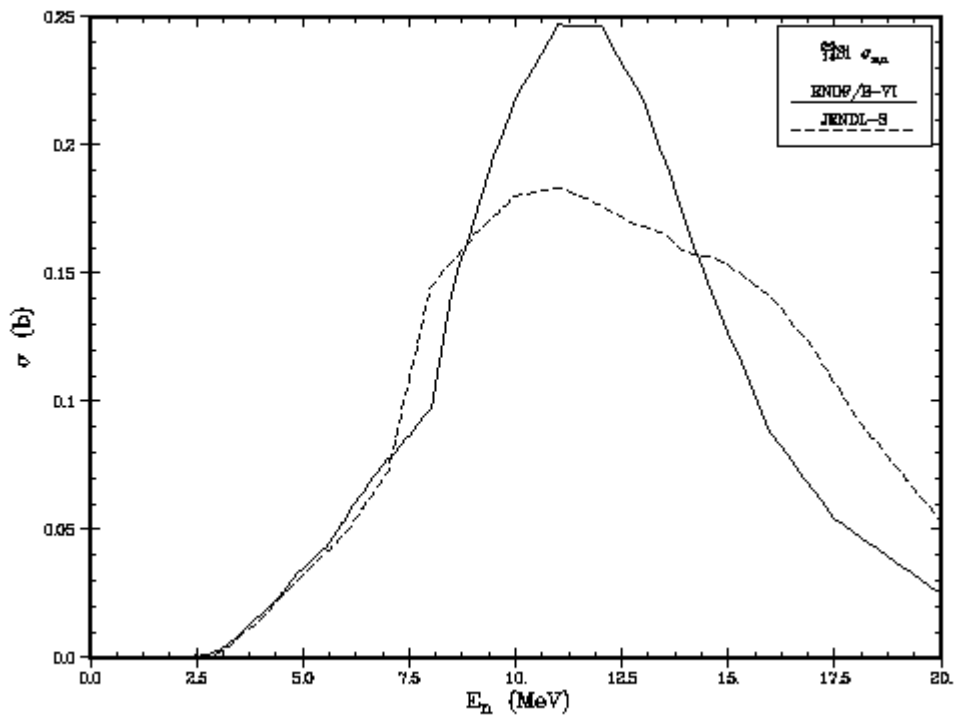


Figure 5.6: $^{29}\text{Si}(n,\alpha)$ reaction cross section

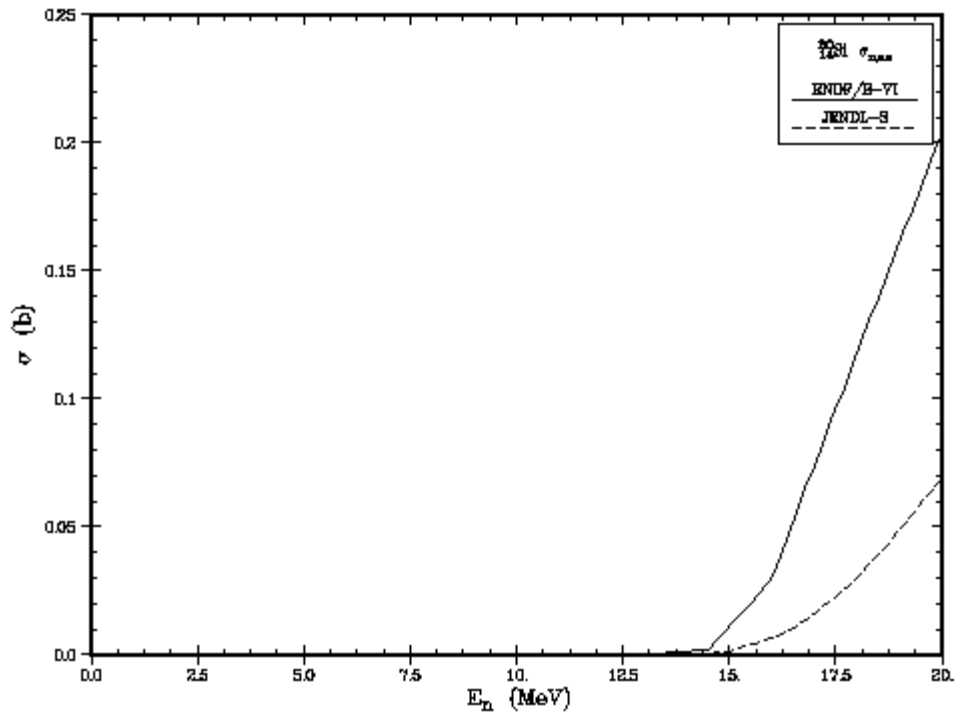


Figure 5.7: $^{30}\text{Si}(n,n\alpha)$ reaction cross section

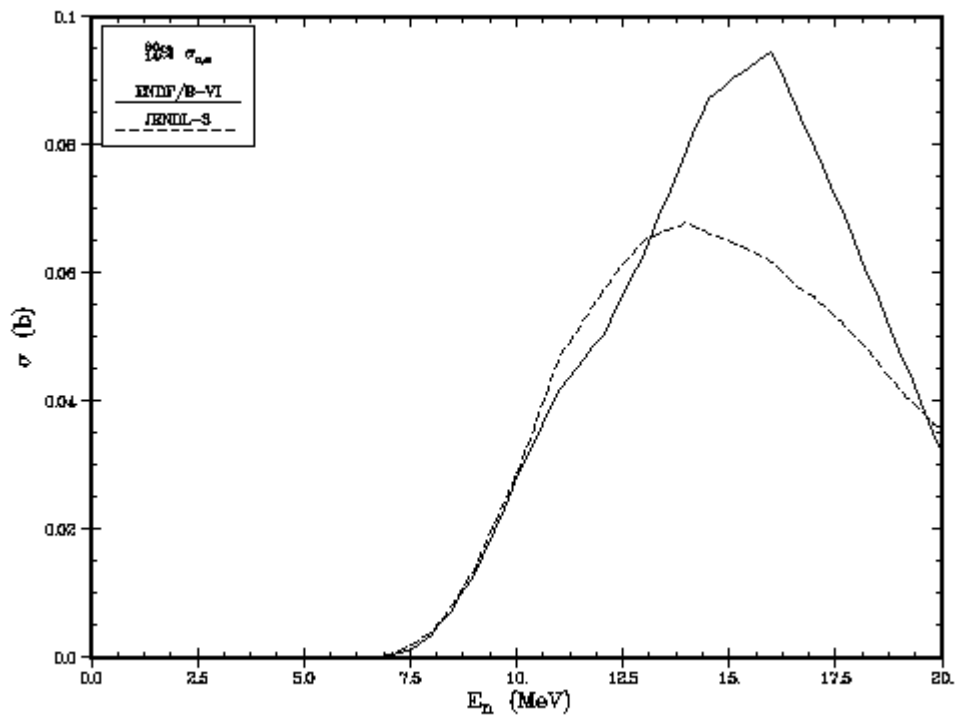


Figure 5.8: $^{30}\text{Si}(n,\alpha)$ reaction cross section

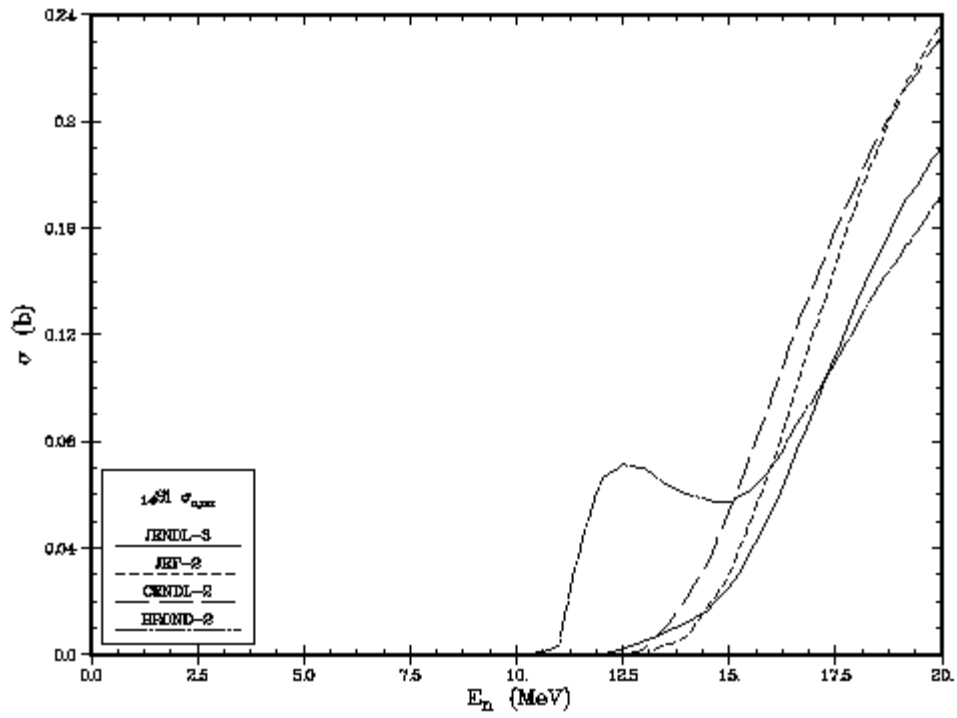


Figure 5.9: $^{14}\text{Si}(n,\alpha)$ reaction cross section

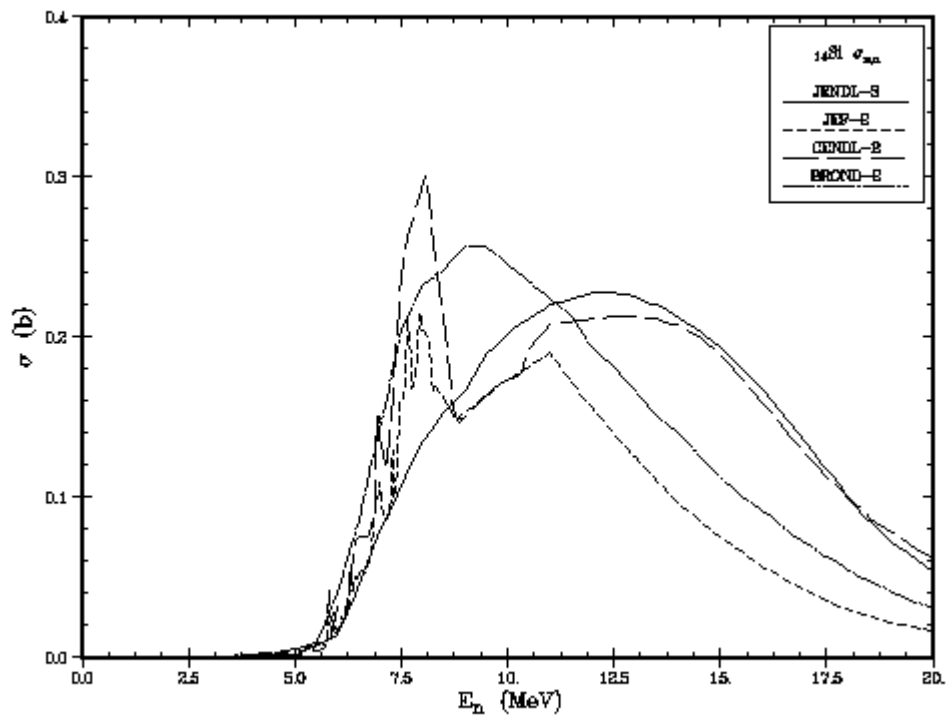


Figure 5.10: $^{14}\text{Si}(n,\alpha)$ reaction cross section

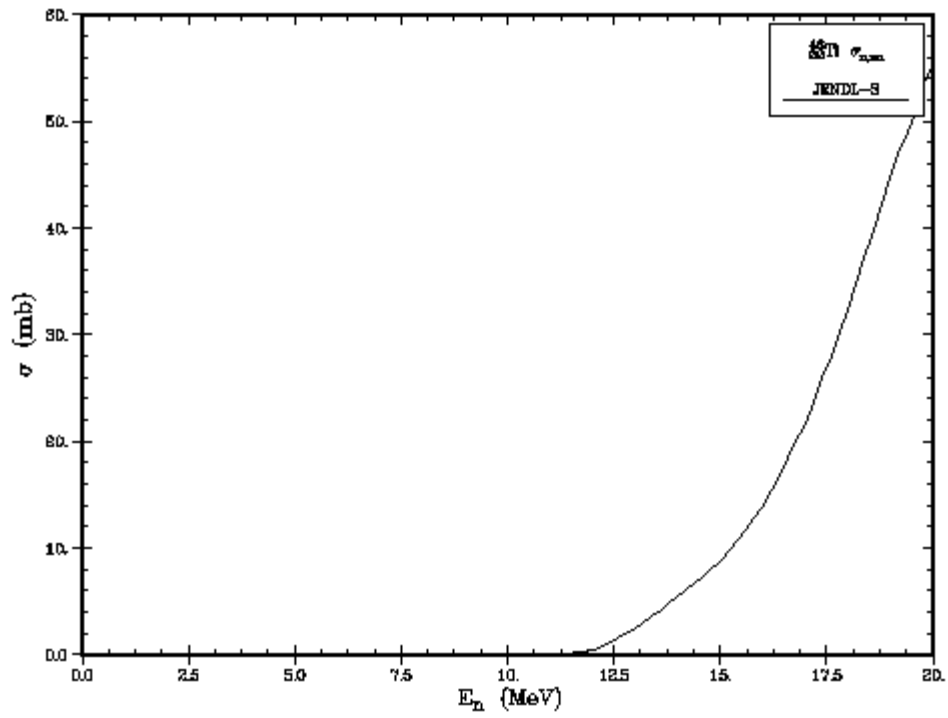


Figure 5.11: $^{46}\text{Ti}(n, n\alpha)$ reaction cross section

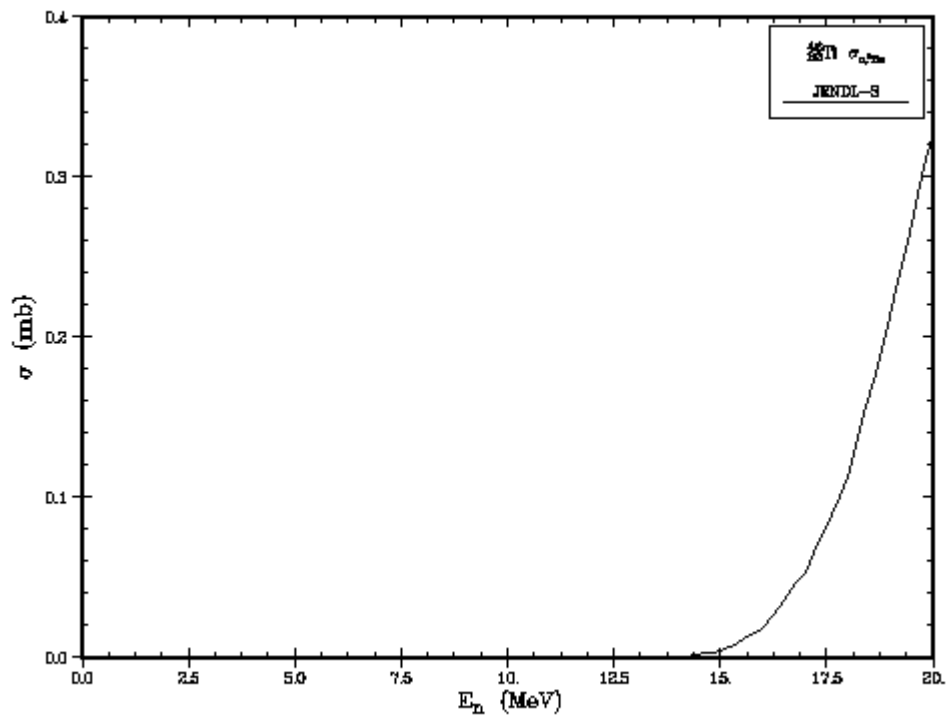


Figure 5.12: $^{46}\text{Ti}(n, ^3\text{He})$ reaction cross section

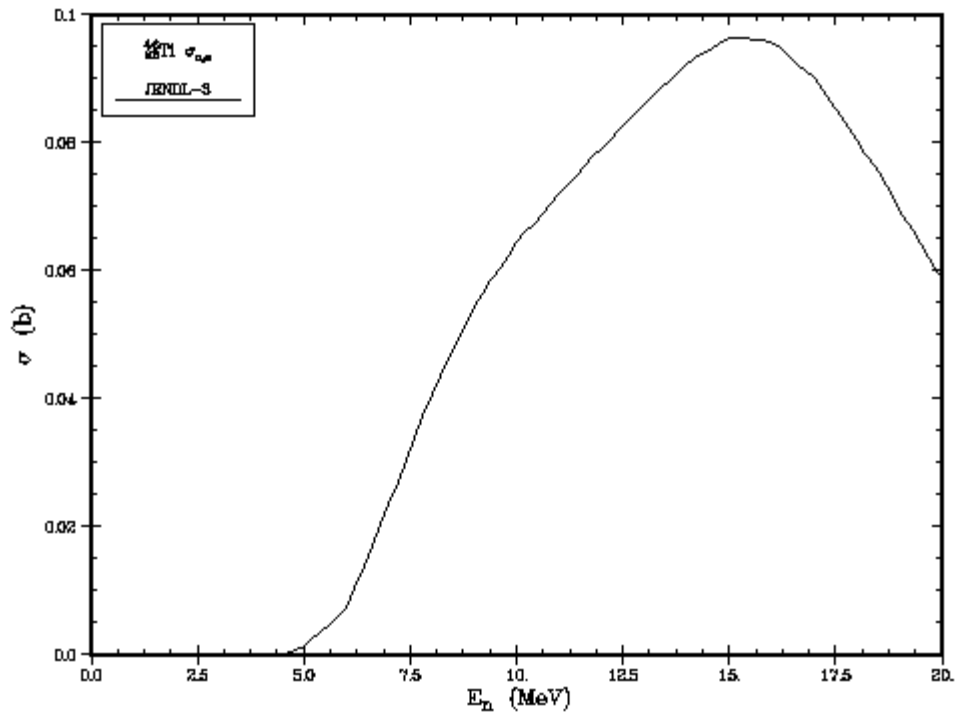


Figure 5.13: $^{46}\text{Ti}(n,\alpha)$ reaction cross section

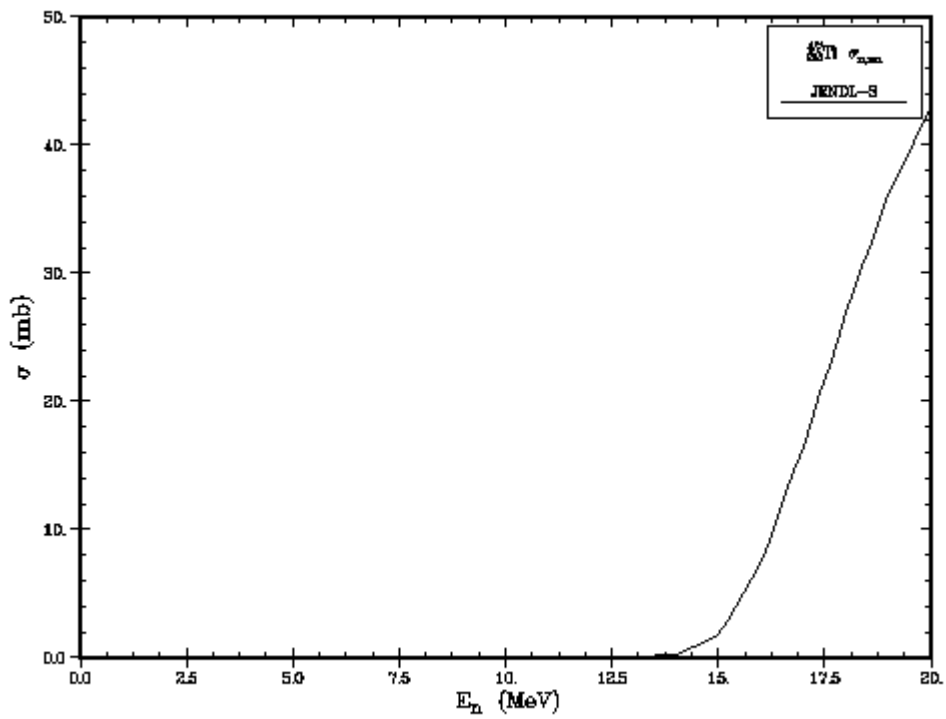


Figure 5.14: $^{47}\text{Ti}(n,n\alpha)$ reaction cross section

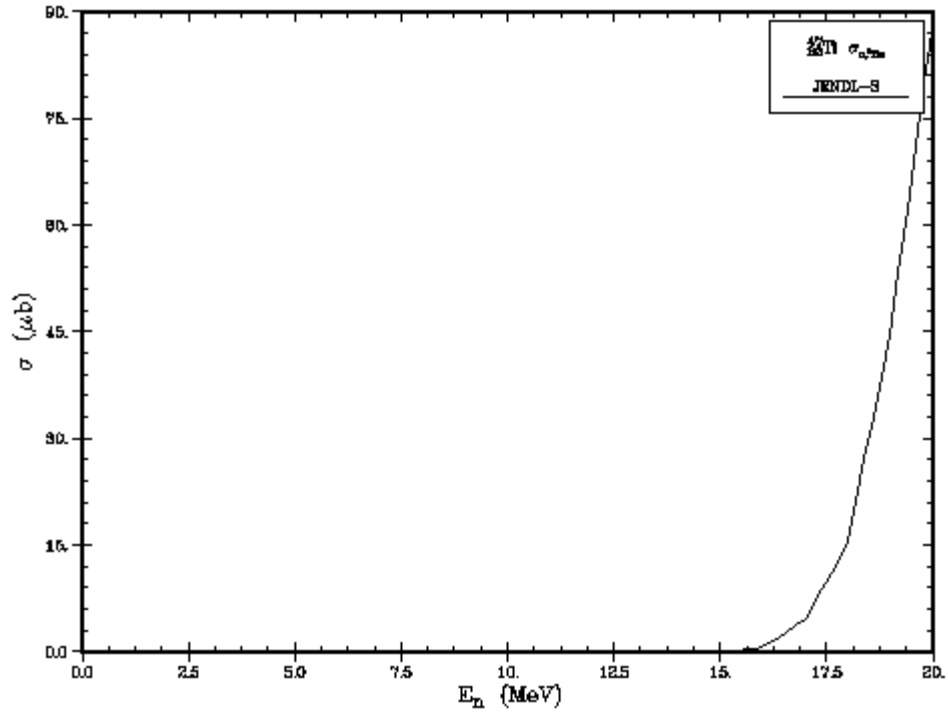


Figure 5.15: $^{47}\text{Ti}(n,^3\text{He})$ reaction cross section

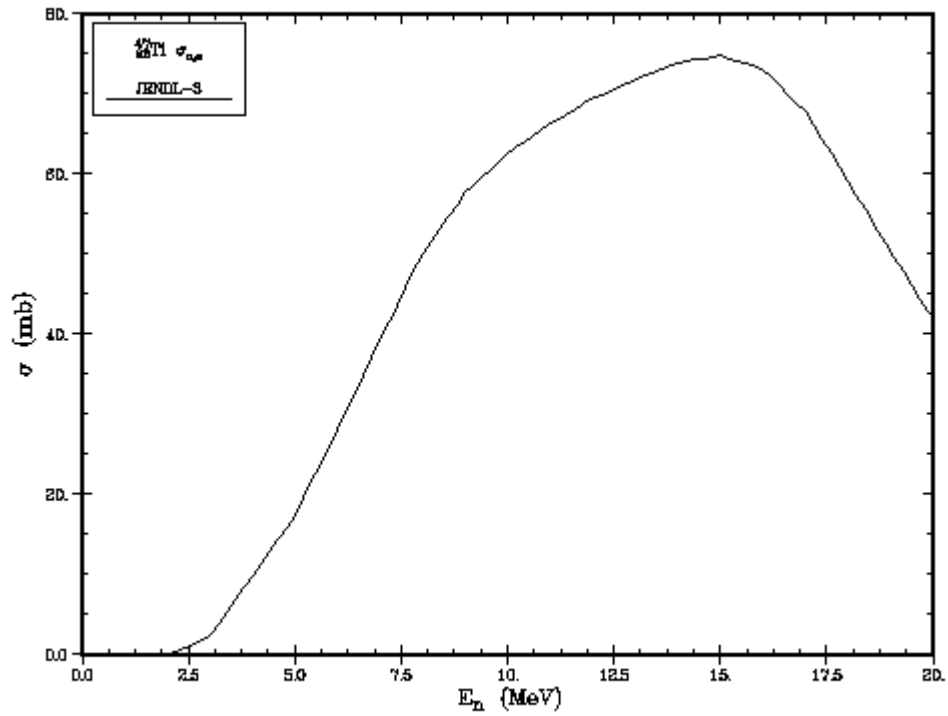


Figure 5.16: $^{47}\text{Ti}(n,\alpha)$ reaction cross section

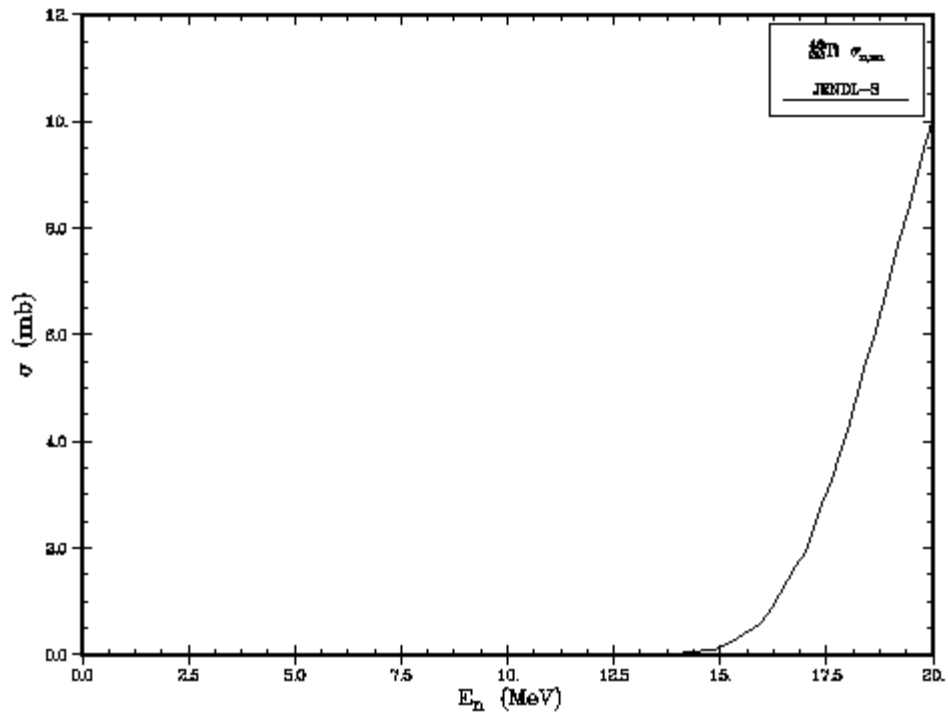


Figure 5.17: $^{48}\text{Ti}(n, n\alpha)$ reaction cross section

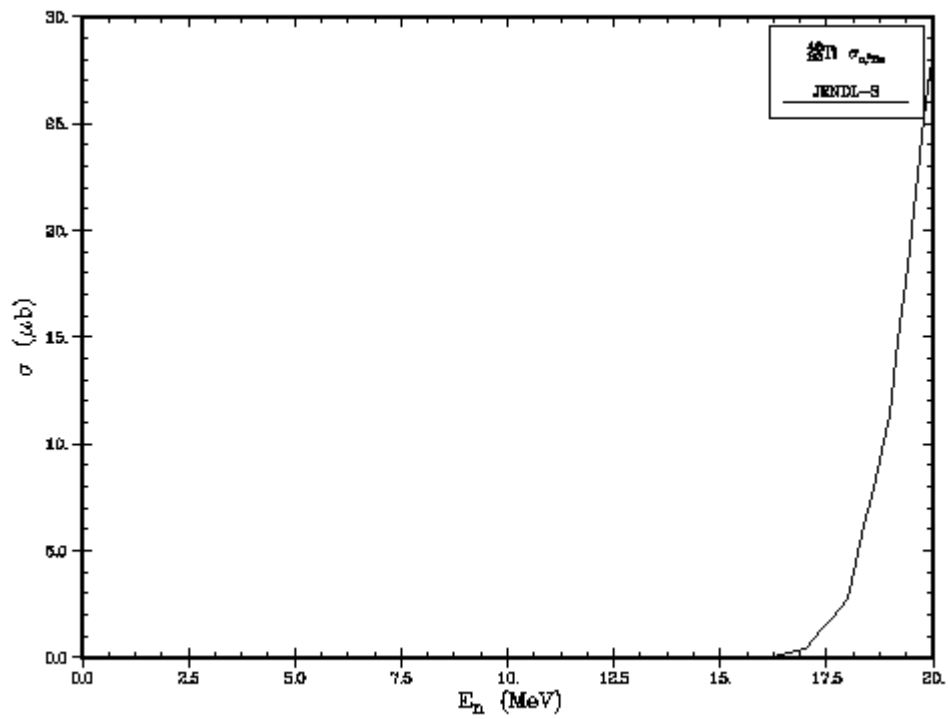


Figure 5.18: $^{48}\text{Ti}(n, ^3\text{He})$ reaction cross section

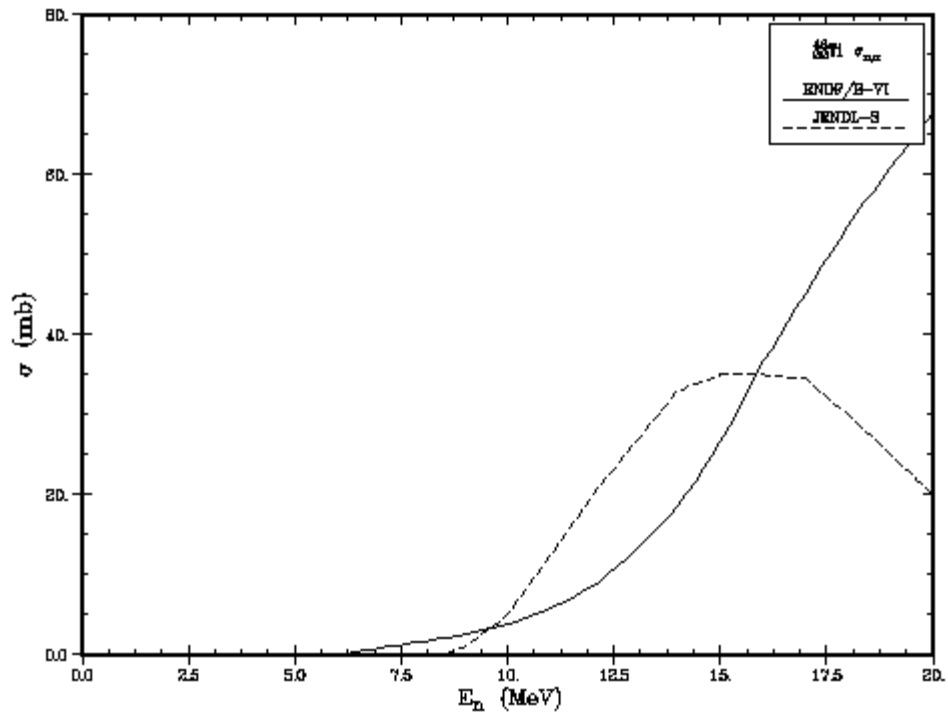


Figure 5.19: $^{48}\text{Ti}(n,\alpha)$ reaction cross section

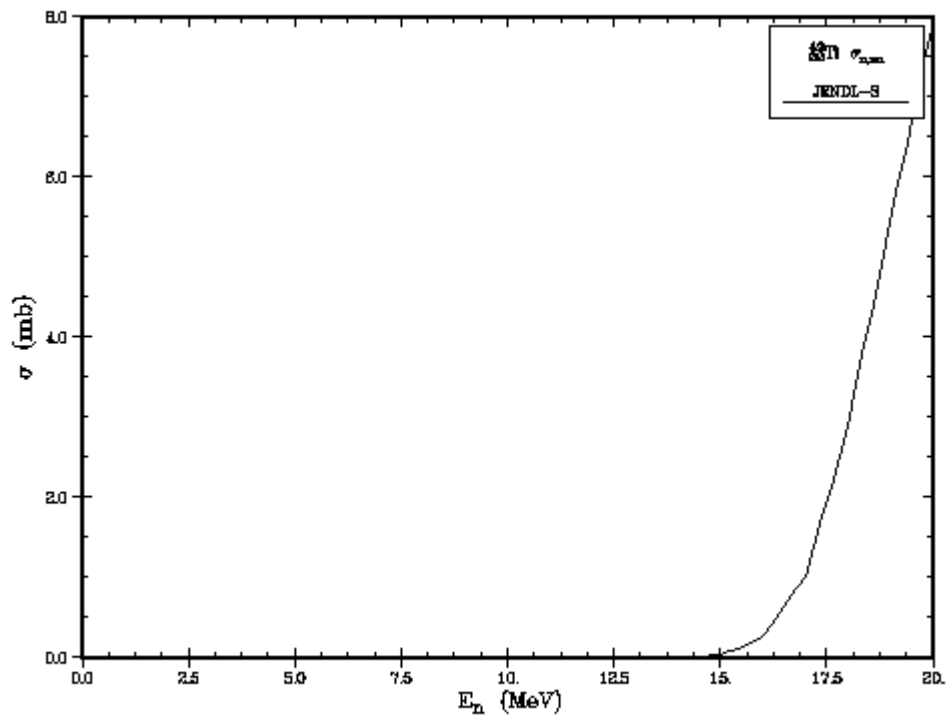


Figure 5.20: $^{49}\text{Ti}(n,n\alpha)$ reaction cross section

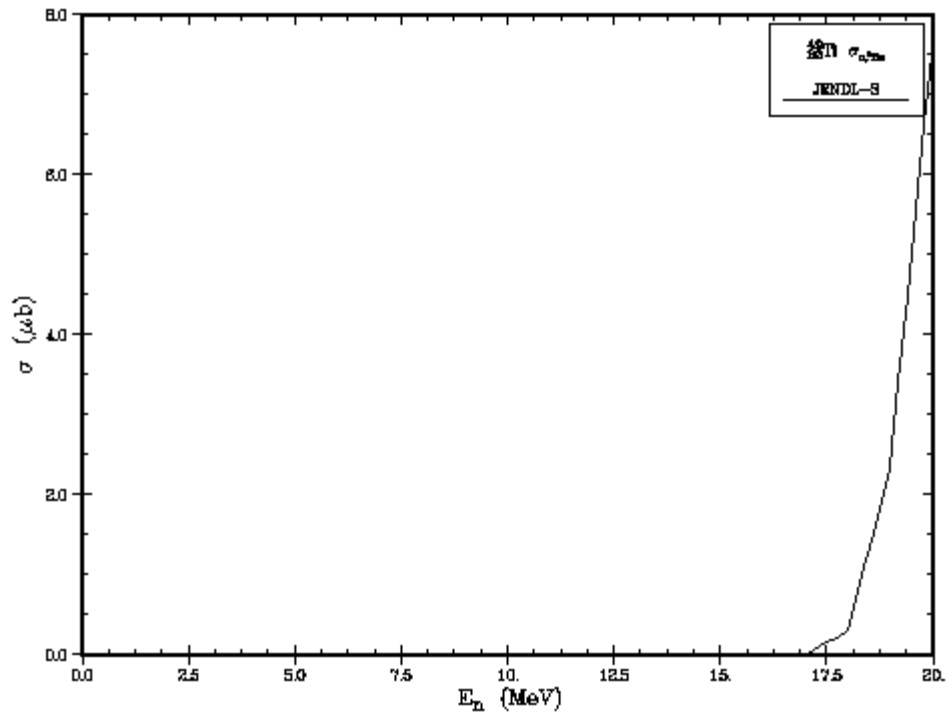


Figure 5.21: $^{49}\text{Ti}(n,^3\text{He})$ reaction cross section

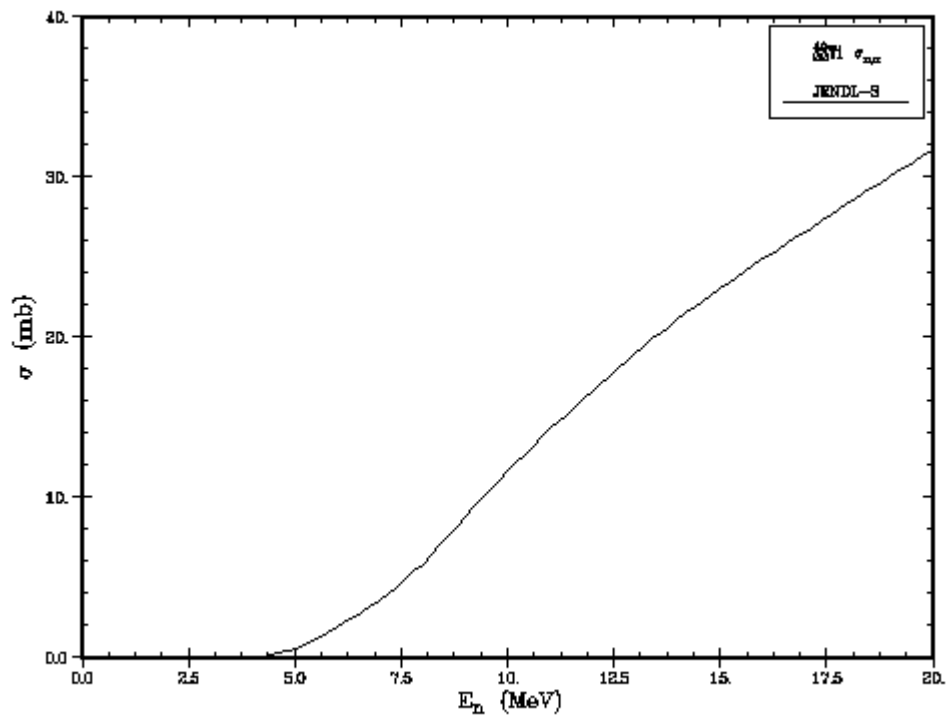


Figure 5.22: $^{49}\text{Ti}(n,\alpha)$ reaction cross section

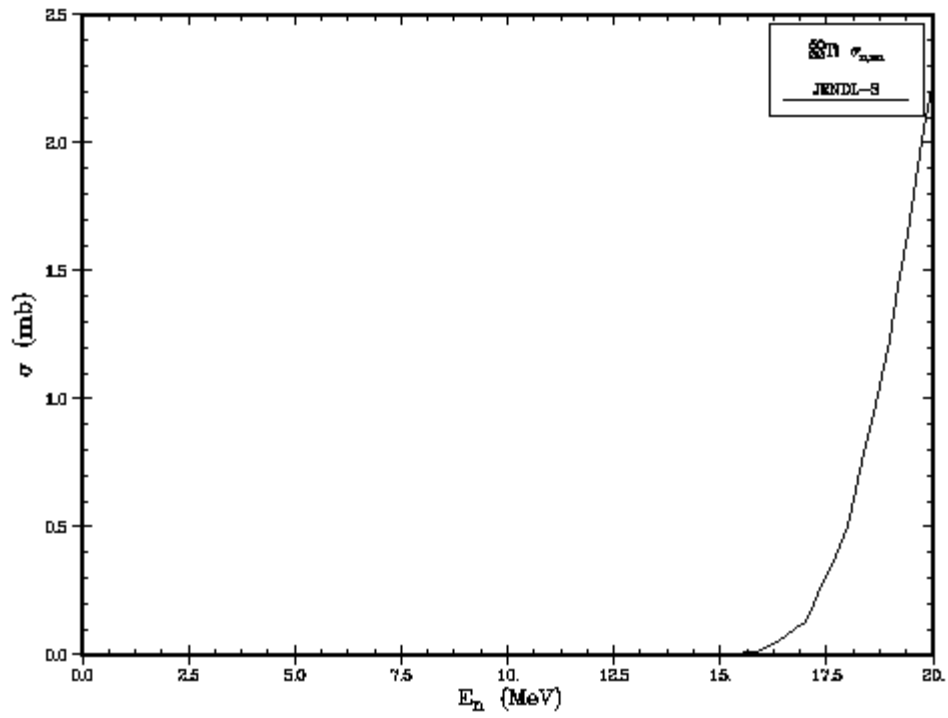


Figure 5.23: $^{50}\text{Ti}(n,n\alpha)$ reaction cross section

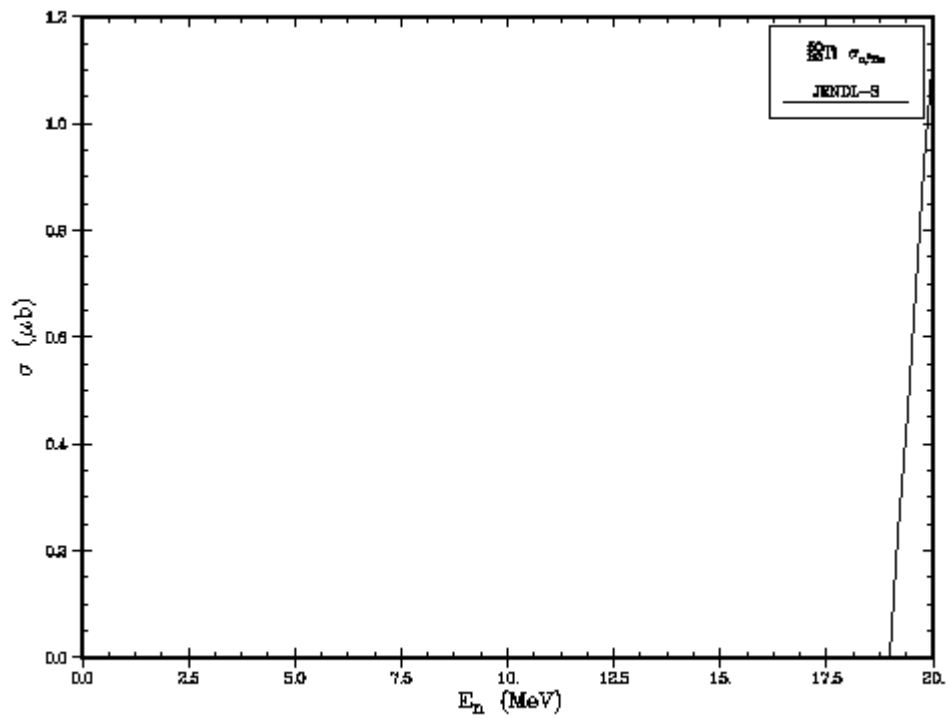


Figure 5.24: $^{50}\text{Ti}(n,^3\text{He})$ reaction cross section

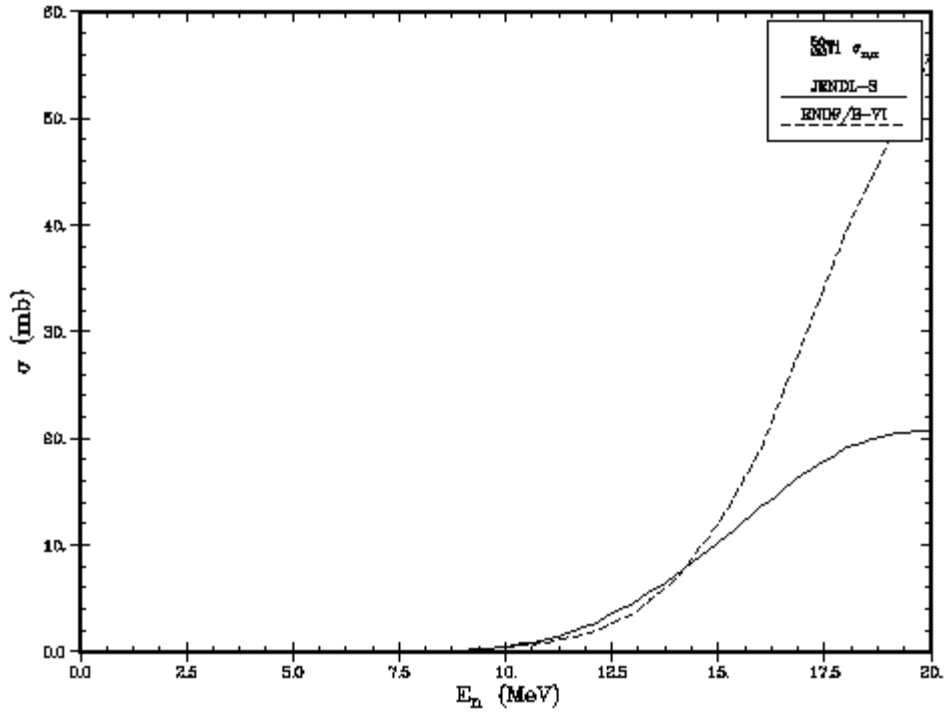


Figure 5.25: $^{50}\text{Ti}(n,\alpha)$ reaction cross section

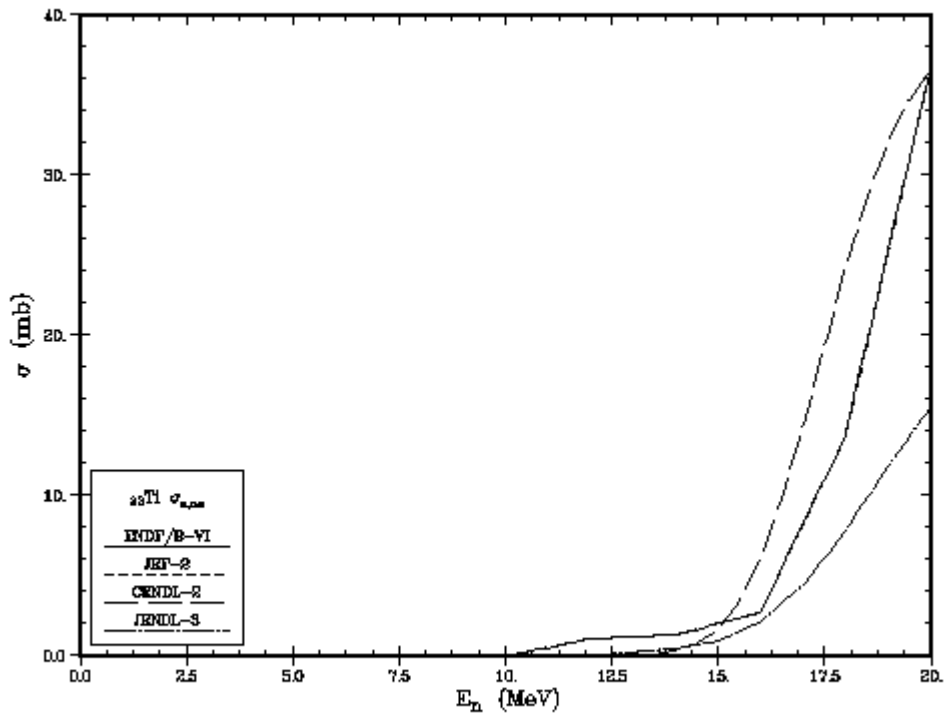


Figure 5.26: $^{\text{nat}}\text{Ti}(n,n\alpha)$ reaction cross section

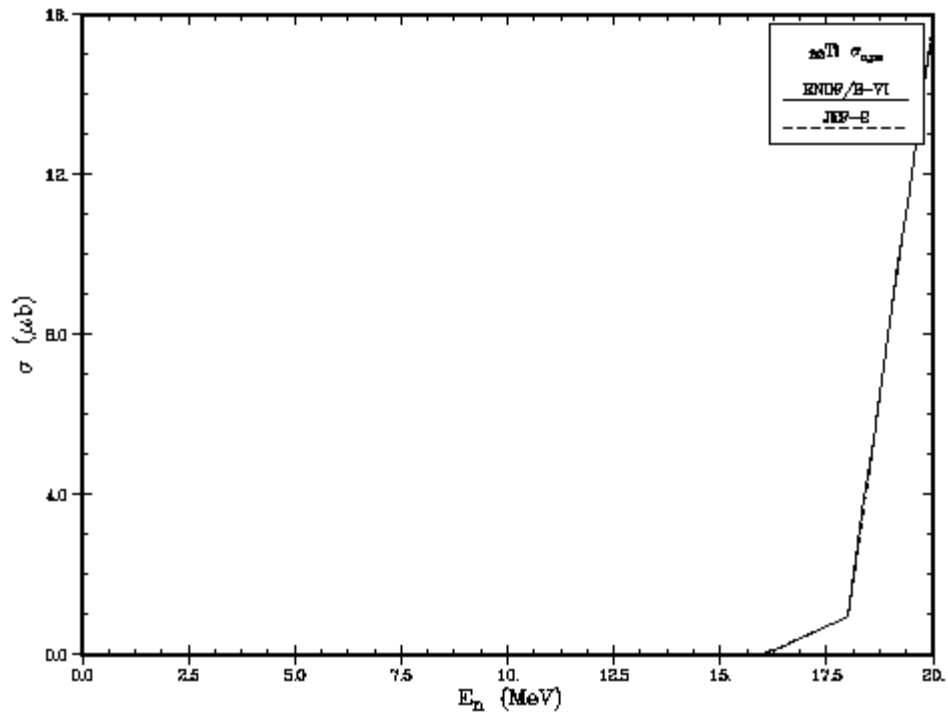


Figure 5.27: $^{nat}\text{Ti}(n,p)\alpha$ reaction cross section

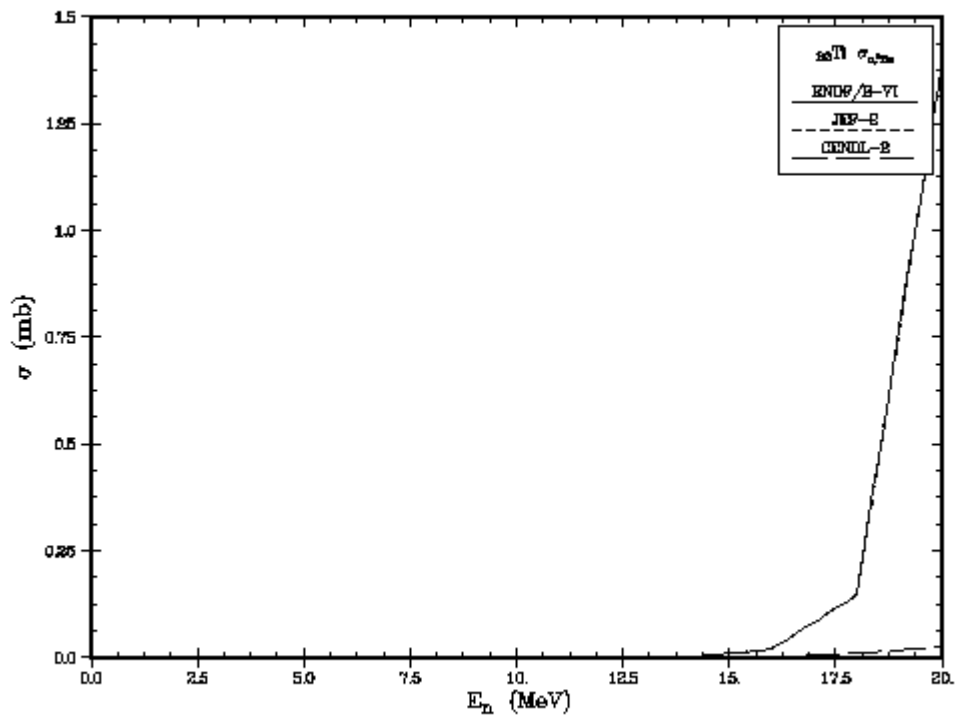


Figure 5.28: $^{nat}\text{Ti}(n,^3\text{He})$ reaction cross section

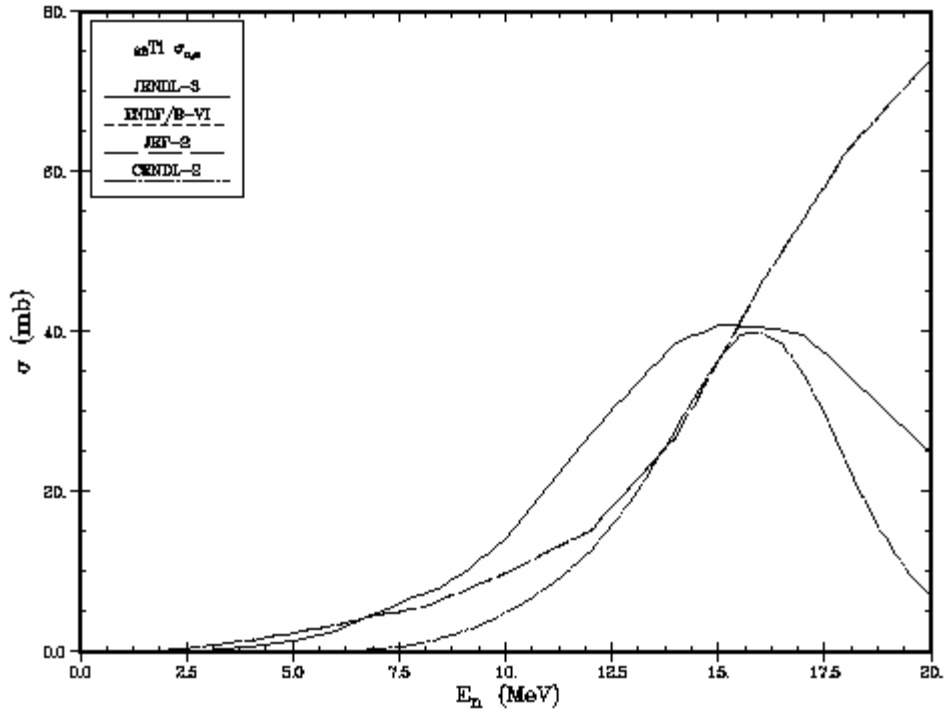
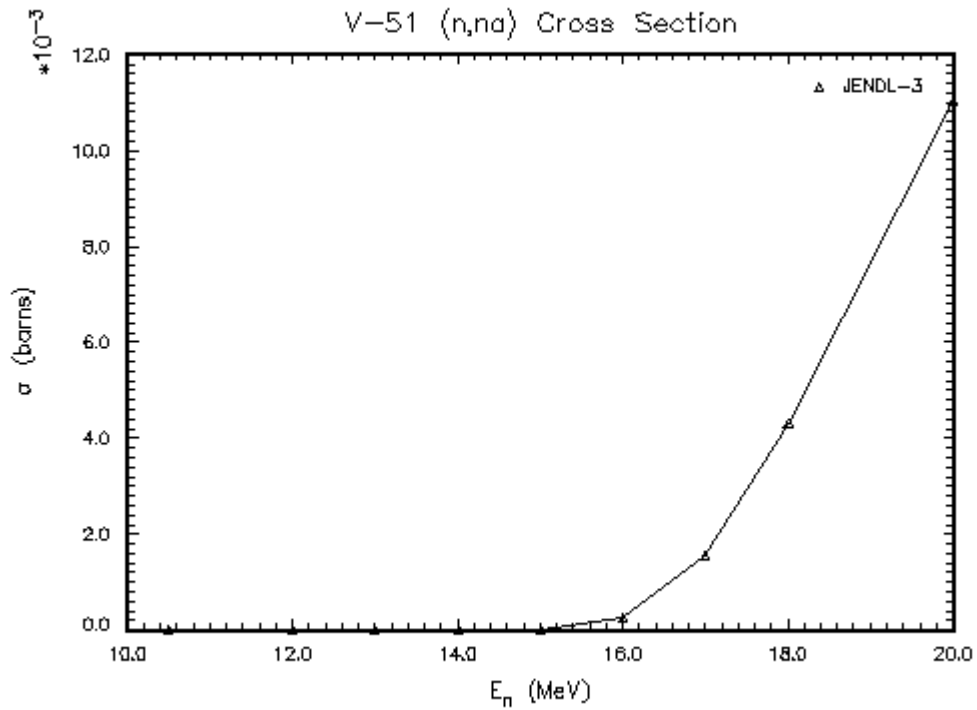
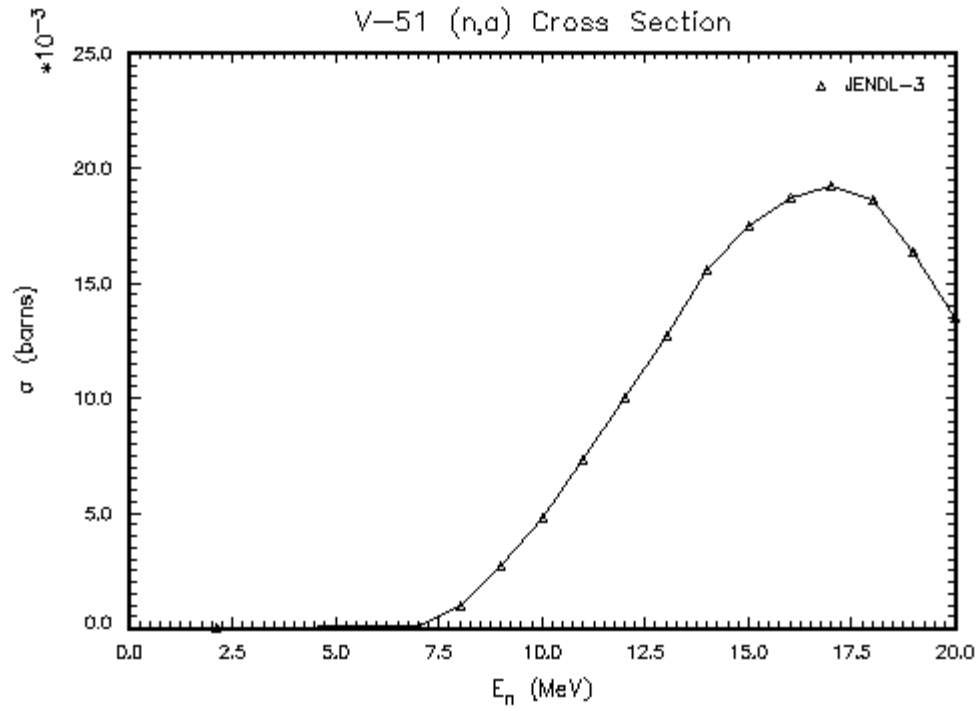


Figure 5.29: $^{nat}\text{Ti}(n,\alpha)$ reaction cross section



15-MAR-2004

Figure 5.30: $^{51}\text{V}(n,n\alpha)$ reaction cross section



15-MAR-2004

Figure 5.31: $^{51}\text{V}(n,\alpha)$ reaction cross section

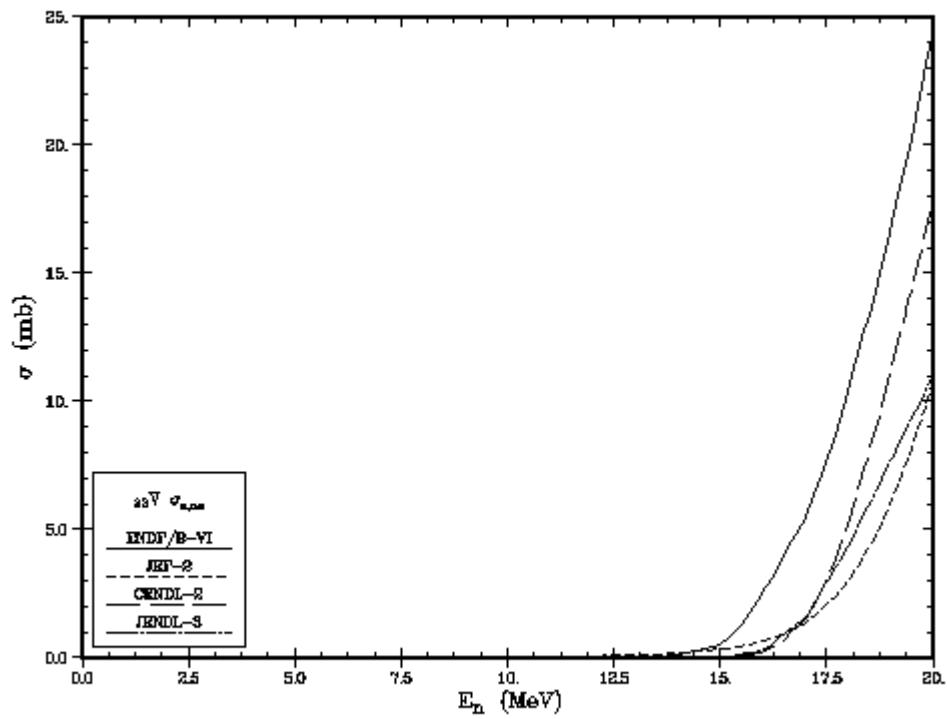


Figure 5.32: $^{\text{nat}}\text{V}(n,n\alpha)$ reaction cross section

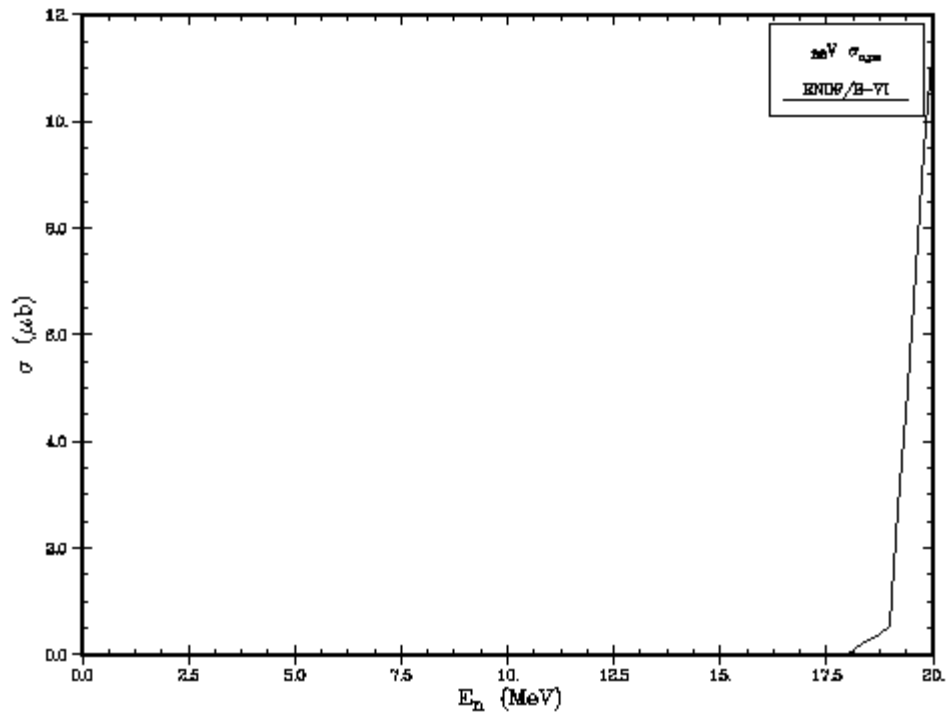


Figure 5.33: ${}^{\text{nat}}\text{V}(n,\alpha)$ reaction cross section

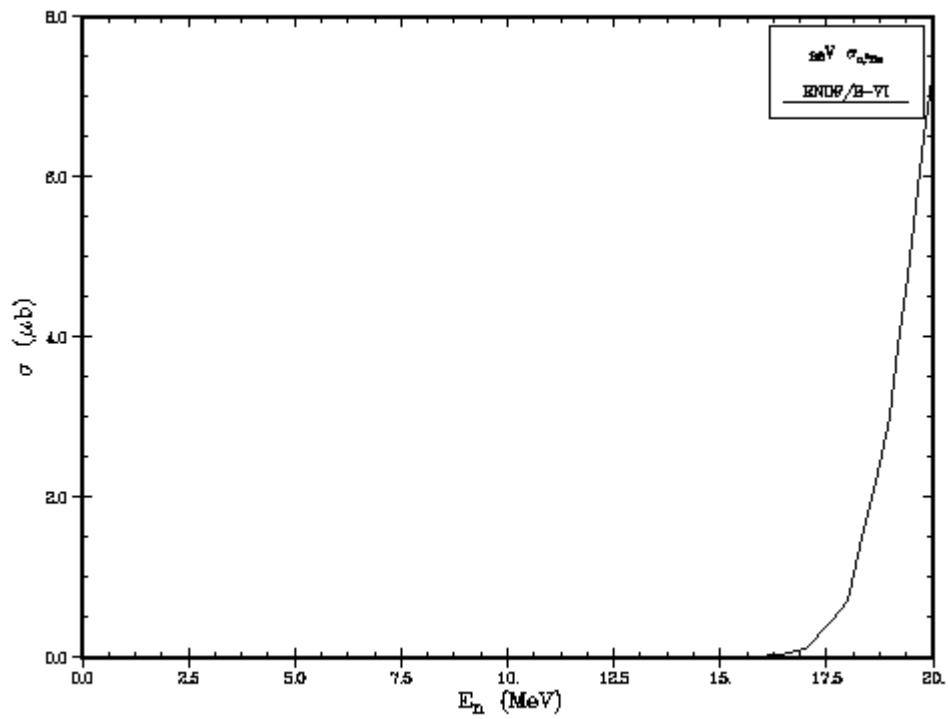


Figure 5.34: ${}^{\text{nat}}\text{V}(n,{}^3\text{He})$ reaction cross section

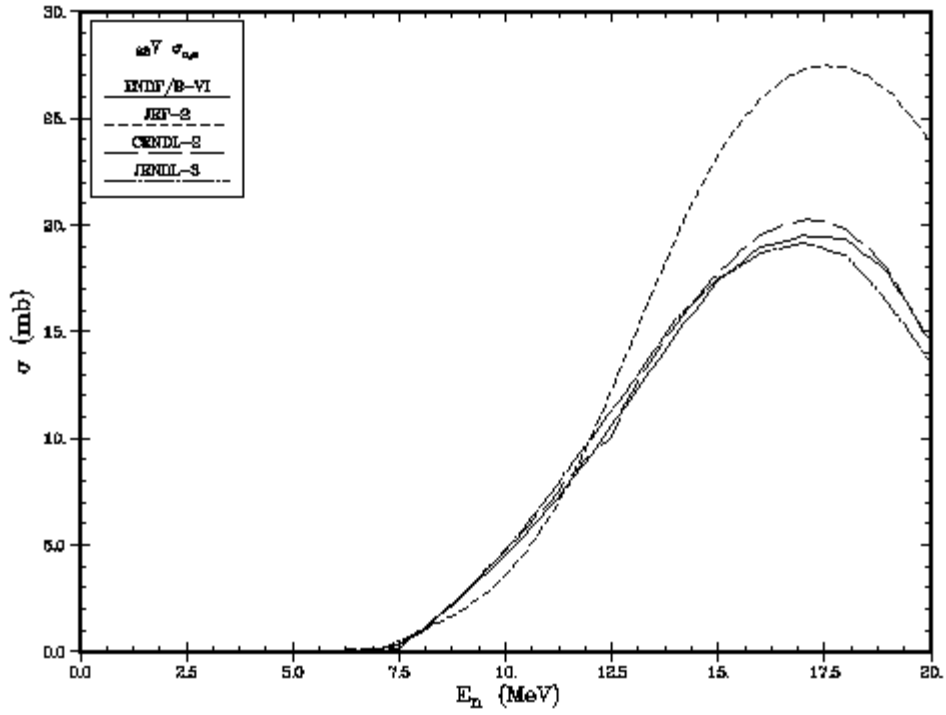


Figure 5.35: ${}^{\text{nat}}\text{V}(n,\alpha)$ reaction cross section

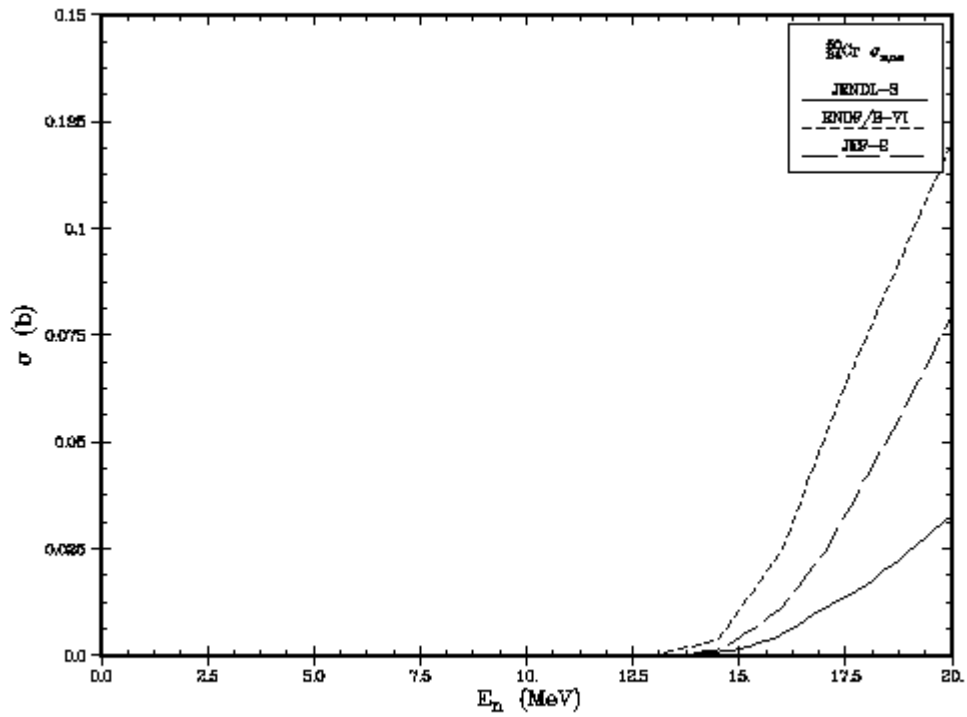


Figure 5.36: ${}^{50}\text{Cr}(n,n\alpha)$ reaction cross section

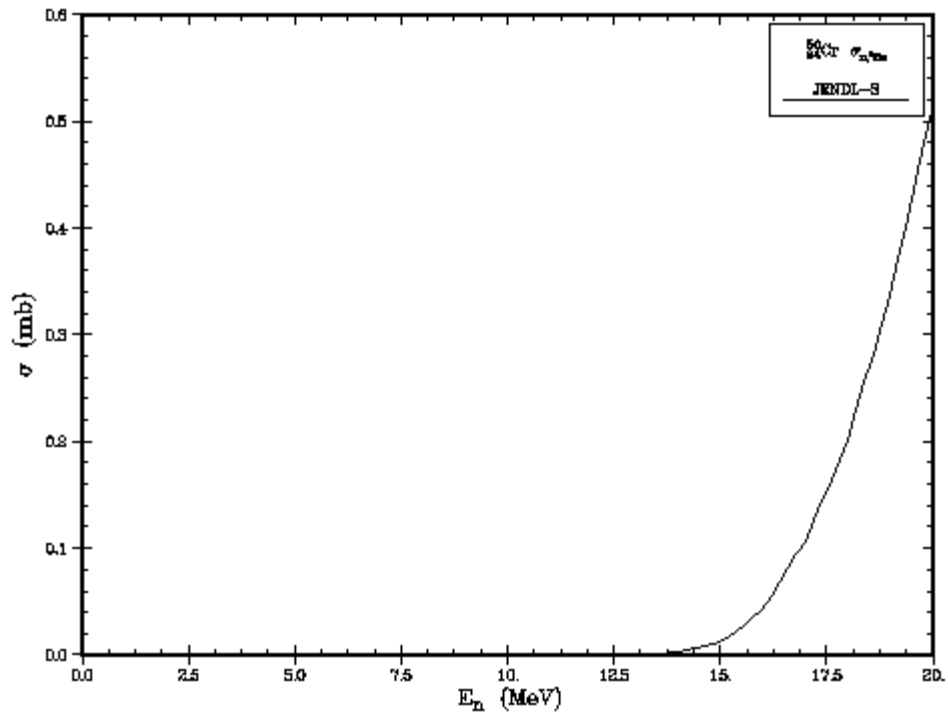


Figure 5.37: $^{50}\text{Cr}(n,^3\text{He})$ reaction cross section

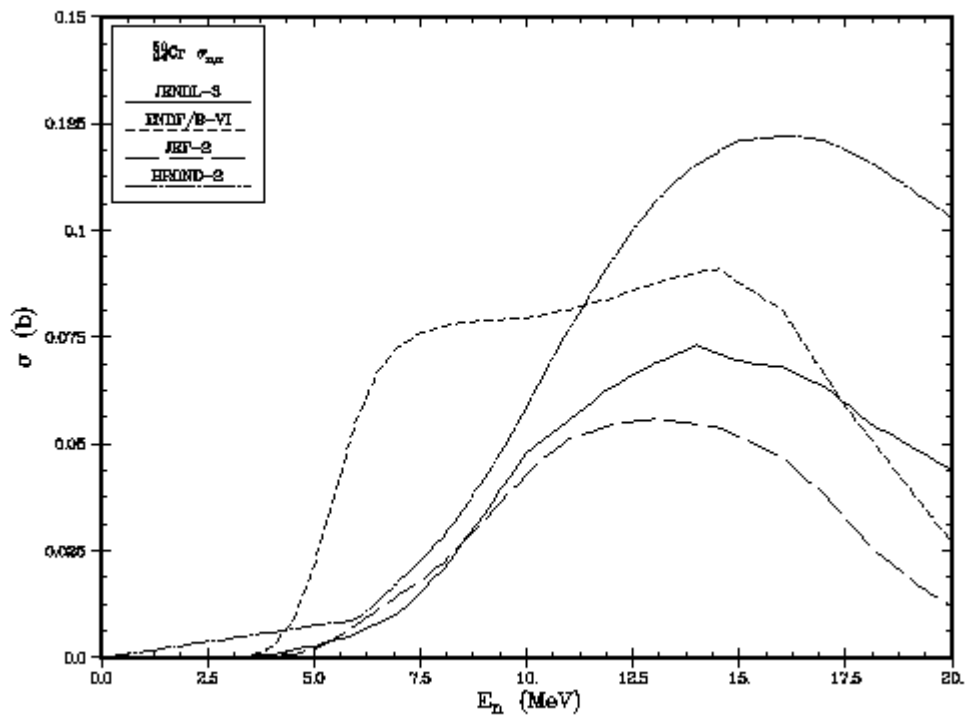


Figure 5.38: $^{50}\text{Cr}(n,\alpha)$ reaction cross section

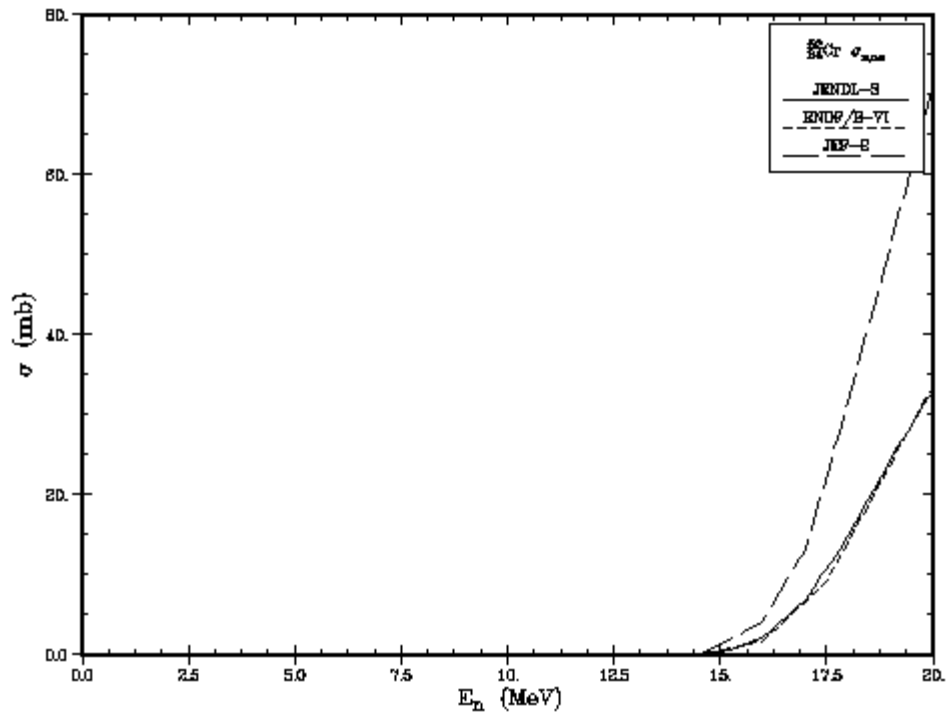


Figure 5.39: $^{52}\text{Cr}(n,n\alpha)$ reaction cross section

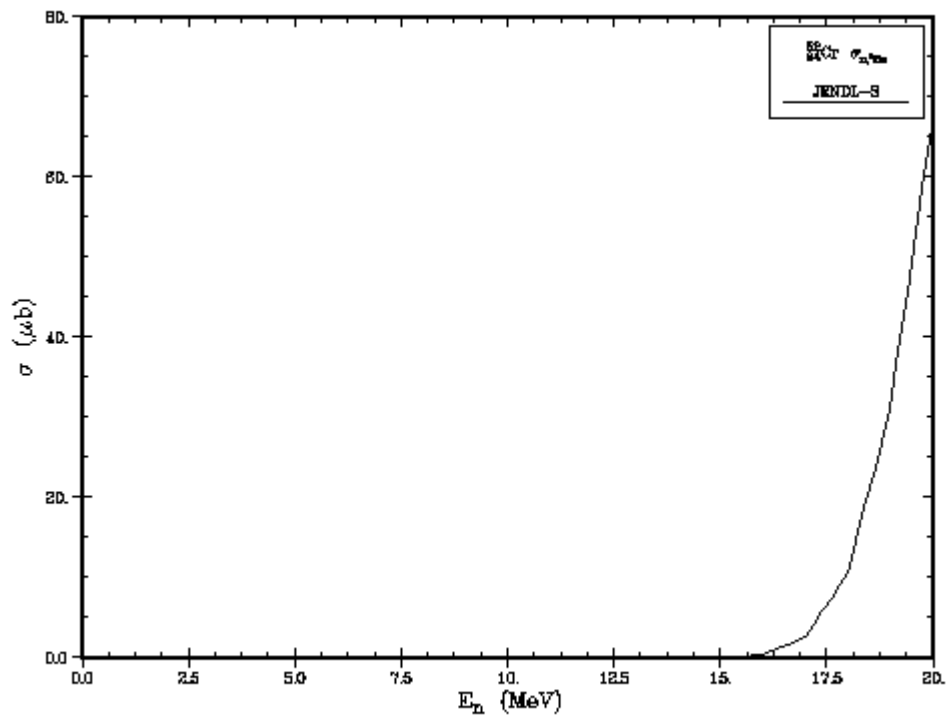


Figure 5.40: $^{52}\text{Cr}(n,^3\text{He})$ reaction cross section

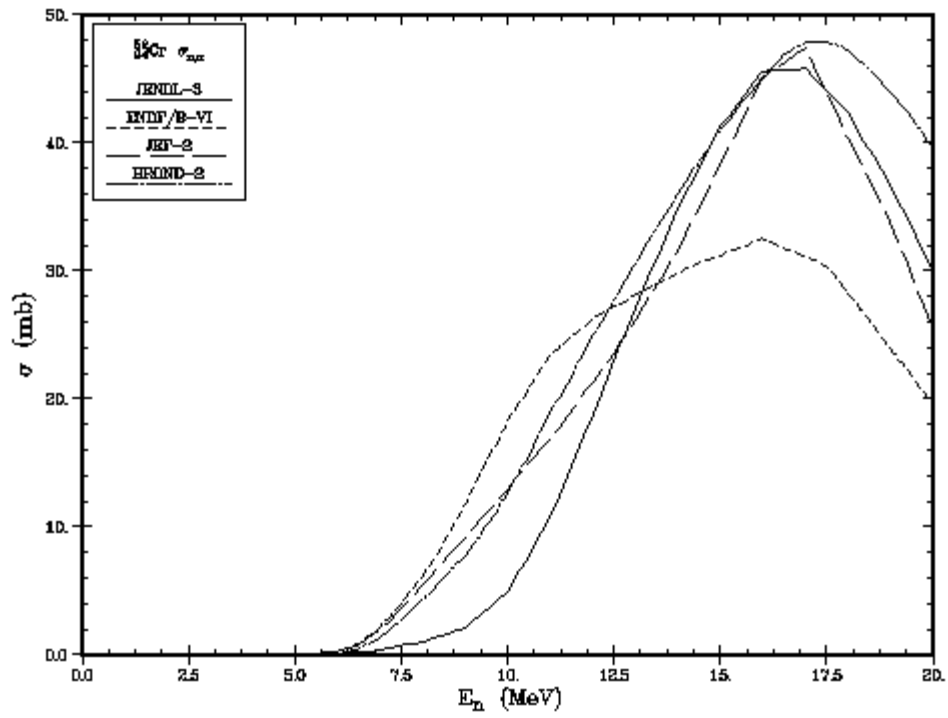


Figure 5.41: $^{52}\text{Cr}(n,\alpha)$ reaction cross section

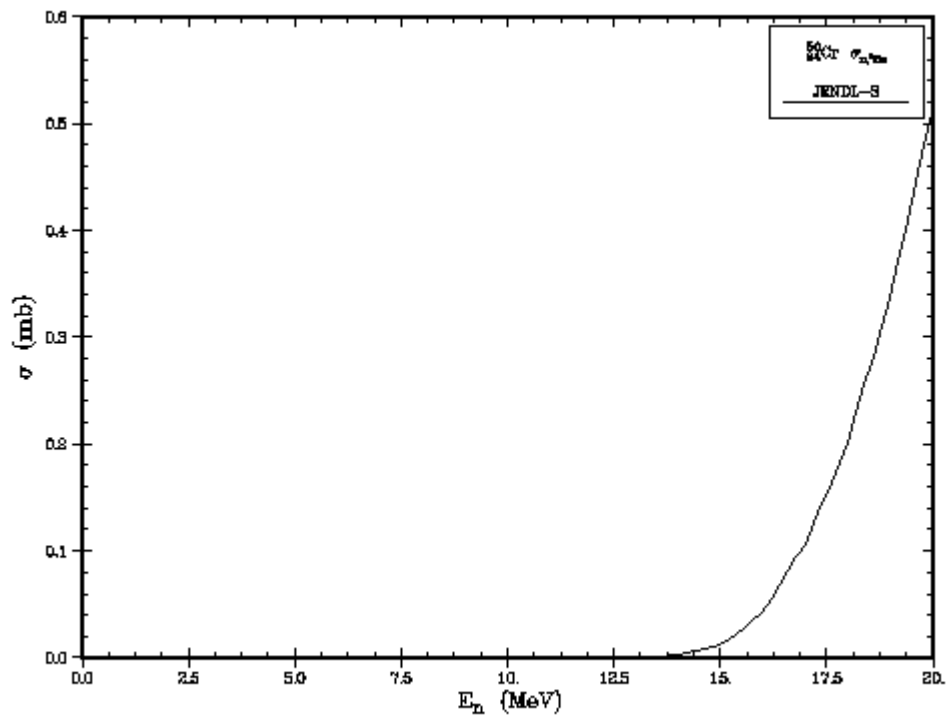


Figure 5.42: $^{53}\text{Cr}(n,\alpha)$ reaction cross section

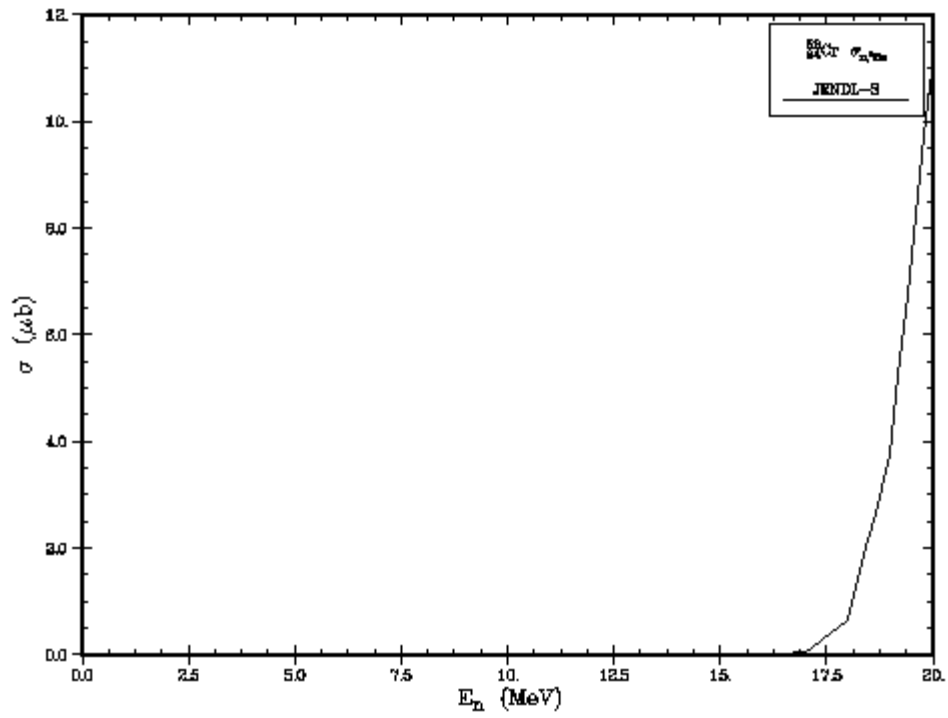


Figure 5.43: $^{53}\text{Cr}(n,^3\text{He})$ reaction cross section

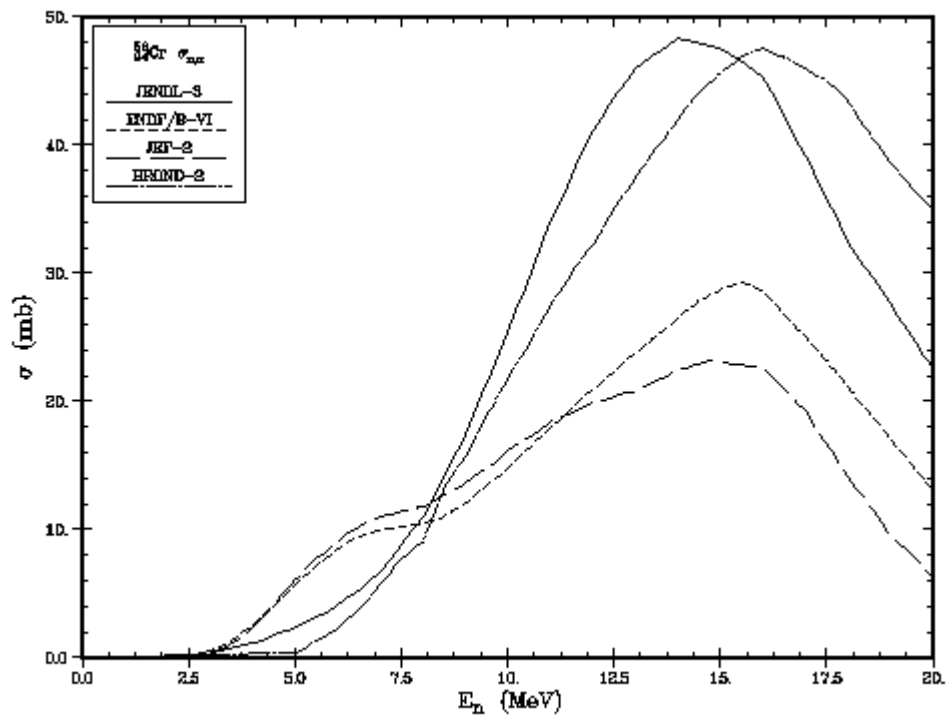


Figure 5.44: $^{53}\text{Cr}(n,\alpha)$ reaction cross section

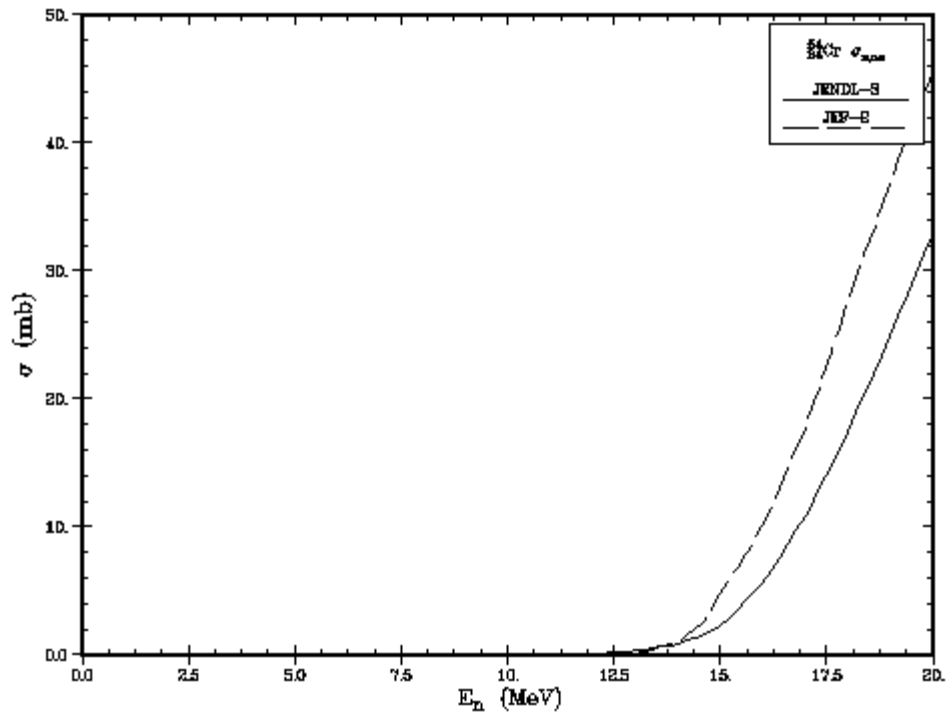


Figure 5.45: $^{54}\text{Cr}(n, n\alpha)$ reaction cross section

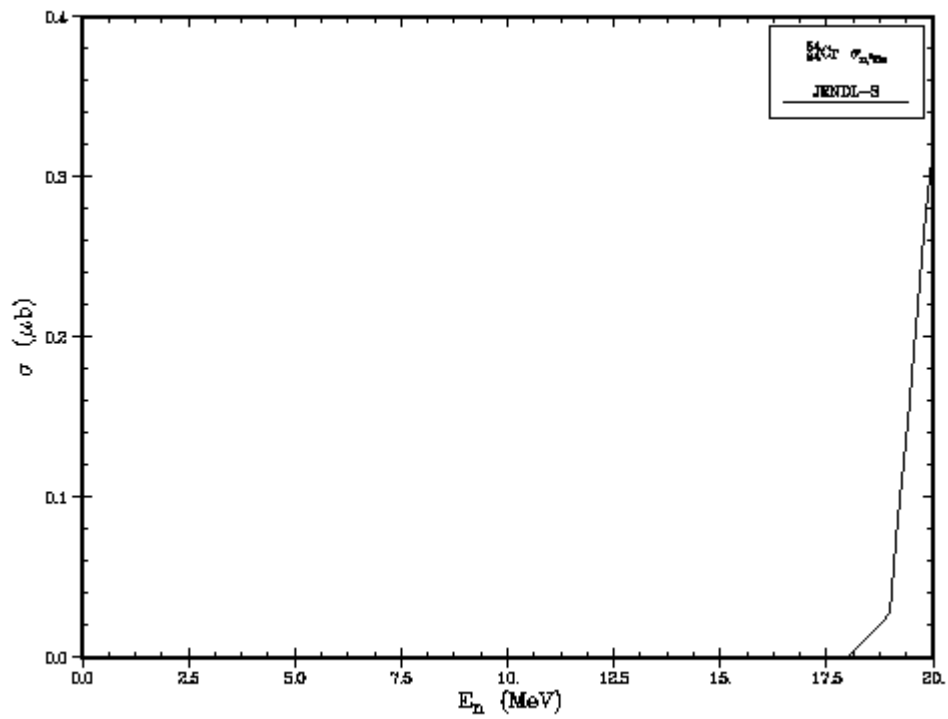


Figure 5.46: $^{54}\text{Cr}(n, ^3\text{He})$ reaction cross section

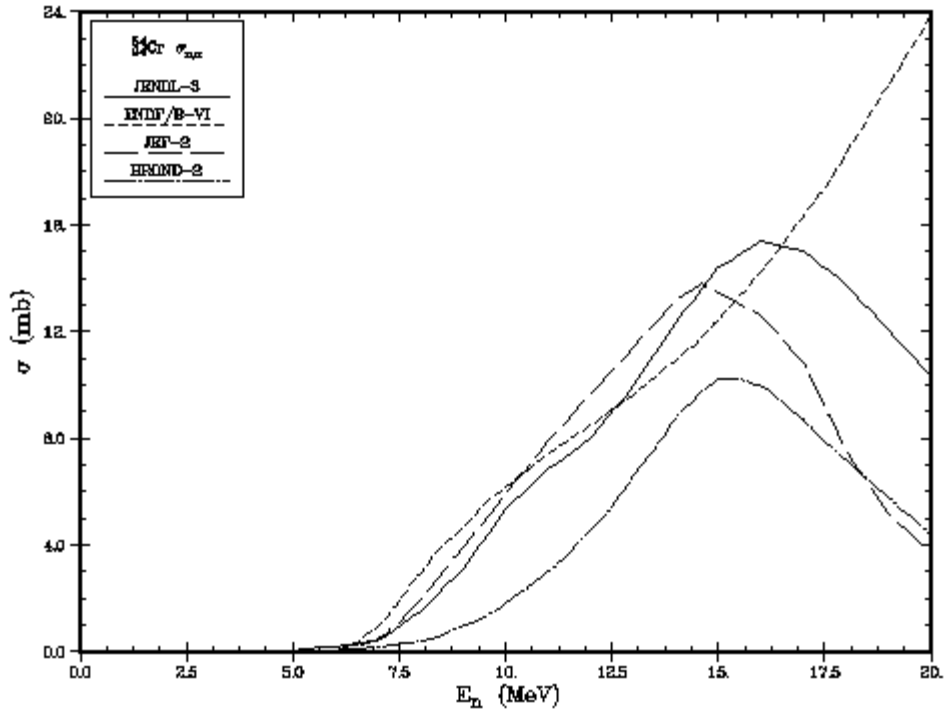


Figure 5.47: $^{54}\text{Cr}(n,\alpha)$ reaction cross section

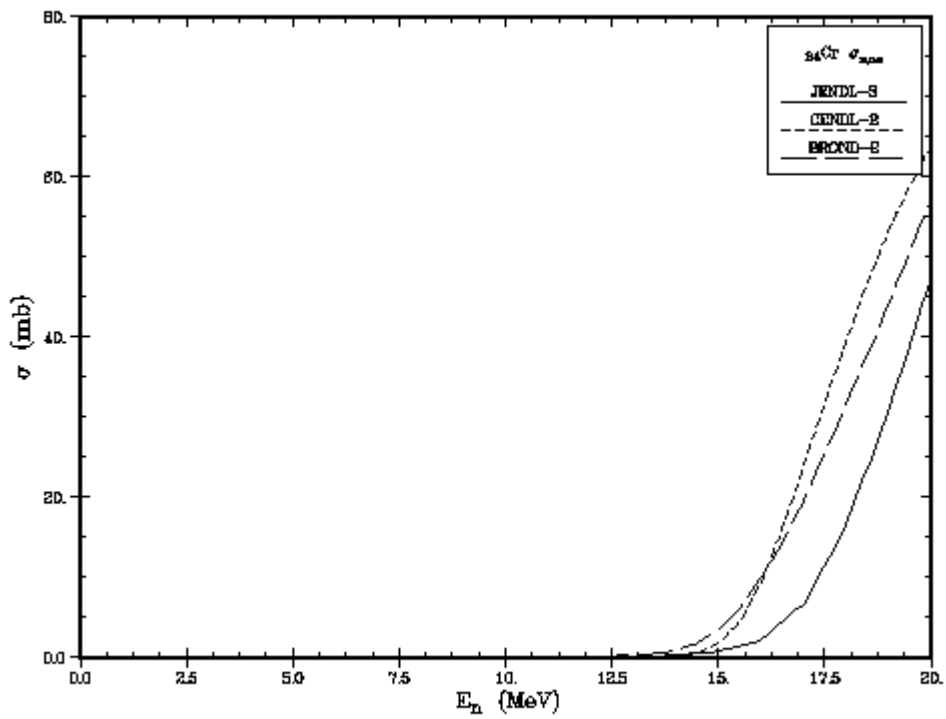


Figure 5.48: $^{\text{nat}}\text{Cr}(n,\alpha)$ reaction cross section

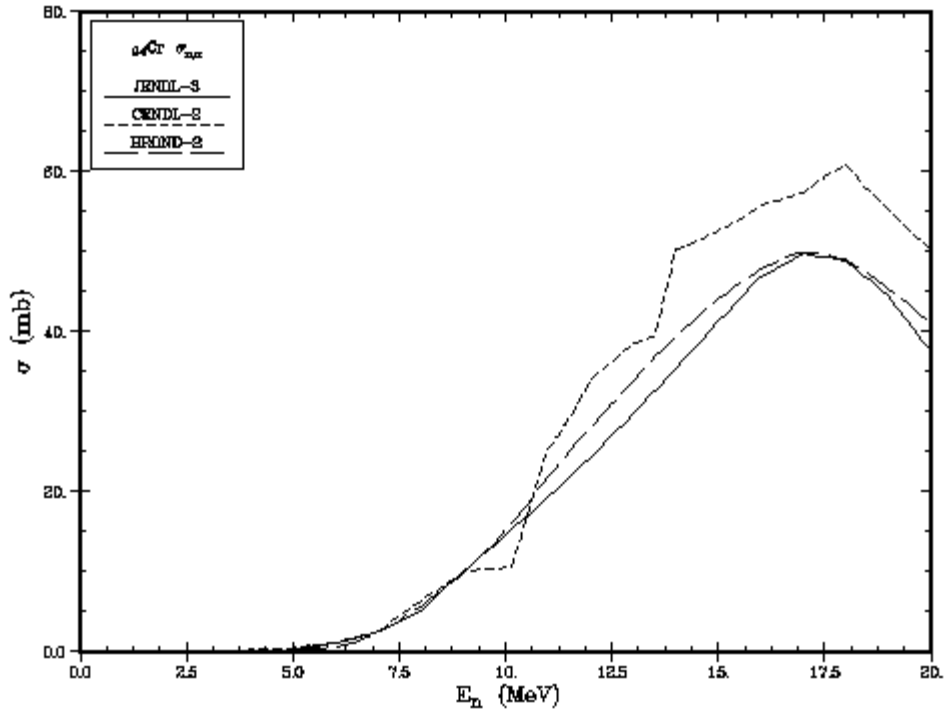


Figure 5.49: $^{nat}\text{Cr}(n,\alpha)$ reaction cross section

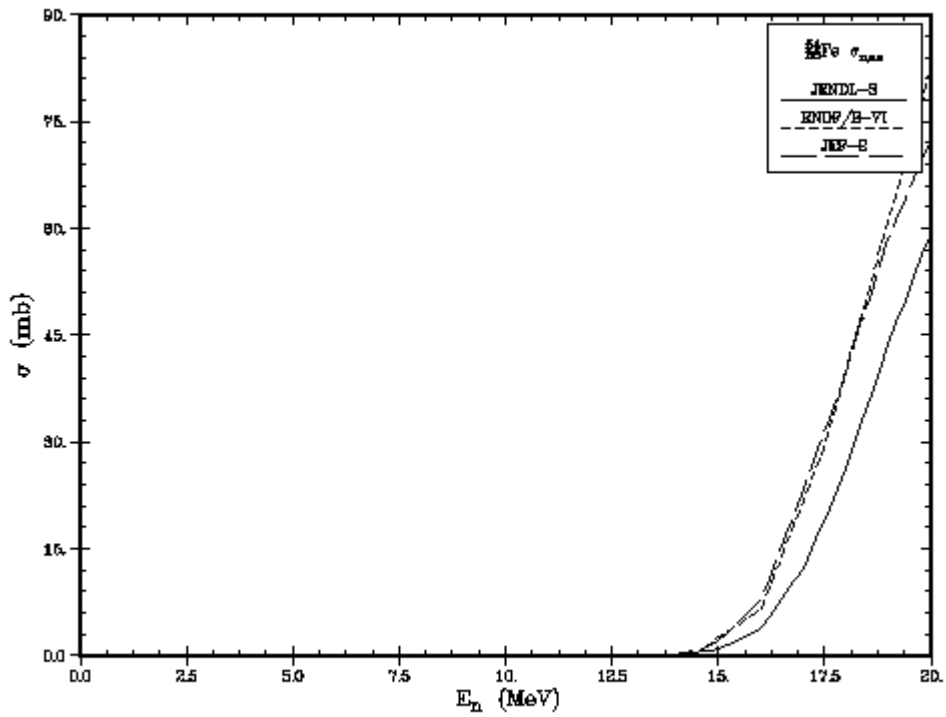


Figure 5.50: $^{54}\text{Fe}(n,\alpha)$ reaction cross section

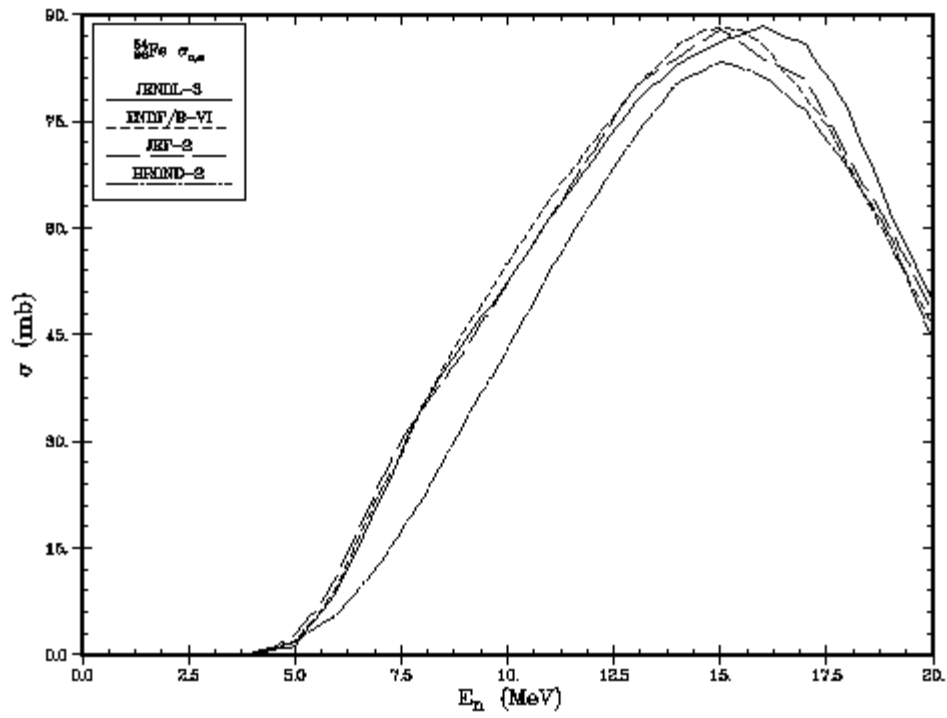


Figure 5.51: $^{54}\text{Fe}(n,\alpha)$ reaction cross section

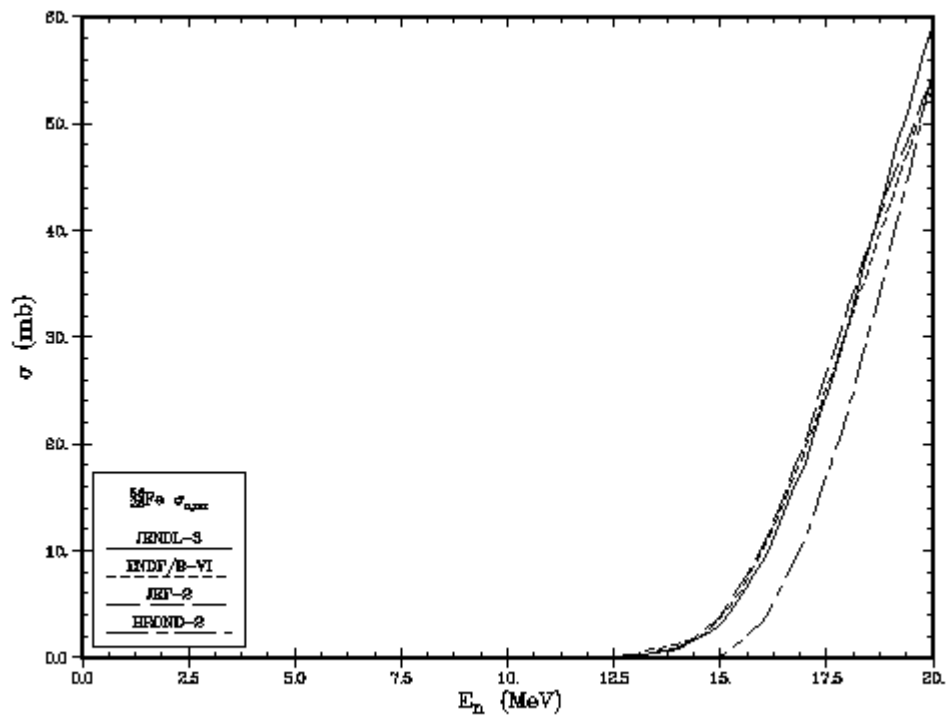


Figure 5.52: $^{56}\text{Fe}(n,n\alpha)$ reaction cross section

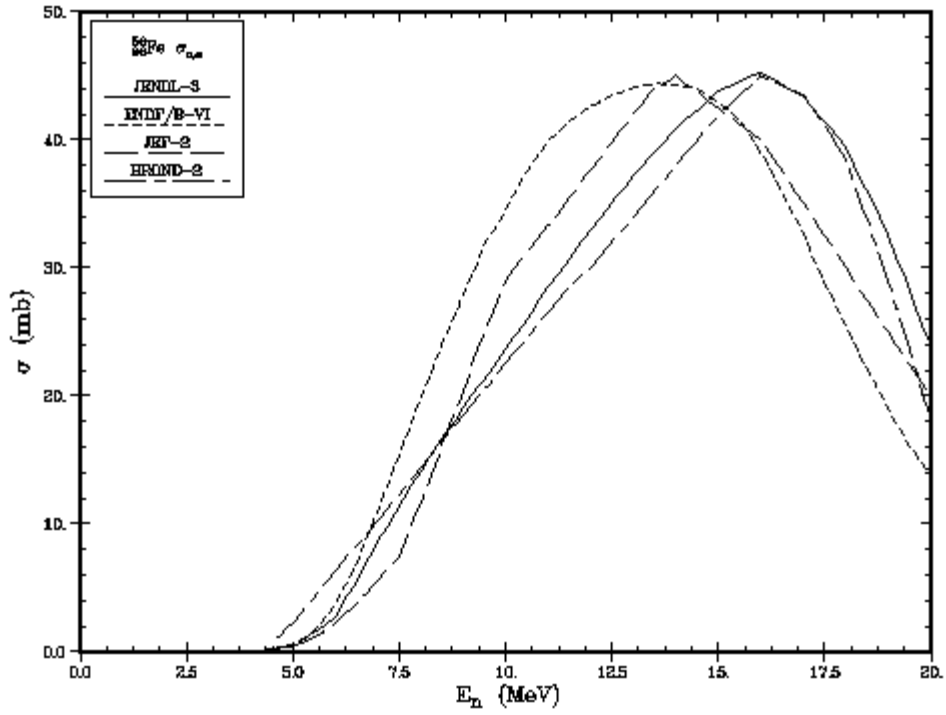


Figure 5.53: $^{56}\text{Fe}(n,\alpha)$ reaction cross section

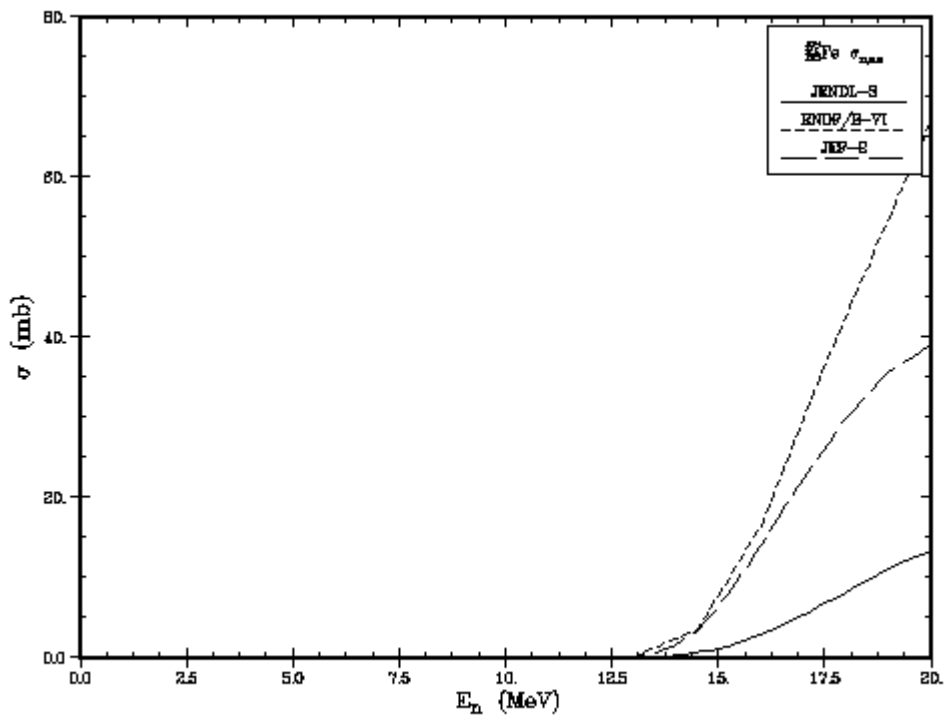


Figure 5.54: $^{57}\text{Fe}(n,n\alpha)$ reaction cross section

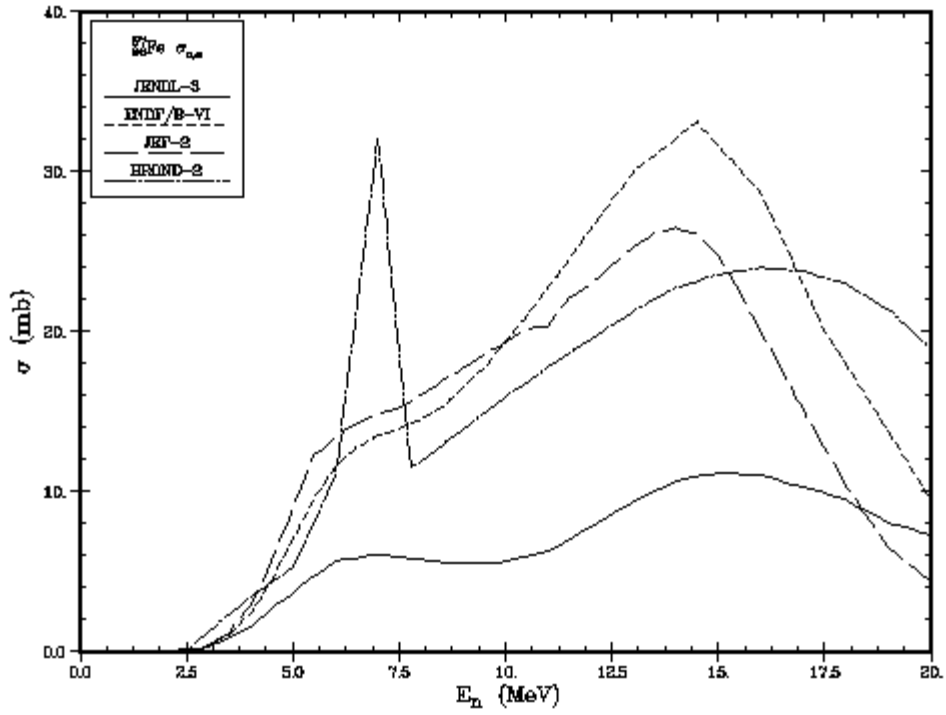


Figure 5.55: $^{57}\text{Fe}(n,\alpha)$ reaction cross section

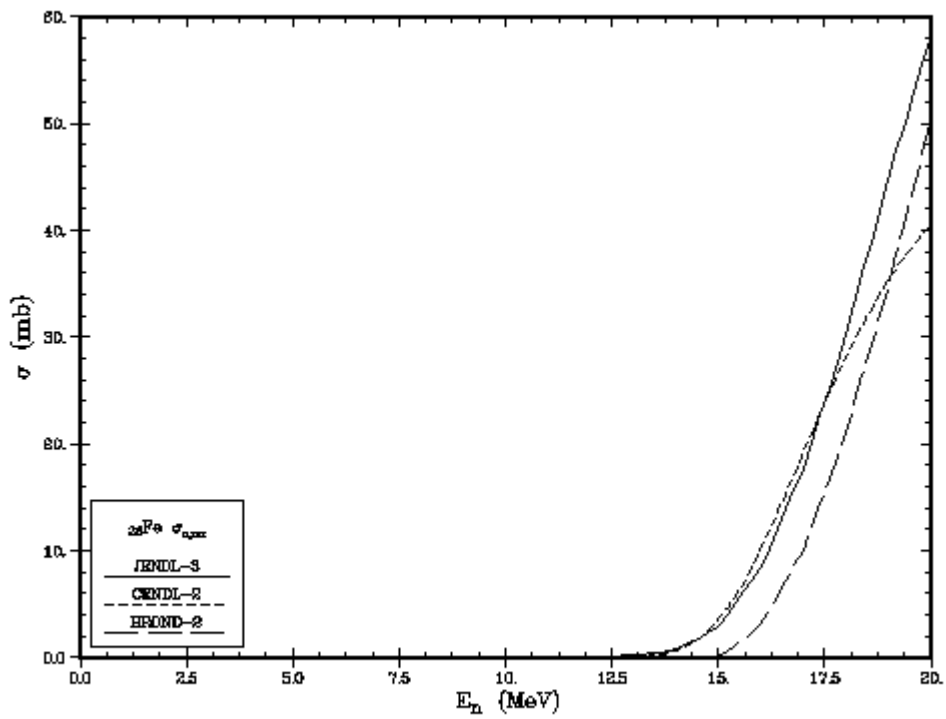


Figure 5.56: $^{\text{nat}}\text{Fe}(n,\alpha)$ reaction cross section

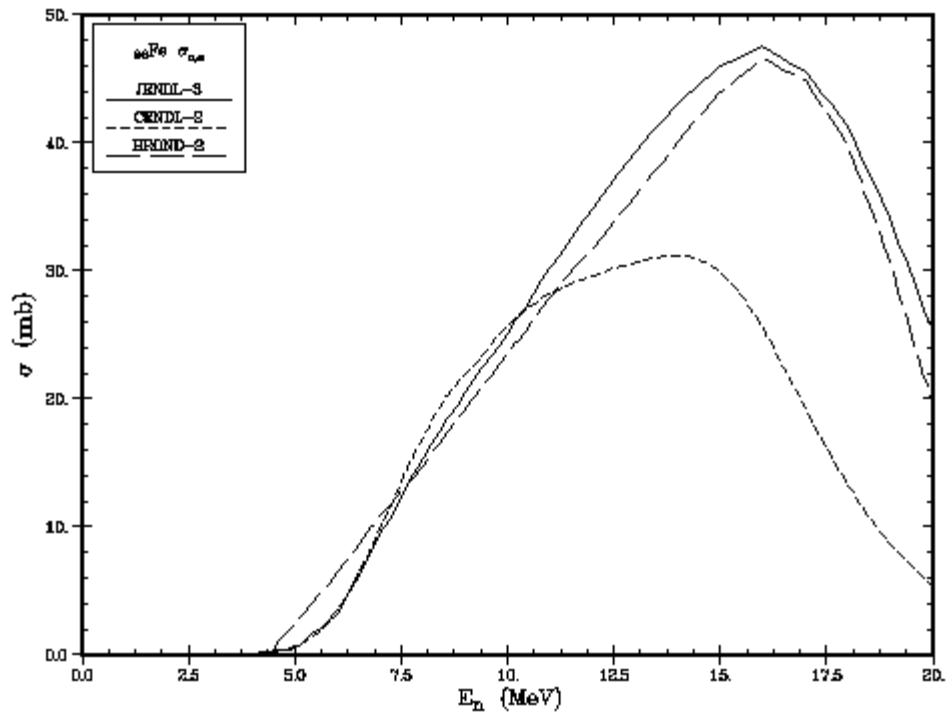


Figure 5.57: $^{nat}\text{Fe}(n,\alpha)$ reaction cross section

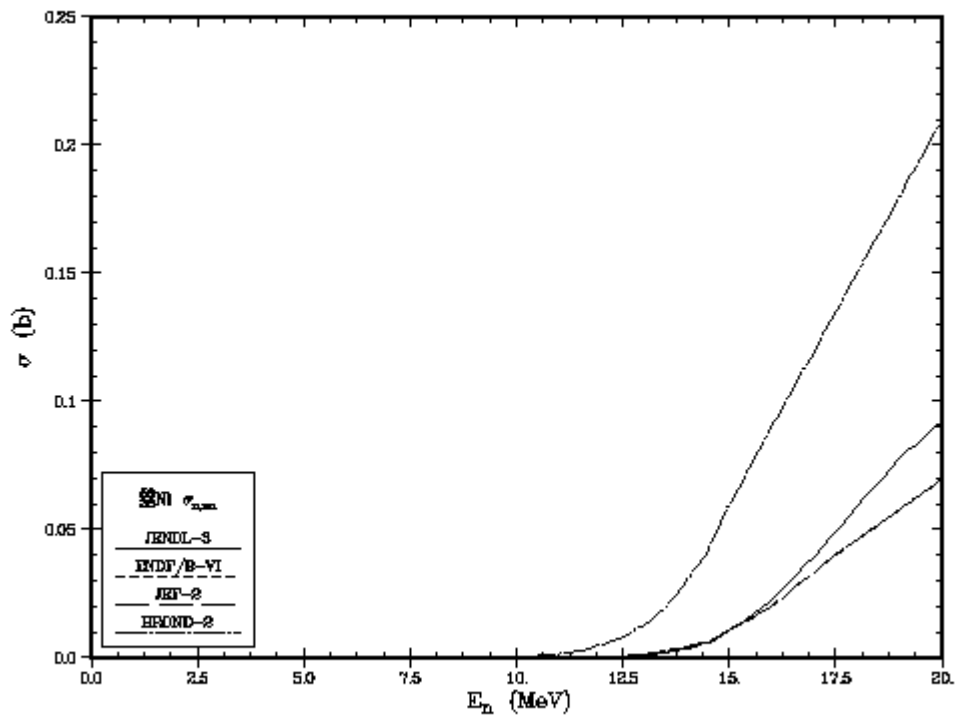


Figure 5.58: $^{58}\text{Ni}(n,n\alpha)$ reaction cross section

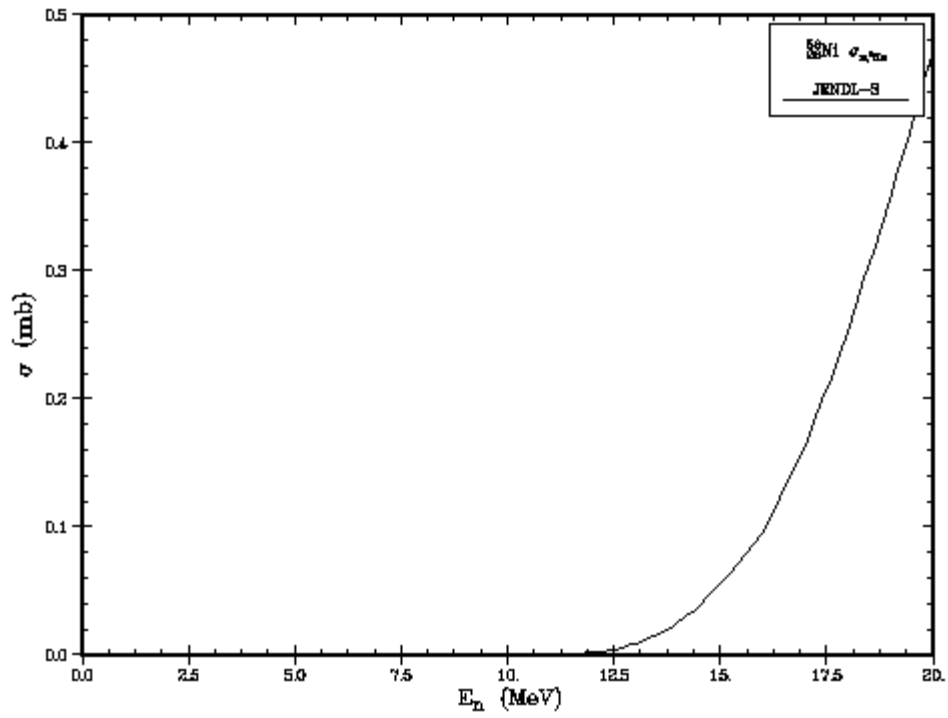


Figure 5.59: $^{58}\text{Ni}(n,^3\text{He})$ reaction cross section

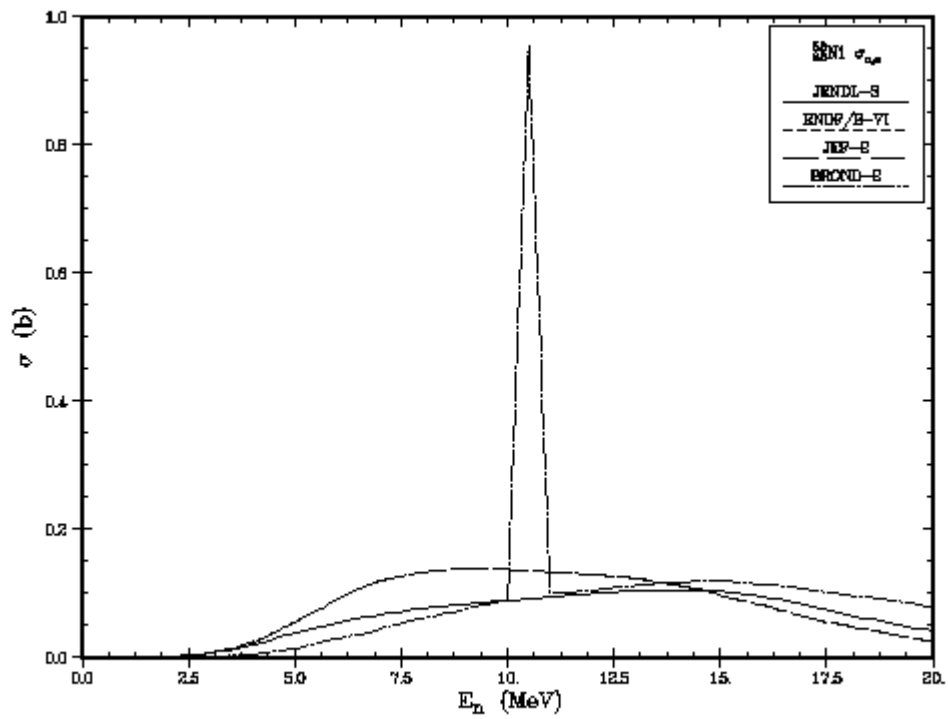


Figure 5.60: $^{58}\text{Ni}(n,\alpha)$ reaction cross section

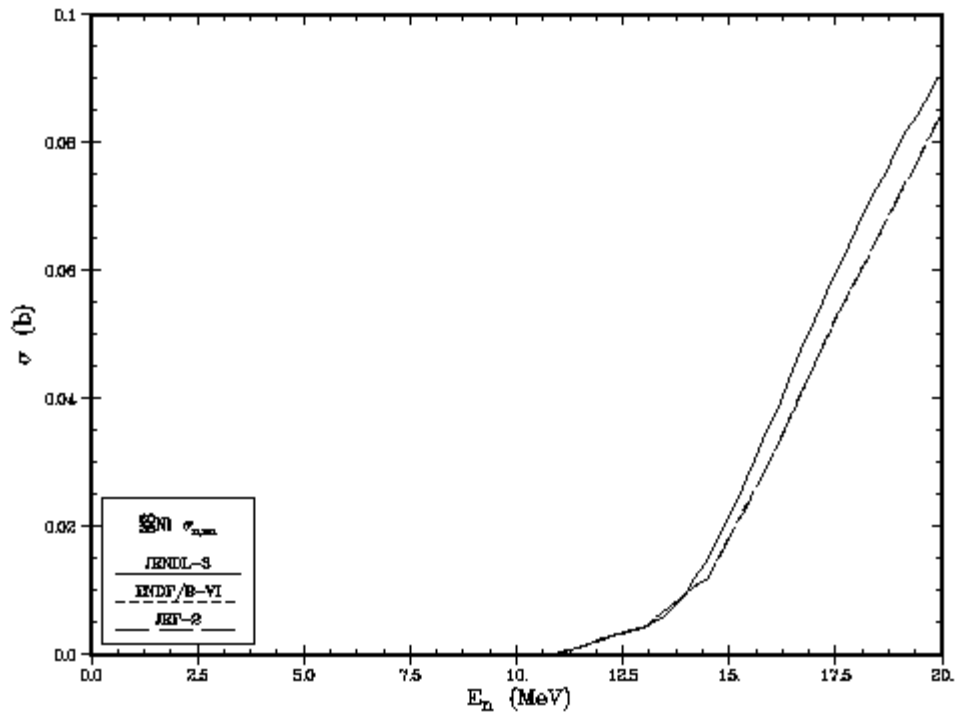


Figure 5.61: $^{60}\text{Ni}(n, n\alpha)$ reaction cross section

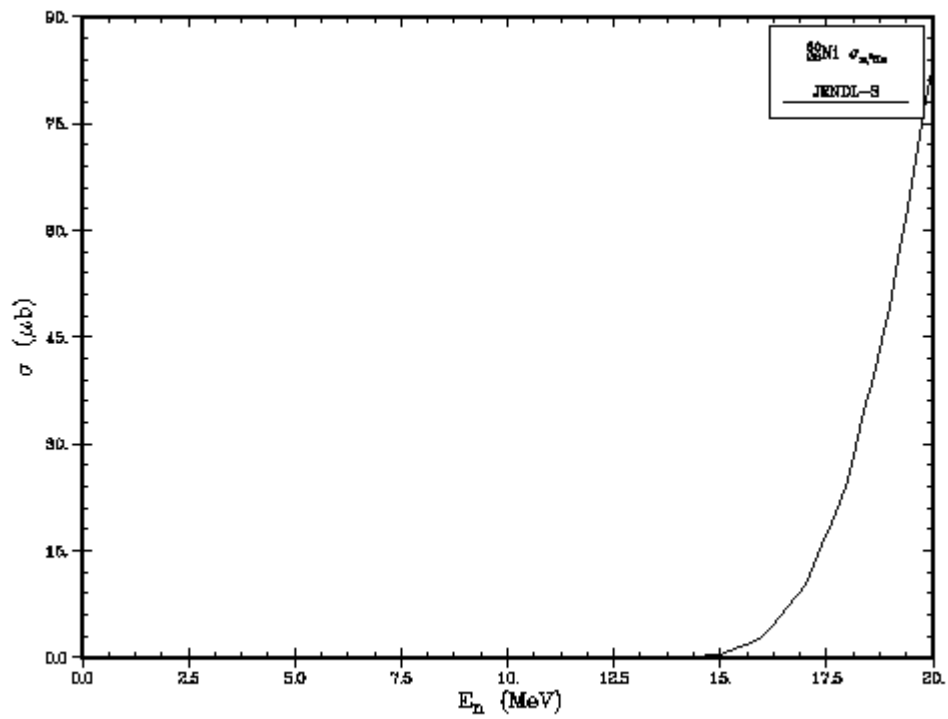


Figure 5.62: $^{60}\text{Ni}(n, ^3\text{He})$ reaction cross section

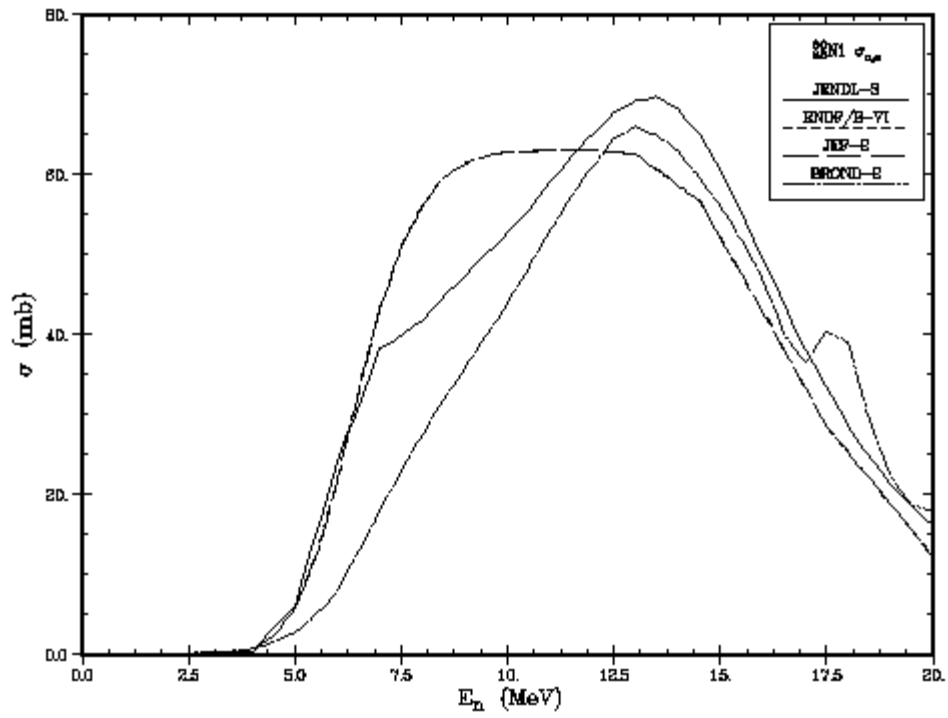


Figure 5.63: $^{60}\text{Ni}(n,\alpha)$ reaction cross section

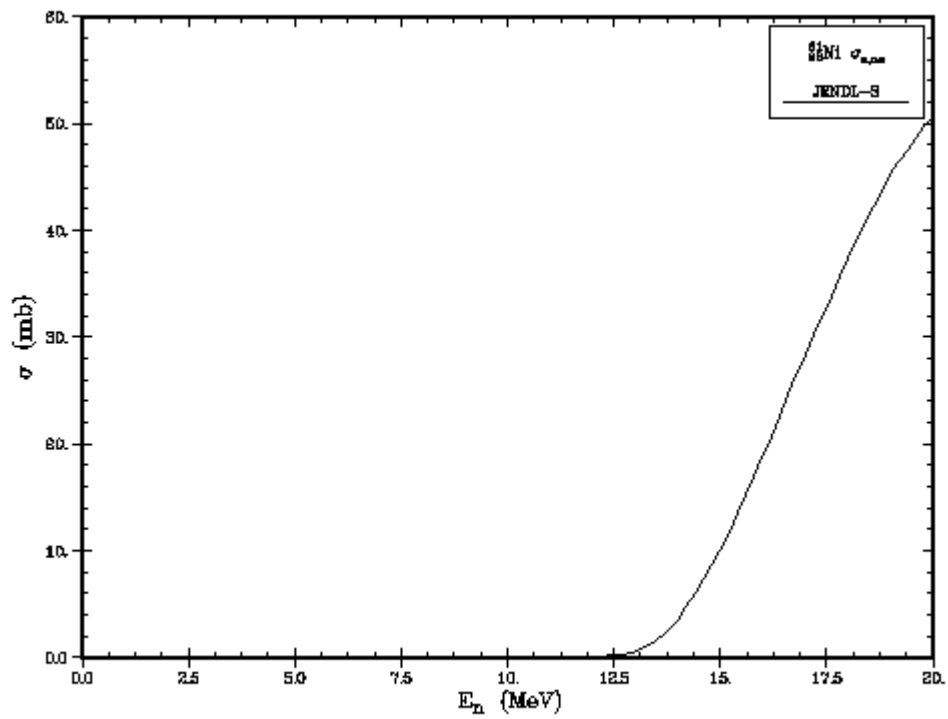


Figure 5.64: $^{61}\text{Ni}(n,n\alpha)$ reaction cross section

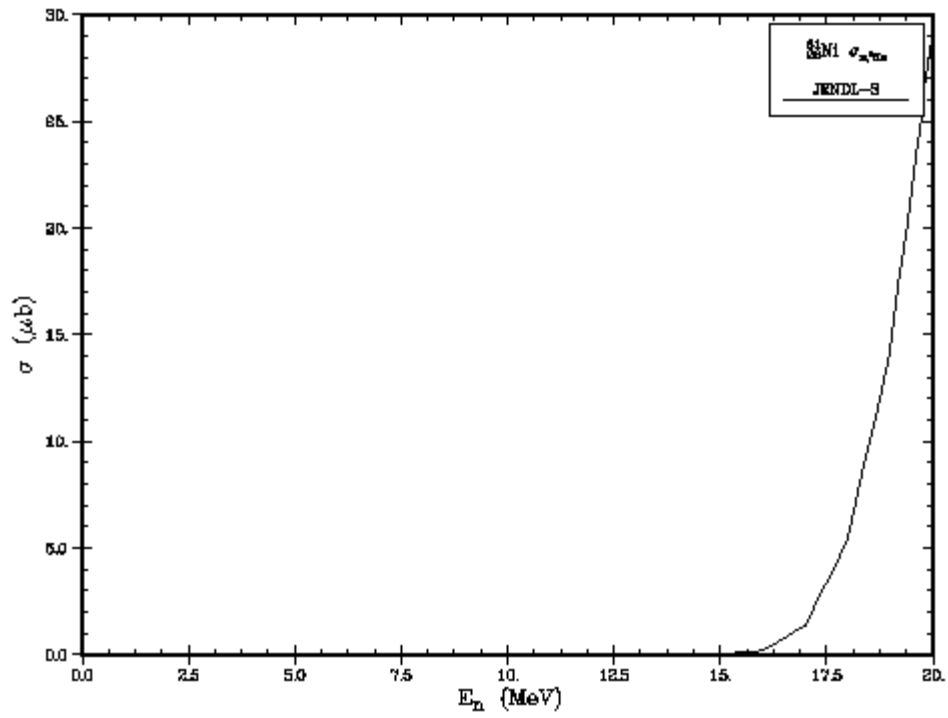


Figure 5.65: $^{61}\text{Ni}(n,^3\text{He})$ reaction cross section

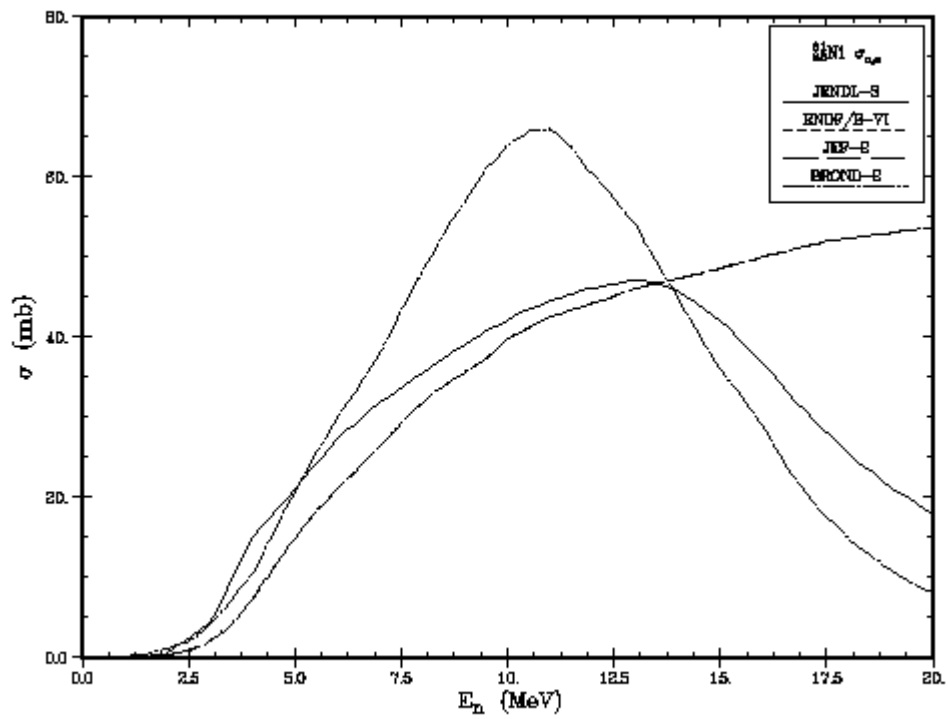


Figure 5.66: $^{61}\text{Ni}(n,\alpha)$ reaction cross section

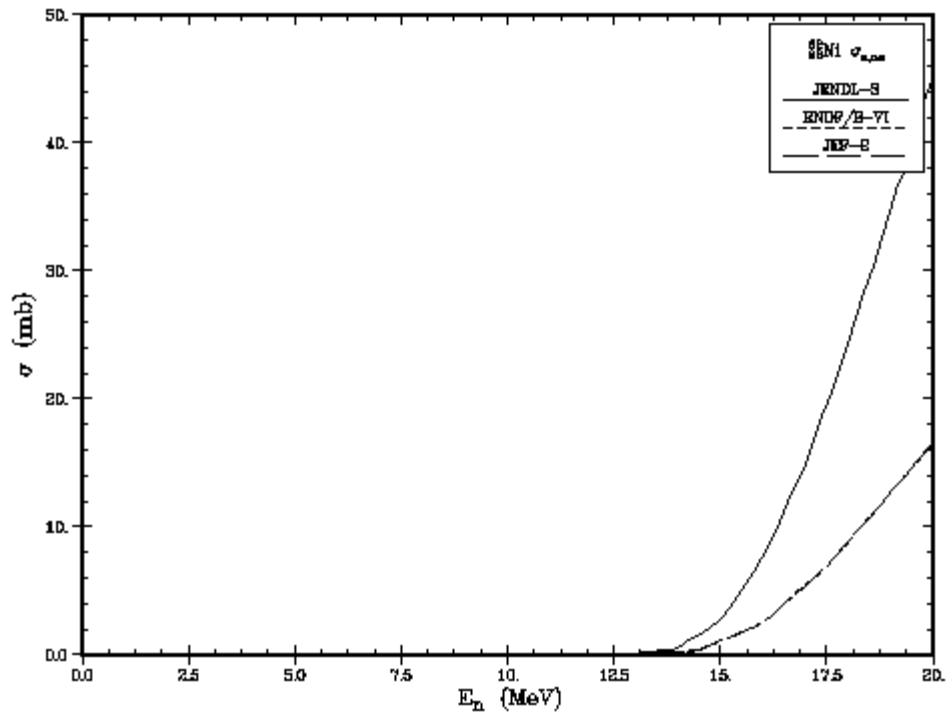


Figure 5.67: $^{62}\text{Ni}(n, n\alpha)$ reaction cross section

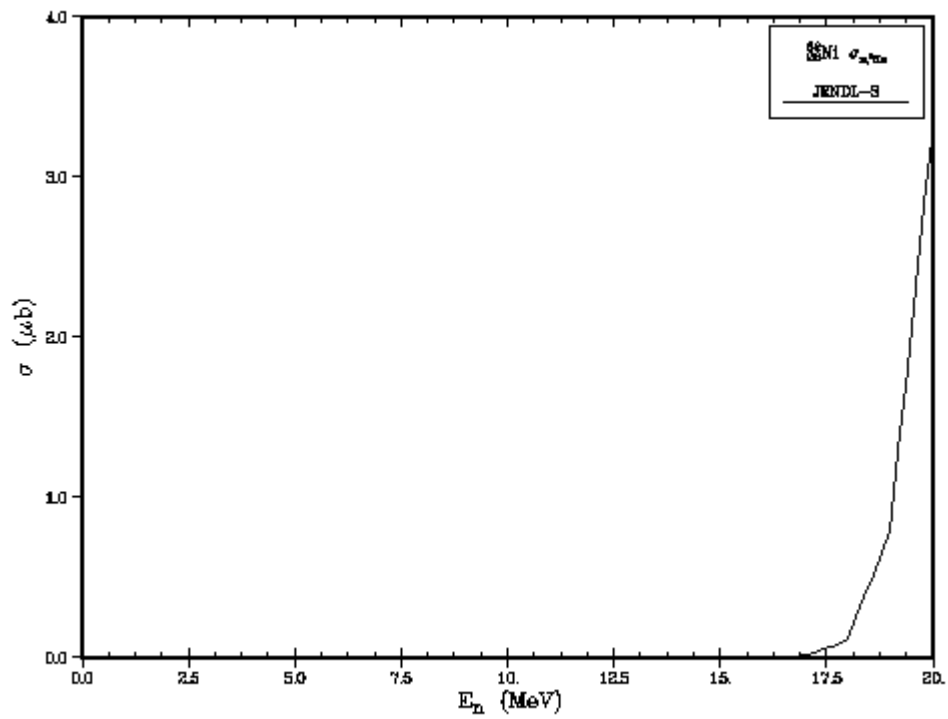


Figure 5.68: $^{62}\text{Ni}(n, ^3\text{He})$ reaction cross section

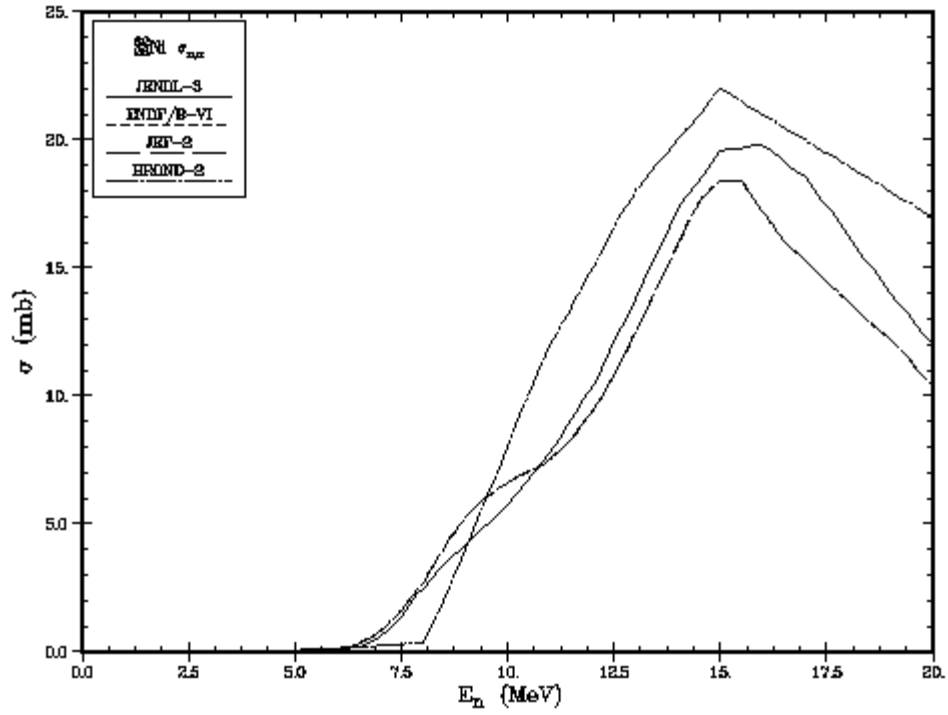


Figure 5.69: $^{62}\text{Ni}(n,\alpha)$ reaction cross section

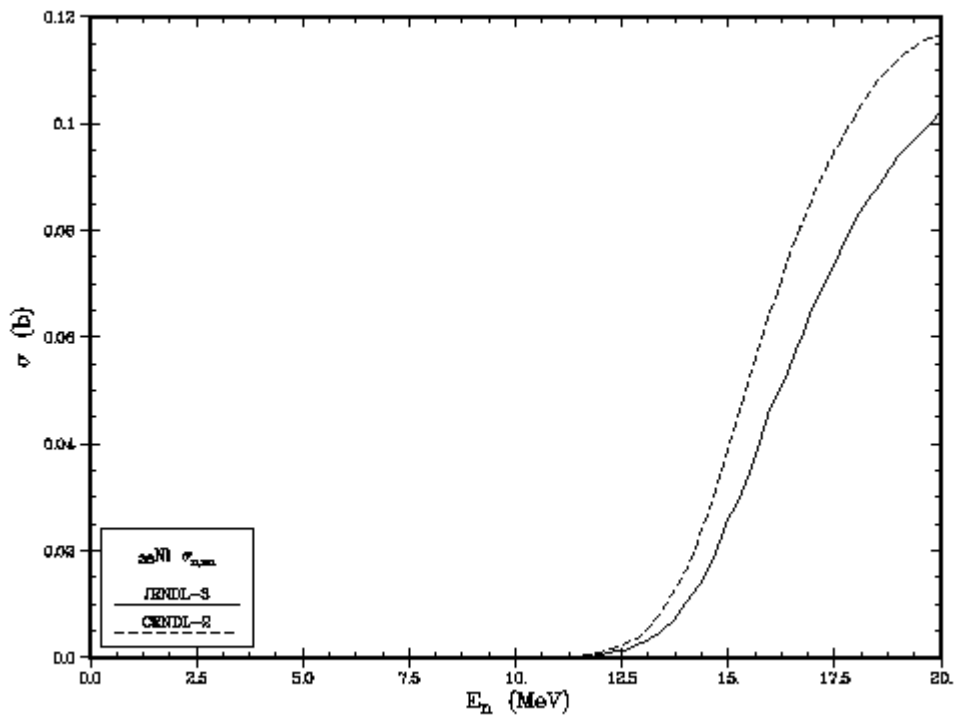


Figure 5.70: $^{\text{nat}}\text{Ni}(n,\alpha)$ reaction cross section

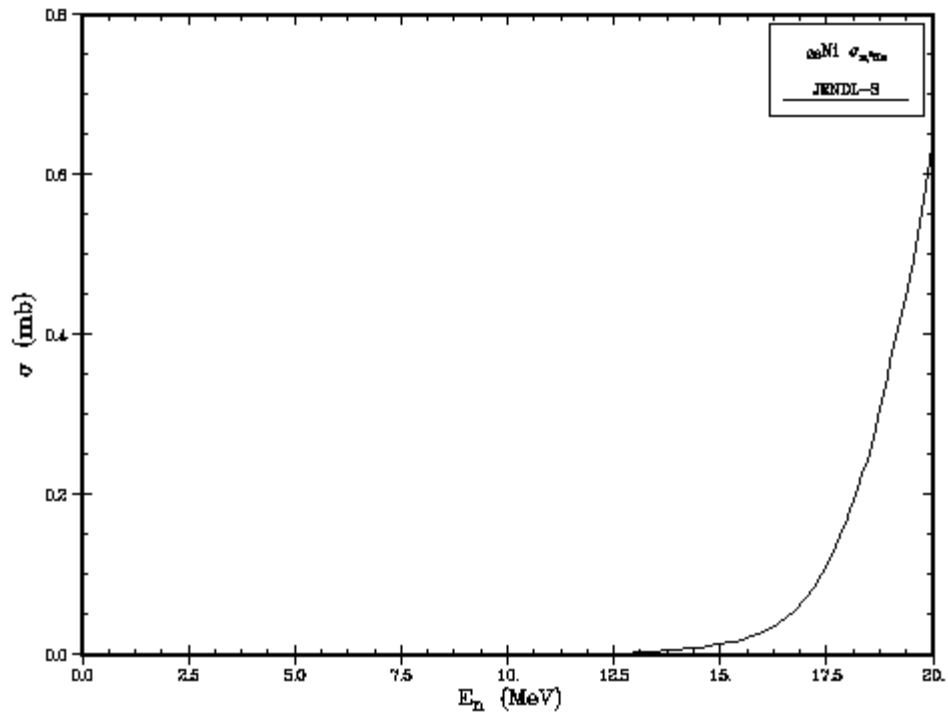


Figure 5.71: ${}^{\text{nat}}\text{Ni}(n, {}^3\text{He})$ reaction cross section

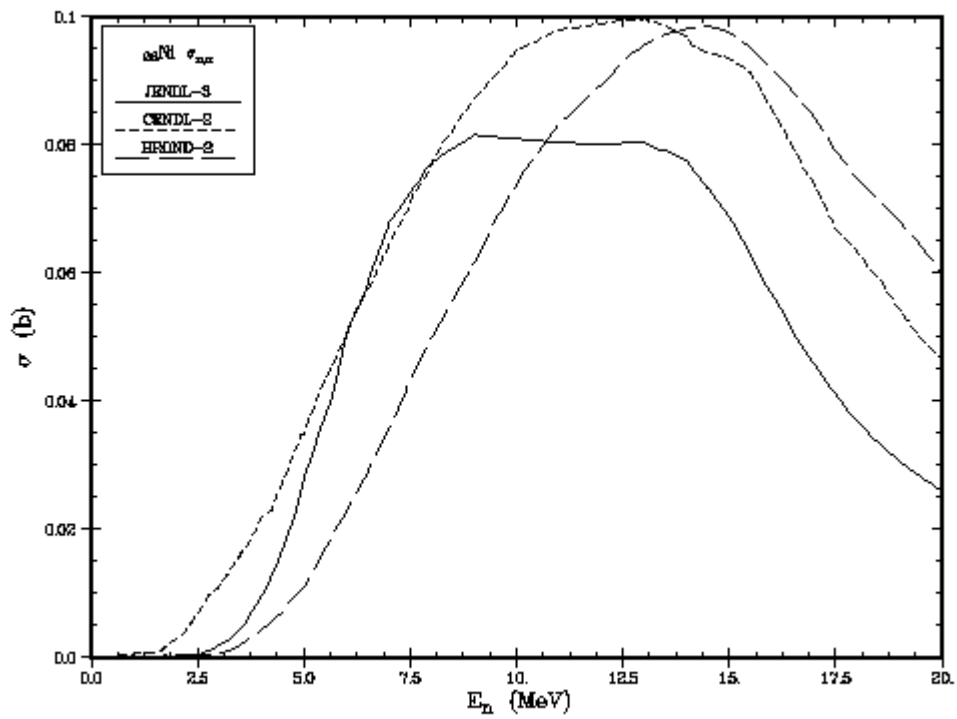


Figure 5.72: ${}^{\text{nat}}\text{Ni}(n, \alpha)$ reaction cross section

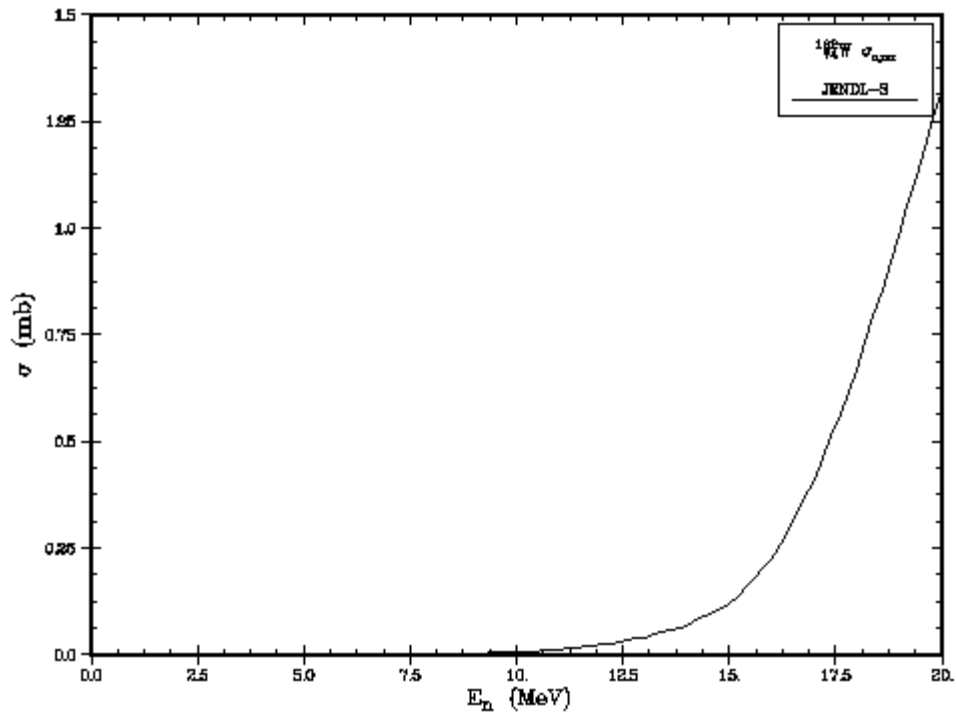


Figure 5.73: $^{182}\text{W}(n,\alpha)$ reaction cross section

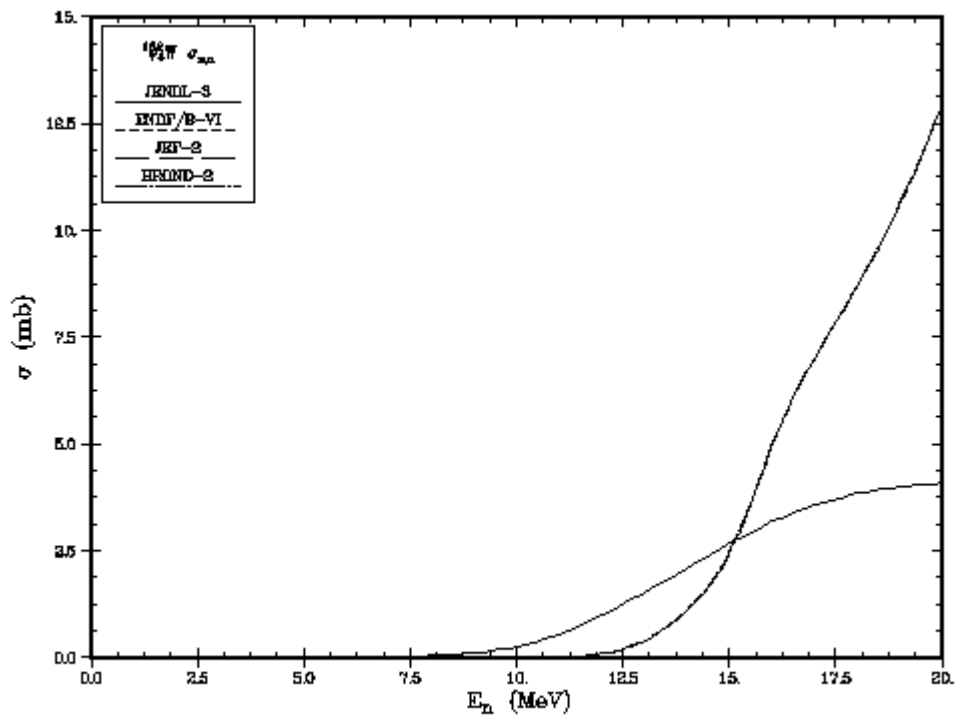


Figure 5.74: $^{182}\text{W}(n,\alpha)$ reaction cross section

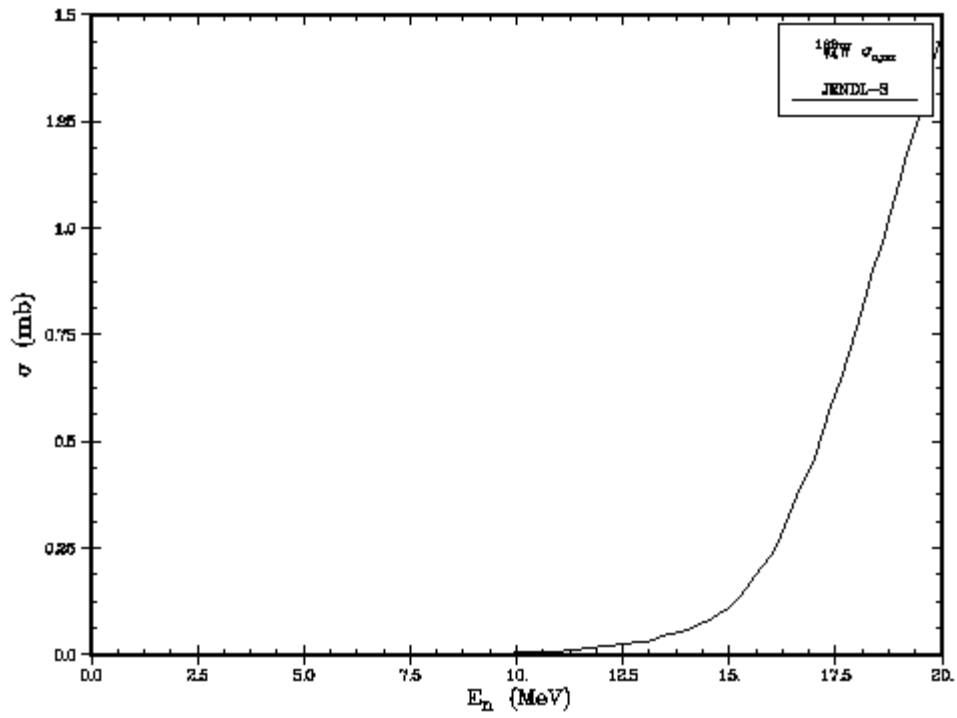


Figure 5.75: $^{183}\text{W}(n,\alpha)$ reaction cross section

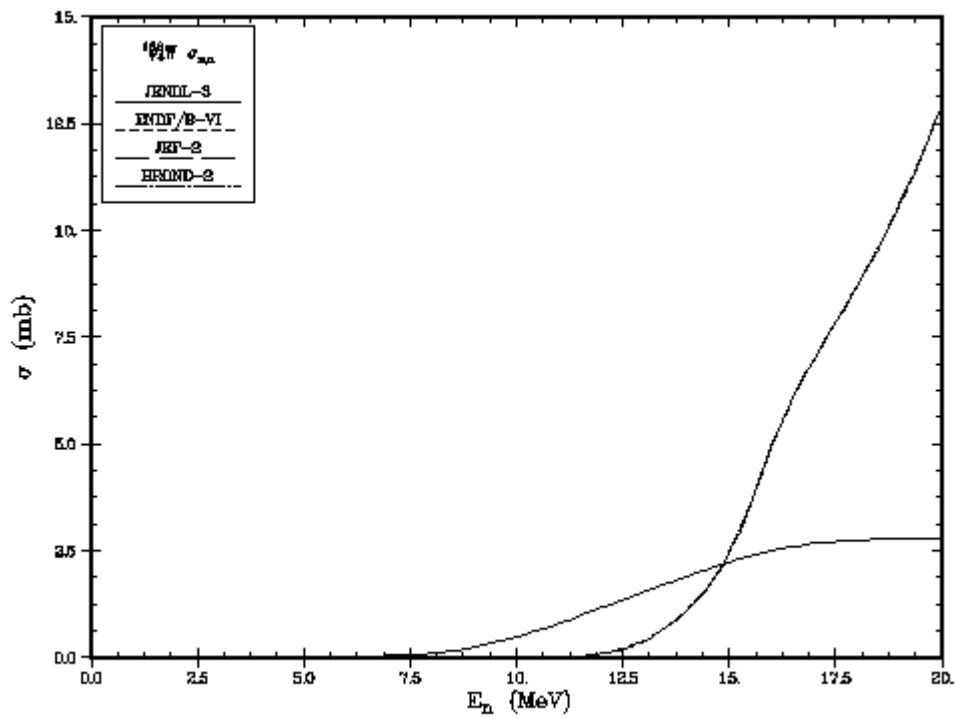


Figure 5.76: $^{183}\text{W}(n,\alpha)$ reaction cross section

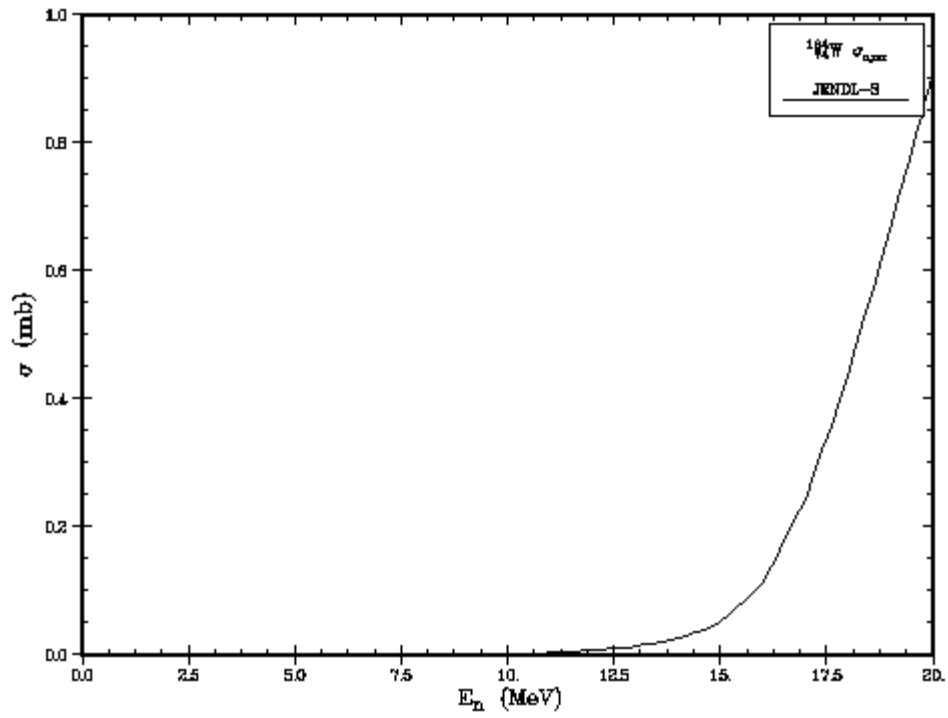


Figure 5.77: $^{184}\text{W}(n,\alpha)$ reaction cross section

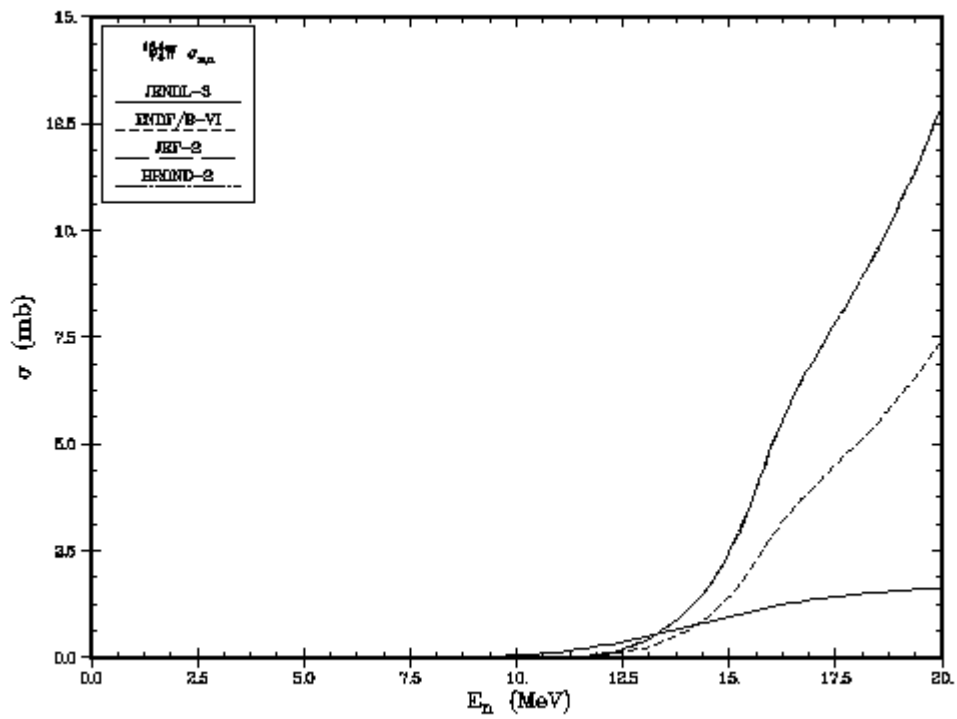


Figure 5.78: $^{184}\text{W}(n,\alpha)$ reaction cross section

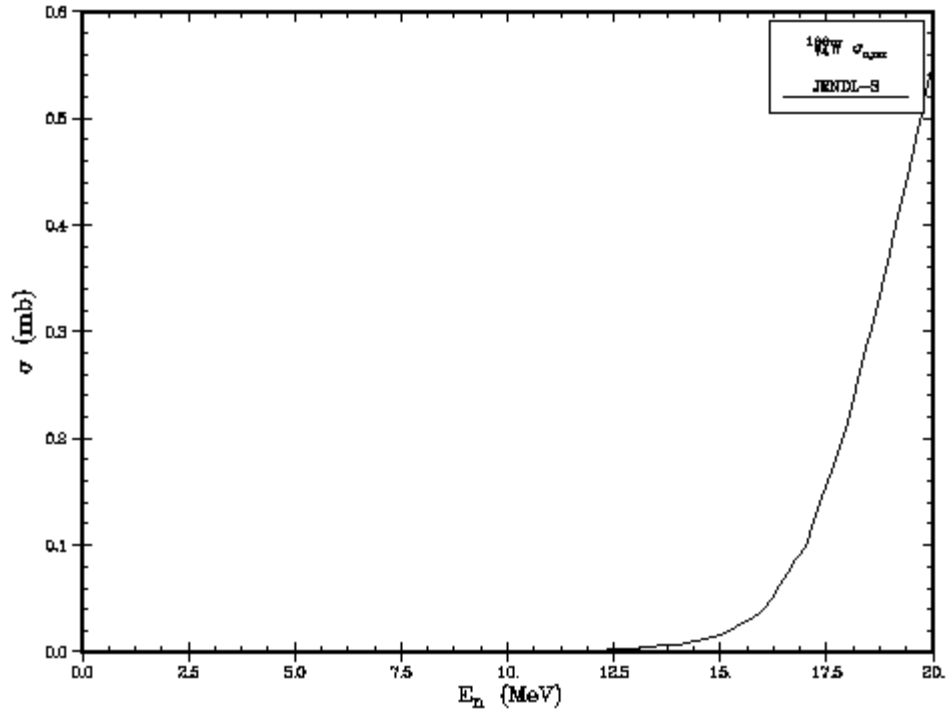


Figure 5.79: $^{186}\text{W}(n,\alpha)$ reaction cross section

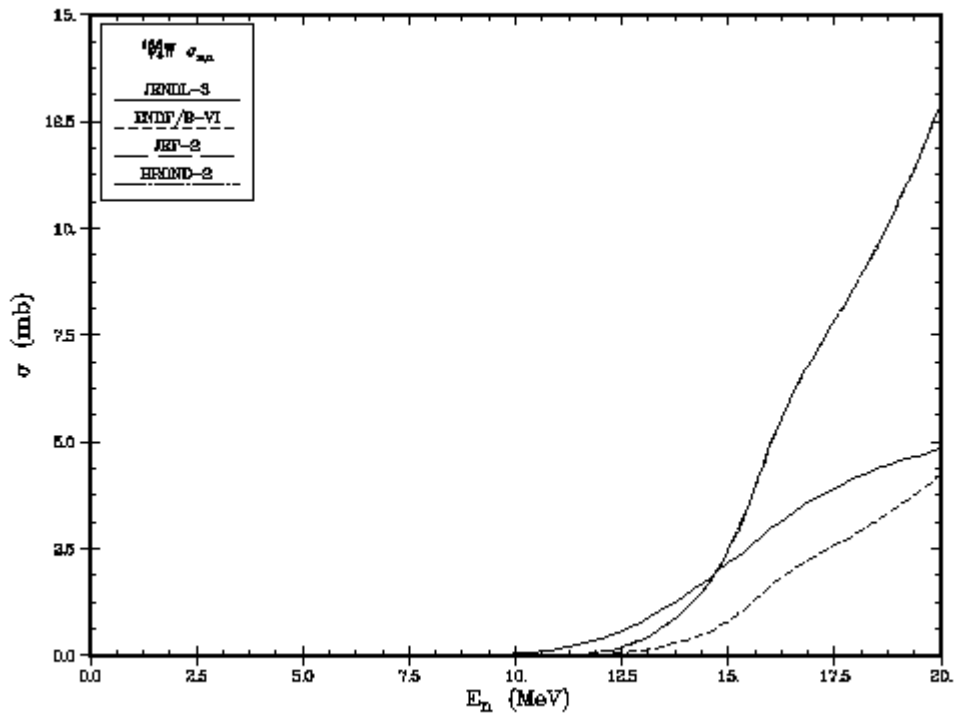


Figure 5.80: $^{186}\text{W}(n,\alpha)$ reaction cross section

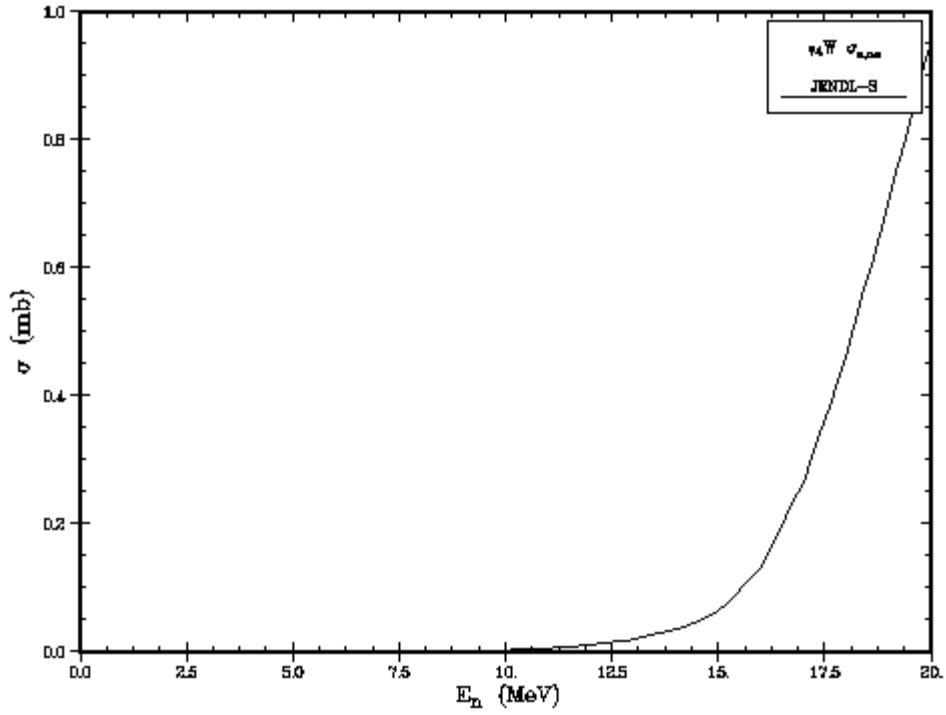


Figure 5.81: ${}^{\text{nat}}\text{W}(n,\alpha)$ reaction cross section

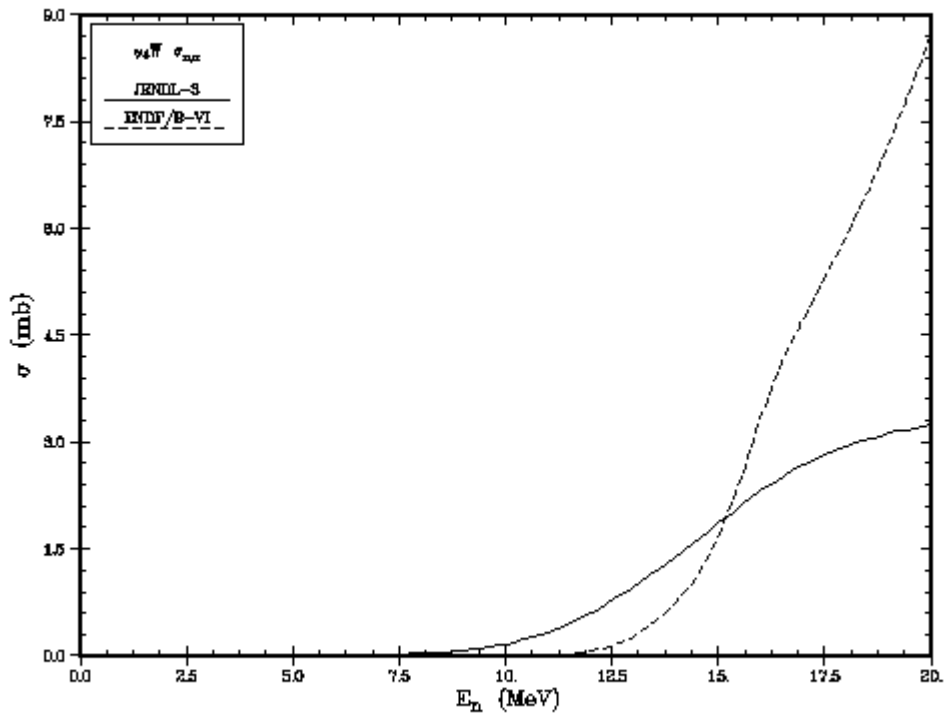


Figure 5.82: ${}^{\text{nat}}\text{W}(n,\alpha)$ reaction cross section

One of the salient features seen in many of the preceding plots is that independent evaluations of particular helium producing reaction cross sections often exhibit radically different shapes. How could this happen? One possible explanation lies in the nature of nuclear model calculations. It is well known that for most nuclei the average neutron total cross section above the resonance region (normally above 100 keV) tends to vary rather gradually with neutron energy. Also, this is generally true for the neutron elastic scattering cross section and, to some extent, for the neutron capture cross section as well. However, such gradual variation is not characteristic of other partial cross sections that exhibit threshold behavior, e.g., neutron inelastic scattering and charged particle emission cross sections. The rise and eventual decline of these individual cross sections with increasing energy is a consequence of competition between the various open reaction channels that must share the relatively constant total non-elastic cross section strength. This corresponds to a zero sum situation, so to speak. Under these circumstances, small changes in one or more of the many parameters that govern nuclear model calculations can lead to very different shapes being obtained by different evaluators from nuclear modeling for the smaller partial cross sections such as $(n,n\alpha)$, (n,α) , or $(n,^3\text{He})$,

While physical effects might explain some of the differences in these evaluations in cases where few if any data are available to guide calculations, other examples from the plots shown above suggest that there are errors present in the files, e.g., the observance of sharp spikes or sudden discontinuities in what should be essentially smoothly varying cross sections. The excitation curves for some of the reactions even suggest that they might not have been generated by nuclear modeling at all (e.g., straight lines or sudden changes in slope) but actually reflect rough “guesses” by an evaluator.

A perusal of the preceding plots generated from general purpose neutron cross section files is indeed sobering. It is often said that what we don't know can hurt us. As a corollary, one should be aware of the fact that what we THINK we know (but is actually flawed or completely wrong) can also hurt us.

5.3 Evaluated Cross Sections from FENDL

The Fusion Evaluated Nuclear Data Library (FENDL) was produced for use in the analysis of conceptual fusion energy systems through the auspices of the International Atomic Energy Agency (IAEA) Nuclear Data Section (NDS), in collaboration with a number of consultants and advisors recruited from the nuclear data evaluation community. The following description of FENDL is quoted from the IAEA-NDS website (<http://www-nds.iaea.org/>): “A comprehensive, validated, and extensively tested nuclear data library developed for fusion (thermonuclear) applications and actually used for the ITER design. Evaluations contained in the library are judged to be the best available by February 1997.” FENDL is a hybrid, isotopic library that draws from various sources what are deemed by evaluation experts to be the best available evaluations, at least in the context of fusion energy applications. The most recent version posted is FENDL 2.0. Various sub-library components also exist. A number of reactions of interest for neutron-induced helium production are contained in the sub-library FENDL/A-2.0 (FENDL Activation Library). Plots of these have been prepared by the IAEA and they are readily available for downloading from the NDS website in GIF format. Table 5.2 summarizes the information obtained from the IAEA-NDS website. This list and the following individual plots form a fairly extensive set of pertinent results drawn from the FENDL/A-2.0 library. Only a sampling of plots for the tungsten isotopes is shown since both ground

states and isomeric states are often involved. Comparisons with other evaluations are not shown in these plots, but experimental data, where available, are shown as an aid in assessing the extent to which the FENDL cross sections are supported by experimental data. These data serve to provide a gauge of the probable reliability of the evaluations.

Table 5.2: Helium-producing neutron cross section plots obtained from FENDL/A-2.0 ^a

<u>Element</u>	<u>Isotope</u>	(N,A)	(N,NA)	(N,2A)	(N,N2A)	(N,3He)	(N,N3He)
<i>Carbon</i>	C-12						
	C-13						
<i>Silicon</i>	Si-28						
	Si-29						
	Si-30						
<i>Titanium</i>	Ti-46						
	Ti-47						
	Ti-48						
	Ti-49						
	Ti-50						
<i>Vanadium</i>	V-51						
<i>Chromium</i>	Cr-50						
	Cr-52						
	Cr-53						
	Cr-54						
<i>Iron</i>	Fe-54						
	Fe-56						
	Fe-57						
<i>Nickel</i>	Ni-58						
	Ni-60						
	Ni-61						
	Ni-62						
<i>Tungsten</i>	W-182	g	g,m1			g	
	W-183	g	g				
	W-184		g				
	W-186		g				

^a Green shading indicates plots obtained from FENDL/A-2.0. g = ground state; m1 = isomer "m1"; otherwise data correspond to the total reaction cross section.

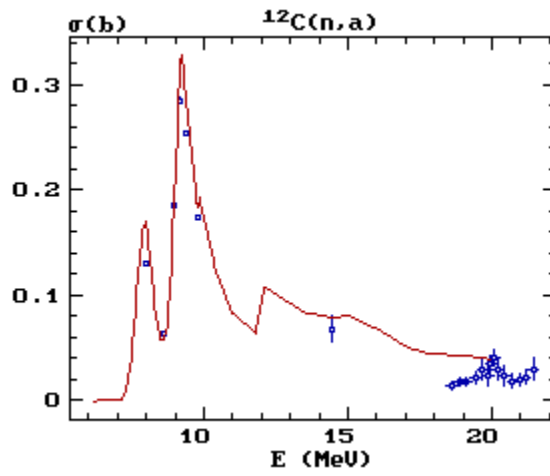


Figure 5.83: $^{12}\text{C}(n,\alpha)$ reaction cross section from FENDL/A-2.0

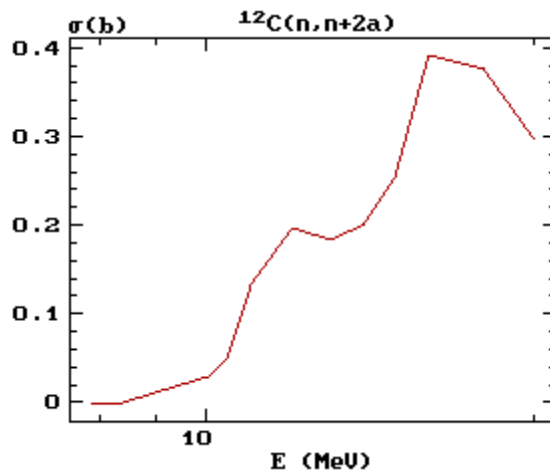


Figure 5.84: $^{12}\text{C}(n,n+2\alpha)$ reaction cross section from FENDL/A-2.0

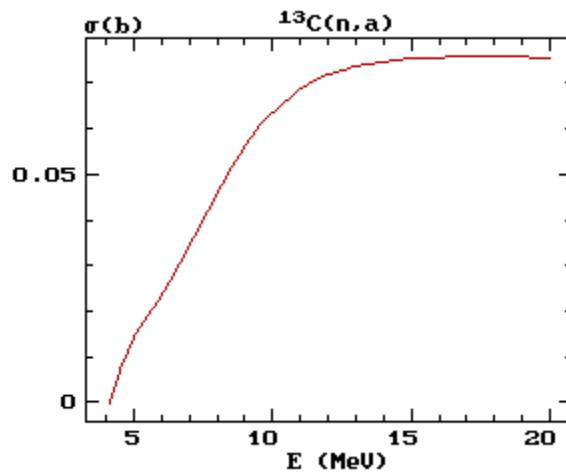


Figure 5.85: $^{13}\text{C}(n,\alpha)$ reaction cross section from FENDL/A-2.0

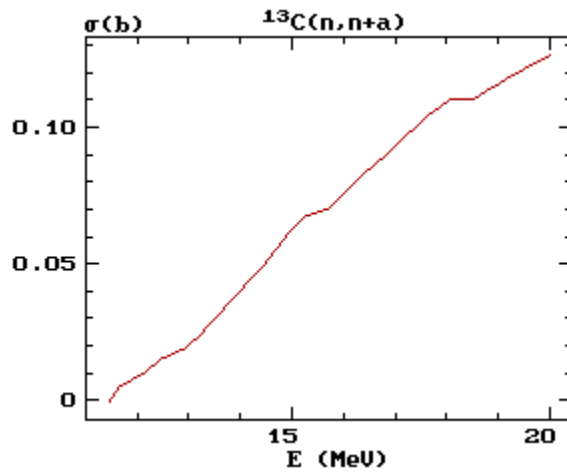


Figure 5.86: $^{13}\text{C}(n, n\alpha)$ reaction cross section from FENDL/A-2.0

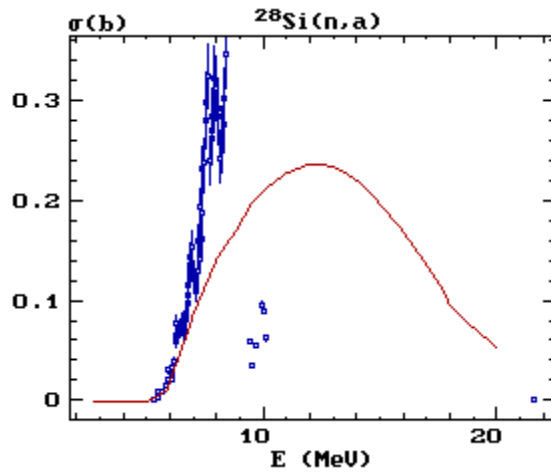


Figure 5.87: $^{28}\text{Si}(n, \alpha)$ reaction cross section from FENDL/A-2.0

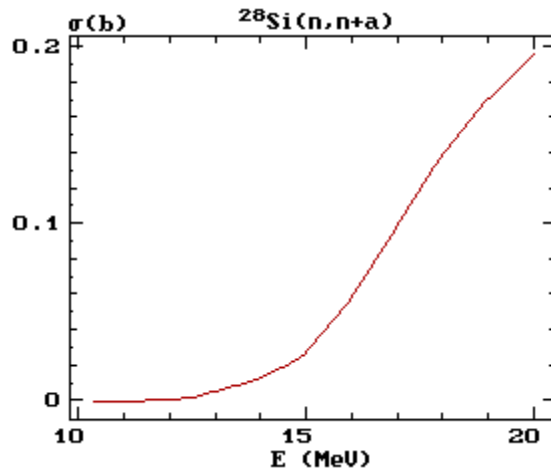


Figure 5.88: $^{28}\text{Si}(n, n\alpha)$ reaction cross section from FENDL/A-2.0

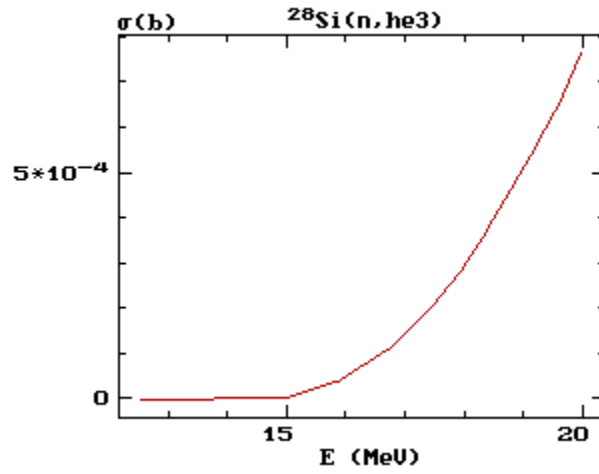


Figure 5.89: $^{28}\text{Si}(n, ^3\text{He})$ reaction cross section from FENDL/A-2.0

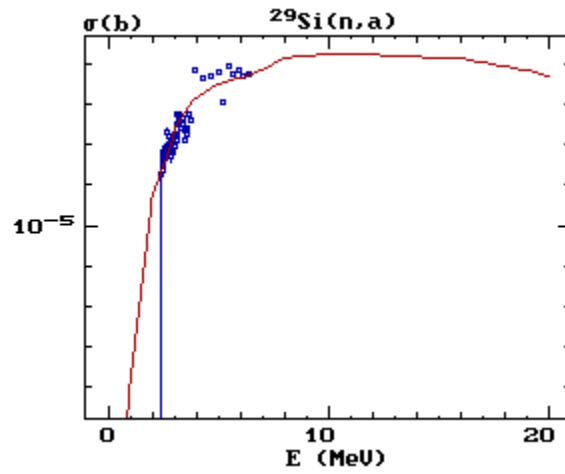


Figure 5.90: $^{29}\text{Si}(n, \alpha)$ reaction cross section from FENDL/A-2.0

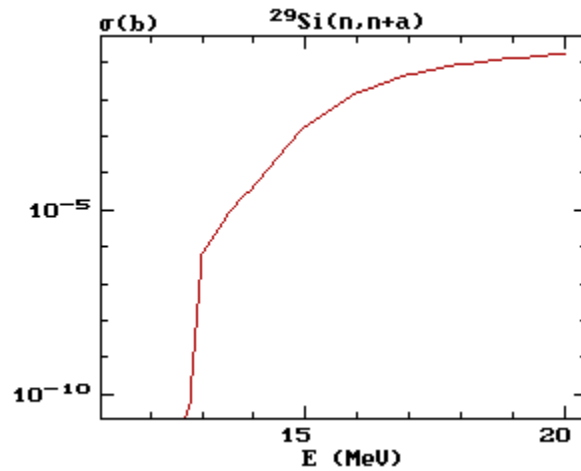


Figure 5.91: $^{29}\text{Si}(n, n\alpha)$ reaction cross section from FENDL/A-2.0

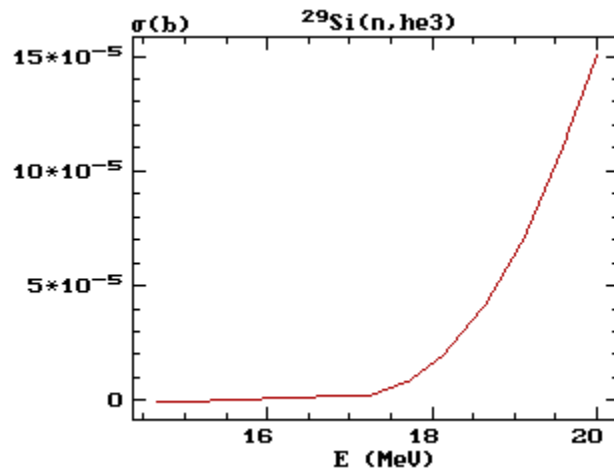


Figure 5.92: $^{29}\text{Si}(n, ^3\text{He})$ reaction cross section from FENDL/A-2.0

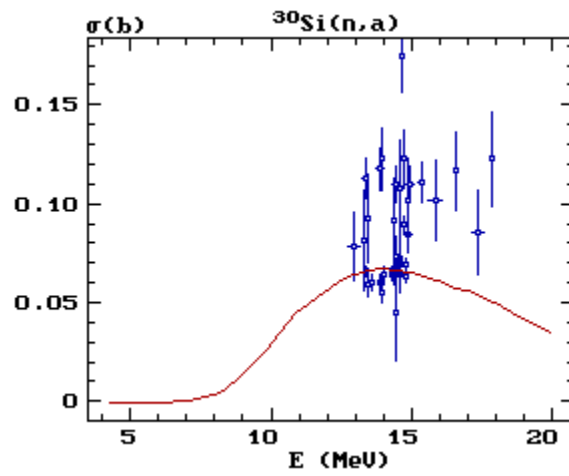


Figure 5.93: $^{30}\text{Si}(n, \alpha)$ reaction cross section from FENDL/A-2.0

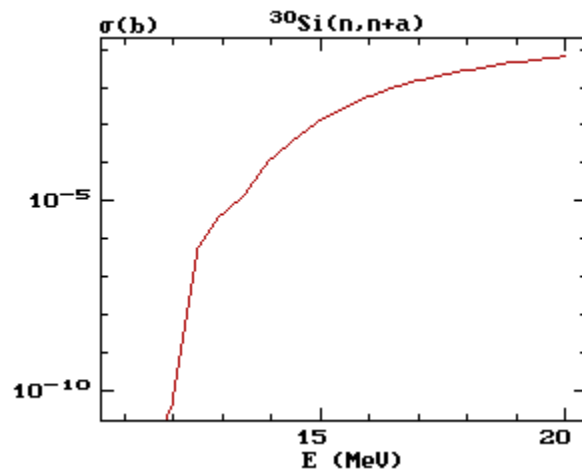


Figure 5.94: $^{30}\text{Si}(n, n\alpha)$ reaction cross section from FENDL/A-2.0

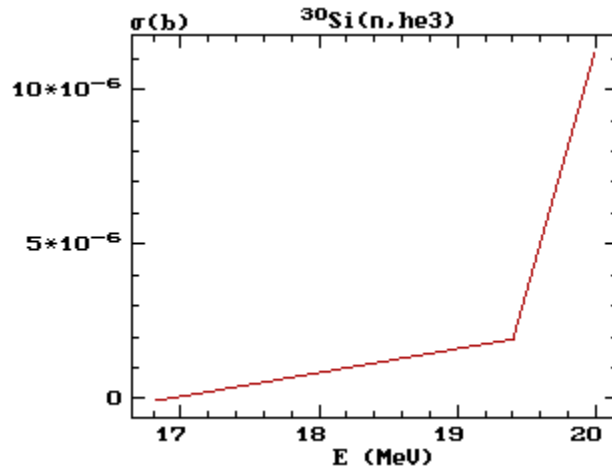


Figure 5.95: $^{30}\text{Si}(n, ^3\text{He})$ reaction cross section from FENDL/A-2.0

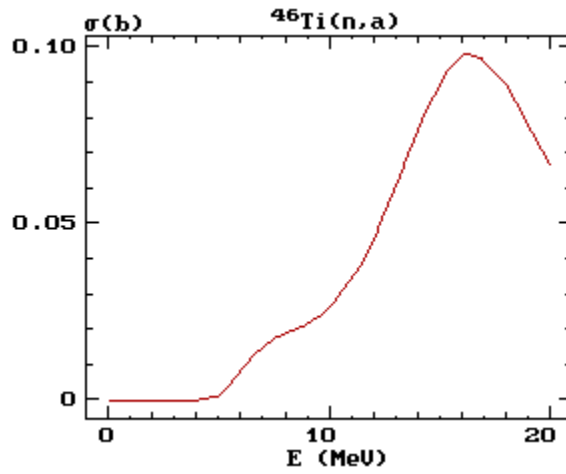


Figure 5.96: $^{46}\text{Ti}(n, \alpha)$ reaction cross section from FENDL/A-2.0

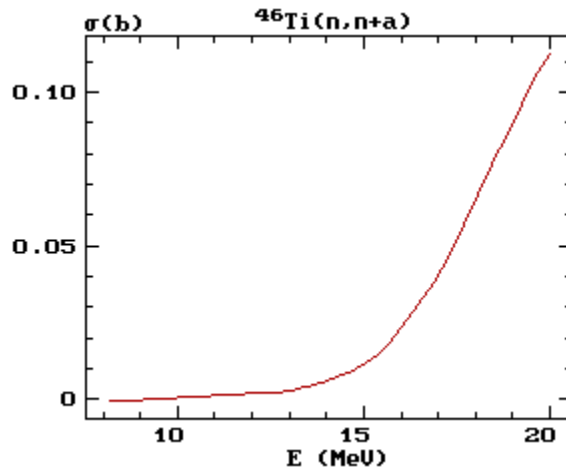


Figure 5.97: $^{46}\text{Ti}(n, n\alpha)$ reaction cross section from FENDL/A-2.0

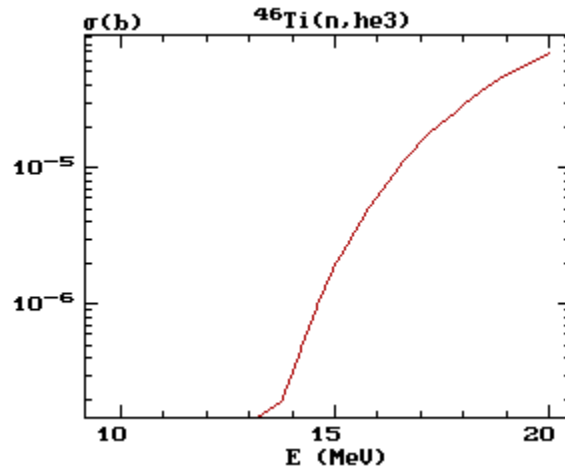


Figure 5.98: $^{46}\text{Ti}(n, ^3\text{He})$ reaction cross section from FENDL/A-2.0

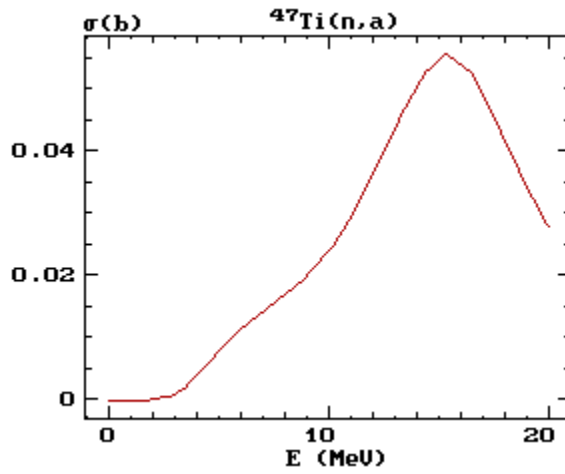


Figure 5.99: $^{47}\text{Ti}(n, \alpha)$ reaction cross section from FENDL/A-2.0

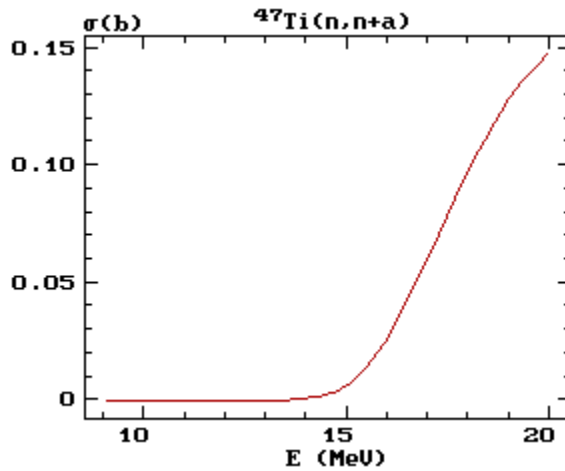


Figure 5.100: $^{47}\text{Ti}(n, n+\alpha)$ reaction cross section from FENDL/A-2.0

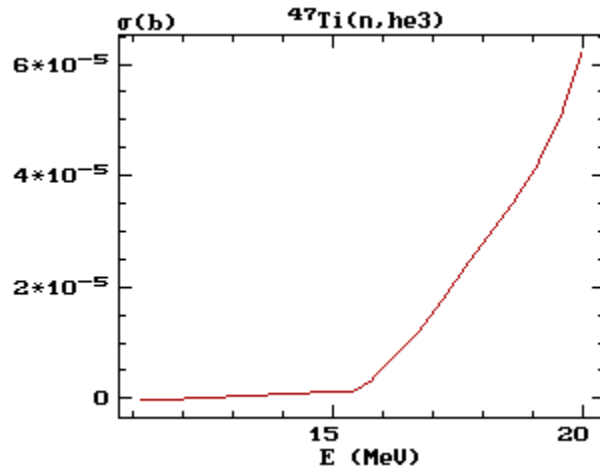


Figure 5.101: $^{47}\text{Ti}(n, ^3\text{He})$ reaction cross section from FENDL/A-2.0

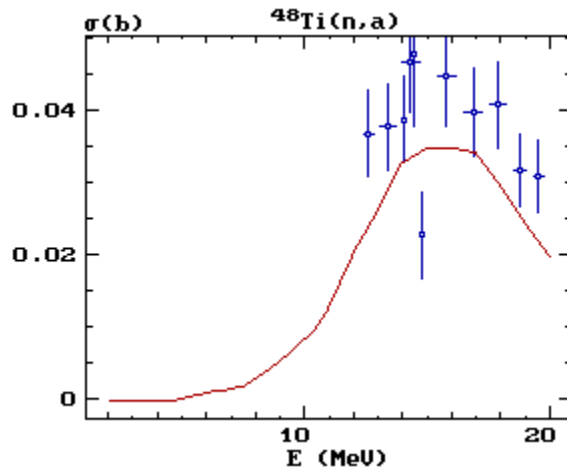


Figure 5.102: $^{48}\text{Ti}(n, \alpha)$ reaction cross section from FENDL/A-2.0

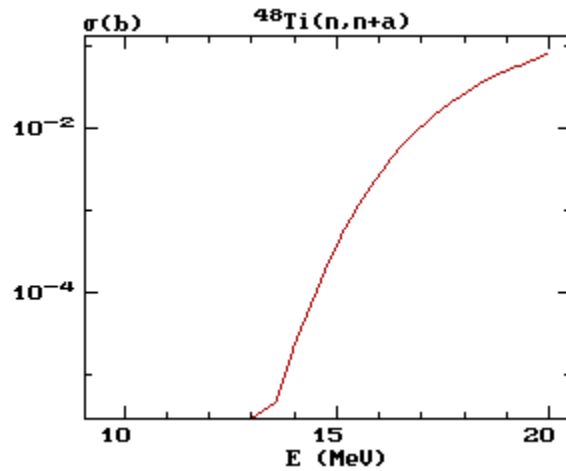


Figure 5.103: $^{48}\text{Ti}(n, n\alpha)$ reaction cross section from FENDL/A-2.0

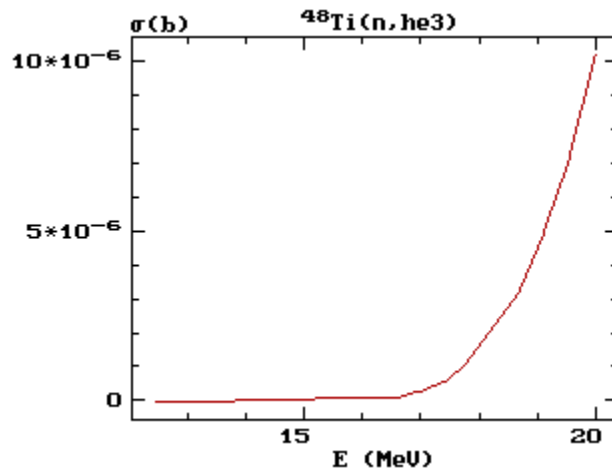


Figure 5.104: $^{48}\text{Ti}(n, ^3\text{He})$ reaction cross section from FENDL/A-2.0

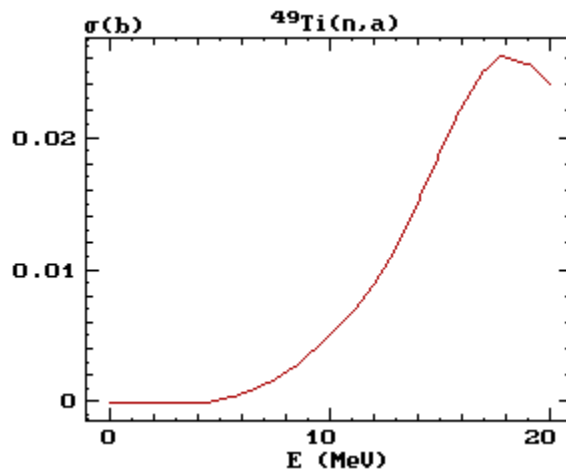


Figure 5.105: $^{49}\text{Ti}(n, \alpha)$ reaction cross section from FENDL/A-2.0

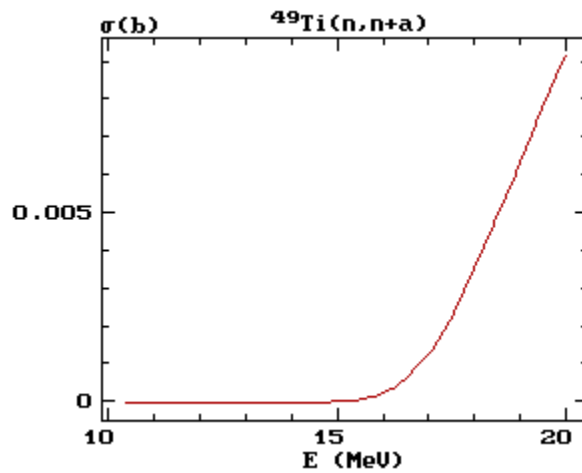


Figure 5.106: $^{49}\text{Ti}(n, n\alpha)$ reaction cross section from FENDL/A-2.0

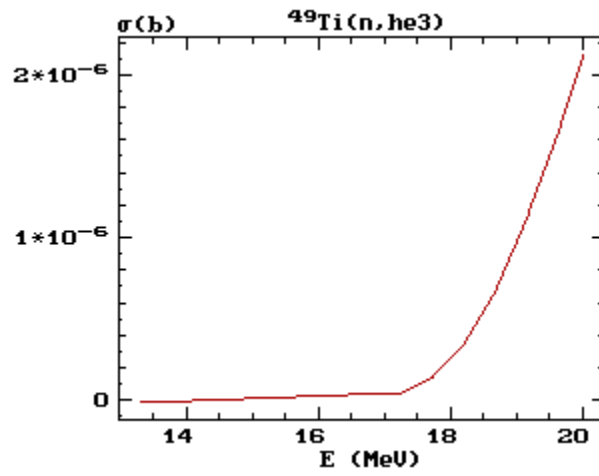


Figure 5.107: $^{49}\text{Ti}(n, ^3\text{He})$ reaction cross section from FENDL/A-2.0

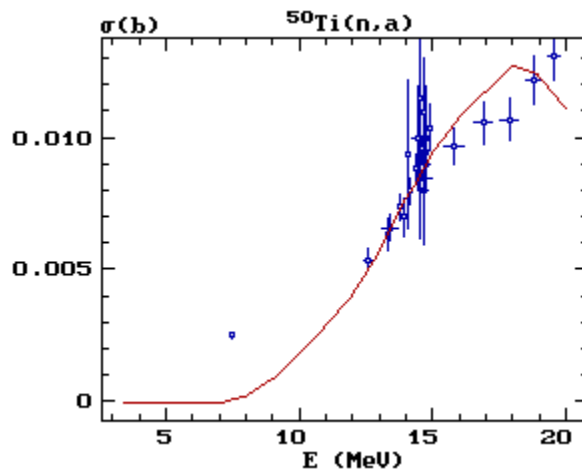


Figure 5.108: $^{50}\text{Ti}(n, \alpha)$ reaction cross section from FENDL/A-2.0

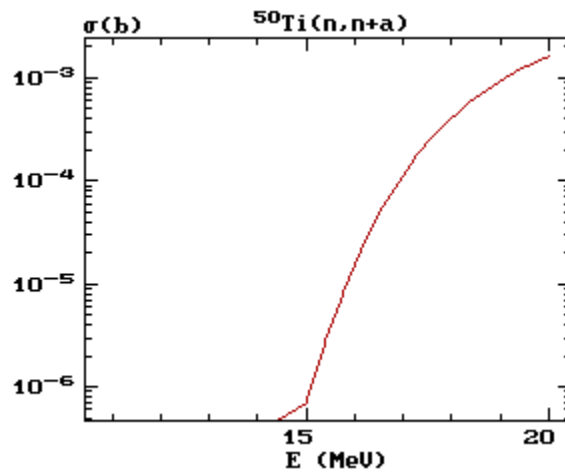


Figure 5.109: $^{50}\text{Ti}(n, n\alpha)$ reaction cross section from FENDL/A-2.0

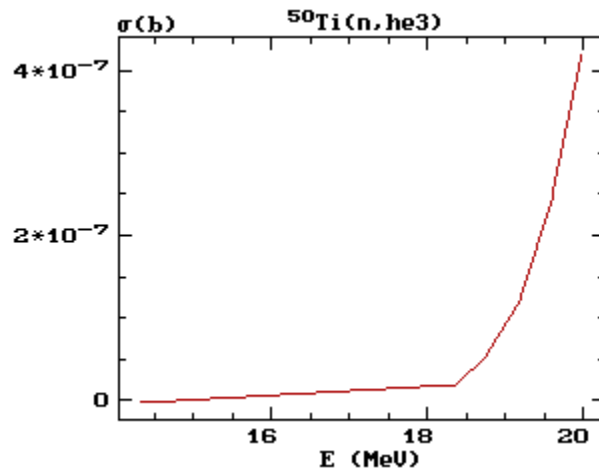


Figure 5.110: $^{50}\text{Ti}(n, \text{He})$ reaction cross section from FENDL/A-2.0

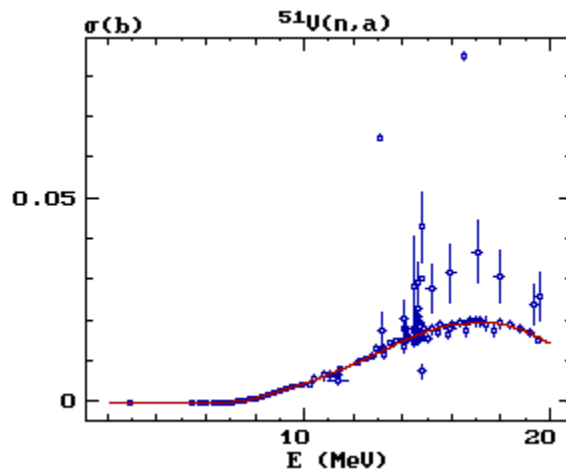


Figure 5.111: $^{51}\text{V}(n, \alpha)$ reaction cross section from FENDL/A-2.0

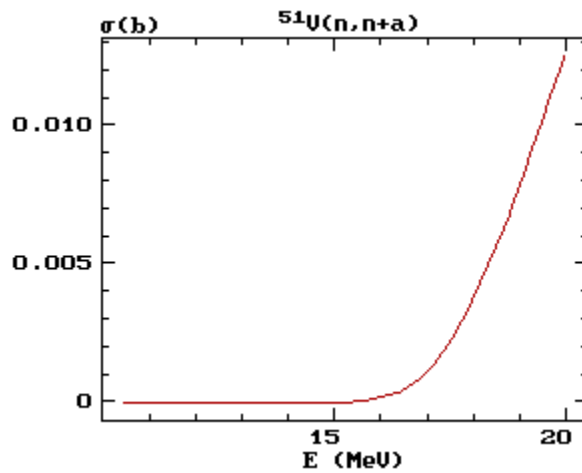


Figure 5.112: $^{51}\text{V}(n, n\alpha)$ reaction cross section from FENDL/A-2.0

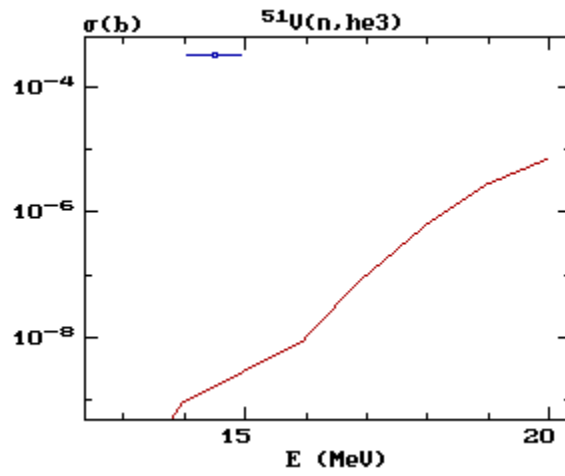


Figure 5.113: $^{51}\text{U}(n, ^3\text{He})$ reaction cross section from FENDL/A-2.0

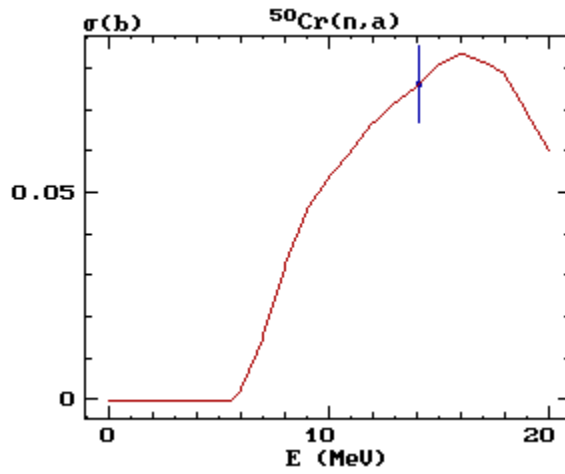


Figure 5.114: $^{50}\text{Cr}(n, \alpha)$ reaction cross section from FENDL/A-2.0

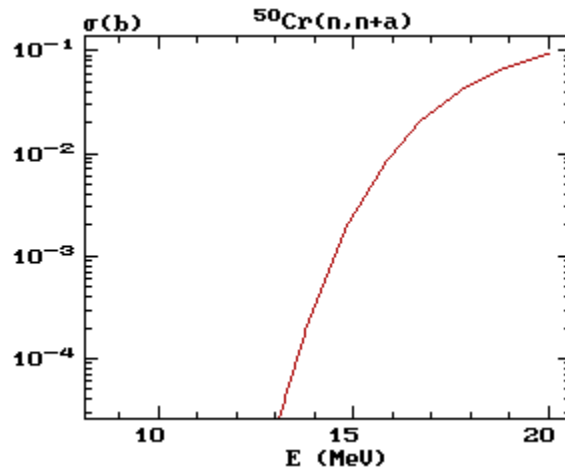


Figure 5.115: $^{50}\text{Cr}(n, n+\alpha)$ reaction cross section from FENDL/A-2.0

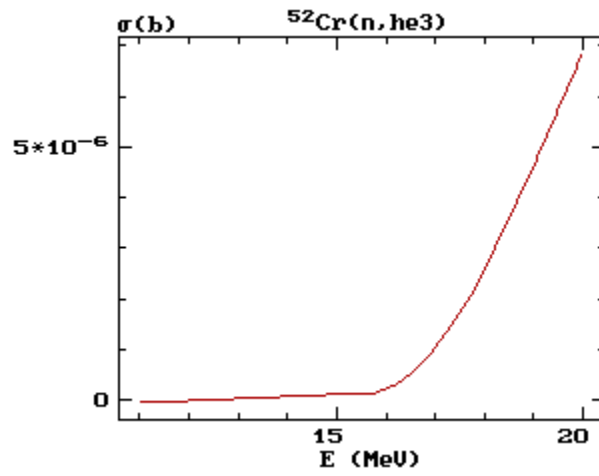


Figure 5.116: $^{50}\text{Cr}(n, ^3\text{He})$ reaction cross section from FENDL/A-2.0

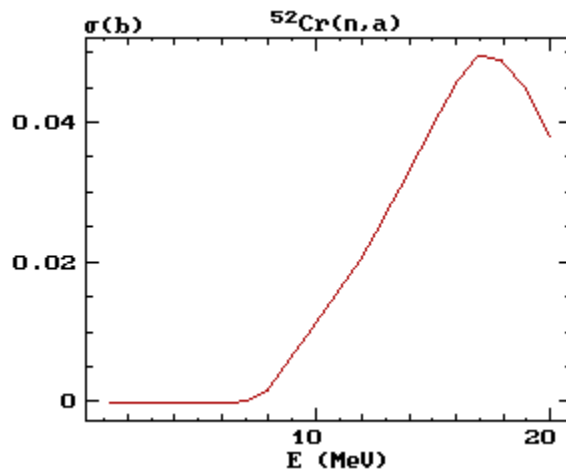


Figure 5.117: $^{52}\text{Cr}(n, \alpha)$ reaction cross section from FENDL/A-2.0

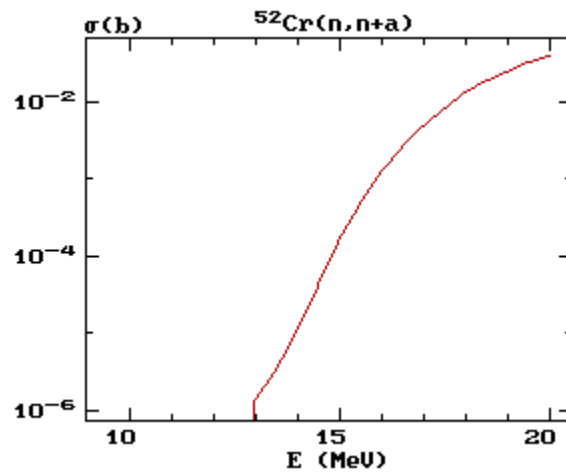


Figure 5.118: $^{52}\text{Cr}(n, n\alpha)$ reaction cross section from FENDL/A-2.0

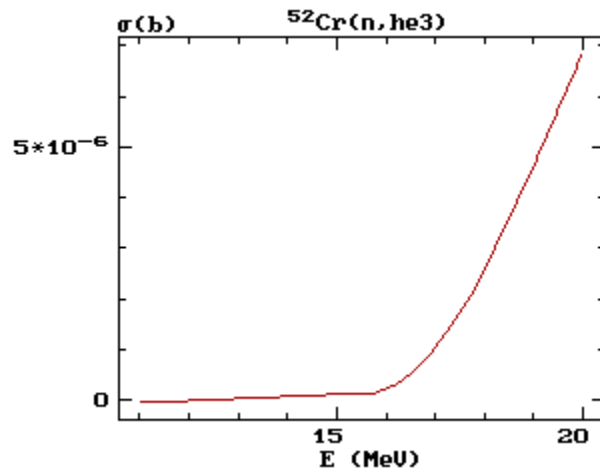


Figure 5.119: $^{52}\text{Cr}(n, ^3\text{He})$ reaction cross section from FENDL/A-2.0

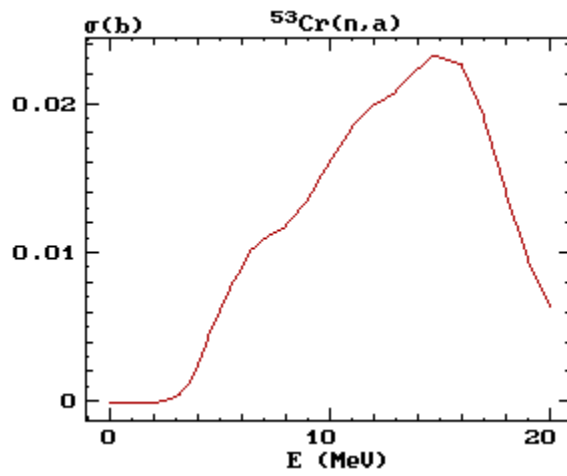


Figure 5.120: $^{53}\text{Cr}(n, \alpha)$ reaction cross section from FENDL/A-2.0

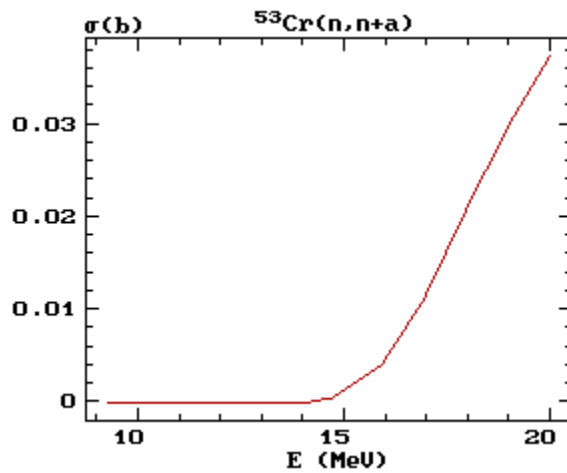


Figure 5.121: $^{53}\text{Cr}(n, n\alpha)$ reaction cross section from FENDL/A-2.0

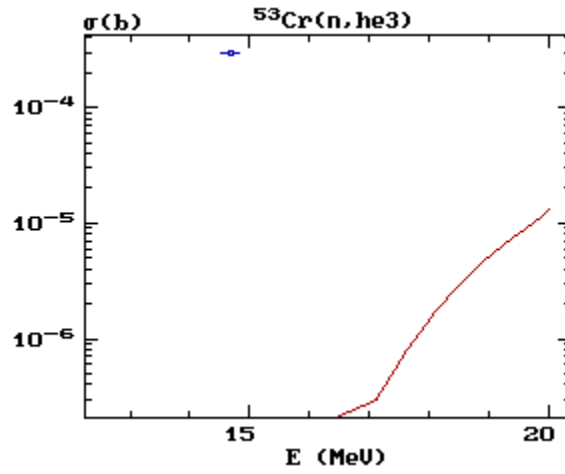


Figure 5.122: $^{53}\text{Cr}(n, ^3\text{He})$ reaction cross section from FENDL/A-2.0

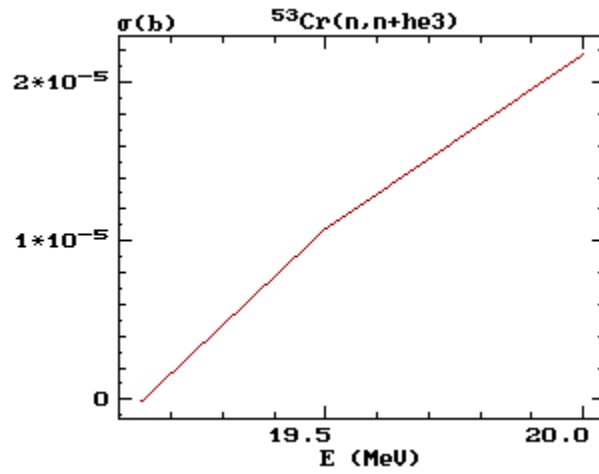


Figure 5.123: $^{53}\text{Cr}(n, n^3\text{He})$ reaction cross section from FENDL/A-2.0

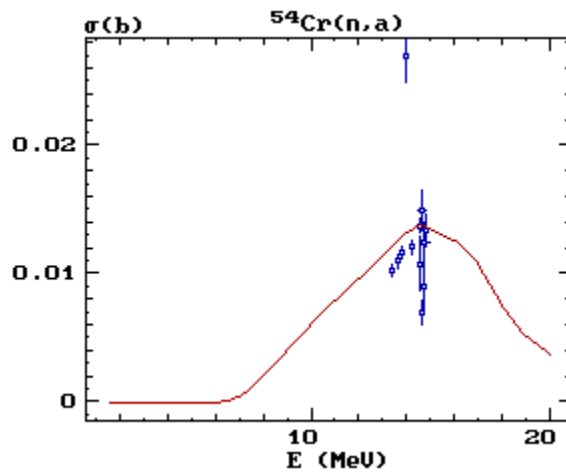


Figure 5.124: $^{54}\text{Cr}(n, \alpha)$ reaction cross section from FENDL/A-2.0

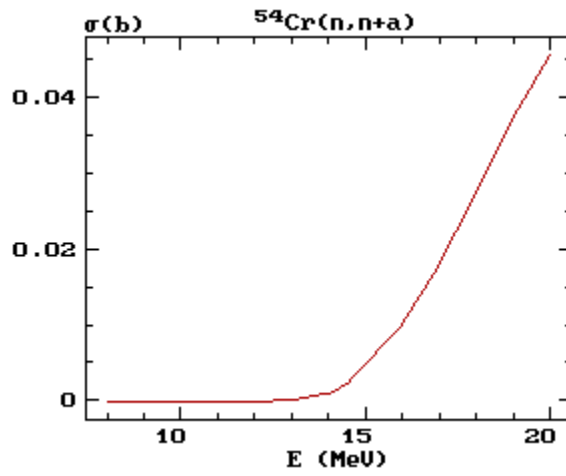


Figure 5.125: $^{54}\text{Cr}(n, n+a)$ reaction cross section from FENDL/A-2.0

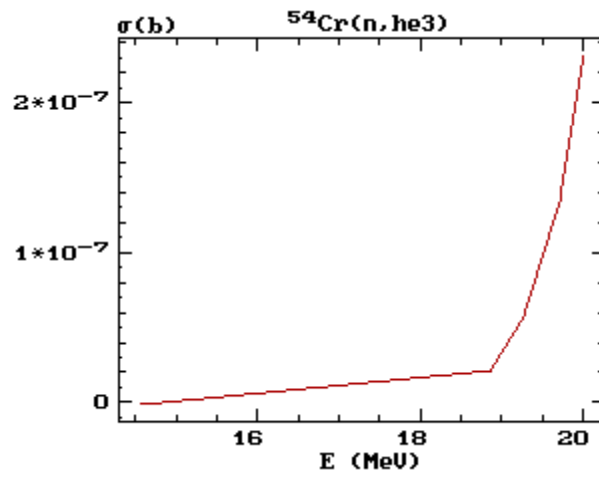


Figure 5.126: $^{54}\text{Cr}(n, {}^3\text{He})$ reaction cross section from FENDL/A-2.0

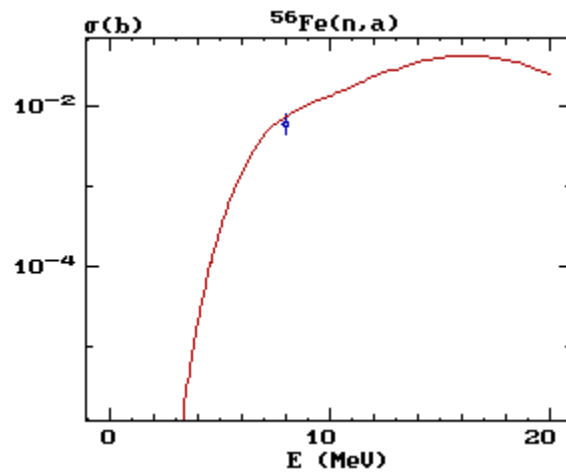


Figure 5.127: $^{56}\text{Fe}(n, \alpha)$ reaction cross section from FENDL/A-2.0

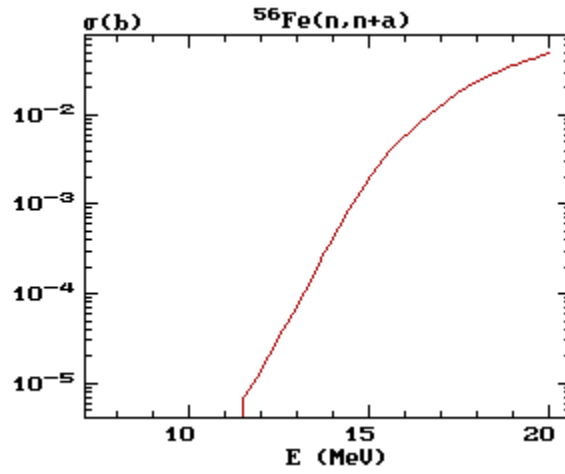


Figure 5.128: $^{56}\text{Fe}(n,\alpha)$ reaction cross section from FENDL/A-2.0

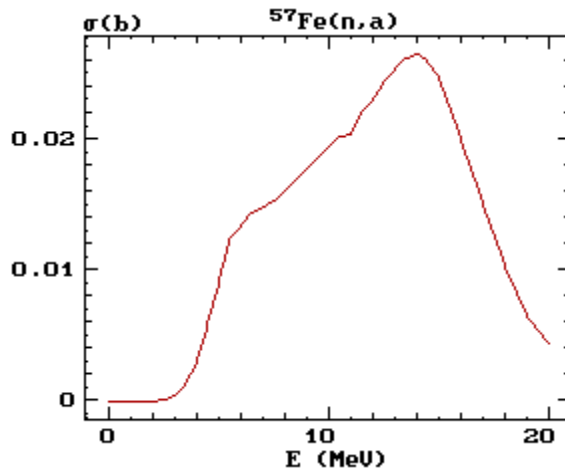


Figure 5.129: $^{57}\text{Fe}(n,\alpha)$ reaction cross section from FENDL/A-2.0

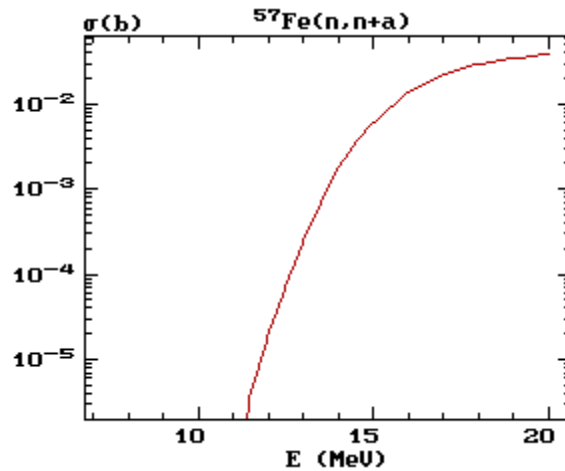


Figure 5.130: $^{57}\text{Fe}(n,\alpha)$ reaction cross section from FENDL/A-2.0

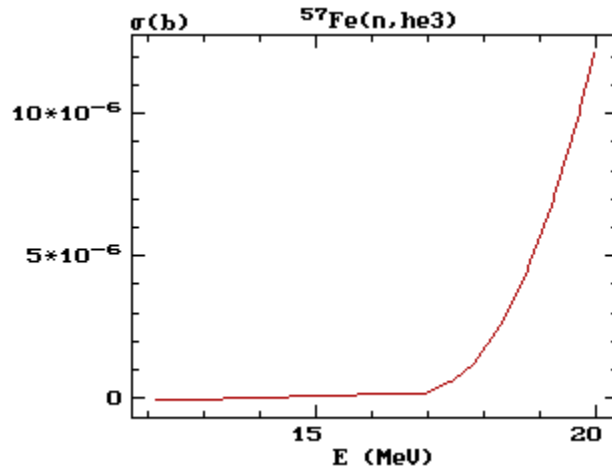


Figure 5.131: $^{57}\text{Fe}(n, ^3\text{He})$ reaction cross section from FENDL/A-2.0

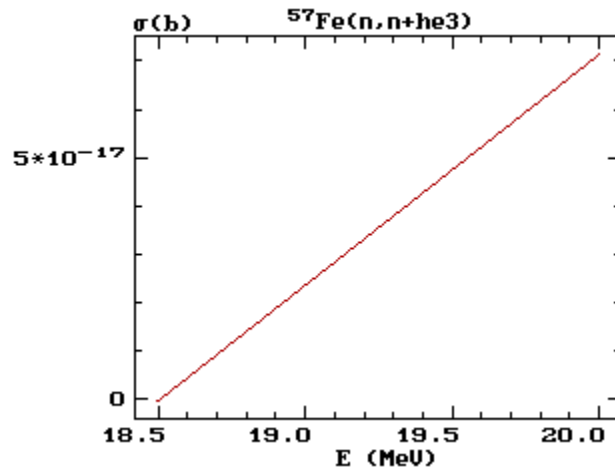


Figure 5.132: $^{57}\text{Fe}(n, n^3\text{He})$ reaction cross section from FENDL/A-2.0

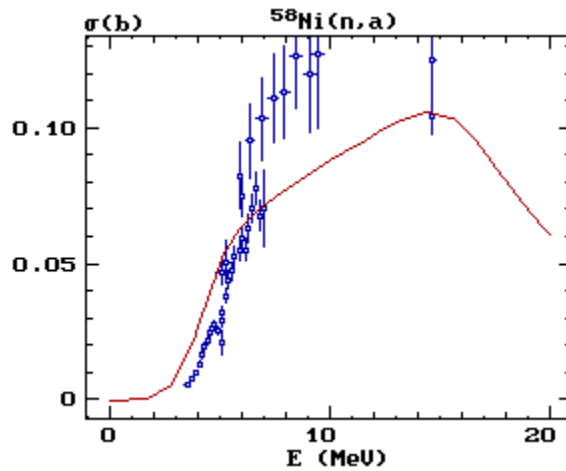


Figure 5.133: $^{58}\text{Ni}(n, \alpha)$ reaction cross section from FENDL/A-2.0

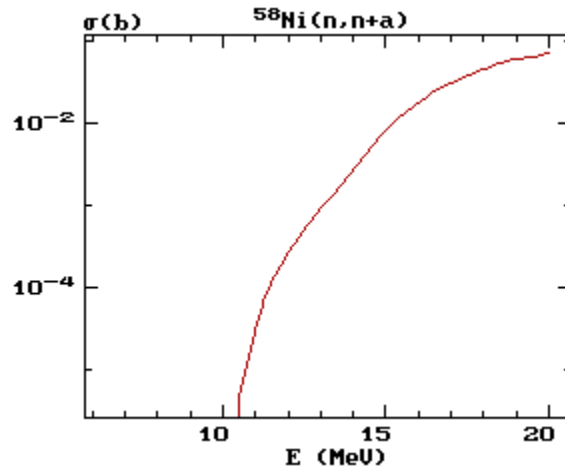


Figure 5.134: $^{58}\text{Ni}(n, n\alpha)$ reaction cross section from FENDL/A-2.0

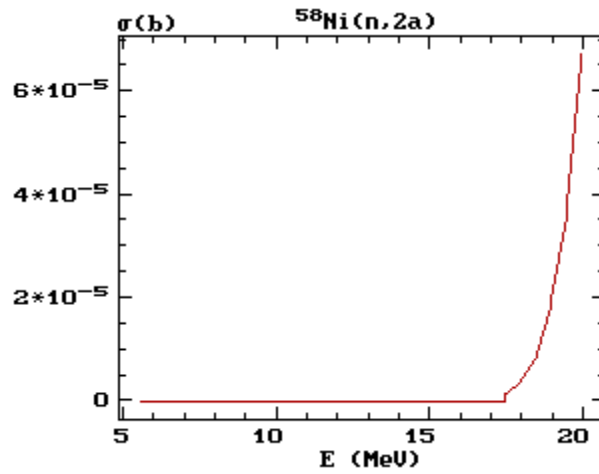


Figure 5.135: $^{58}\text{Ni}(n, 2\alpha)$ reaction cross section from FENDL/A-2.0

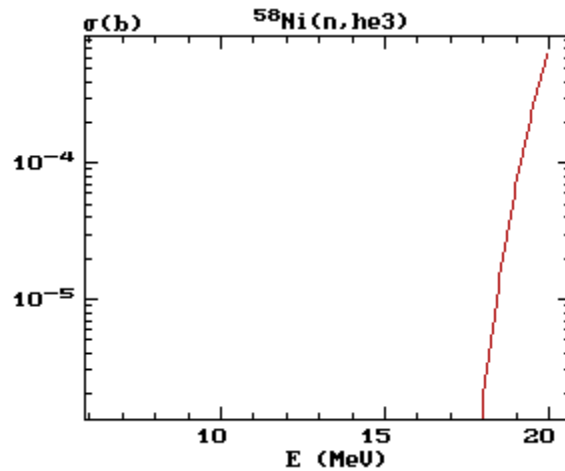


Figure 5.136: $^{58}\text{Ni}(n, ^3\text{He})$ reaction cross section from FENDL/A-2.0

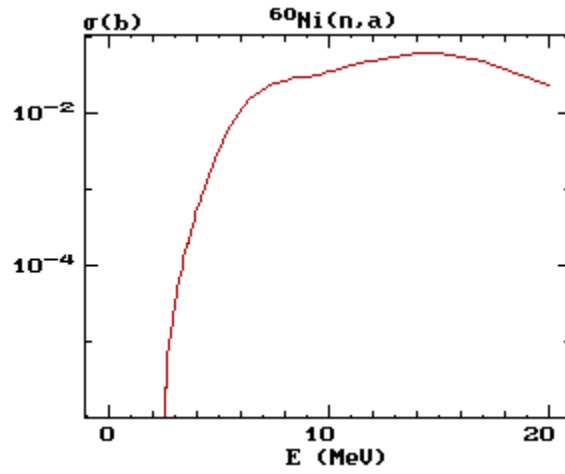


Figure 5.137: $^{60}\text{Ni}(n, \alpha)$ reaction cross section from FENDL/A-2.0

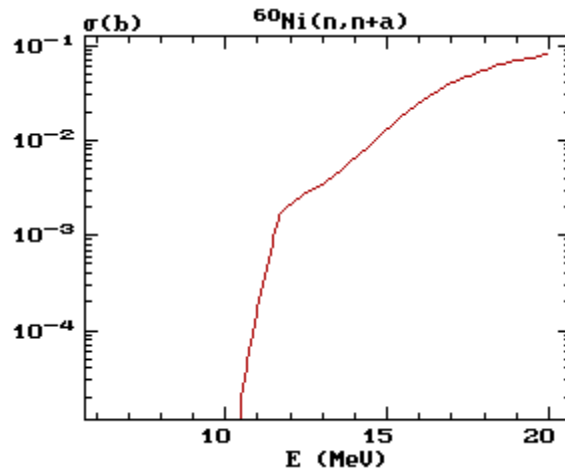


Figure 5.138: $^{60}\text{Ni}(n, n+\alpha)$ reaction cross section from FENDL/A-2.0

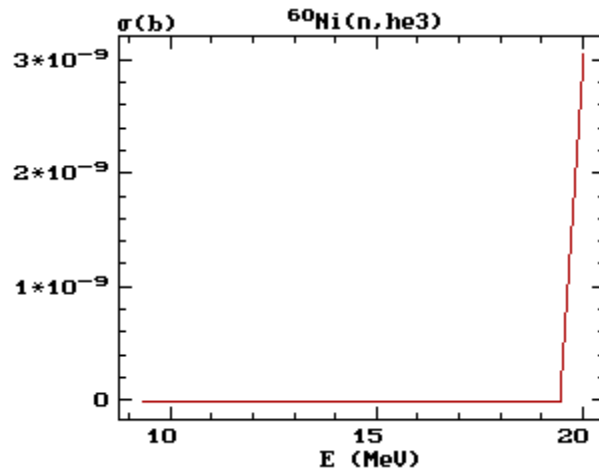


Figure 5.139: $^{60}\text{Ni}(n, ^3\text{He})$ reaction cross section from FENDL/A-2.0

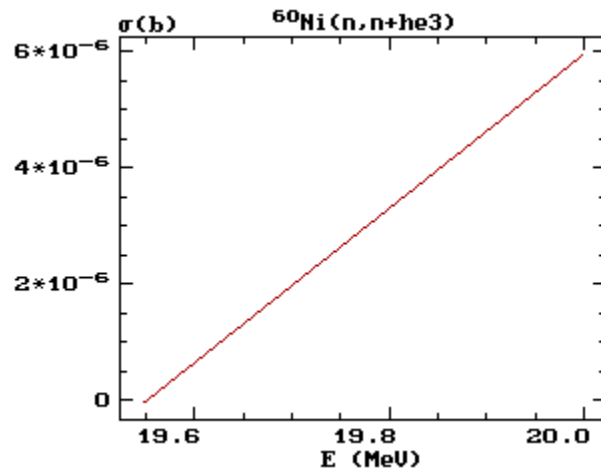


Figure 5.140: $^{60}\text{Ni}(n, n+^3\text{He})$ reaction cross section from FENDL/A-2.0

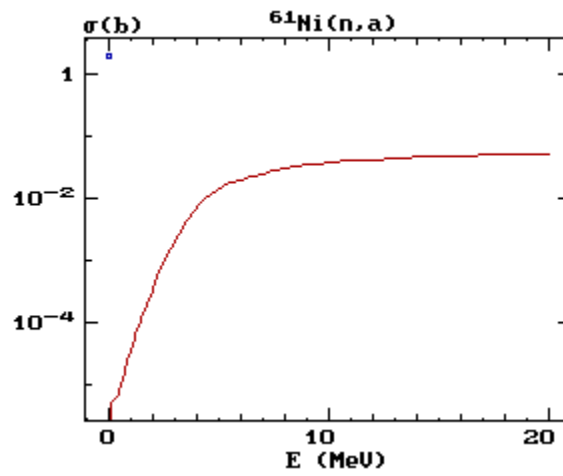


Figure 5.141: $^{61}\text{Ni}(n, \alpha)$ reaction cross section from FENDL/A-2.0

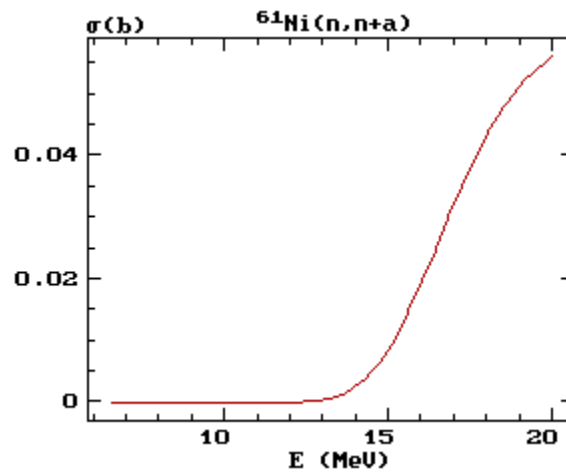


Figure 5.142: $^{61}\text{Ni}(n, n+\alpha)$ reaction cross section from FENDL/A-2.0

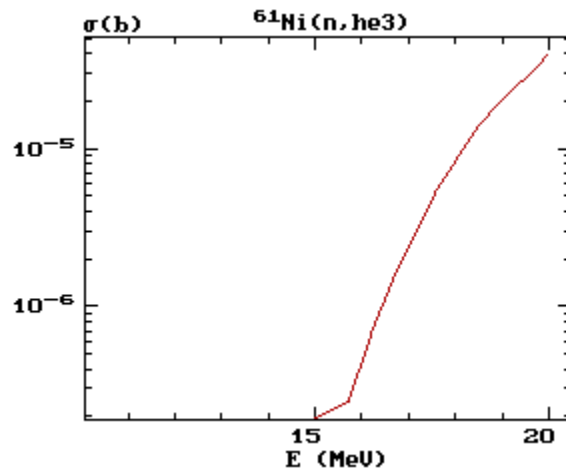


Figure 5.143: $^{61}\text{Ni}(n, ^3\text{He})$ reaction cross section from FENDL/A-2.0

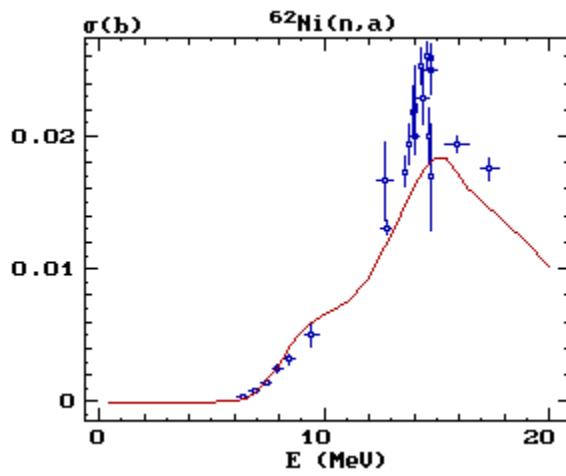


Figure 5.144: $^{62}\text{Ni}(n, \alpha)$ reaction cross section from FENDL/A-2.0

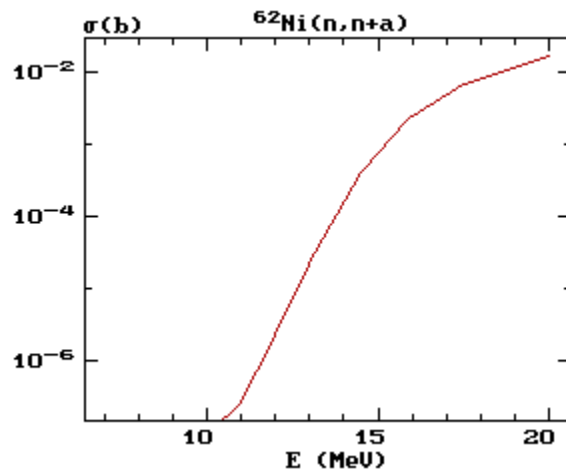


Figure 5.145: $^{62}\text{Ni}(n, n\alpha)$ reaction cross section from FENDL/A-2.0

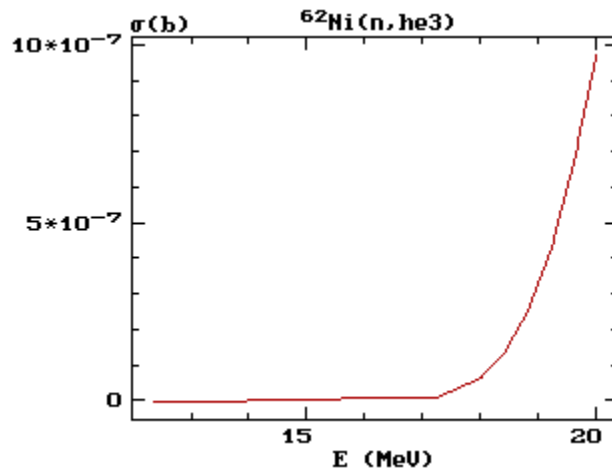


Figure 5.146: $^{62}\text{Ni}(n, ^3\text{He})$ reaction cross section from FENDL/A-2.0

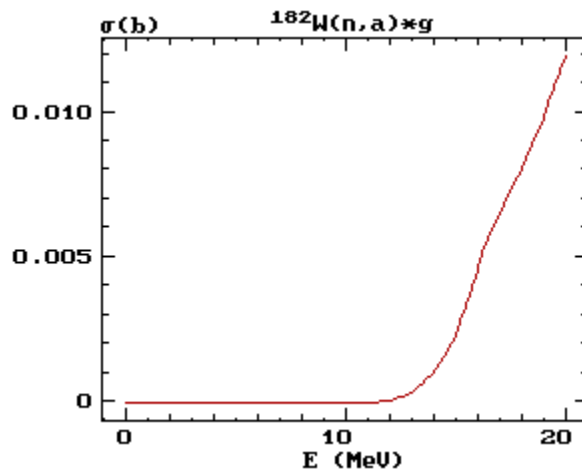


Figure 5.147: $^{182}\text{W}(n, \alpha)^g$ reaction cross section from FENDL/A-2.0

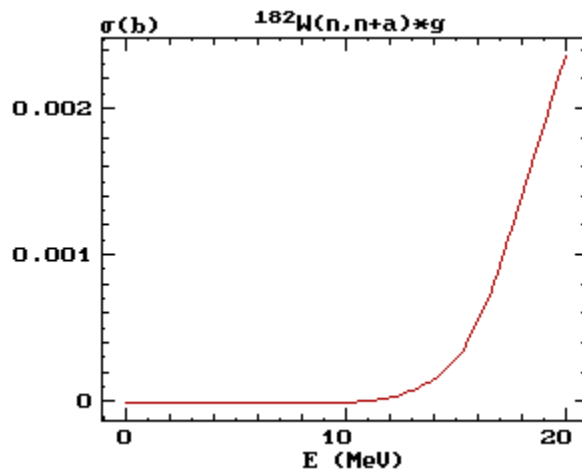


Figure 5.148: $^{182}\text{W}(n, n\alpha)^g$ reaction cross section from FENDL/A-2.0

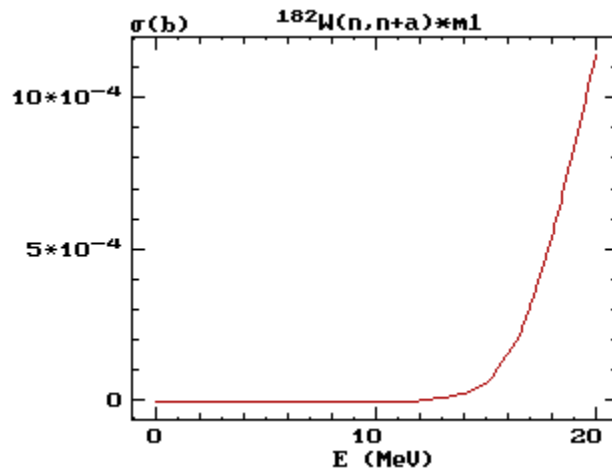


Figure 5.149: $^{182}\text{W}(n, n\alpha)^{m1}$ reaction cross section from FENDL/A-2.0

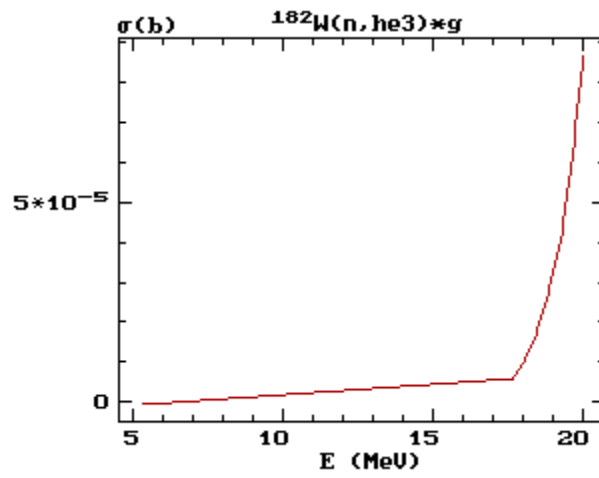


Figure 5.150: $^{182}\text{W}(n, {}^3\text{He})^g$ reaction cross section from FENDL/A-2.0

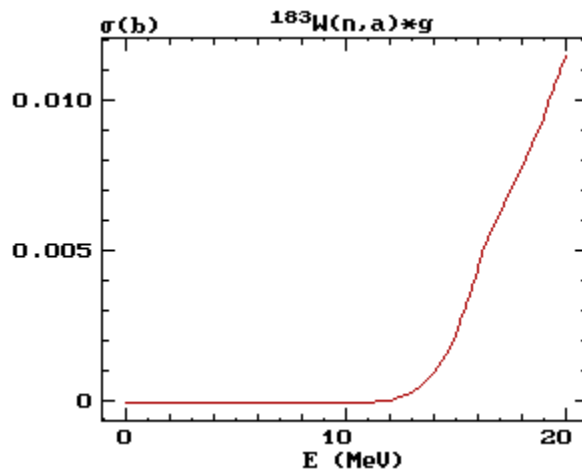


Figure 5.151: $^{183}\text{W}(n, \alpha)^g$ reaction cross section from FENDL/A-2.0

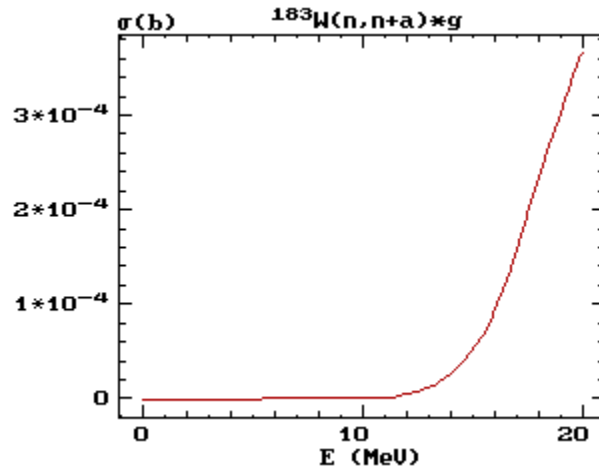


Figure 5.152: $^{183}\text{W}(n, n\alpha)^g$ reaction cross section from FENDL/A-2.0

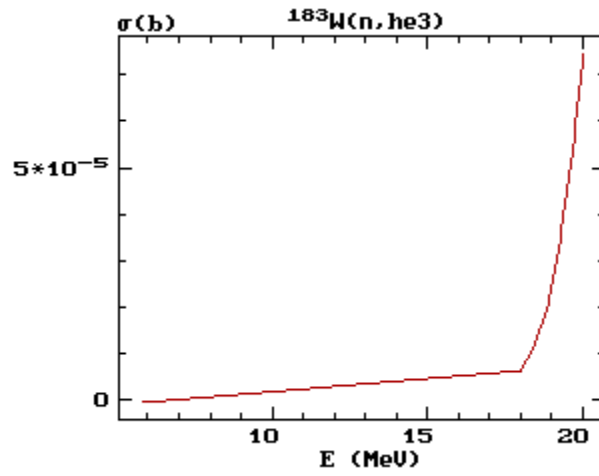


Figure 5.153: $^{183}\text{W}(n, {}^3\text{He})$ reaction cross section from FENDL/A-2.0

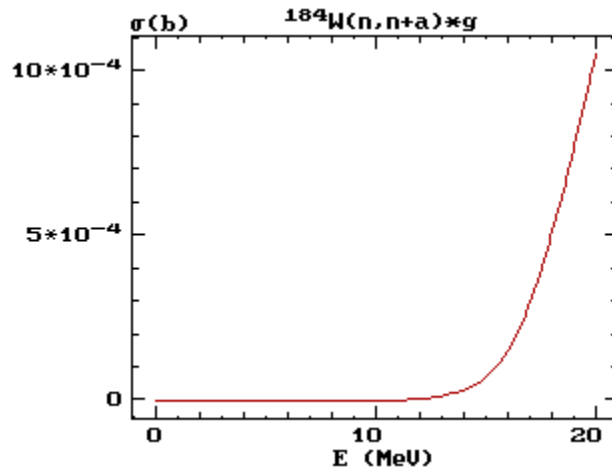


Figure 5.154: $^{184}\text{W}(n, n\alpha)^g$ reaction cross section from FENDL/A-2.0

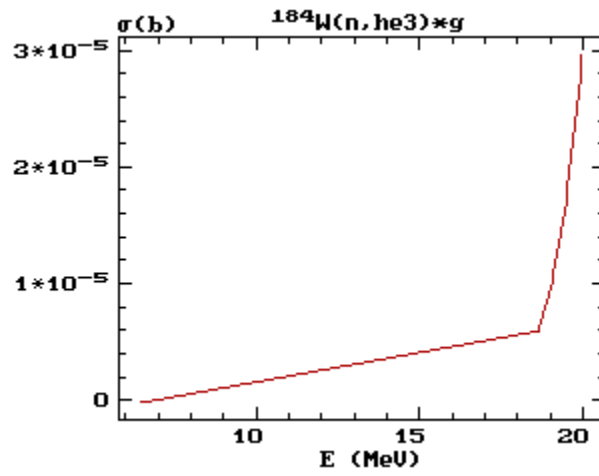


Figure 5.155: $^{184}\text{W}(n, ^3\text{He})^g$ reaction cross section from FENDL/A-2.0

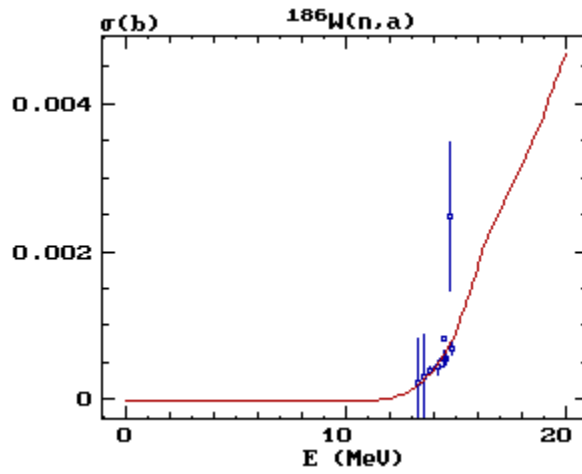


Figure 5.156: $^{186}\text{W}(n, \alpha)$ reaction cross section from FENDL/A-2.0

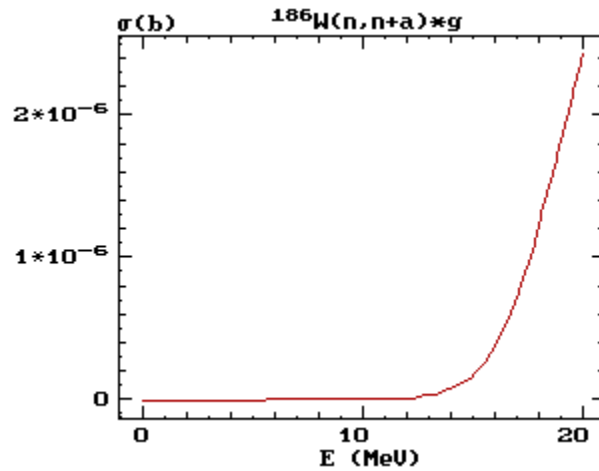


Figure 5.157: $^{186}\text{W}(n, n\alpha)^g$ reaction cross section from FENDL/A-2.0

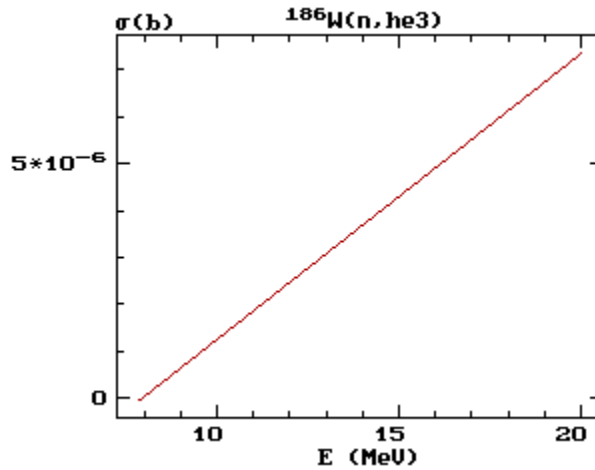


Figure 5.158: $^{186}\text{W}(n, ^3\text{He})$ reaction cross section from FENDL/A-2.0

A glance at these FENDL plots leaves one with several impressions. First, one is struck with how many of the cross sections are unsubstantiated by experimental data, or at best there exist one or two points that perhaps give some indication as to the overall normalization (magnitude) of the cross section but provide no real guidance as to the shape of the excitation function. In cases where there are no supportive experimental data and the evaluation relies entirely on nuclear modeling, it is suggested by the plots in Section 5.2 that the uncertainty has to be considered to be rather large (up to a factor or two or three in some cases). On a more positive note, in cases where there are substantial experimental data that serve to define both the shape and normalization of the cross section excitation function, e.g., for $^{51}\text{V}(n, \alpha)$, there is strong consistency observed between the majority of the more accurate experimental data points and the FENDL evaluation. The reader should not be led to believe, however, that just because an evaluation from a particular library appears to be quite reliable for an individual reaction channel of a particular isotope that the same holds true for the other reaction channels of that isotope. For example, there are apparently no experimental data to support the FENDL evaluation for the $^{51}\text{V}(n, n\alpha)$ reaction so the cross section for that process has to be treated as quite uncertain.

On the whole, the status of neutron induced helium production cross section information for most of the elements, isotopes, and reaction channels surveyed is in quite poor shape, even below 20 MeV. Above 20 MeV, the situation is even worse. One might be tempted to argue that although many of the individual reactions are uncertain, collectively, the situation might be somewhat better. This is risky speculation; this quasi-statistical argument is fundamentally flawed since certain reactions stand out as being more important than others because of the magnitude of the cross sections and relative abundance in a fusion system of the various elements and isotopes in question.

6. Comments on a Neutron Materials Test Facility for Fusion

Radiation damage is a well established phenomenon in fission power reactors. The mechanisms involved are primarily the displacement of atoms from lattice positions by neutrons and charged particles, followed by incomplete annealing, and the production of chemical and gaseous byproducts, especially helium, that lead to a weakening of the reactor structural components. The neutron energies that will be encountered in D-T fusion power reactors will be far greater, on average, than is the case for fission reactors. Consequently, there is an urgent need for testing candidate fusion reactor materials in neutron environments that bear at least some resemblance to those that will be encountered in actual fusion reactors. In order to induce in test specimens a level of radiation damage adequate to indicate how various materials might perform in fusion power reactor environments, a powerful materials irradiation test facility will be required. Furthermore, this facility will need to provide neutron spectra and fluence levels adequate for the intended purpose. While lower fluence levels and long exposure times might appear upon casual reflection to be acceptable, this assumption overlooks the fact that radiation damage induced at a slow rate is much more likely to be annealed, especially at elevated temperatures, than is the case for higher fluences and lower duration exposures. In some sense, materials resemble living organisms in that a portion of the structural defects induced by exposure to radiation can disappear with time, i.e., the materials can “heal.” The goal of this section is to examine briefly some properties of a neutron spectrum that has been proposed by the fusion community for materials testing purposes and to comment on its relationship to the helium producing nuclear reactions addressed in this report.

6.1 Fast Neutron Test Spectrum

The fast neutron environment of a D-T fusion reactor is likely to be a particularly punishing one for the materials selected for use in constructing such a device. While the predominant neutron yield will be in the 13 - 15 MeV energy range, it is anticipated that there will also be a few even more energetic neutrons produced in the D-T plasma, as well as in the walls of the containment vessel, by various secondary nuclear reaction processes. In the plasma, the energies of the contained tritium and deuterium particles will normally be mostly in the thermal range. However, some tritons may be impacted by energetic neutrons or recoiling alpha particles, thereby gaining kinetic energy so that in collisions with deuterons there can be production of neutrons with energies up to perhaps as much as 20 MeV. Note that the much more loosely bound deuterons found in the plasma are prone to break apart into neutrons and protons when struck by few MeV recoiling alpha particles or other energetic particles (besides tritons). Fusion neutrons impinging on the plasma containment vessel wall can initiate $(n, X\alpha)$ reactions ($X =$ other particles) with the elements encountered there, thereby leading to emission of energetic alpha particles that may also collide with tritons in the plasma, and so on. Although these are largely secondary processes, with relatively low probability of occurring, the potential for production of neutrons at energies above 15 MeV cannot be overlooked when

attempting to understand the various radiation damage and radiation producing mechanisms that might be influential during long term operation of a fusion reactor.

While it might seem reasonable to incorporate intense D-T neutron sources involving low energy and high current accelerators (14-MeV neutron generators) for materials testing, in practice this approach is beset with limitations that have led the fusion research community to examine alternative options for a neutron test facility. One limitation is that D-T neutron generators, even those designed to operate near the limits of current technology such as the FNS facility in JAERI-Tokai, Japan, do not produce sufficiently intense neutron fluxes for practical testing of materials. The neutron output from these facilities is generally limited to 10^{12} to 10^{13} neutrons/sec, due mainly to target survival problems (dissipation of heat, retention of tritium, etc.). The available test volumes with fluxes high enough to induce damage for study purposes at the threshold of measurability are very small. The second limitation follows from the issue mentioned above, i.e., the neutron energies produced by a D-T reaction are limited mainly to $\approx 13 - 15$ MeV. Thus, testing of materials for effects of higher energy neutrons is not feasible.

Given these physical considerations, the fusion community is considering other accelerator based neutron source options. The most promising one among these possibilities involves employing the Li(d,n) reaction. That is, neutrons are produced by bombardment of natural lithium with energetic deuterons in the energy range of a few tens of MeV. This approach has been explored for nearly two decades. However, its implementation in a full scale engineering test facility has been delayed, largely due to the cost that would be involved in its construction as well as uncertainty regarding the time scale for development of a D-T fusion test reactor. Recently, the schedule for construction of the International Tokamak Experimental Reactor (ITER) has firmed and a site selection process is now in progress. Thus, the fusion community is strongly committed to the timely construction of a companion materials test facility that will be needed to gain an understanding of how candidate materials for ITER (and future fusion power reactors) are likely to perform in the intense neutron radiation environments of these machines.

The materials irradiation test facility that is presently being considered is denoted as the International Fusion Materials Irradiation Facility (IFMIF); it is based on 40-MeV deuteron bombardment of natural lithium targets that are sufficiently thick to stop the incident charged particles. Information regarding this proposed project, including general operating features of the facility, can be obtained from the Internet (http://insdell.tokai.jaeri.go.jp/IFMIFHOME/if_overview_e.html). Contemporary design specifications for IFMIF call for a 40-MeV deuteron beam with 250 mA of current incident on a high speed liquid lithium flow (20 m/s). Achievement of neutron output levels of the order of 4.5×10^{17} neutrons/m²/sec is envisioned for this machine. The facility design aims to generate up to 20 dpa per year in test samples. The current projected time schedule seeks to have this facility operational at full beam current capacity by the year 2020, with a projected 20-year operating lifetime thereafter prior to decommissioning in 2040.

What is of interest in the present context is the nature of the neutron spectrum that would be produced in IFMIF. Relevant spectral measurements have been made at various accelerator facilities during that past two decades. Figure 6.1 is a recent example of such work. This neutron emission spectrum, corresponding to a zero-degree laboratory angle, has been obtained from measurements performed at Tohoku University in Japan. That reference, with spectral plots, is available from the Internet (Masayuki Hagiwara, et al.; <http://www.cyric.tohoku.ac.jp/english/report/report2002/V1Hagiwara.pdf>). Since Fig. 6.1 corresponds to a semi-log representation of the results, a different perspective may be had by showing the same information using a linear plot. This is shown in Fig. 6.2.

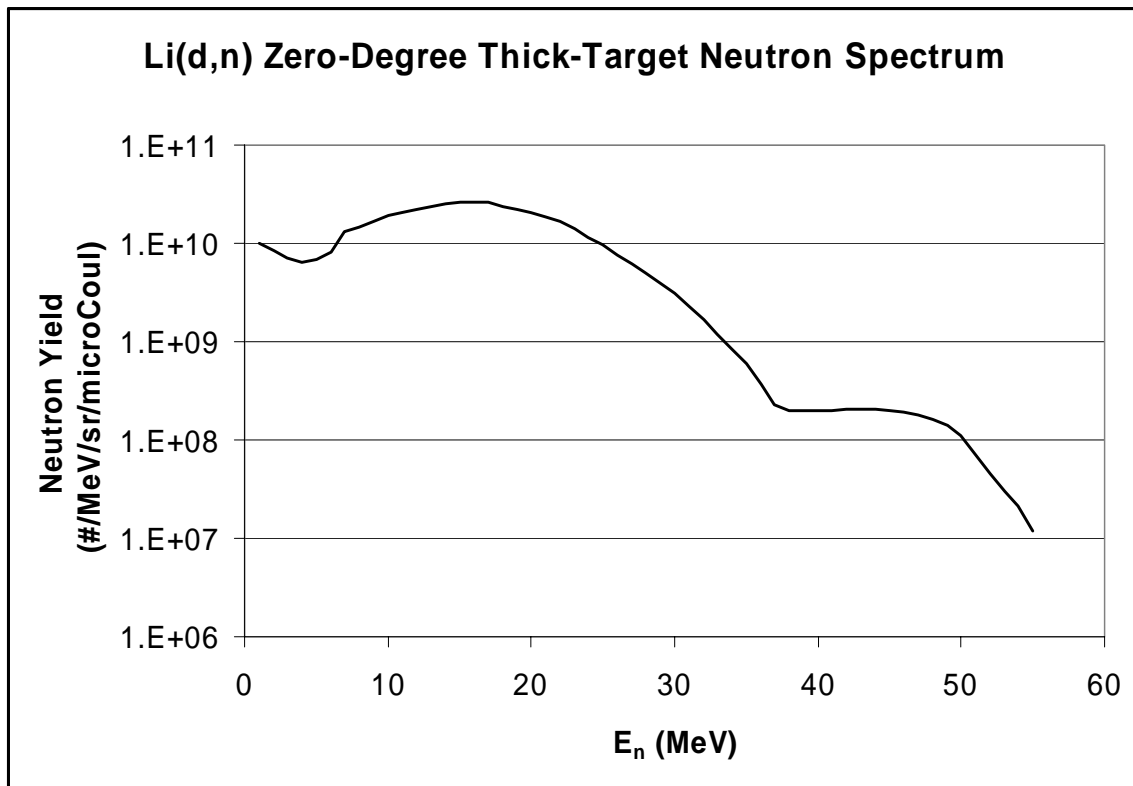


Figure 6.1: Li(d,n) zero-degree thick-target neutron spectrum (semi-log plot)

It is seen that the spectrum of neutrons emitted in the forward direction corresponds roughly to a very broad peak centered on 15 MeV. The neutron yield above 55 MeV is negligible (relatively speaking), whereas the large number of neutrons observed at relatively low energies (< 5 MeV) probably results mainly from neutron scattering in the target assembly, since the Li(d,n) source reactions tend to be exoergic (i.e., they have positive Q-values). The contributions to the total neutron yield from various portions of the spectrum represented in Figs. 6.1 and 6.2 can be discerned best from Fig. 6.3 which shows the cumulative neutron yield versus neutron energy. That is, Fig. 6.3 is a plot of $\int_0^{E_n} Y(E)dE$, where $Y(E)$ is the energy differential neutron yield shown in Figs. 6.1 and 6.2, but renormalized so that the integral over the entire spectrum

equals unity (100%). Since the deuteron bombarding energy ($E_d = 40$ MeV) for the IFMIF design was no doubt selected so that, on average, the spectrum would peak around 14 - 15 MeV, it should come as no surprise that roughly 50% of the neutrons have energies below 15 MeV while the remaining neutrons have energies above 15 MeV. This is also intuitively clear from a glance at Fig. 6.2. The information provided in Fig. 6.3 is expressed in a more quantitative fashion in Table 6.1. Be advised that although the percentage values shown in this table are given to three decimal points, in order to permit small yield differences at the higher neutron energies to be shown, the accuracy of these results is actually considerably less than implied. The spectral data appearing in Figs. 6.1 – 6.3 are based on a single experiment (Hagiwara, et al., Tohoku University, Japan) that, quite naturally, is subject to reasonable experimental error. An additional uncertainty is introduced by the numerical procedures used to generate the figures and table presented in this section. Furthermore, results obtained from various other experiments reported in the literature during the past two decades (e.g, see the reference list provided at the IFMIF Internet site mentioned above) tend to differ quantitatively, although not qualitatively, from these values. Thus, there is a clear need for careful evaluation of the existing database of experimental results for the important Li(d,n) benchmark neutron spectrum, not only at zero degree emission angle but at other neutron emission angles as well. Such information is required for Monte Carlo calculations of neutron energy and flux profiles within the test volume of IFMIF and inside the individual test specimens of fusion materials that will be subjected to irradiation at this facility.

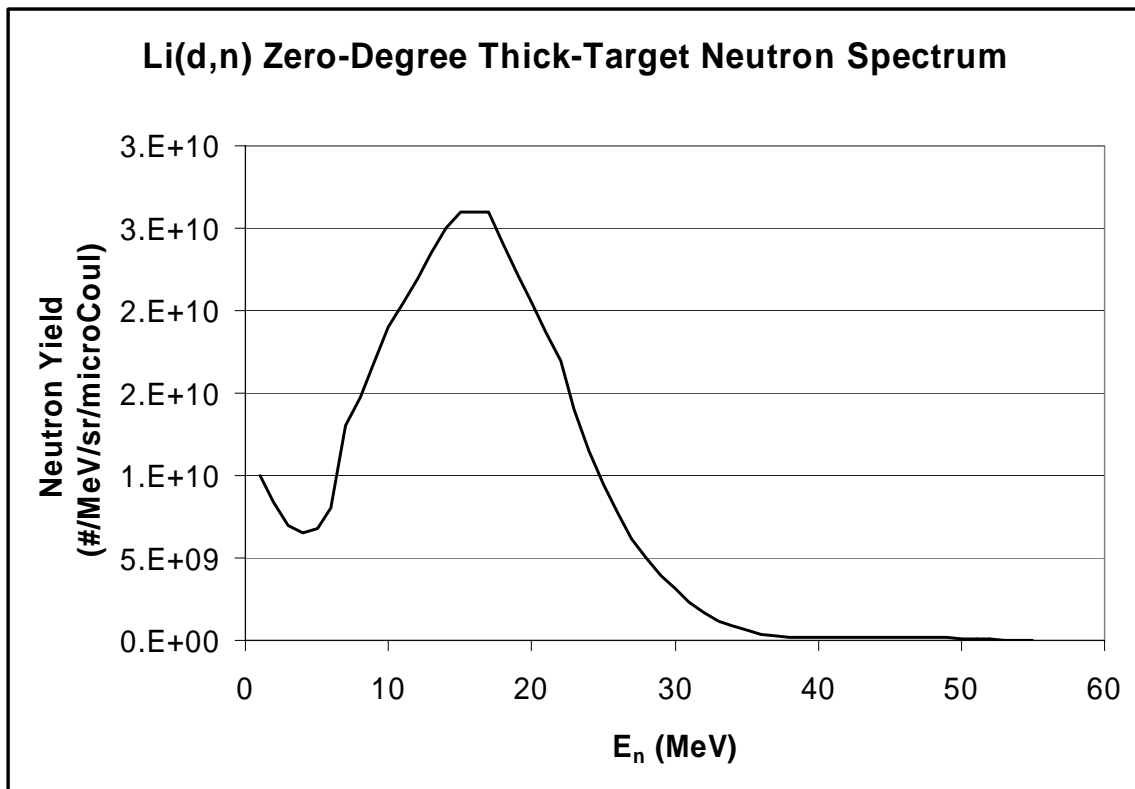


Figure 6.2: Li(d,n) zero-degree thick-target neutron spectrum (linear plot)

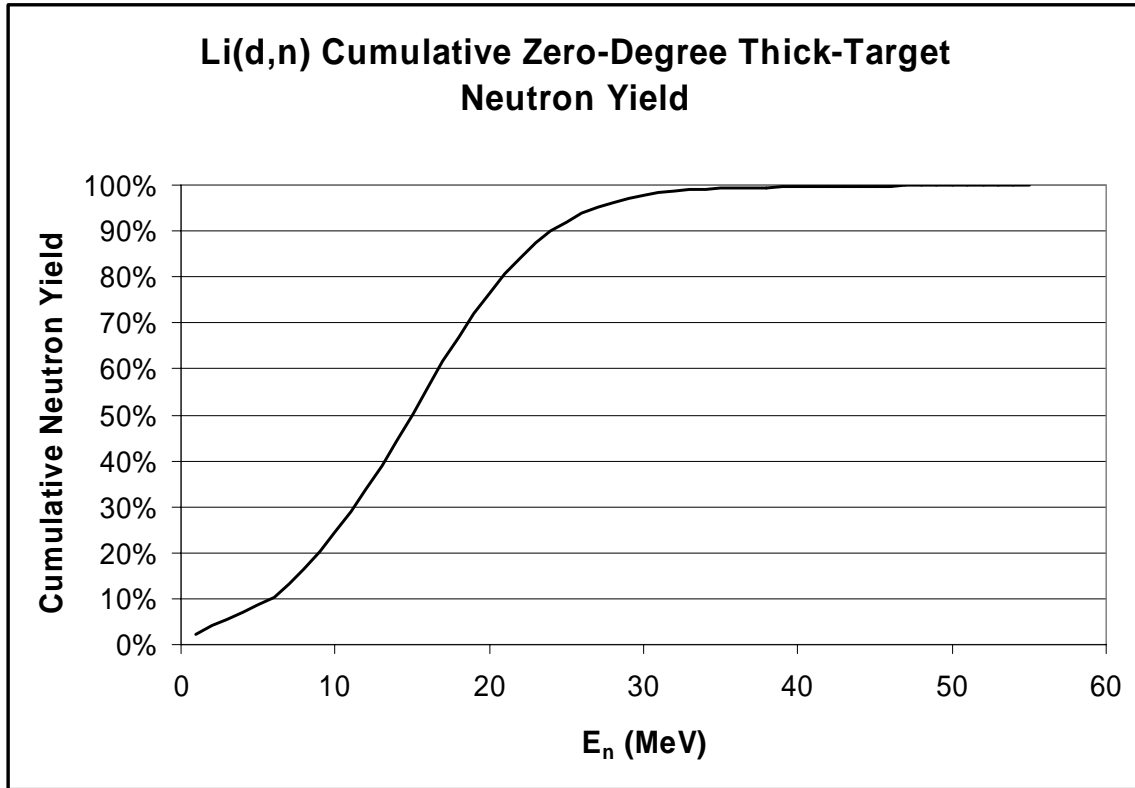


Figure 6.3: Cumulative neutron yield vs. neutron energy for 40-MeV deuterons incident on lithium

The experimental spectral database is probably adequate for such an evaluation to be performed now, though detailed examination of the available information may uncover unacceptable discrepancies that would have to be resolved by additional laboratory work. As a general rule, new measurements should never be undertaken until a careful review of the existing database has been completed and the existing uncertainties and discrepancies are thoroughly revealed and documented. Measurements are costly while reviews and evaluations of existing data are relatively inexpensive to carry out.

Table 6.1: Cumulative neutron yield for 40-MeV deuterons on a thick lithium target

E_n (MeV)	Cumulative Neutron Yield ^a
1	2.212%
2	4.062%
3	5.611%
4	7.048%
5	8.552%
6	10.322%
7	13.197%

8	16.460%
9	20.164%
10	24.366%
11	28.888%
12	33.754%
13	38.941%
14	44.471%
15	50.222%
16	55.972%
17	61.723%
18	67.032%
19	71.938%
20	76.472%
21	80.601%
22	84.361%
23	87.454%
24	89.997%
25	92.099%
26	93.795%
27	95.165%
28	96.271%
29	97.142%
30	97.827%
31	98.335%
32	98.711%
33	98.977%
34	99.165%
35	99.297%
36	99.379%
37	99.430%
38	99.475%
39	99.519%
40	99.563%
41	99.608%
42	99.653%
43	99.698%
44	99.743%
45	99.787%
46	99.830%
47	99.870%
48	99.905%
49	99.936%
50	99.961%

51	99.976%
52	99.986%
53	99.993%
54	99.997%
55	≈100.000%

^a Tabulated values correspond to percentages of all neutrons having energies lower than the listed energies.

6.2: Significance of the IFMIF Spectrum

The focus of the present study is an assessment of the adequacy of the existing cross section database for neutron induced helium production relevant to several important fusion reactor materials. At the outset of this investigation it was assumed that cross section data would be required for neutron energies up to 60 MeV. Many different reaction channels that produce helium were identified and discussed in preceding sections of this report. From the information presented in the present section, it is evident that knowledge of the Li(d,n) neutron for 40 MeV deuterons is very sketchy for $E_n > 50$ MeV. In fact, it is evident from Table 6.1 that less than 0.04% of all the neutrons produced have energies greater than 50 MeV. It is shown in earlier sections of this report that (n, α) and (n,n α) reactions tend to dominate helium production for neutron energies < 15 MeV. Above 15 MeV, many reaction channels that produce helium are energetically allowed but they must compete with other open reaction channels, especially with (n,xn) reactions ($x = 2,3,4\dots$). It is well known that the neutron total cross section varies rather slowly with increasing neutron energy. In fact, it exhibits a mildly oscillatory behavior known as the Ramsauer effect with increasing energy. Nevertheless, the general trend is toward lower total cross sections with increasing energy due to shorter deBroglie wavelengths of the incident neutrons and thus reduced interaction ranges. The elastic scattering cross section behaves in a somewhat similar manner to the total cross section. Thus, the non-elastic cross section, of which helium production is one portion, is clearly capped. This ultimately prevents helium production from increasing steadily without limits at higher neutron energies. It is possible to provide a rough numerical estimate of the relative helium production for neutrons above and below 15 MeV, respectively, for the IFMIF spectrum, but this would be beyond the scope of the present study. The main uncertainty associated with such a determination would originate from uncertainty in the cross sections for the various helium producing reaction channels. In the opinion of this author, the yield of helium from neutrons with energies above 15 MeV is likely to exceed that from neutrons below this energy for the IFMIF spectrum, but the actual difference may not be as large as one might expect because of the physical constraints mentioned above. In any event, there are likely to be significant differences between the responses of materials in the high fluences of a d + Li neutron spectrum (e.g., in IFMIF) than for an intense source of D-T neutrons with energies predominantly in the 13 – 15 MeV range. The effects of these differences need to be understood from a theoretical point of view and, if possible, tested experimentally in order to be able to interpret results derived from materials damage tests to be carried out at IFMIF. In particular, the implications of differences between damage produced in IFMIF irradiations and damage likely to be

produced in a true fusion reactor need to be thoroughly explored. This is primarily a materials science issue rather than a nuclear physics issue.

7. Summary and Recommendations

The study upon which the present report is based was undertaken to examine various technical issues that pertain to the production of helium by fast neutrons interacting with several important candidate fusion reactor materials. This section summarizes the content of the present report and offers three recommendations for near term research activities that are designed to achieve significant further progress in this area of fusion technology.

7.1 Summary

Section 1 defines the scope of the present investigation. The elements considered here are carbon, silicon, titanium, vanadium, chromium, iron, nickel, and tungsten. Section 2 explores the key physics issues associated with production of helium by fast neutron reactions on the elements considered. The present investigation is limited to those isotopes whose abundances exceed 1% in the selected elements. Helium consists of two isotopes: ^4He (alpha particle) and ^3He . Those reactions that produce ^4He are the more prevalent ones, primarily due to the tight binding energy of the alpha particle and, thus, to the relatively higher Q-values of reactions that produce ^4He . It is shown that the number of reaction channels that are energetically allowed to produce helium particles increases approximately exponentially with increased neutron energy. However, various nuclear physics limitations conspire, in practice, to limit these lists to considerably fewer significant reactions. At energies below 15 MeV, the (n, α) and (n,n α) reaction mechanisms tend to dominate, although in some case the (n, ^3He) reaction contributes as well. Above 15 MeV, the situation becomes considerably more complicated. Section 3 examines the scope of citations to helium producing nuclear reaction data given in the index CINDA. It is demonstrated that considerable information has been reported. The citations encompass experiments, theory, evaluations, compilations, and reviews. In general, the information available relevant to energies above 20 MeV neutron energy is quite sparse. Studies reported for iron and nickel are the most prevalent among these citations, and experimental references dominate over all the other categories. Section 4 explores the database of experimental information on helium producing reactions found in CSISRS (EXFOR). Plots are provided, where data are available, in order to indicate energy coverage, discrepancies, etc. It is concluded from this survey that experimental results alone are insufficient to define the cross sections for most isotopes and reaction types. An explanation is offered as to why such deficiencies exist. The principal culprit is limitations of experimental technique and facilities. The need to supplement experiment with theory is thus established. Contemporary evaluations draw information from both experiment and nuclear modeling (based on theory). Comparisons between evaluations produced by various nuclear data projects are shown in Section 5 in the form of plots. In some instances the evaluated curves are compared explicitly with experimental data. Significant differences between independent evaluations are observed in many of these plots. These can usually be attributed to the limitations of contemporary nuclear modeling practice as well as to the uncertainty in specifying model parameters required

for these calculations. Since it is likely that testing of candidate fusion reactor materials for radiation damage vulnerability will be carried out in a neutron spectrum produced by 40-MeV deuterons on thick lithium targets (IFMIF), Section 6 presents a brief discussion of the nature of this spectrum, points out its differences relative to the D-T fusion neutron spectrum of a fusion reactor, and discusses how these differences might impact on the interpretation of radiation damage test data carried out in IFMIF vis-a-vis damage by neutrons that could be anticipated in a D-T fusion reactor.

7.2: Recommendations

The main conclusion from the present review of fast neutron helium producing reaction data is that the existing database, derived from both experiments and theory, is inadequate for the purpose of assessing the importance of helium production as a radiation damage mechanism. The main shortcoming stems from inadequate knowledge of reaction cross sections. Many reactions are involved and they can be difficult, if not impossible, to distinguish experimentally. While the dominant reactions at energies below 15 MeV are generally understood, at least qualitatively if not quantitatively, the situation at energies above 15 MeV is completely unsatisfactory. Further design efforts for ITER are likely to be hampered by this lack of adequate knowledge of this important radiation damage mechanism. With this in mind, two practical recommendations are offered here. If they are fully implemented, these suggestions would be likely to improve the current situation significantly within a few years, at relatively modest cost. These recommendations involve organizing and utilizing technical resources that currently exist. Thus, no capability development would be required to obtain valuable answers to a number of important technical questions.

Recommendation #1: Nuclear modeling studies

Comprehensive calculations of reaction cross sections for all helium producing reaction channels up to at least 50 MeV should be carried out systematically for candidate elements using the best available contemporary nuclear modeling procedures. These calculations should address particle emission angle and energy distributions as well as integrated reaction cross sections. Computational code packages such as TALYS (Petten, Netherlands), GNASH (Los Alamos, U.S.A.), etc., that incorporate both compound and pre-compound reaction mechanisms, should be employed for this purpose. Comparisons between corresponding results generated by two or more independent groups would provide a better understanding of the uncertainties involved. Furthermore, these results, though subject to considerable uncertainty, would enable the fusion community to judge, at least qualitatively, the relative importance of various reaction mechanisms, and to eliminate from consideration those individual processes that appear to be insignificant. The model calculated cross sections could then be energy and angle integrated and summed according to isotopic abundance weighting so as to provide data that could be compared to direct measurements (see Recommendations #2 and #3 below). Furthermore, these model calculations would yield helium particle energy and angle emission spectra that could be used in computer codes that are designed to predict radiation damage

resulting from atomic displacements (dpa) associated with these helium particles. Such information is very difficult – in fact impossible in many cases – to obtain by means of direct experimentation.

Recommendation #2: Li(d,n) spectrum evaluation

The available experimental data pertaining to the spectrum of neutrons emitted from 40-MeV deuterons on thick natural lithium targets should be evaluated with the objective of producing an agreed upon representation for this spectrum, including uncertainties. Knowledge of this spectrum is required to calculate the response of computed helium producing reaction cross sections (see Recommendation #1) in the IFMIF neutron environment, as discussed in Section 6.

Recommendation #3: Experimental studies

Based on the experience of the last half century, it is very unlikely, even if a “crash” program were to be implemented, that all the detailed cross section information for the individual helium producing reactions applicable to fusion could be obtained by experimental work. The reasons are discussed in this report. However, it would be of great value to know the total helium production to be expected when individual materials are irradiated with neutrons having a spectrum characteristic of a fusion reactor (mainly 13 – 15 MeV) and a Li(d,n) test spectrum, respectively. Comprehensive measurements could be performed using contemporary experimental techniques, in particular the helium fluence accumulation method (HAFM) based on helium mass spectrometry. This approach is well developed and it has been used for a number of years. Furthermore, the capability for performing these measurements still exists (e.g., refer to Greenwood et al., PNL, on the Internet at <http://www.pnl.gov/etd/solutions/rDOSim.htm>). Therefore, it is recommended that specimens of all candidate materials be irradiated for as long as is reasonably feasible at both an intense D-T neutron generator facility (13 – 15 MeV) and at an accelerator facility that can produce a spectrum characteristic of IFMIF. These samples should then be analyzed for helium (either total helium or ^4He and ^3He separately) as desired by the fusion community. These measurements would provide information that is really needed by the fusion community for design purposes, namely, total helium production without regard to the details of the plethora of individual reaction channels discussed in Section 2.

The investigation indicated by the three recommendations offered above could be implemented as an international project, e.g., under the auspices of a collaboration coordinated by either the ITER Project, the IAEA, the NEA, or the IEA, etc. The important point is that individual researchers selected to participate in this collaboration should be equipped and willing to offer, with minimal preparation, those resources required to carry out the suggested tasks (i.e., well tested nuclear model codes and parameter sets, accelerator facilities appropriate to produce the suggested intense neutron irradiation environments, sample preparation techniques and facilities, and direct helium production measurement capabilities). It is envisioned that a great deal of valuable information of direct and timely relevance to the fusion community could be acquired

during a project time period of 3 - 5 years that would commence as soon as such a collaboration can be organized.